

## **4 RESULTS AND DISCUSSION**

### **4.1 Characterization of Ore**

#### **4.1.1 Thermal analysis & x-ray diffraction:**

The size analysis and chemical composition of the ore is indicated in table 4.1 and table 4.2. The analysis indicates that lime, silica and alumina are the other constituents of the ore along with iron bearing minerals. The results of x-ray diffraction of raw ore, with search match analysis from standard charts,<sup>55</sup> is tabulated in table 4.3. The result indicates that hematite is the main constituent of the ore along with goethite ( $\text{FeO} \cdot \text{OH}$ ) and iron oxalate hydrate ( $\text{FeC}_2\text{O}_4 \cdot 2\text{H}_2\text{O}$ ) as associated minerals. Kaolinite ( $\text{Al}_2\text{Si}_2\text{O}_5(\text{OH})_4$ ) and eudialyte having composition  $\{\text{Na}_4(\text{Ca},\text{Fe}^{''})_2\text{ZrSi}_6\text{O}_{17}(\text{OH},\text{Cl})_2\}$  are the best match for other peaks, indicating their presence. Many investigators have reported the association of goethite, kaolinite and other clay minerals with iron ores<sup>14, 18, 19, 23</sup>.

Figure 4.1 indicates the results of simultaneous thermal analysis of iron ore powder for one set of experiment with heating rate of  $10^0\text{C}/\text{min}$ . Similar plots were observed for other sets of experiment. The result of TG analysis of the ore in air for heating rates of  $10^0\text{C}/\text{min}$  to  $30^0\text{C}/\text{min}$  is indicated in figure 4.2 as multiple plots. The figure indicates four stages of weight losses followed by a weight gain at later stages in all the cases reported. The first loss of about 0.6% ( $10^0\text{C}/\text{min}$ ) is due

**Table No.4.1**  
**Size analysis of ore powder**

Mesh	Microns	% Weight Retained
- 100+170	- 152+86	1.90
- 170+200	- 88+76	6.00
-- 200+300	- 76+54	56.0
- 300+pan	-54	36.1
		Total 100%

**Table No.4.2**  
**Chemical analysis of iron ore**

Element	Percentage (mass %)
Total iron (Fe)	63.0
SiO <sub>2</sub>	3.30
CaO	1.00
Al <sub>2</sub> O <sub>3</sub>	2.02
Loss on ignition	4.00
	100%

TABLE NO: 4.3  
: X-ray data of iron ore with analysis (Target : Cu & Filter : Ni)

Sr.No	Observed Peak d (Å <sup>o</sup> )	Hematite			Goethite			Iron oxalate hydrate			Eudialyte			Kaolinite		
		I/I <sub>0</sub>	d (Å <sup>o</sup> )	I/I <sub>0</sub>	D (Å <sup>o</sup> )	I/I <sub>0</sub>	d (Å <sup>o</sup> )	I/I <sub>0</sub>	d (Å <sup>o</sup> )	I/I <sub>0</sub>	I/I <sub>0</sub>	d (Å <sup>o</sup> )	I/I <sub>0</sub>	d (Å <sup>o</sup> )	I/I <sub>0</sub>	
1	7.155	13												7.19	100	7.15
2	6.482	13												6.48	60	50
3	5.989	14												6.07	10	
4	5.061	13														
5	4.951	19														
6	4.808	30														
7	4.724	14														
8	4.667	14														
9	4.465	14														
10	4.229	16														
11	4.160	20														
12	3.664	41														
13	3.545	15														
14	3.013	14														
15	2.813	26														
16	2.718	19														
17	2.689	100														
18	2.507	70	2.51	50	2.49	16										
19	2.475	16														
20	2.442	22														
21	2.293	15														
22	2.199	26														
23	2.183	17														
24	1.836	36	1.838	40	1.838	40										
25	1.692	42	1.690	60	1.690	60										
26	1.598	17	1.596	16	1.596	16										
27	1.484	28	1.484	85	1.484	85										
28	1.457	16	1.452	35	1.452	35										
29	1.451	32	1.452	35	1.452	35										
30	1.345	15	1.345	23	1.345	23										
31	1.310	23	1.310	20	1.310	20										

Sample : Iron ore ( 9058  $\mu$ g), Heating rate:  $10^{\circ}\text{C}/\text{min}$

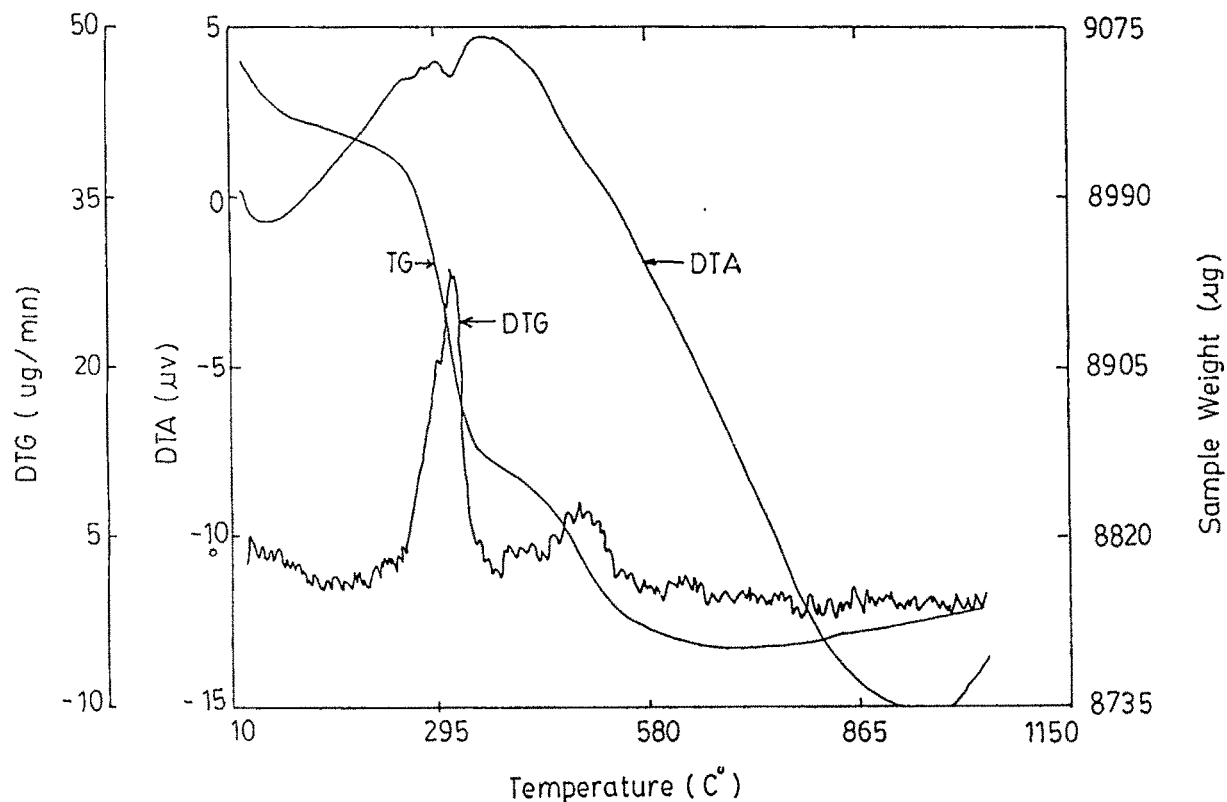


Fig. 4.1 Simultaneous analysis curve for one set (Sample iron ore heating rate  $10^{\circ}\text{C}/\text{min}$ )

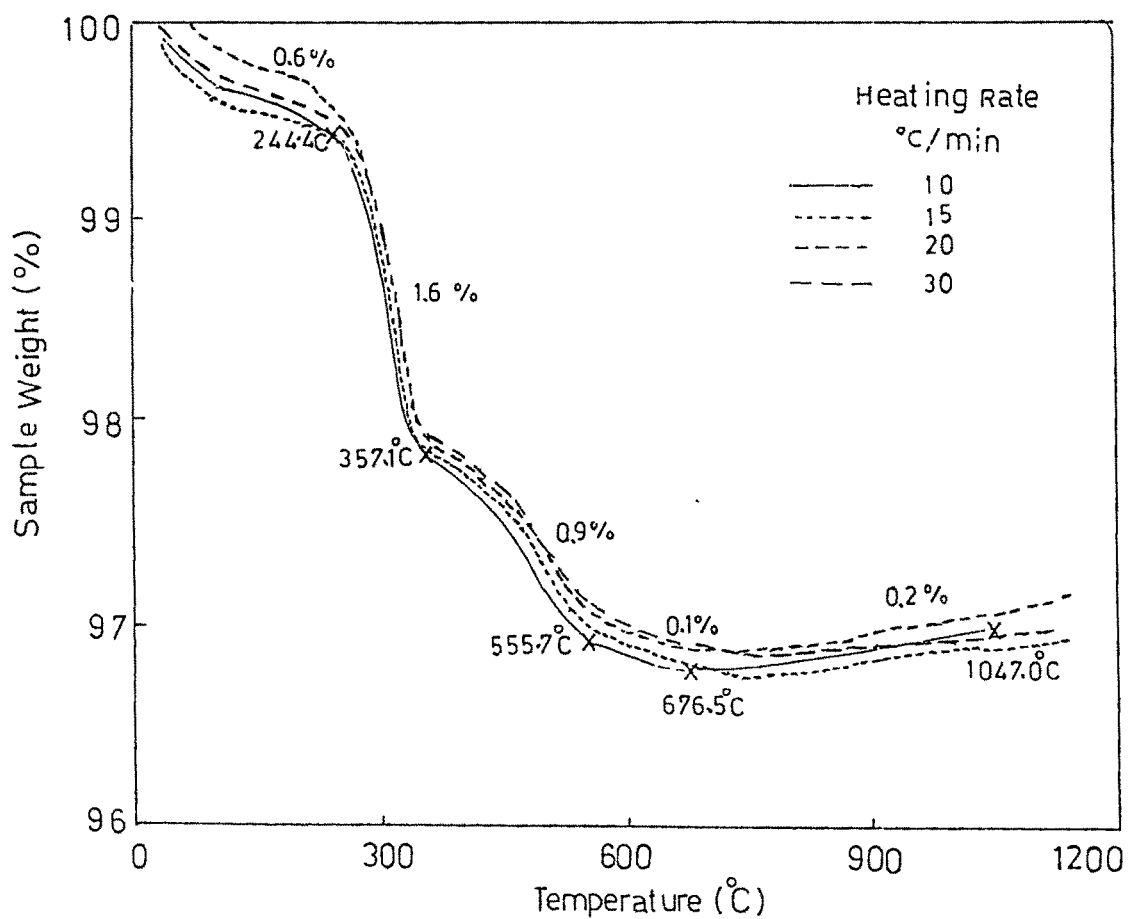


Fig. 4.2 Multiple plot of TG for heating rate  $10^{\circ}\text{C}/\text{min}$  to  $30^{\circ}\text{C}/\text{min}$

to the absorbed moisture. The second stage of weight loss, in the temperature range of  $244^{\circ}\text{C}$  to  $357^{\circ}\text{C}$  and amounting to 1.6% is due to the decomposition of goethite and iron oxalate hydrate. The third and fourth stages in temperature range of  $357^{\circ}\text{C}$  to  $676^{\circ}\text{C}$  and amounting to 0.9% and 0.1% respectively is attributed to the decomposition of gangue materials. At final stages after around  $676^{\circ}\text{C}$  the samples gradually gained weight by about 0.2%, indicating the probable oxidation of the products of gangue decomposition. The gangue decomposition is better resolved by TG analysis in nitrogen atmosphere and is discussed at later stages of this text.

Figure 4.3 indicates the DTG plot of the same data. The result shows a major peak of weight loss corresponding to goethite and iron oxalate hydrate decomposition and a small hump attributed to gangue decomposition. As expected the peaks shift to higher temperature with increase in the rate of heating. The maximum rate of decomposition (peak value) also increases with heating rate from 0.3260 %/min for  $10^{\circ}\text{C}/\text{min}$  to 0.935%/min for  $30^{\circ}\text{C}/\text{min}$  for goethite decomposition. Similar trend is observed for gangue decomposition also.

The multiple DTA plots of the sample are represented in Figure 4.4. The endothermic peak in temperature range of  $318^{\circ}\text{C}$  to  $335.8^{\circ}\text{C}$  for heating rates of  $10^{\circ}\text{C}/\text{min}$  to  $30^{\circ}\text{C}/\text{min}$  corresponds to decomposition of goethite<sup>20,21</sup>. The results indicate the right shift of the peak temperature from  $318^{\circ}\text{C}$  to  $336^{\circ}\text{C}$ . The  $\Delta T$  value increases from 3.6  $\mu\text{V}$  to 11.90  $\mu\text{V}$  with heating rate. However the area of the curve, which is proportional to the amount of heat absorbed and quantity of goethite present, remains almost same around 10  $\mu\text{Vs}/\text{mg}$ .

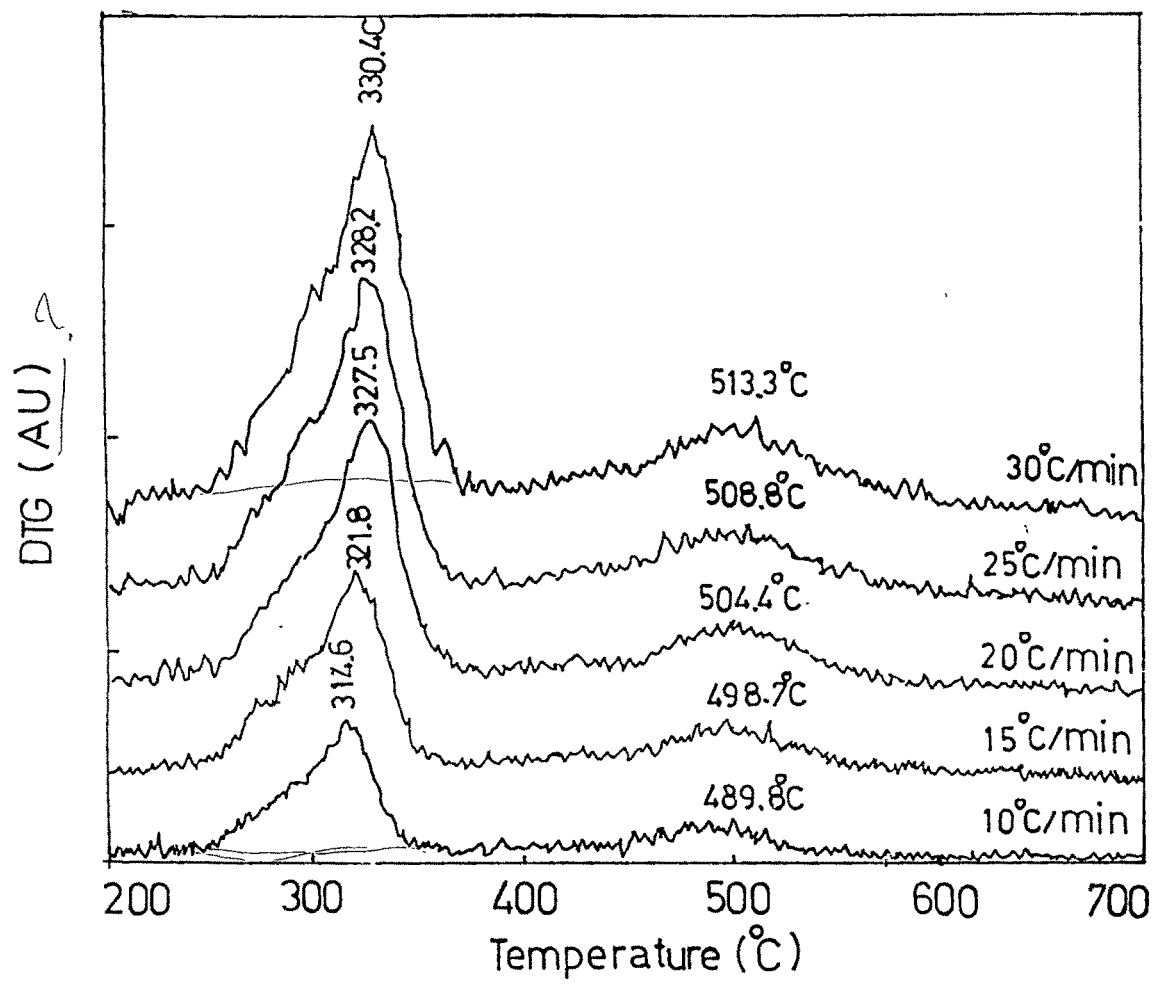


Fig. 4.3 Multiple plot of DTG for heating rate  $10\text{ }^{\circ}\text{C}/\text{min}$  to  $30\text{ }^{\circ}\text{C}/\text{min}$

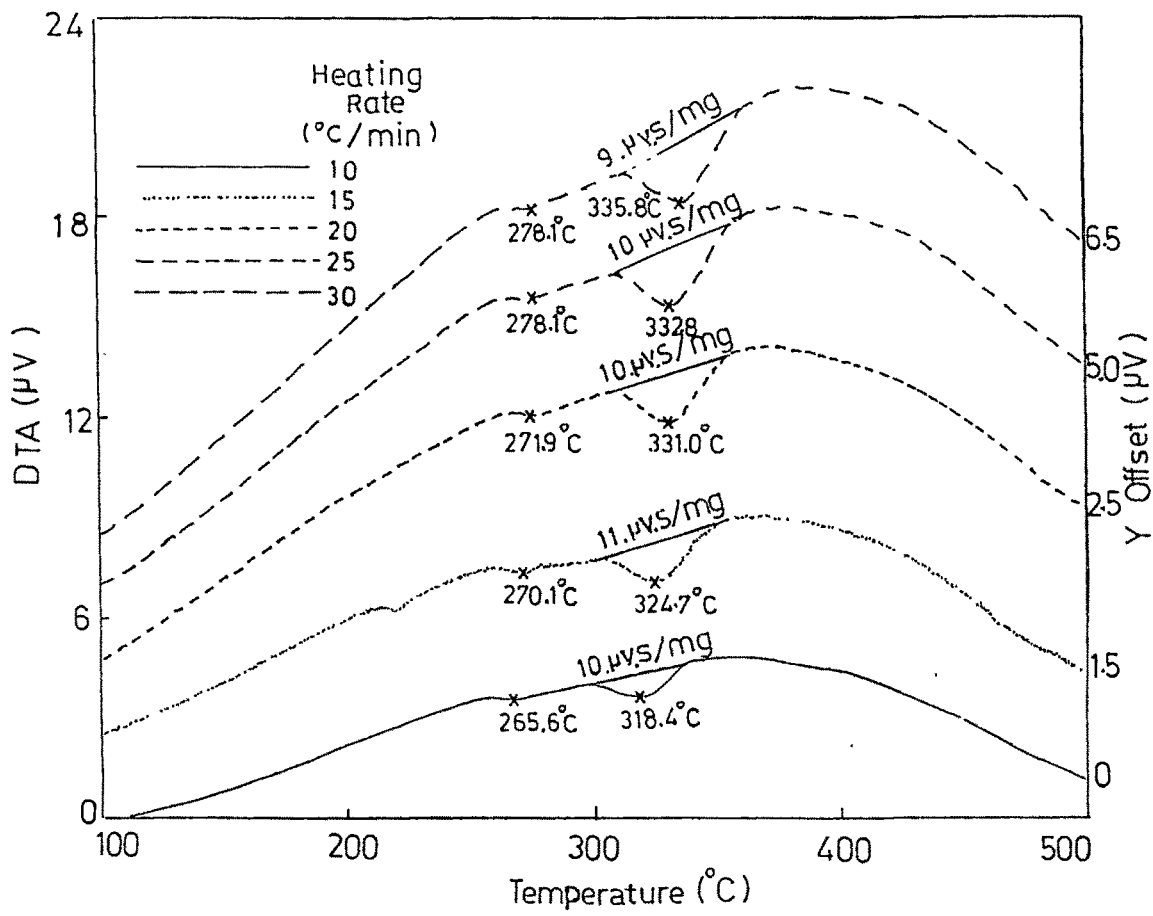


Fig. 4.4 Multiple plot of DTA for heating rate  $10\text{ }^{\circ}\text{C}/\text{min}$  to  $30\text{ }^{\circ}\text{C}/\text{min}$   
(Reference  $\alpha$ -Alumina)

The literature<sup>20, 21</sup> on DTA of hydrated iron oxide indicate that goethite decomposes around this temperature and a well-crystallized goethite decomposes around 380°C. There are, however fine grain goethites, with disordered structure, which dehydrate much below this temperature. The decomposition of Australian iron ore was studied by Akiyama<sup>10,14</sup> et al and reported that the decomposition of associated goethite occurs around 300°C and was indicated by an endothermic peak in DSC plot (figure 2.1). This supports our observation confirming the presence of goethite in present ore as indicated by x-ray analysis.

The DTA plot also indicates shallow endothermic peaks at temperatures of 270°C. This peak is attributed to the decomposition of iron oxalate hydrate phase indicated in x-ray analysis. The oxalates on heating in air decomposes<sup>20</sup> to CO, CO<sub>2</sub>, metal oxide and water molecule. It is reported that, <sup>reference</sup> this decomposition yields two endothermic peaks in the range of 270°C - 280°C coinciding with present observation and confirming the presence of iron oxalate hydrate.

To confirm the presence of these phases and their decomposition an x-ray analysis of iron ore heated to 355°C and cooled was carried out. The results (figure 4.5) indicate that peak representing goethite at 'd' values 4.16A°, 2.475A° and 2.442A° in ore analysis were absent. Similarly peaks corresponding to the iron oxalate hydrate phase at 'd' values of 4.808A°, 4.724A° and 2.298A° were also not observed.

#### 4.1.2 Quantitative phase analysis of minerals:

As indicated in chapter 2, the decomposition of goethite can be written as<sup>20</sup>:

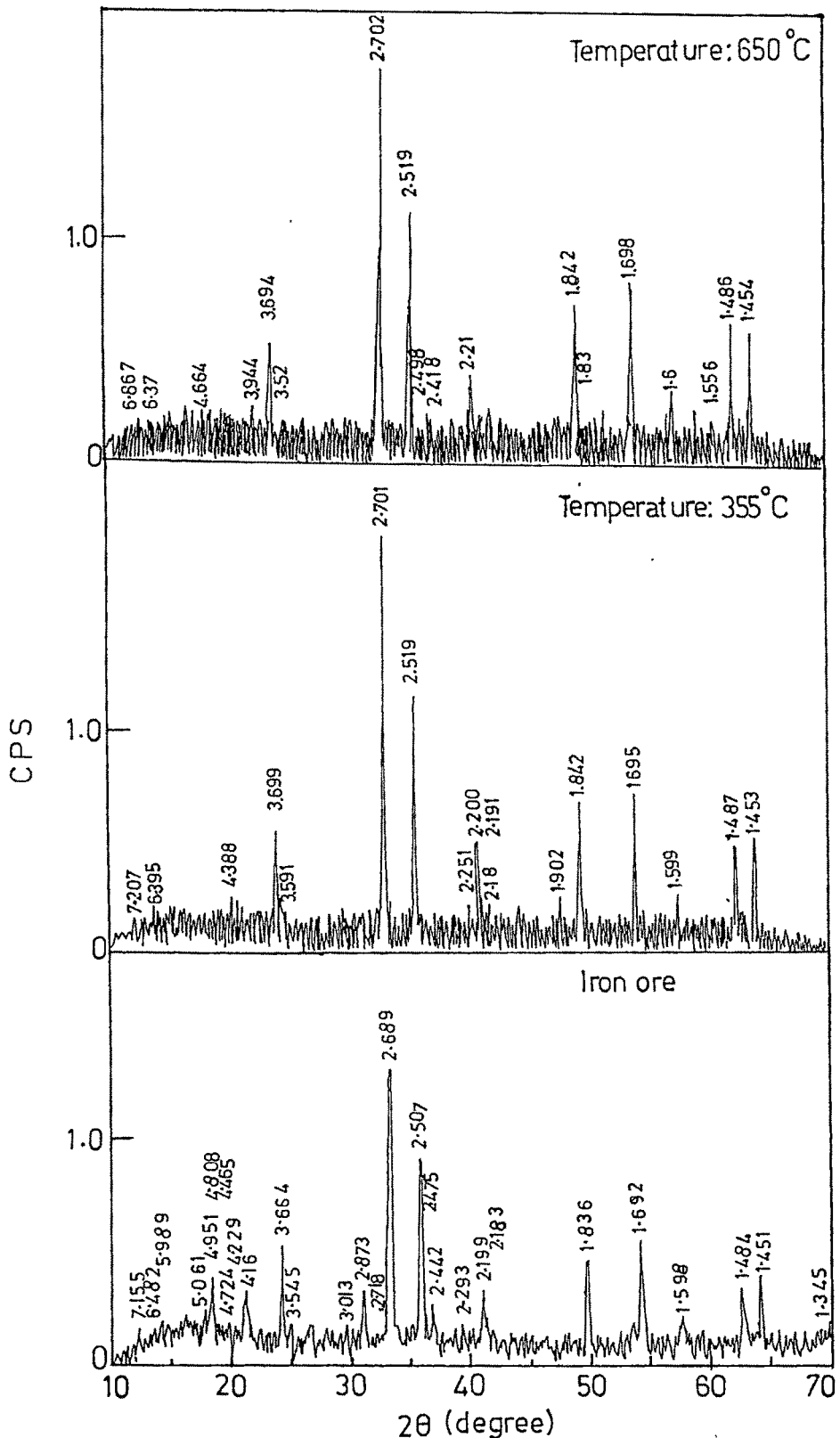
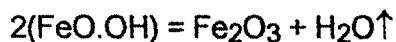
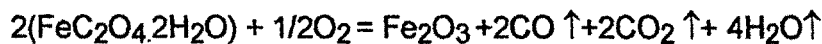
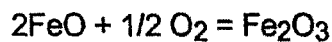


Fig. 4.5 X-ray diffraction pattern of partially decomposed iron ore with original sample



with stoichiometric weight loss of 10.11%.

Similarly the oxalate decomposes in air as<sup>20</sup>:



with net stoichiometric loss of 55.56%.

This aspect could be used to estimate the amount of these phases present in ore. Weight losses corresponding to each of these individual reactions could be ascertained by TG analysis.

One of the methods is to consider the onset point of DTA endothermic peak of goethite decomposition as the cut off point of the two reactions mentioned above. Figure 4.10 indicates the 2<sup>nd</sup> stage weight loss region of TG along with corresponding DTA and DTG plots for one of the experiments with 30°C/min heating-rate. For this case, the second stage weight loss commences at 250.3°C and completes at 371.1°C with net weight loss of 152.8μg. The onset point of goethite decomposition is at 311.6°C. The weight of the sample at this temperature is 9484.3μg. Thus the sample lost 58.3 μg out of total 152.8μg due to oxalate decomposition. It could be noticed that the slope of DTG curve also changes at this point of 311.6°C. The results of other sets of experiments is shown in figure 4.7 to figure 4.9..

2m  
Hf4.10 before  
H.7 - 4.9  
Reference

Decomposition  
peak needed to  
separate two peaks

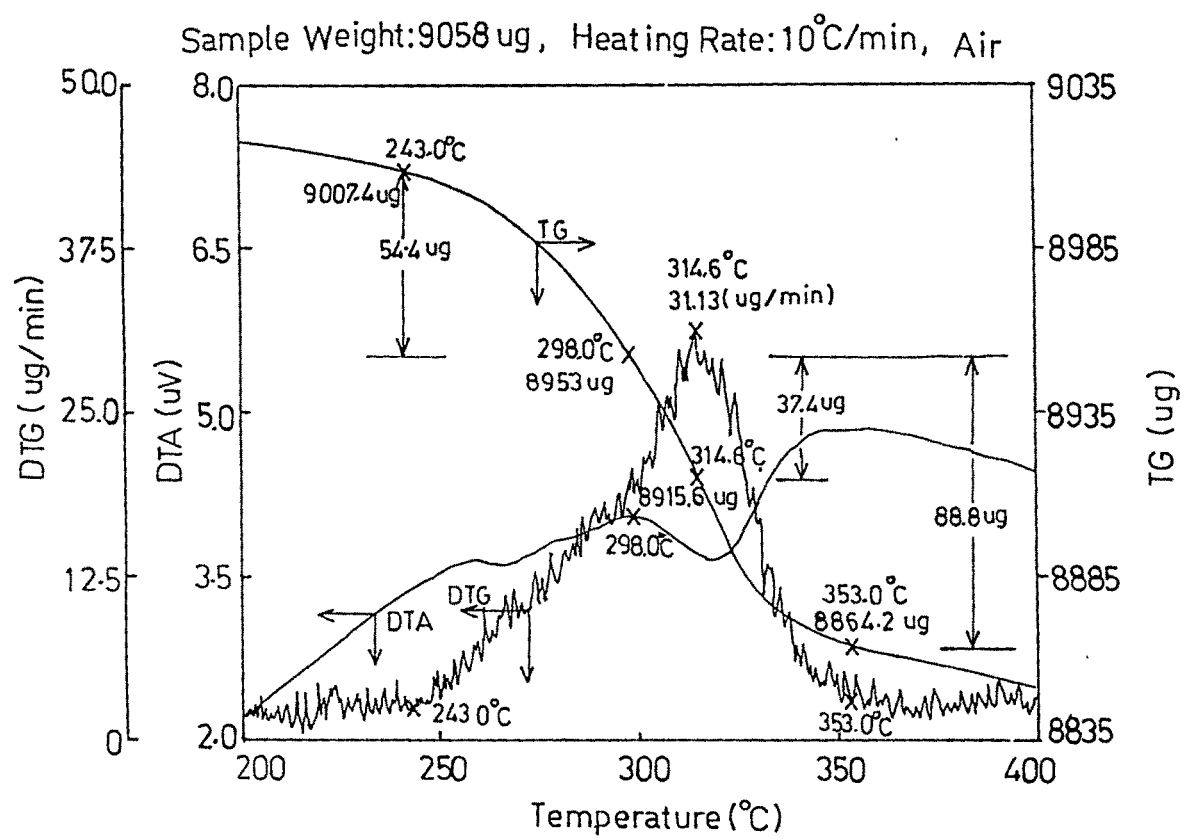


Fig. 4.6 Simultaneous plot (TG/DTA/DTG) for decomposition.  
(Heating rate: $10^0\text{C} / \text{min}$ )

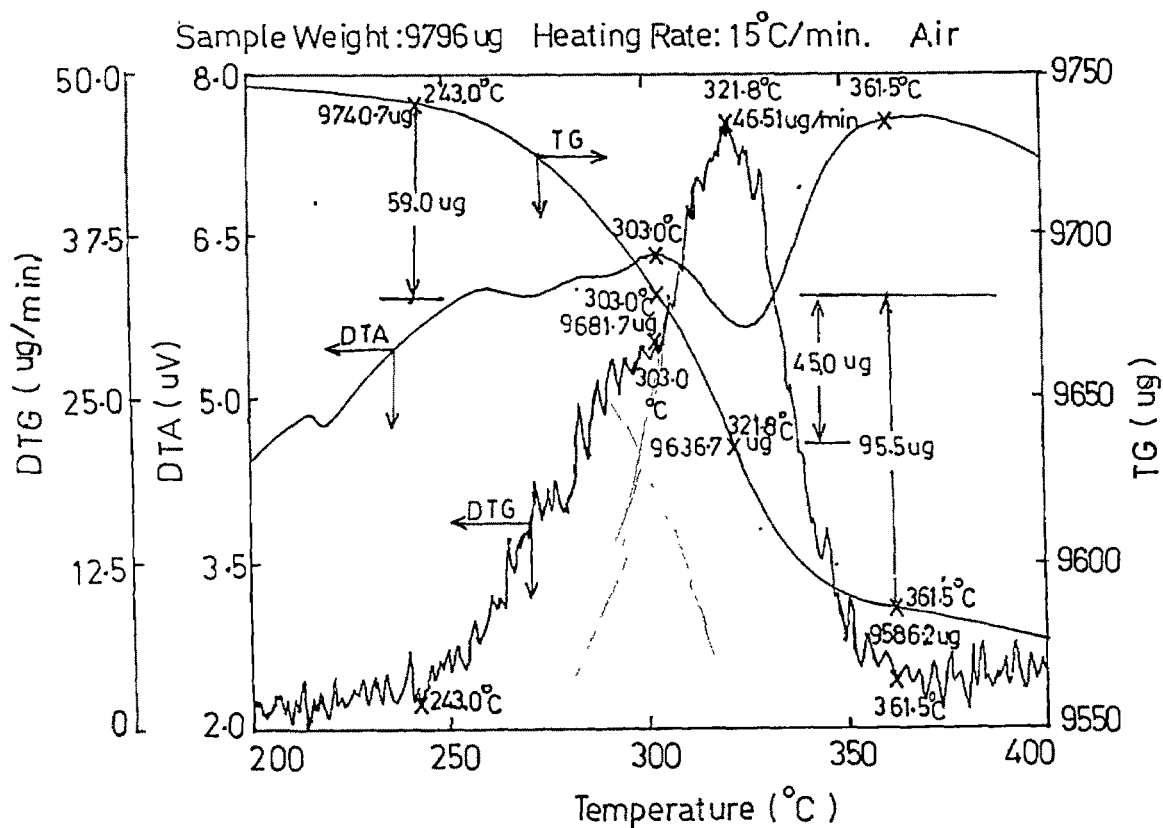


Fig. 4.7 Simultaneous plot (TG/DTA/DTG) for decomposition.  
(Heating rate: 15<sup>o</sup>C/ min)

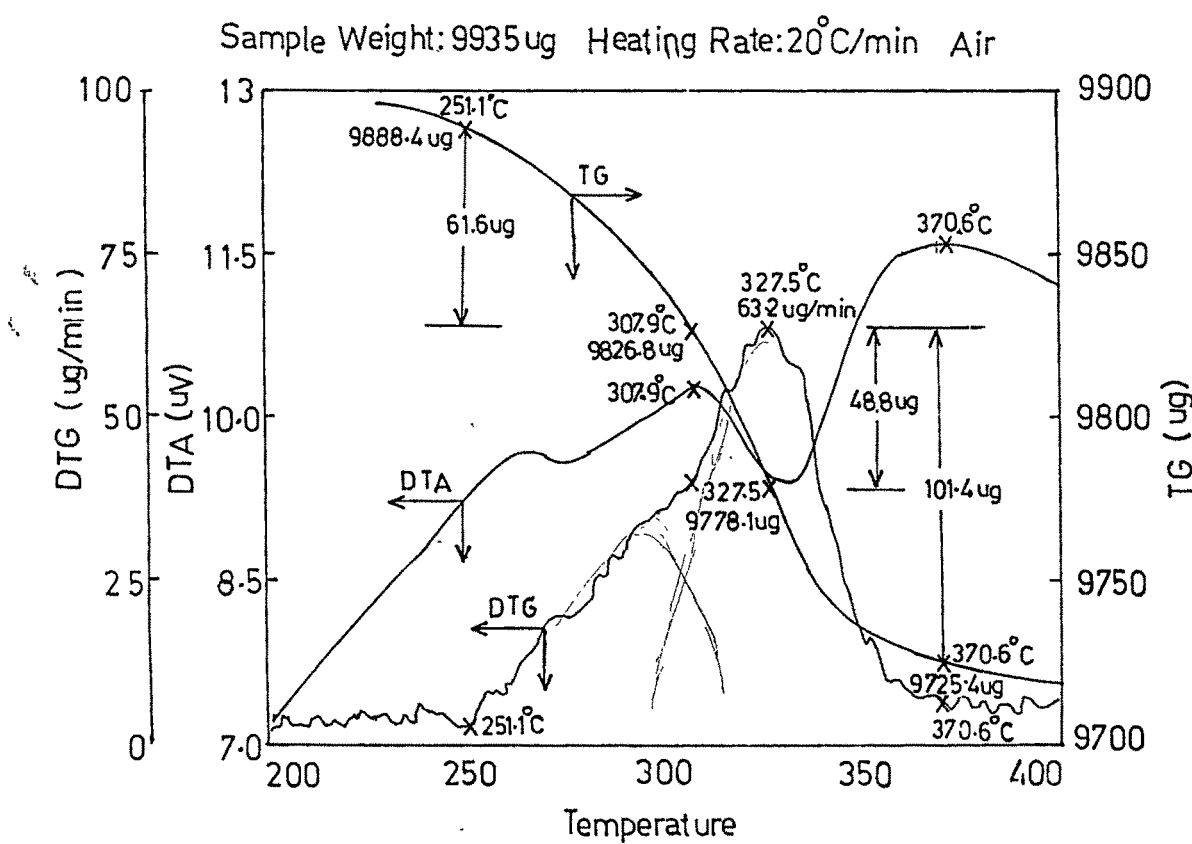


Fig. 4.8 Simultaneous plot (TG/DTA/DTG) for decomposition.  
(Heating rate: 20°C / min)

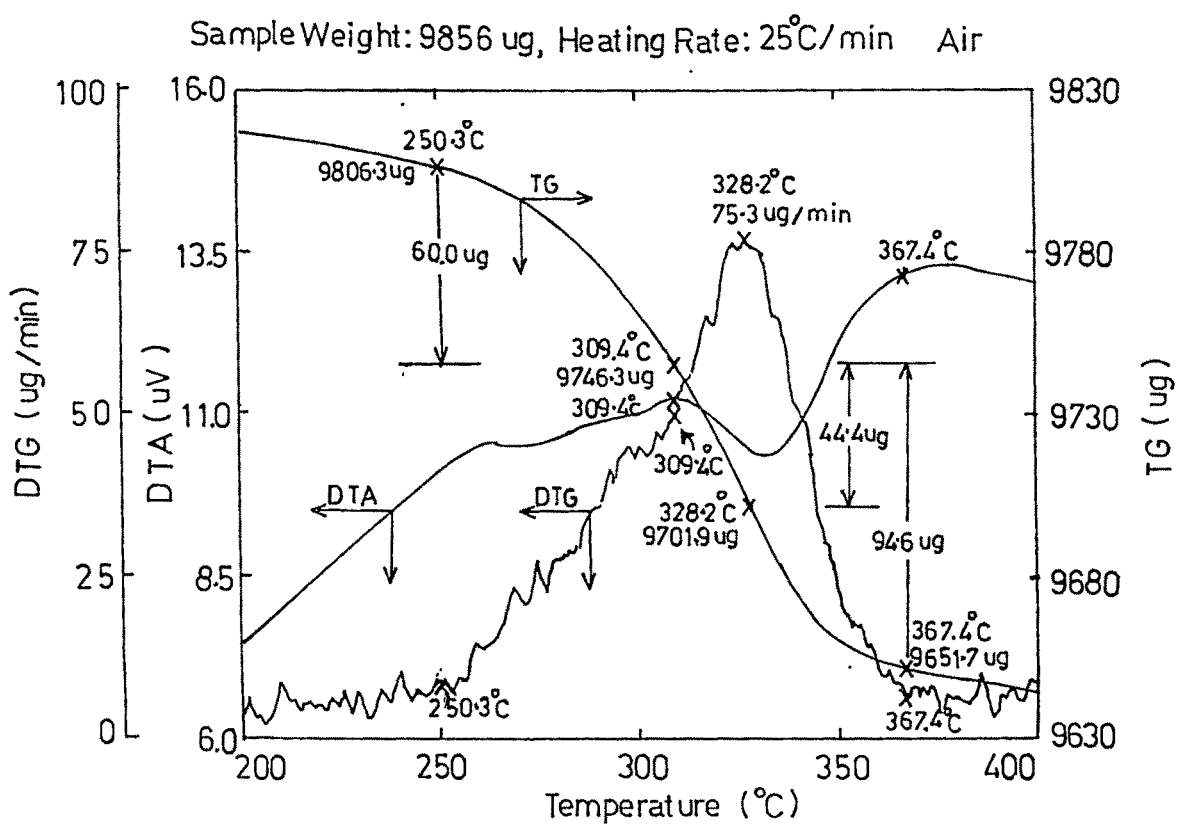


Fig. 4.9 Simultaneous plot (TG/DTA/DTG) for decomposition.  
(Heating rate: 25 $^{\circ}\text{C} / \text{min}$ )

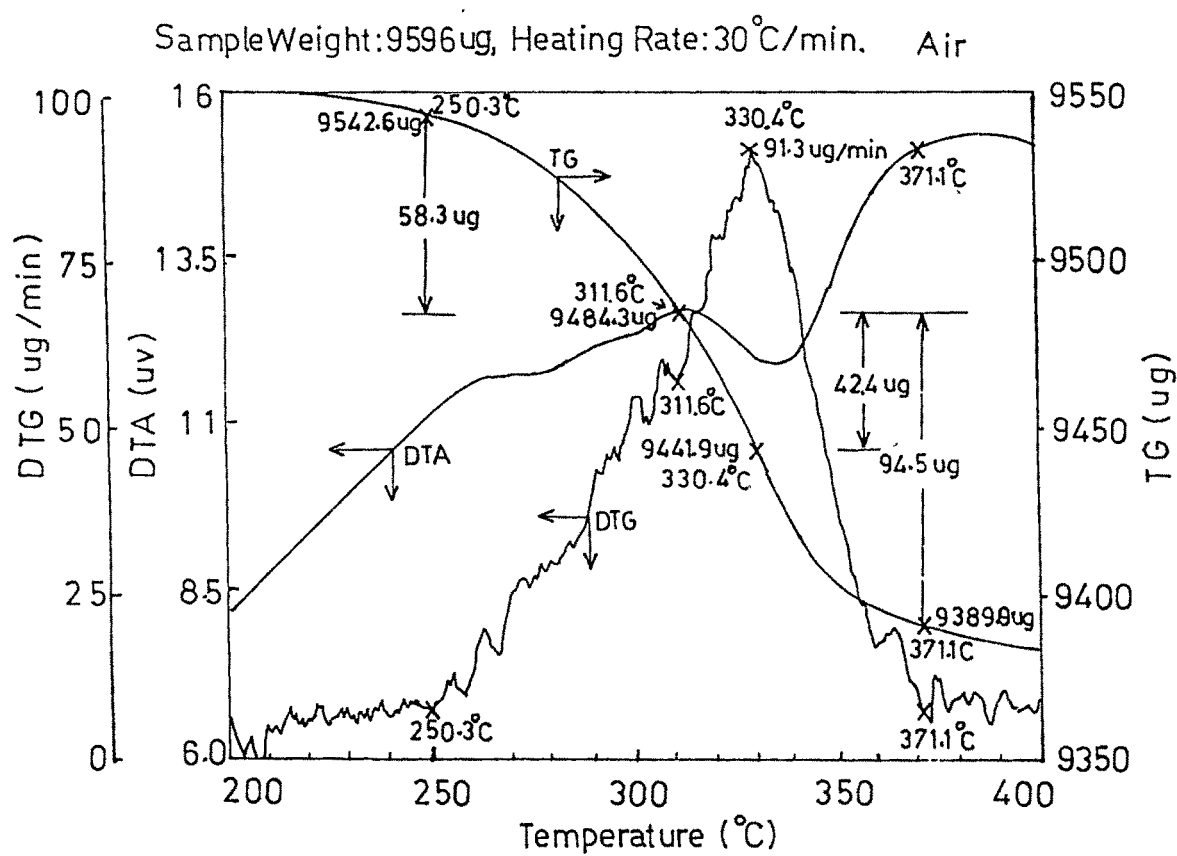


Fig. 4.10 Simultaneous plot (TG/DTA/DTG) for decomposition.  
(Heating rate : 30  $^{\circ}\text{C}/\text{min}$  )

The selection of this cut off points is crucial in quantitative phase analysis hence it was also checked by evaluating the activation energy of the decomposition reaction at various stages. One of the method to do so is by Broido's method<sup>56, 57</sup> which is represented by equation:

$$\ln(\ln(m_0/m)) = -E/R(1/T) + \text{constant} \quad (4.1)$$

' $m_0$ ' is the original weight of the sample, ' $m$ ' is the weight of sample at an instant when temperature is ' $T$ ', ' $E$ ' is the activation energy and ' $R$ ' the gas constant. In this method, plot between  $\ln(\ln(m_0/m))$  Vs  $(1/T)$  yields a straight line and the slope gives the value of activation energy. The point of change in slope of the line indicates change in activation energy and hence the change in reaction.

Figure 4.11 indicates the multiple plot of second stage weight loss of TG analysis for different heating rates of  $10^0\text{C}/\text{min}$  to  $30^0\text{C}/\text{min}$ . The points on curves indicate the temperature values at 0%, 20%, 30%, 40%, 60%, 80% and 100% change of second stage weight loss. The fraction of reaction ( $x$ ) is given by:

$$x = (m_0 - m) / (m_0) \quad (4.2)$$

$$x = (1 - m / m_0) \quad (4.3)$$

$$m_0/m = (1-x)^{-1} \quad (4.4)$$

Substituting in equation (4.1) we get:

$$\ln\{\ln(1-x)^{-1}\} = -E/R(1/T) + \text{constant.} \quad (4.5)$$

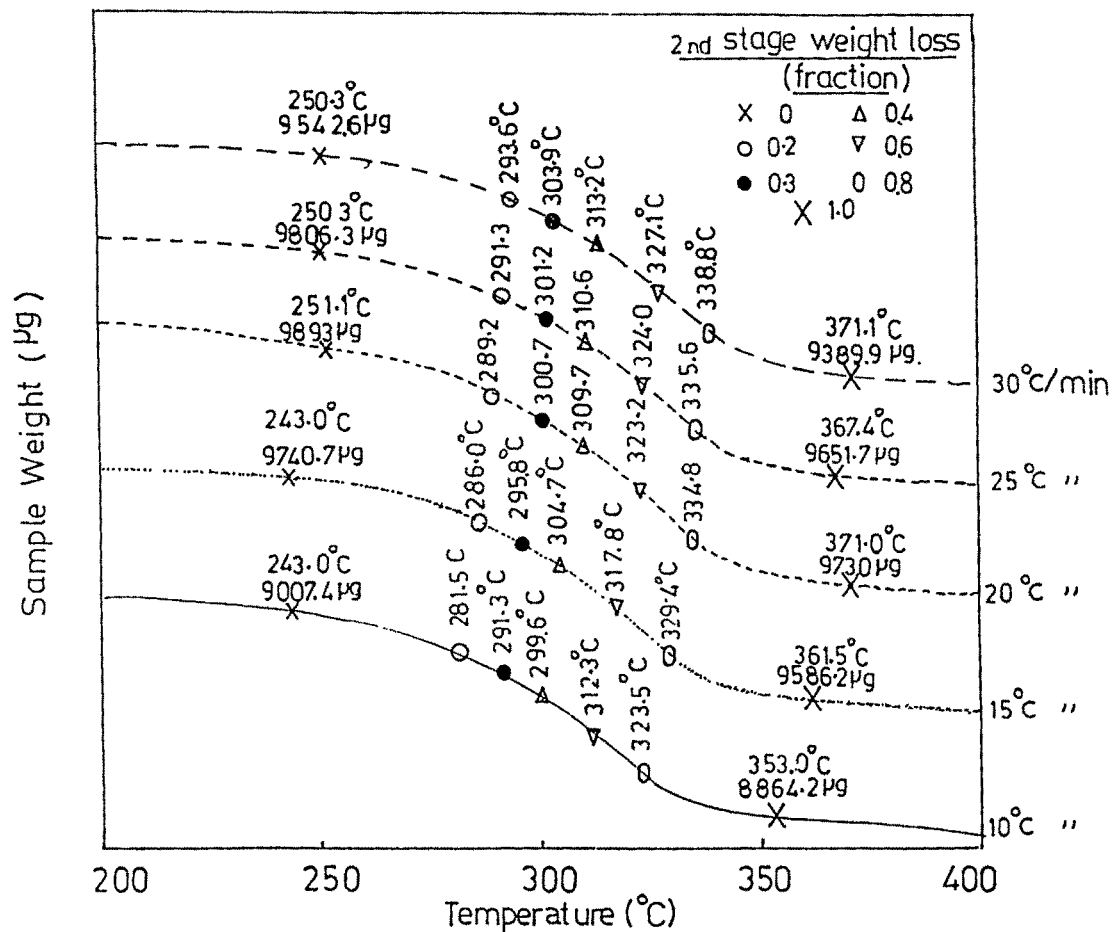


Fig. 4.11 Multiple plot-TG second stage weight loss for different heating rates (with off-set)

This equation is identical to the equation (2.19) as discussed in chapter 2. The LHS of the above equation was calculated for 'x' values of 0.2, 0.3, 0.4, 0.6 and 0.8 for three sets of heating rates, and plotted in figure 4.12. The change in slope of this plot is observed at 'x' value of 0.38 indicating that the cut off point for above two reactions is at 38% weight change point of TG curve. This point coincides with onset of DTA curve for goethite decomposition as discussed earlier.

(After annealing)

Once this point is identified, the weight loss contributed by each of the individual reaction is evaluated and tabulated in table 4.4, along with the quantity and percentage of phases for all sets. The table shows that average amount of iron oxalate hydrate present in the ore is 1.09% and that of goethite is 9.74%. *Such analysis?*

#### 4.1.3 Activation energy and order of reaction:

The activation energy value for goethite decomposition is calculated by Kissinger<sup>41</sup> method. The equation is discussed in chapter 2. In this method  $\ln(B/T_m^2)$  Vs  $1/T_m$  for different heating rates 'B' to get a straight line with slope  $(-E/R)$ . Here ' $T_m$ ' is the minimum temperature at DTA endothermic peak. The peak temperatures and heating rates are noted from figure 4.4 and plotted in figure 4.13. The activation energy value is 175 kJ/mole. Table 4.5 indicates the calculation of activation energy. *See Fig 4.2 calculation?*

An attempt has been made to determine the mechanism of goethite decomposition by evaluating the parameter 'n' in function equation<sup>37, 41</sup>

$$F(x) = (1-x)^n \quad (4.6)$$

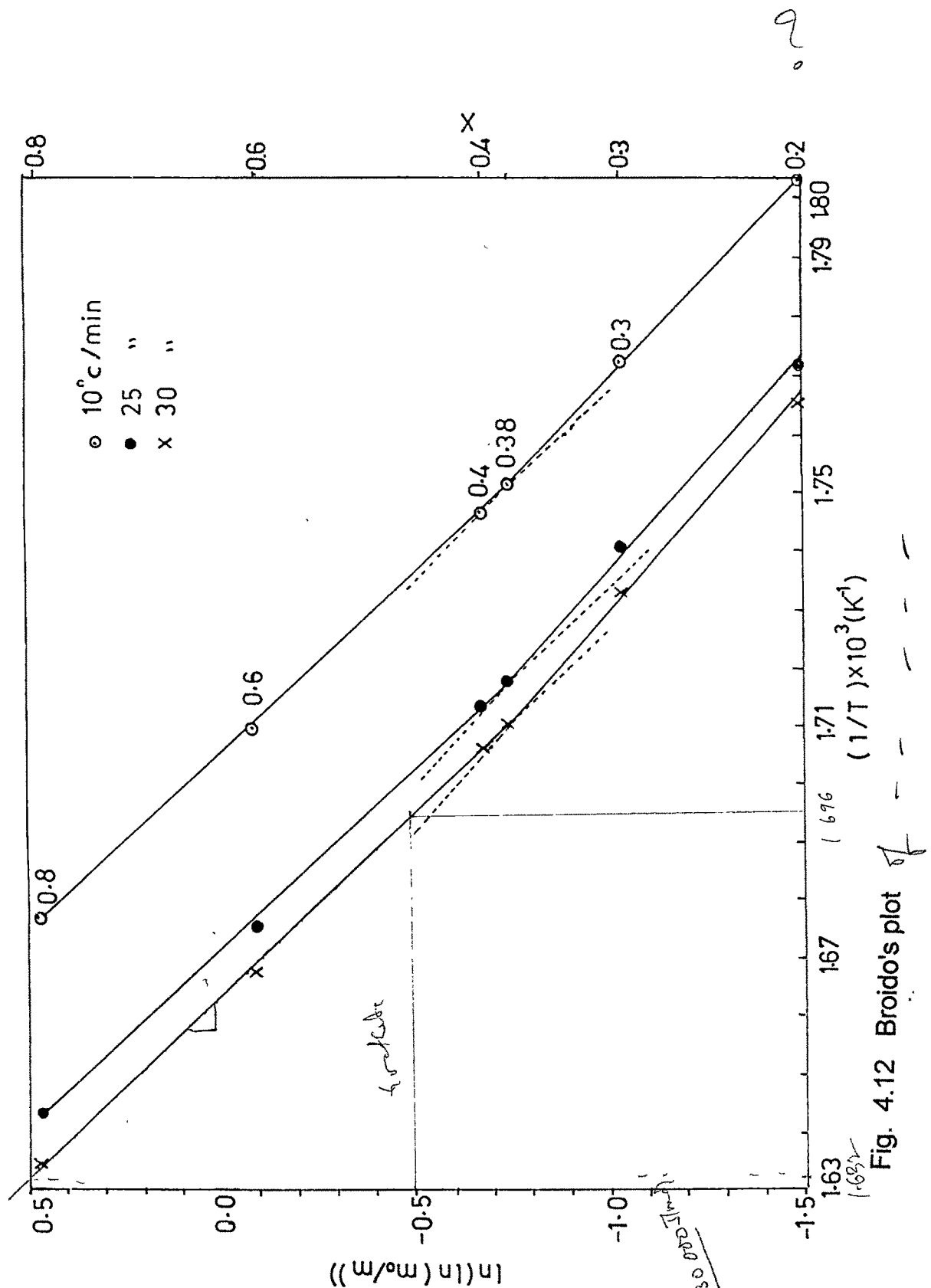


Fig. 4.12 Broido's plot

**Table No. 4.4**  
**Quantitative Analysis of Mineral Matter in Iron Ore**

Sr.No.	Rate of Heating ( C/min)	Sample weight ( $\mu\text{g}$ )	Weight loss in second stage of TG analysis			Amount of minerals			
			Oxalate Decompo.	Goethite Decompo.	Total	Iron oxalate Hydrate		Goethite	
			( $\mu\text{g}$ )	( $\mu\text{g}$ )	( $\mu\text{g}$ )	( $\mu\text{g}$ )	%	( $\mu\text{g}$ )	%
1	10	9058	54.4	88.8	143.1	97.91	1.081	873.34	9.697
2	15	9796	59	95.5	154.5	106.19	1.084	944.61	9.643
3	20	9935	61.6	101.4	163	110.87	1.115	1002.96	10.10
4	25	9856	60	94.6	154.6	107.99	1.096	935.7	9.49
5	30	9596	58.3	94.5	152.8	104.93	1.093	934.72	9.74
					Average	1.094	Average	Average	9.74

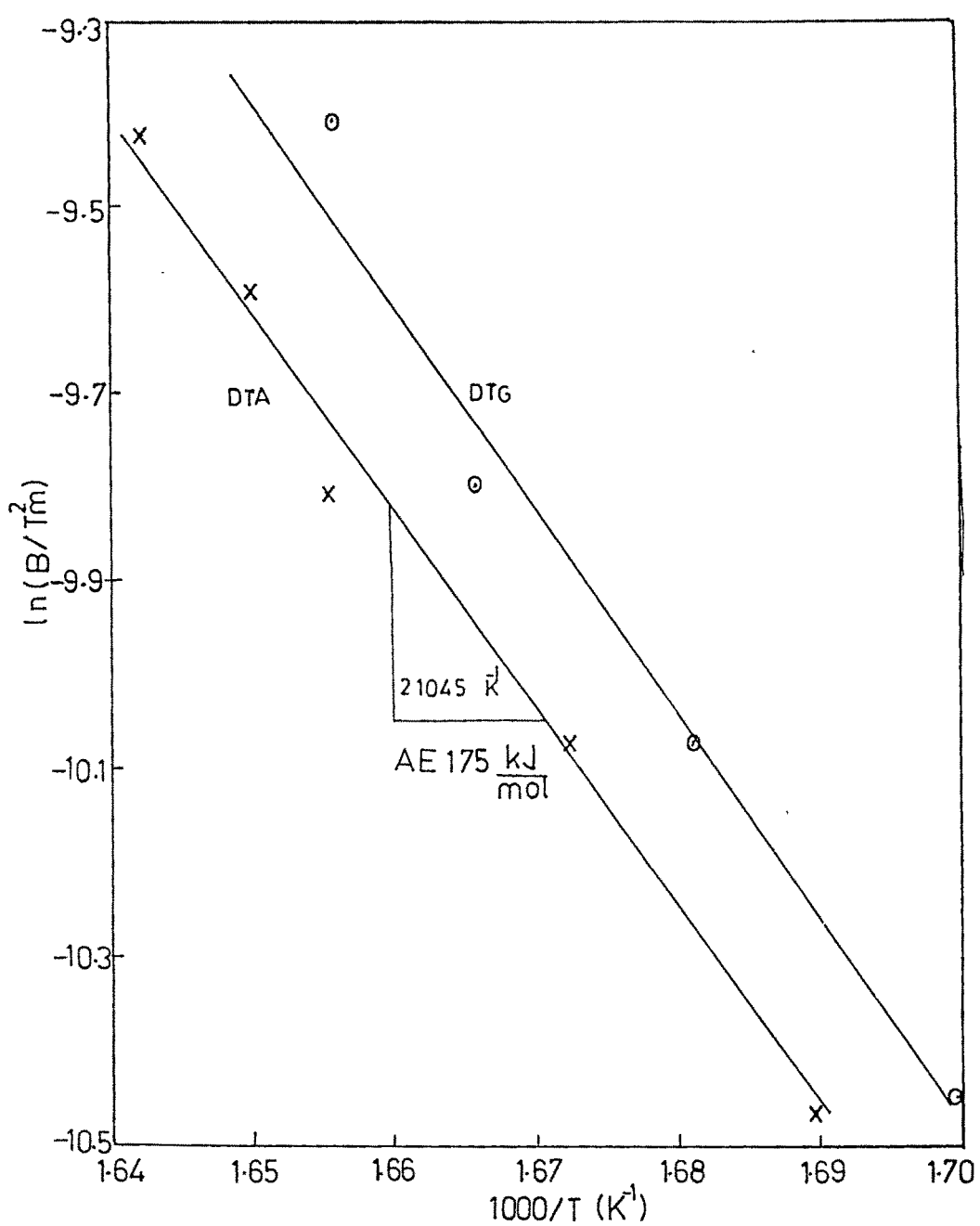


Fig. 4.13 Kissinger method - Calculation of activation energy

*rudimentary calculations  
not valid*

Table: 4.5 Calculation of Activation Energy (Kissinger Method)

S.N	Rate of Heating °C/min	Peak Temp. °C	Peak Temp. (K)	$1/T \times 10^3$ (K <sup>-1</sup> ) (X)	$\ln(B/T_m^2)$ (Y)	XY
1	10	318.4	591.4	1.6909	-10.4624	-.01769087
2	15	324.7	597.7	1.6731	-10.078127	-.01686171
3	20	331.0	604.0	1.6556	-9.81142	-.01624378
4	25	332.8	605.8	1.6507	-9.59422	-.01583717
5	30	335.8	608.8	1.6426	-9.42178	-.01547621
$\Sigma$	-	-	-	8.3129	-49.367947	-.08210974

$$\text{Slope} = \frac{\Sigma XY - (\Sigma X \Sigma Y)/n}{\Sigma X^2 - (\Sigma X)^2/n} = \frac{-0.08210974 - (-0.08207816)}{13.82236303 - 13.82086128}$$

$$= \frac{-0.00003158}{0.00150175} \times 10^6$$

$$= -21028.8 \text{ K}^{-1}$$

$$\begin{aligned}\text{Activation Energy} &= 21028.8 \times 8.314 \text{ Joules/mol/K} \\ &= 174833.441 \text{ Joules/mol} \\ &= 175 \text{ k.J/mol}\end{aligned}$$

used in non-isothermal kinetic analysis. As discussed in chapter 2, at inflexion point of TG curve, when the second derivative is zero.

$$\frac{E.B}{RT_{\max}^2} = \frac{n (dx/dt)_{\max}}{(1-x_{\max})} \quad (4.7)$$

$$\frac{B}{T_{\max}^2} = \left[ \frac{nR (dx/dt)_{\max}}{E (1-x_{\max})} \right] \quad (4.8)$$

here:

$T_{\max}$  = Temperature of TG influx

The plot between function of RHS in brackets with  $B/T_{\max}^2$  will give a straight line with positive slope of  $nR/E$ . The value of parameter 'n' could be evaluated for above calculated value of activation energy (175kJ/mole). Figure 4.10 indicates that goethite decomposition commences at  $311.6^{\circ}\text{C}$  and completes at  $371.1^{\circ}\text{C}$  with weight change of  $94.5\mu\text{g}$ . The maximum rate of this decomposition is at  $330.4^{\circ}\text{C}$  and is  $91.3\mu\text{g}/\text{min}$ . The corresponding weight at TG curve is  $9441.9\mu\text{g}$  i.e. the sample loses  $42.4\mu\text{g}$  up to this point. The fraction of goethite decomposed at this point of time is  $0.4487$  ( $42.4/94.5$ ) corresponding to  $dm/dt$  of  $91.3\mu\text{g}/\text{min}$  and  $dx/dt$  of  $0.966$ . These values are similarly calculated for other sets of experiments and the plot between the function  $\{(dx/dt)_{\max}/(1-x_{\max})\}$  and  $B/T_{\max}^2$  is shown in figure 4.14. The slope of the curve ( $nR/E$ ) is evaluated and the value of 'n' calculated for an

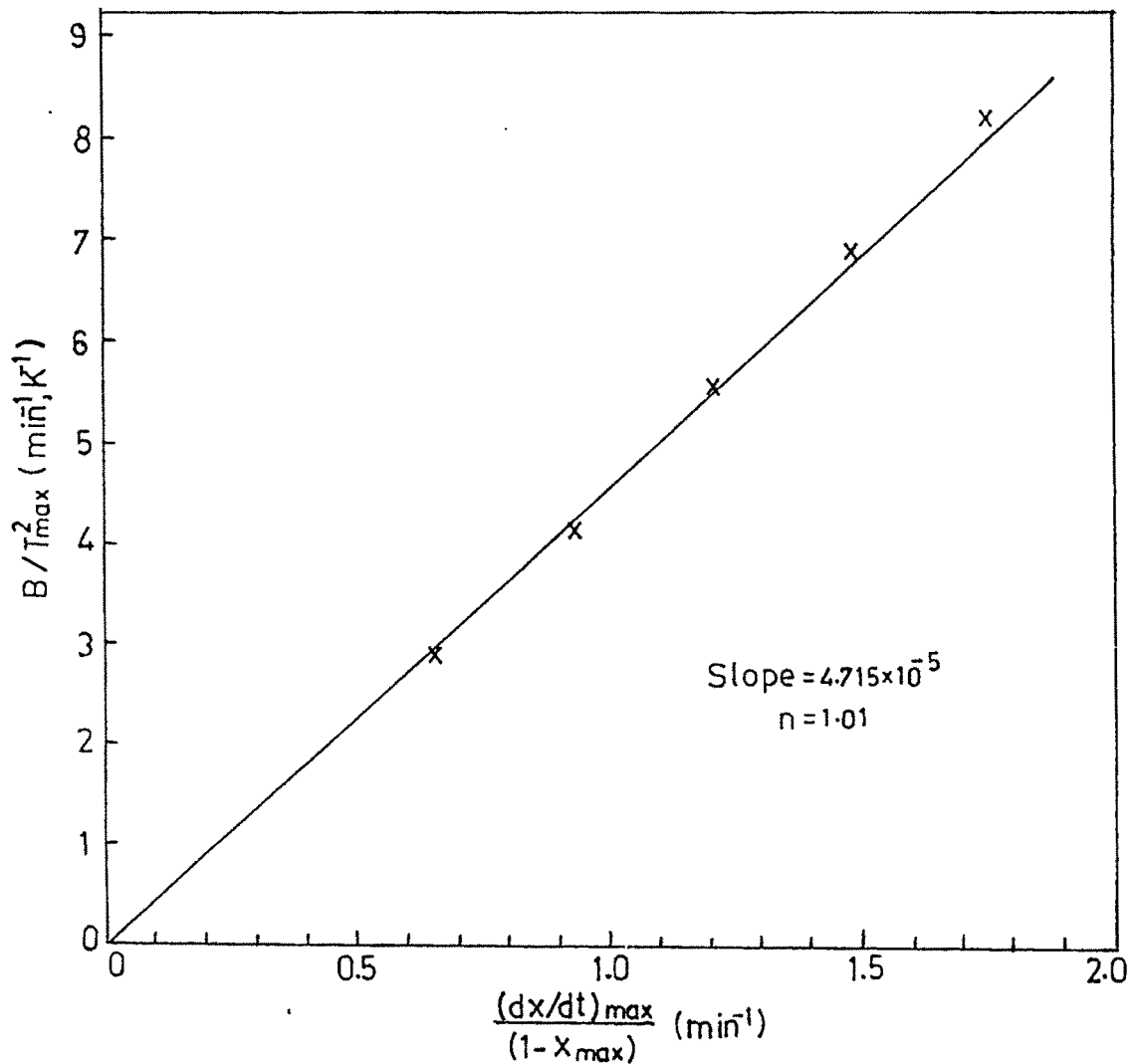


Fig. 4.14 Plot between  $B/T_{\max}^2$  Vs  $(dx/dt)_{\max} / (1-x_{\max})$  for evaluation of order of reaction.

activation energy value of 175 kJ/mole, which is equal to 0.98 as indicated in table 4.6.

The value of 'n' for different kinetic processes is indicated in literature<sup>41,51</sup>. For nucleation controlled reaction mechanism which is represented by the equation:

*that about other mechanism!*

$$\ln(1-x) = kt \quad (4.9)$$

and in differential form

$$dx/dt = k(1-x) \quad (4.10)$$

the value of 'n' is 1. The value of 'n' obtained in present investigation is 0.98 and is comparable to '1' indicating that the goethite decomposition has a nucleation controlled mechanism and is a first order reaction.

#### 4.1.4 Gangue material decomposition.

The x-ray analysis of the ore indicated the presence of two gangue minerals, one 'Kaolinite' and other 'Eudialyte'. Presence of kaolinite as gangue mineral in iron ores is reported in many investigations.<sup>10 23</sup> As discussed earlier this mineral decomposes around  $600^{\circ}\text{C}$  losing water. The x-ray analysis of ore powder heated to  $650^{\circ}\text{C}$  is indicated in figure 4.5 which shows that peaks of kaolinite and eudialyte, present in ore, disappear indicating their decomposition.

The decomposition of these gangues, in present work, is indicated by the third and fourth stage of weight loss in TG curve (figure 4.2). The figure indicates

**TABLE: 4. 6 Calculations for order of reaction 'n'**

Rate of Heating °C/min	DTG (T <sub>max</sub> ) °C	dW/dt μg/min	dx/dt 1/min	Goethite Weight loss (μg)	X <sub>max</sub>	(dx/dt) <sub>max</sub> / (1-x) <sub>max</sub>	B/T <sub>max</sub> <sup>2</sup> 10 <sup>5</sup>
10	314.6	31.13	.3505631	88.8	.4211712	.605642	2.896253
15	321.8	46.51	.4870157	95.5	.4712042	.9209901	4.239839
20	327.5	63.2	.6232742	101.4	.4802761	1.199241	5.546308
25	328.2	75.3	.7959831	94.6	.4693446	1.499999	6.916749
30	330.4	91.3	.9661376	94.5	.4486772	1.752399	8.239686

Calculation of slope by Least Square Method.

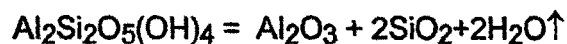
S.N	X	Y X 10 <sup>-5</sup>	XY
1	0.605642	2.896253	1.754092459
2	.9209901	4.239839	3.904849745
3	1.199241	5.546308	6.651359952
4	1.499999	6.916749	10.37511658
5	1.752399	8.239686	14.43921751
$\Sigma$	5.9782711	27.838835	37.12463625

$$\text{Slope} = \frac{\sum XY - (\sum X \sum Y)/n}{\sum X^2 - (\sum X)^2/n} = \frac{37.12463625 - 33.28562055}{7.974103228 - 7.147945069} = 4.647 \times 10^{-5}$$

$$\text{Value of 'n'} = 4.647 \times 10^{-5} \times 175000 = 0.98$$

that for all the cases of heating rates, the samples gain weight. This gain in weight was not observed when the experiment were conducted in nitrogen atmosphere <sup>20</sup> (figure 4.15), which indicates that the weight gain is caused by the oxidation of some of the elements present in the decomposition products.

As reported in chapter 2, the decomposition of kaolinite occurs as:<sup>20</sup>



This reaction yields 13.95% of stoichiometric weight loss due to loss of water molecule and yields terminal oxides of aluminium and silica, probably as silicate, with no further oxidation possible. The other gangue, 'Eudialyte' containing elements as  $\text{Fe}^{+2}$  and zirconium may yield products of decomposition liable to oxidise.

Figure 4.15.depicts that the fourth stage of weight loss is better resolved in nitrogen atmosphere by a sharper weight loss with prominent DTG peak (figure 4.16).This also indicates that the oxidation of the decomposed product of eudialyte and the decomposition of the other gangue, kaolinite are overlapping processes. Any attempts to decrease the oxidation rate or its elimination resolve the decomposition of kaolinite better. This adds to the proof that one of the gangue yields decomposition product which are liable to oxidies.

To analyse the process better x-ray analysis of the ore after heating it to  $900^{\circ}\text{C}$  in air, nitrogen, argon and in oxygen atmosphere were carried out. The results

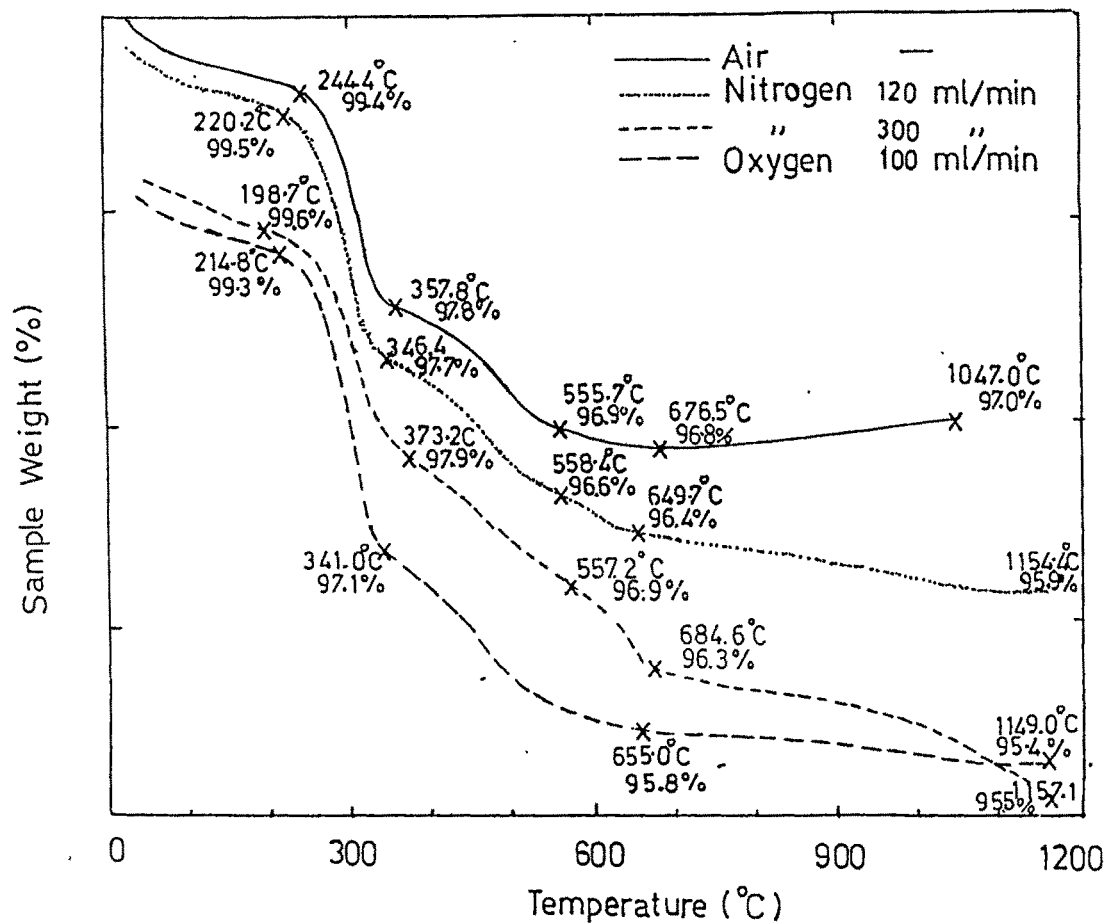


Fig. 4.15 Thermogravimetry (TG) of iron ore in different media

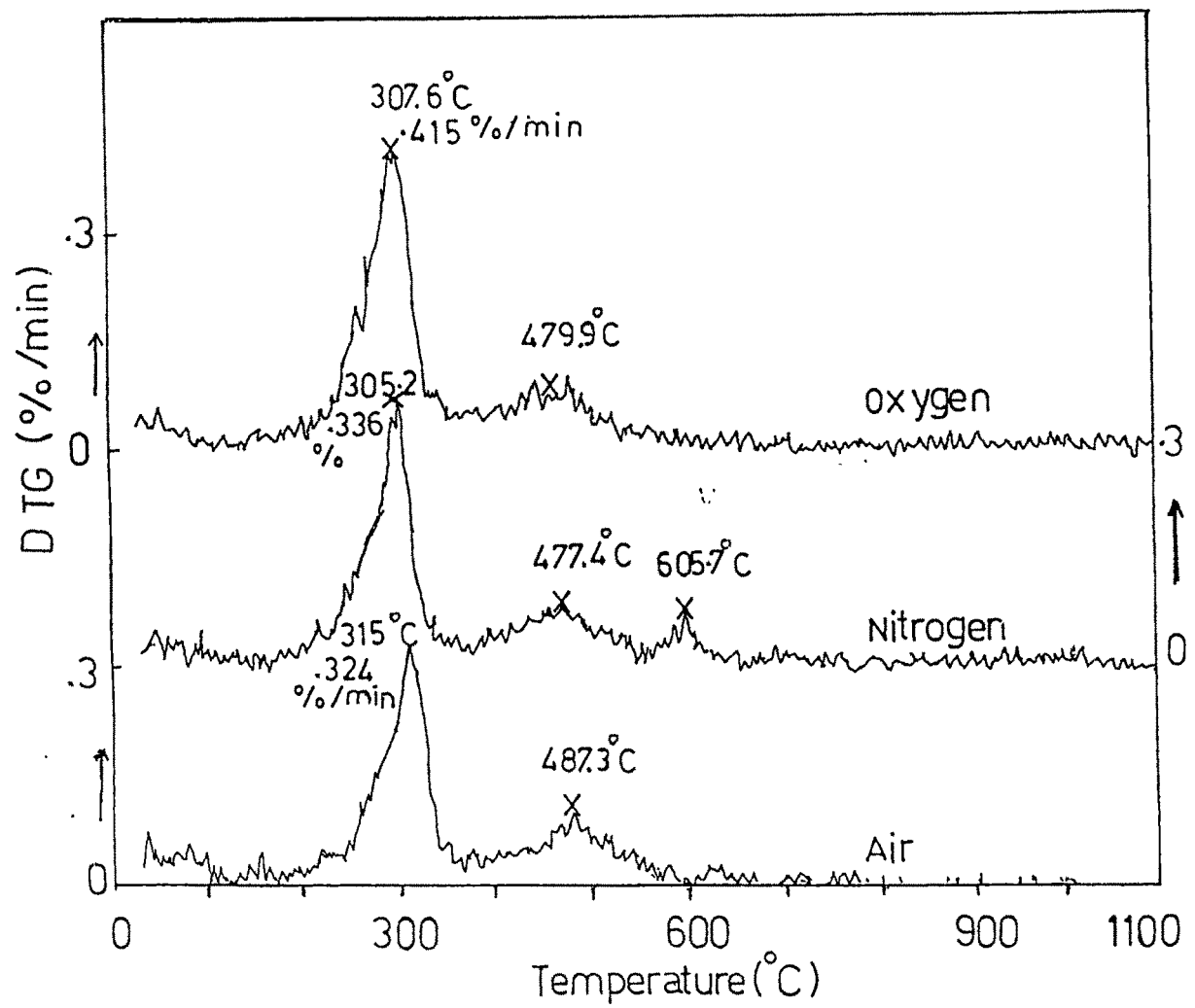


Fig. 4.16 Differential thermogravimetry (DTG) of iron ore in different media.

for range of  $20^\circ$  to  $40^\circ$  and  $40^\circ$  to  $70^\circ$  are indicated separately in figures 4.17 and 4.18 for better presentation. The analysis indicates that  $\beta\text{CaO} \cdot \text{SiO}_2$  (triclinic) and quartz along with hematite are the main phases present. A few peaks of calcium ferrite are seen in case of air. On the other hand, the sample fired in inert atmosphere indicates more probability of presence of phases as  $\text{Ca}_2\text{SiO}_4$ ,  $\text{Fe}_2\text{SiO}_4$  etc than  $\beta\text{CaO} \cdot \text{SiO}_2$ . The peaks at  $2.499\text{\AA}^0$ ,  $2.822\text{\AA}^0$  indicate fayalite and those at  $2.714\text{\AA}^0$ ,  $2.82\text{\AA}^0$ ,  $2.74\text{\AA}^0$  are of  $\text{Ca}_2\text{SiO}_4$ . The split peak at  $2.532\text{\AA}^0$  with other peaks  $2.969\text{\AA}^0$ ,  $2.099\text{\AA}^0$  and  $1.616\text{\AA}^0$  indicate magnetite formed due to incomplete oxidation of  $\text{FeO}$  formed as intermediate phase of goethite and oxalate decomposition. The x-ray diffraction pattern of sample fired in oxygen indicates primarily hematite peaks. The intensity of all other peaks decreases substantially, however, the phases  $\beta\text{CaO} \cdot \text{SiO}_2$ ,  $\text{SiO}_2$  and  $\text{CaO} \cdot \text{Fe}_2\text{O}_3$  could be seen.

Thermodynamically <sup>58</sup> zirconium chloride and oxide are more stable than other possible chlorides of this system as  $\text{SiCl}_4$  or  $\text{FeCl}_3$ . The reaction is dependent on oxygen potential of atmosphere as indicated in figure 4.15 where weight loss in case of oxygen is much higher. The oxidation of zirconium chlorides to its oxide and chlorine gas is also a known reaction in zirconium extraction process. <sup>59</sup>

To check the evolution of any chloride fumes in the reaction, the evolved gas was tested for its chloride content by passing it through a distilled water bubbler. Oxygen, argon nitrogen and air were used as carrying gas. The silver nitrate test indicated a distinct milky colour in case of oxygen but very little change in colour of

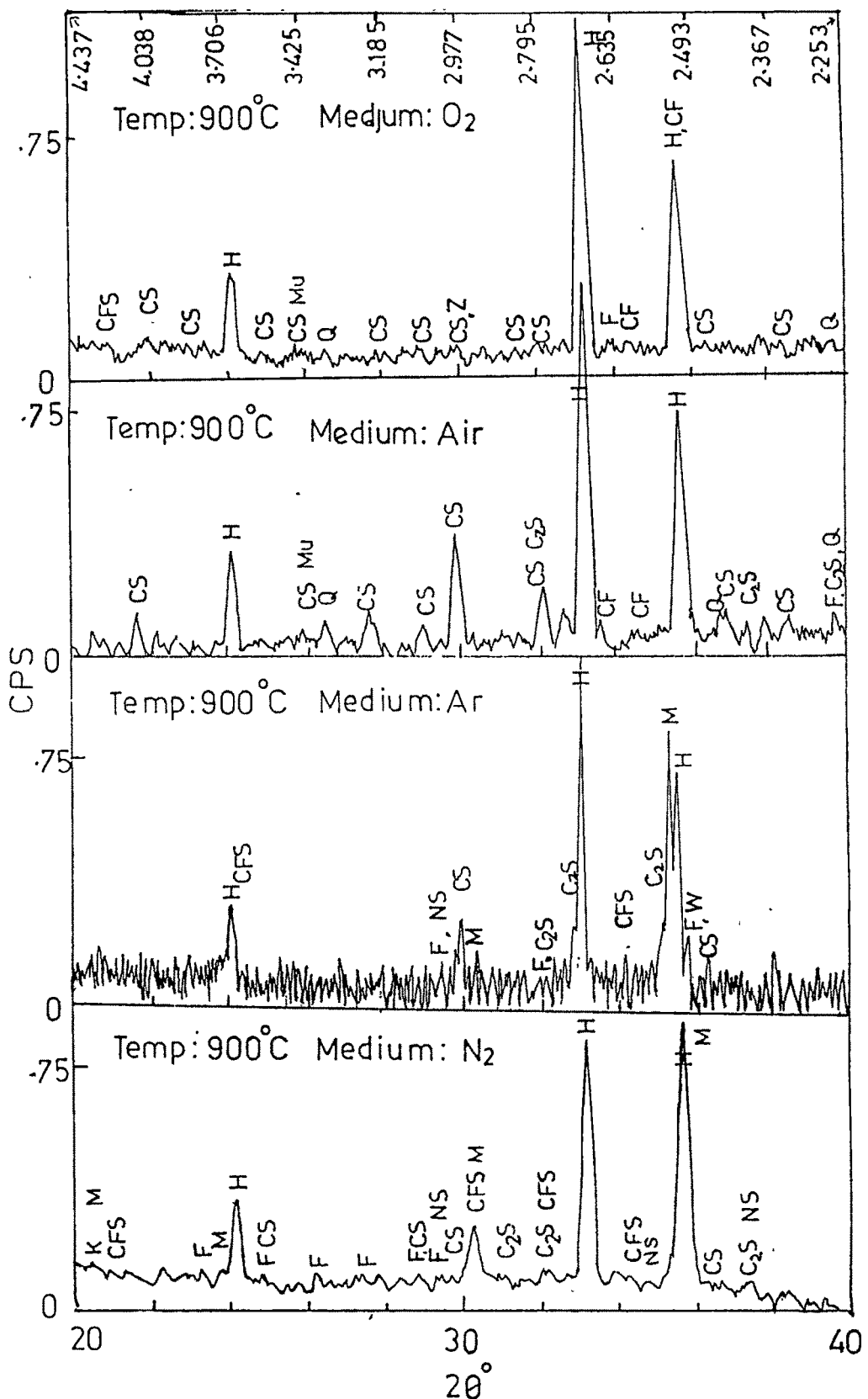


Fig. 4.17 X-ray analysis of iron ore decomposed in different media.

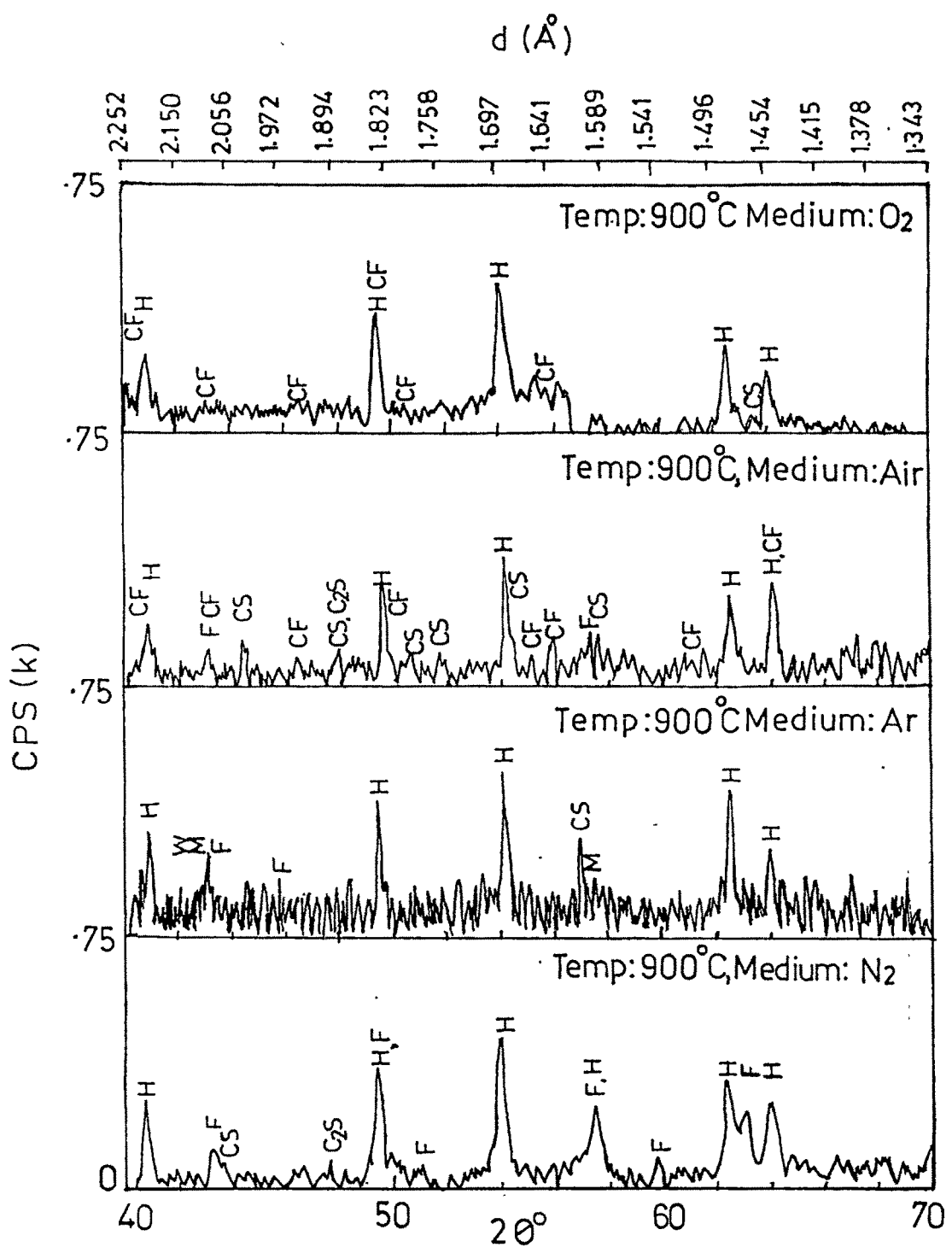


Fig. 4.18 X-ray analysis of iron ore decomposed in different media.

F-Fayalite, M - Magnetite, W-Wustite, M-Mullite, Q-Quartz, Z-Zirconia  
 CF-Calcium ferrite, CS-Calcium silicate, NS-Sodium silicate  
 C<sub>2</sub>S-Di-calcium silicate, N<sub>2</sub>S-Di-sodium silicate, CFS-Calcium iron silicate

water in case of argon, nitrogen and air. This indicates the presence of chlorine fumes in exit gases specifically in oxygen.

Many investigations are reported on mineral formation on heating iron ores containing  $\text{CaO}$ ,  $\text{SiO}_2$ ,  $\text{Al}_2\text{O}_3$ . As discussed in chapter 2 minerals reported<sup>30</sup> are fayalite, calcium silicate, calcium olivine, mono-calcium ferrite and di-calcium ferrite. Matsuno<sup>29</sup> reported that when the mixture of  $\text{Fe}_2\text{O}_3$  -  $\text{CaO}$  -  $\text{SiO}_2$  is heated, melts are formed locally which was indicated by two endothermic peak in the temperature range of  $1200^{\circ}\text{C}$  to  $1240^{\circ}\text{C}$ . Kasai<sup>31</sup> also observed the melt formation and their interaction. The shape and intensity of endothermic peaks depends on composition of ore mixture. In some cases peak broadening was observed due to prolonged melting. Wynnyckyj<sup>4</sup> reports that trivalent iron oxide does not form silicate and the melt formed depends on the oxygen potential of system. In case of higher oxygen potential, calcium ferrite melt is formed but at lower oxygen potential and in the presence of  $\text{Fe}^{+2}$  ion, it forms silicate melt. These observations discussed in chapter 2 are consistent with present observations.

Figure 4.19 indicate the results of DTA of ore sample in air, conducted with slow heating rate, in the range of  $1100^{\circ}\text{C}$ - $1260^{\circ}\text{C}$ . The endothermic peak at  $1209^{\circ}\text{C}$  and a prolonged melting in temperature range  $1213.8^{\circ}\text{C}$  to  $1259.9^{\circ}\text{C}$  indicate the presence of fayalite, calcium-ferrite respectively<sup>60</sup>. The x-ray pattern of ore powder heated to  $1250^{\circ}\text{C}$  is indicated in table 4.7. The results indicate the presence of phases discussed above. The prolonged melting of calcium ferrite is expected as per  $\text{CaO}-\text{Fe}_2\text{O}_3$  equilibrium diagram<sup>60</sup> reproduced in figure 4.20.

Table : 4.7 X-ray data of iron ore heated to 1523K(1250°C) and cooled. ( Target : Cu Filter : Ni )

Observed Peaks.		Standard values JCPDS											
Sr. no	d(A°)	II <sub>o</sub>	Hematite	Fayalite	B <sub>2</sub> CaO <sub>5</sub> SiO <sub>4</sub>	Quartz	Na <sub>2</sub> SiO <sub>3</sub>	Zr <sub>2</sub> Cl <sub>10</sub>	Ca <sub>2</sub> SiO <sub>5</sub>	Mullite			
		II <sub>o</sub>	d(A°)	II <sub>o</sub>	d(A°)	II <sub>o</sub>	d(A°)	II <sub>o</sub>	d(A°)	II <sub>o</sub>	d(A°)	II <sub>o</sub>	d(A°)
1.	3.770	18		3.780	20	3.760	30					3.777	12
2.	3.666	42	3.660	25		*			3.560	40	3.690	40	
3.	3.431	17			3.410	20							3.428
4.	3.326	17			3.310	80	3.340	100					95
5.	3.256	21			3.228	40							
6.	3.089	21			3.080	70			3.160	100			
7.	3.038	20		3.050	40			3.040	100			3.046	14
8.	2.978	33			2.976	100						2.876	35
9.	2.879	17											
10.	2.824	17		2.828	90	2.843	20		2.840	80	2.795	100	
11.	2.774	29			2.790	40					2.780	90	
12.	2.742	17			2.712	40							
13.	2.688	100	2.690	100									
14.	2.619	20							2.630	60	2.608	65	
15.	2.508	79	2.510	50	2.501	100							
16.	2.431	17			2.470	60	2.458	12	2.410	50		2.451	20
17.	2.199	29	2.201	30	2.190	50	2.170	70			2.210	40	2.428
18.	2.036	19					2.040	30			2.010	40	14
19.	1.869	20							1.890	30	1.860	40	1.868
20.	1.835	35	1.838	40		1.838	60				1.820	40	60
21.	1.689	36	1.690	60									
22.	1.655	21			1.650	60							
23.	1.605	18			1.605	40	1.607	30					
24.	1.481	20	1.484	35									
25.	1.469	16					1.467	30					
26.	1.451	17	1.452	35									

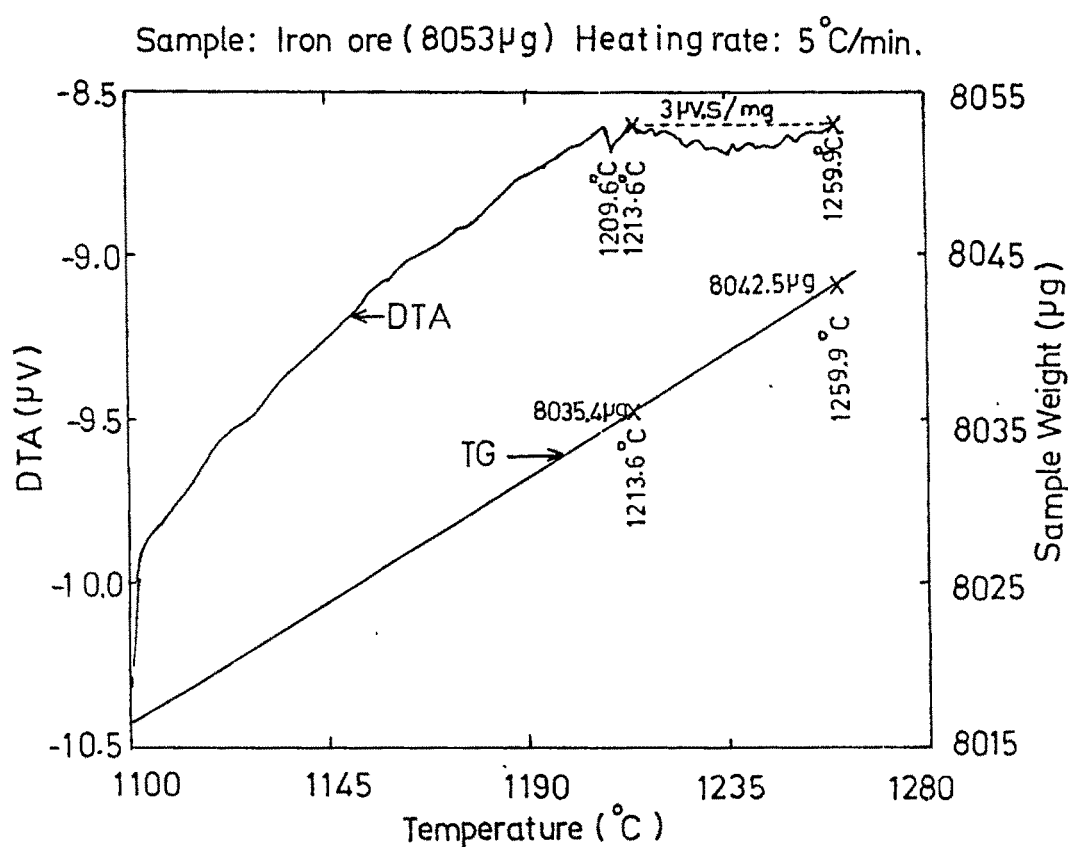


Fig. 4.19 TG, DTA upto 1260 $^{\circ}$ C shows melting of calcium ferrite

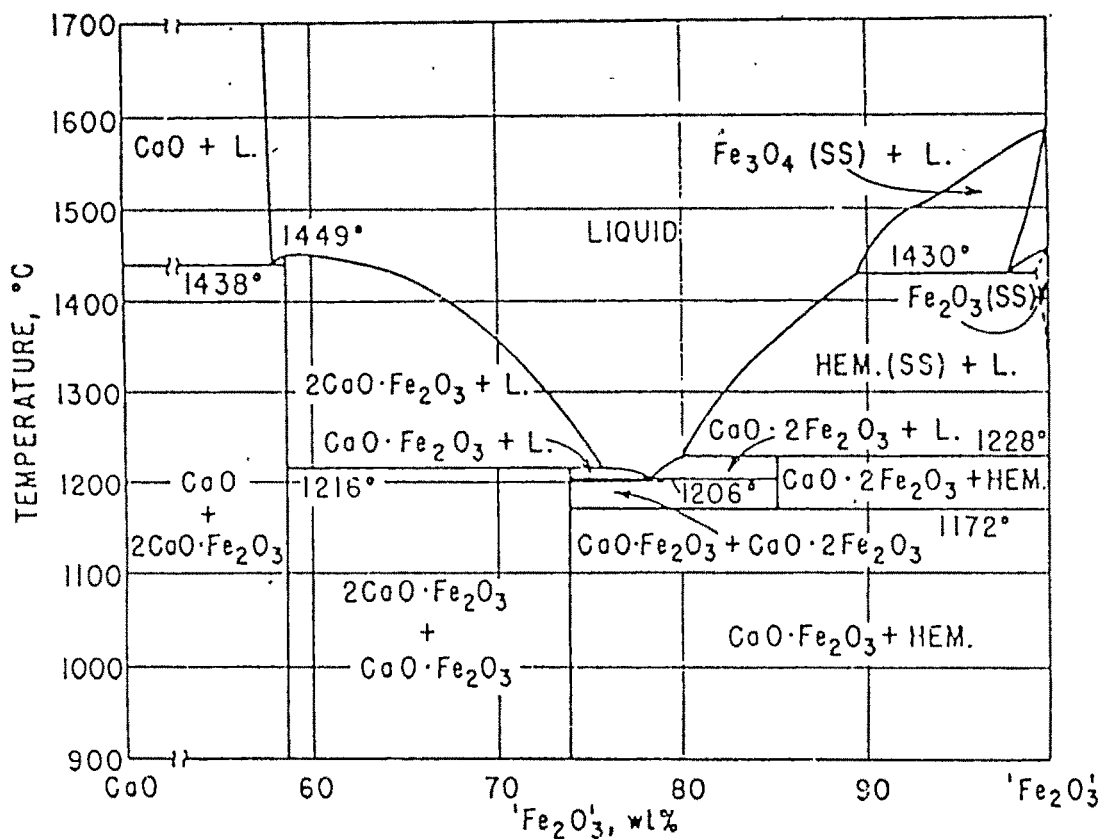
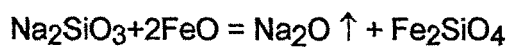


Fig. 4.20 Equilibrium diagram of CaO-Fe<sub>2</sub>O<sub>3</sub> System (Ref No.59)

Figure 4.15 indicates a decrease in sample weight at  $880^{\circ}\text{C}$  to  $1150^{\circ}\text{C}$  in case of nitrogen atmosphere. The decrease was also observed in runs with lower flow rate of nitrogen (150ml/min). This decrease in weight is likely to be due to the localized melting of sodium silicates and its fluxing with 'FeO' available as decomposition product to yield iron silicate and evolve alkali oxides as:



and

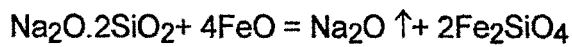
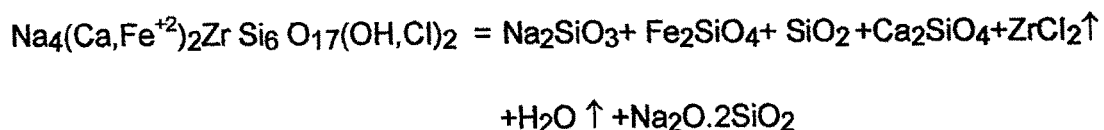


Figure 4.21 and 4.22 indicates this region of TG and DTA peak. The two endothermic peaks in temperature ranges of  $880\text{-}920^{\circ}\text{C}$  and at  $1048\text{-}1087^{\circ}\text{C}$  match with melting region of  $\text{Na}_2\text{O}.2\text{SiO}_2$  ( $874^{\circ}\text{C}$ ) and  $\text{Na}_2\text{SiO}_3$  ( $1087^{\circ}\text{C}$ ) as indicated in equilibrium diagram of  $\text{Na}_2\text{O}-\text{SiO}_2$  system <sup>61</sup> in figure 4.23. The two stages of this weight loss is also notable by slope change in TG curve at about  $1087^{\circ}\text{C}$  and more evidently in DTG curve. These observations indicate the presence of alkali silicates in decomposition product.

In view of the above observation, one can make an attempt to write the probable reaction of 'Eudialyte' decomposition in different atmosphere as:

In air:



Sample Weight: 8730 $\mu$ g , Heating Rate: 20°C/min , Nitrogen: 300ml/min

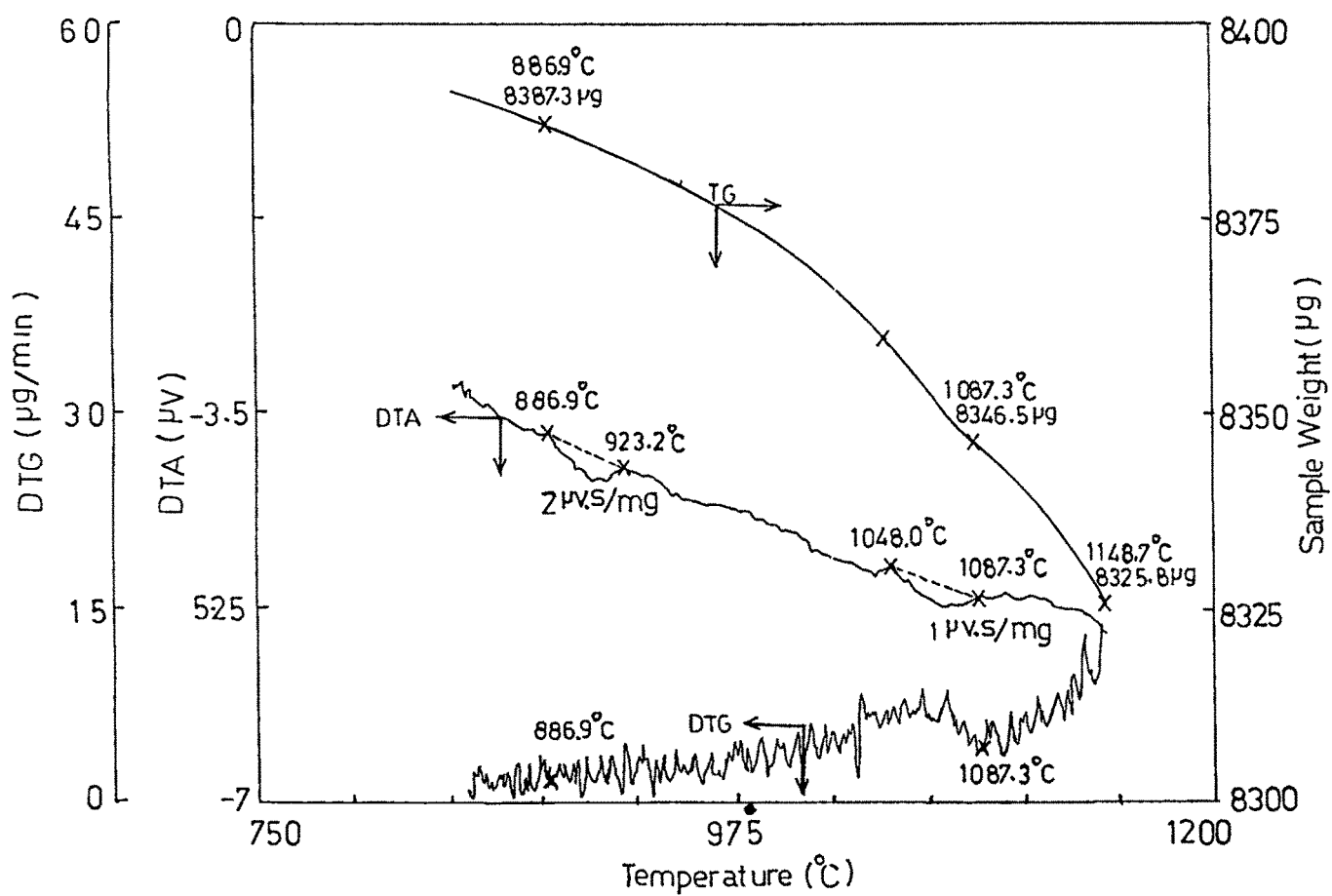


Fig. 4.21 Sodium silicate melting and fluxing  
(Nitrogen flow rate 300 ml / min )

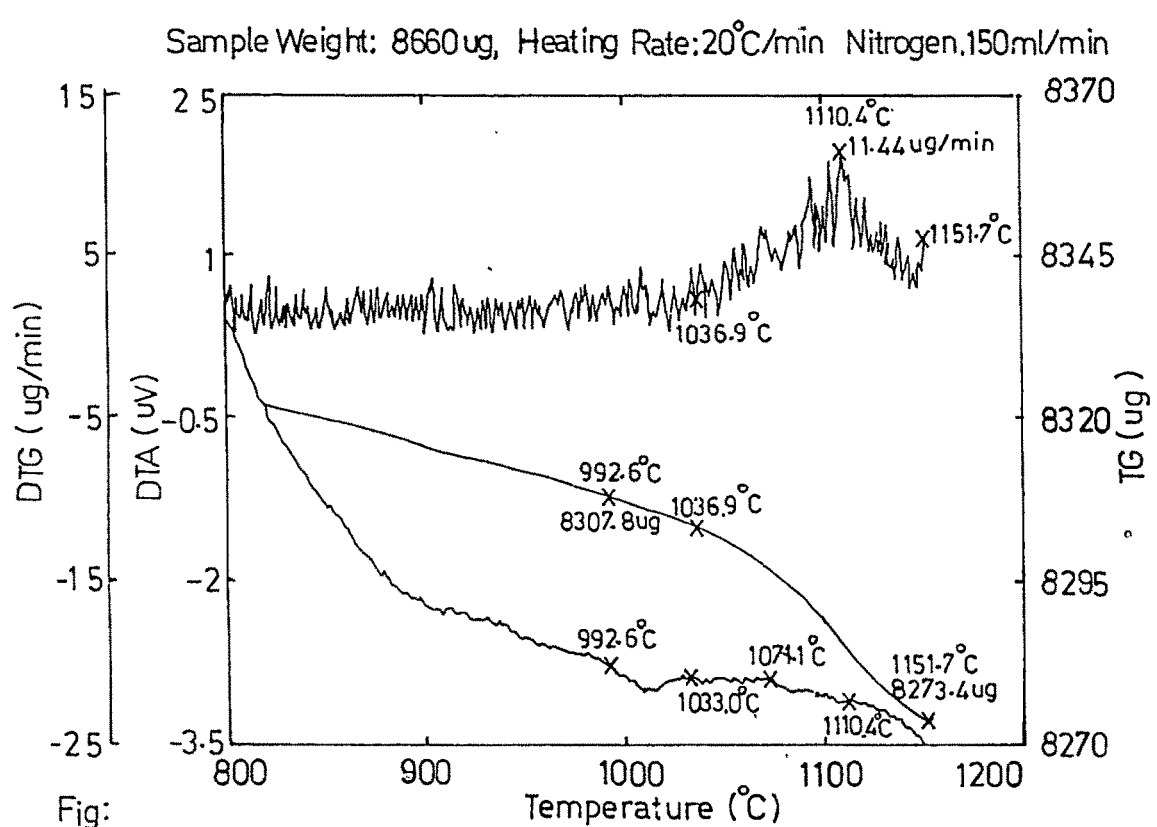


Fig. 4.22 Sodium silicate melting and fluxing  
(Nitrogen flow rate 150 ml / min )

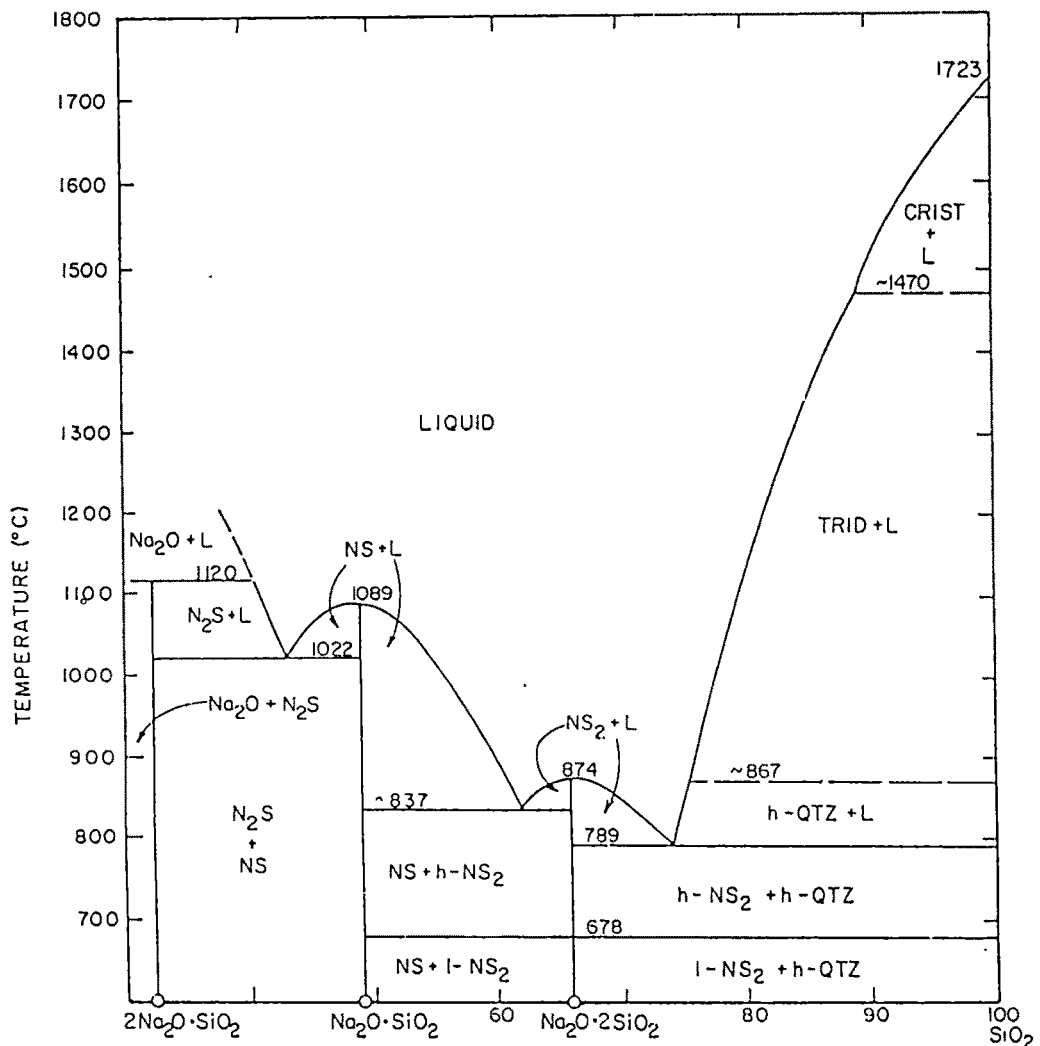


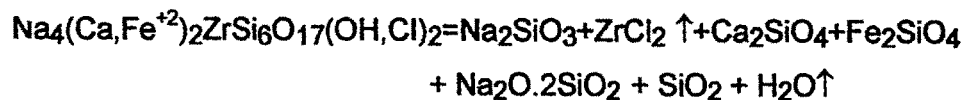
Fig. 4.23 Equilibrium diagram of  $\text{Na}_2\text{O} - \text{SiO}_2$  System (Ref No.59)

Trid=Tridymite, Crist=Cristobalite, Qtz=Quartz, L=liquid  
 $\text{NS} = \text{Na}_2\text{SiO}_3$ ,  $\text{N}_2\text{S} = 2\text{Na}_2\text{SiO}_4$ ,  $\text{NS}_2 = \text{Na}_2\text{SiO}_5$

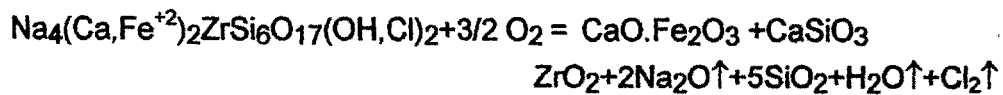
Subsequently:



In nitrogen:



In Oxygen:



In present investigation, the weight losses observed in above reaction are of interest to warrant a quantitative analysis.

The decomposition reaction in nitrogen is selected for quantitative analysis of gangue present. The stoichiometric weight loss in a reaction is 19.67% of eudialyte. Figure 4.24 and Figure 2.25 indicates the thermo-gravimetry curve along with DTG. The onset and completion of a process could be marked on TG curve with the help of DTG peak terminal points. Figure 4.24 indicates that the onset of eudialyte decomposition for this case starts at 359.8 °C and continues to 569.2°C. The weight lost by sample in this region is 95.5 µg. (8483.2 µg - 8390.7 µg) Stoichiometrically this loss corresponds to 470.26 µg of eudialyte phase. This amounts to 5.43% of eudialyte in the ore. Similarly in case of nitrogen flow rate of 300 ml/min, the weight loss in this region (figure 4.25) is 85.7 µg corresponding to

Sample weight : 8660 ug, Heating rate : 20° C/min (150 ml/min)

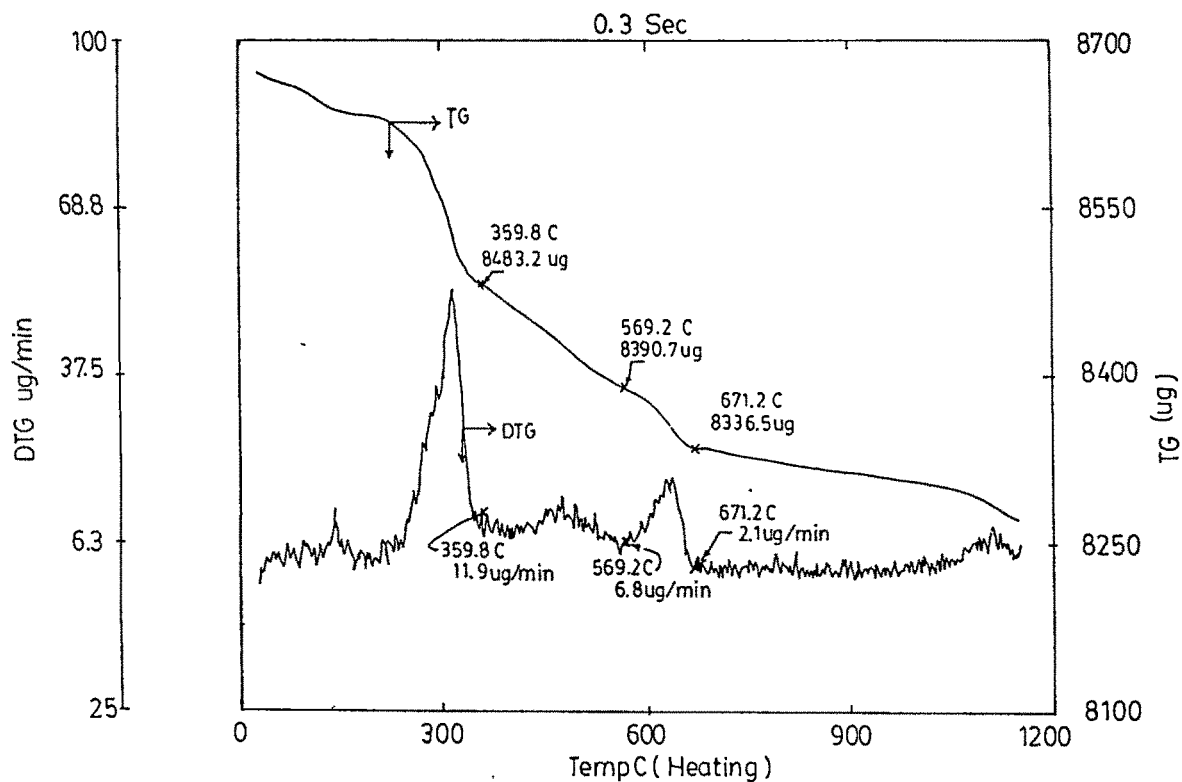


Fig. 4.24 TG/DTG of ore in nitrogen (Flow rate 150ml/min)

Sample weight : 8730 ug , Heating rate : 20° C/min Nitrogen (300 ml/min)

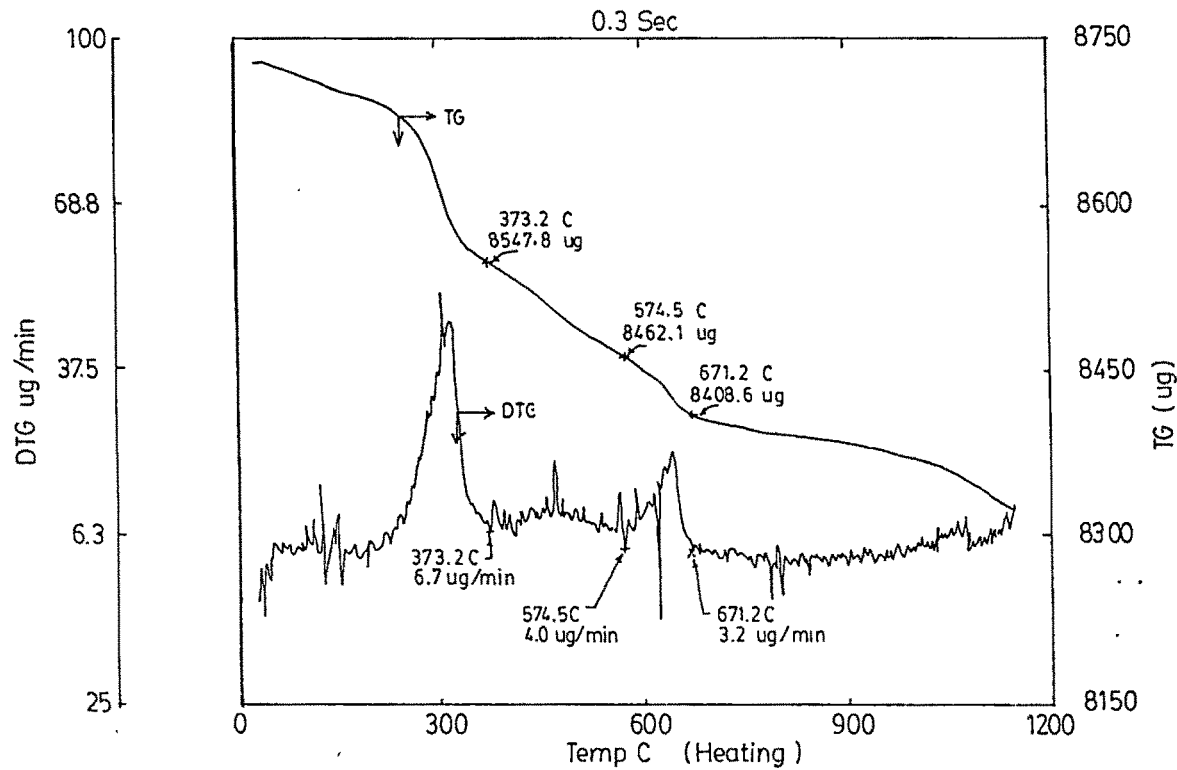


Fig. 4.25 TG/DTG of ore in nitrogen (Flow rate 150ml/min)

$435.69\mu\text{g}$  of eudialyte i.e. 4.995%. Thus the average amount of this clay in ore is 5.21%. The decomposition of kaolinite commences at the  $569.2^{\circ}\text{C}$  and  $574.5^{\circ}\text{C}$  respectively and complete at  $671.2^{\circ}\text{C}$  in both cases. The weight lost is  $54.3\mu\text{g}$  and  $53.5\mu\text{g}$  yielding  $389.25\mu\text{g}$  and  $383.52\mu\text{g}$  of kaolinite. The average percentage of kaolinite is thus 4.44%.

Thus the over all phase analysis of ore is Goethite 9.74% , Iron oxalate hydrate 1.09% Kaolinite 4.44%, Eudialyte 5.21% and rest Hematite 79.52%.

#### 4.1.5 Change in true density of iron ore:

On heating, ore under goes a few physical and chemical changes as discussed in previous section. These transformations change the true density of powder. The following table indicates the value of true density of powder after heating it to given temperature. The trend of change is indicated in figure 4.26.

Temperature( $^{\circ}\text{C}$ )	Density( $\text{Kg/m}^3$ )
950	4350
1030	4370
1050	4380
1100	4420
1120	4450
1200	4600
1215	4650
1250	4750
1275	4820

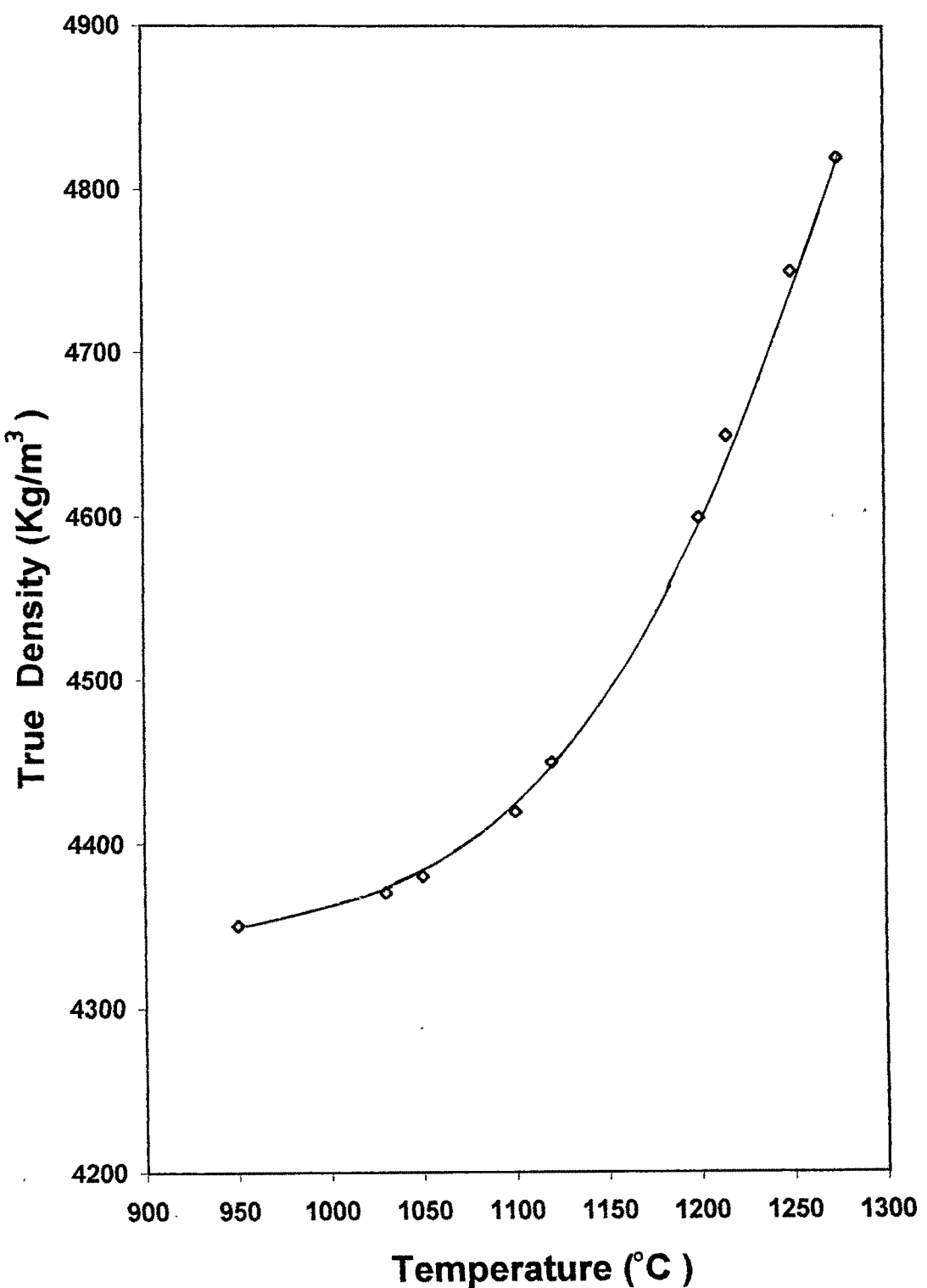


Fig. 4.26 Change in true density of iron ore powder on heating.

## 4.2 Thermal Diffusivity and Conductivity Measurement.

The thermal diffusivity and conductivity studies were made with three types of pellets.

- 1 Pelletized pellets.
- 2 Hand rolled iron oxide pellets.
- 3 Pressed and carved pellets.

The first two categories of pellets are discussed here together and the third at later stage.

Figures 4.27 to 4.38 indicate the rise in surface and centre temperature of a pelletized pellet with time and figures 4.39 to 4.43 for hand rolled iron oxide pellets. The relationship between surface tempearture ( $T_s$ ) and centre tempearture ( $T_c$ ) for one set of reading for pelletized pellet with porosity 32.17% is indicated in figure 4.44. An attempts were made to correlate ' $T_s$ ' and ' $T_c$ ' with time ' $t$ '. Out of the expressions attempted the expression of the type.

$$T_c = T_s (1 - e^{-Kt}) + T_0 e^{-Kt} \quad (4.11)$$

or

$$(T_s - T_c) / (T_s - T_0) = e^{-Kt} \quad (4.12)$$

was found to suit best, ' $T_0$ ' is the initial temperature of pellet and ' $k$ ' is a parameter. Ray<sup>62</sup> et al derived such an equation assuming exponential rate of heating of volume elements of sample. Watts and Wright also used similar equation to correlate the temperatures in their studies.

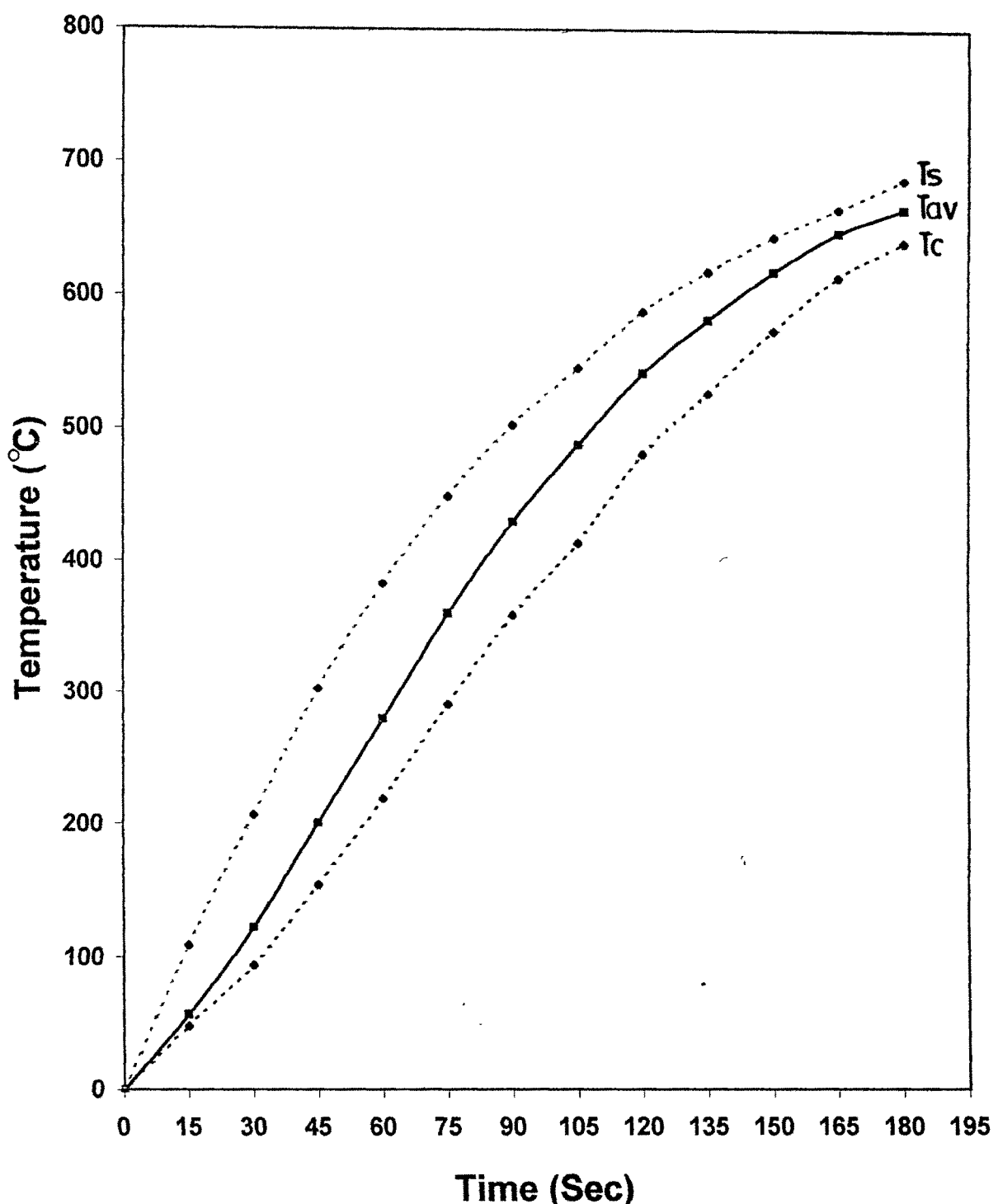


Fig.4.27 Rise in surface, centre and average temperature in pelletized pellet with time.(Size=0.6146cm&Porosity=24.27% )

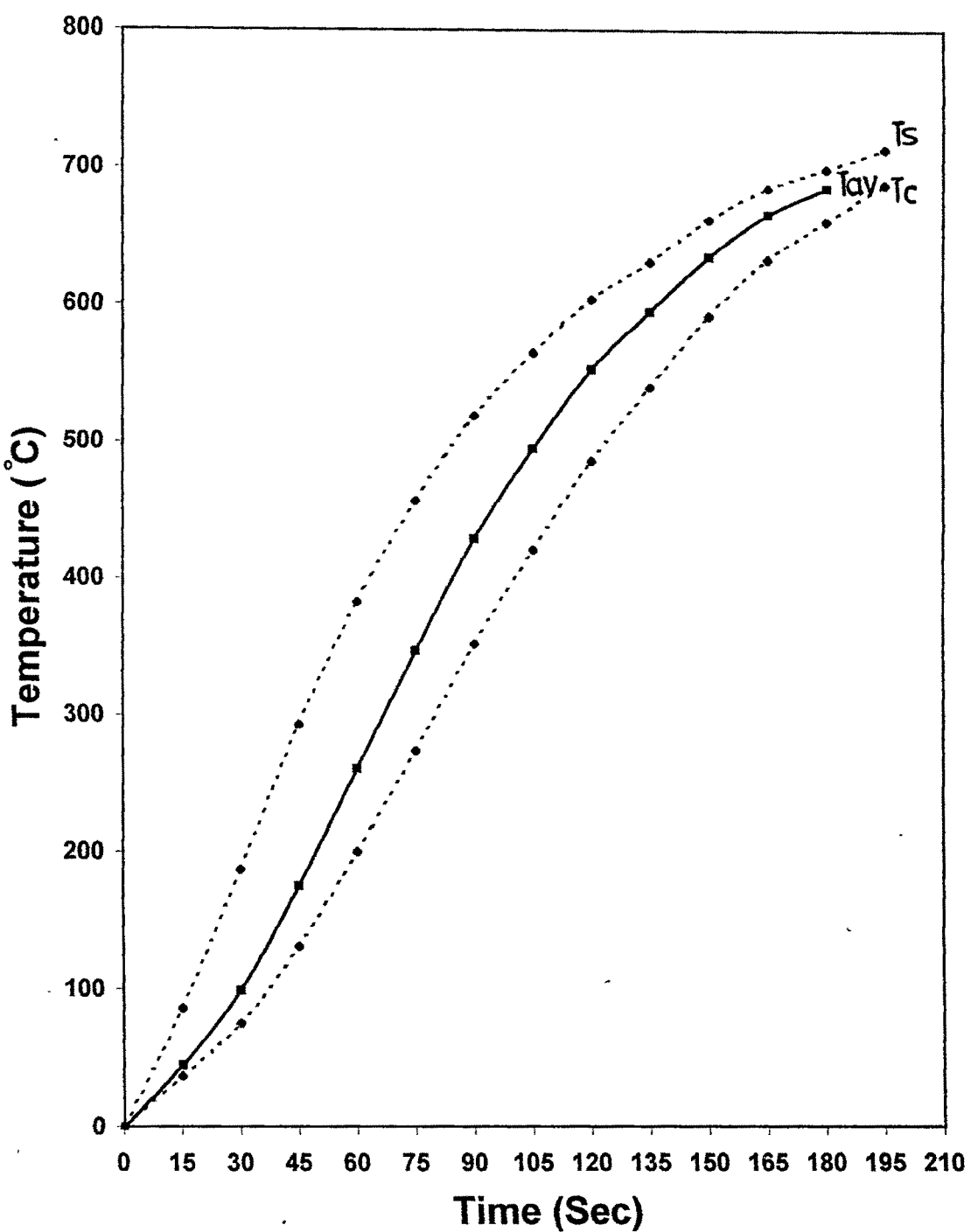


Fig. 4.28 Rise in surface, centre and average temperature in pelletized pellet with time. ( Size=0.5854cm&Porosity=25.87%)

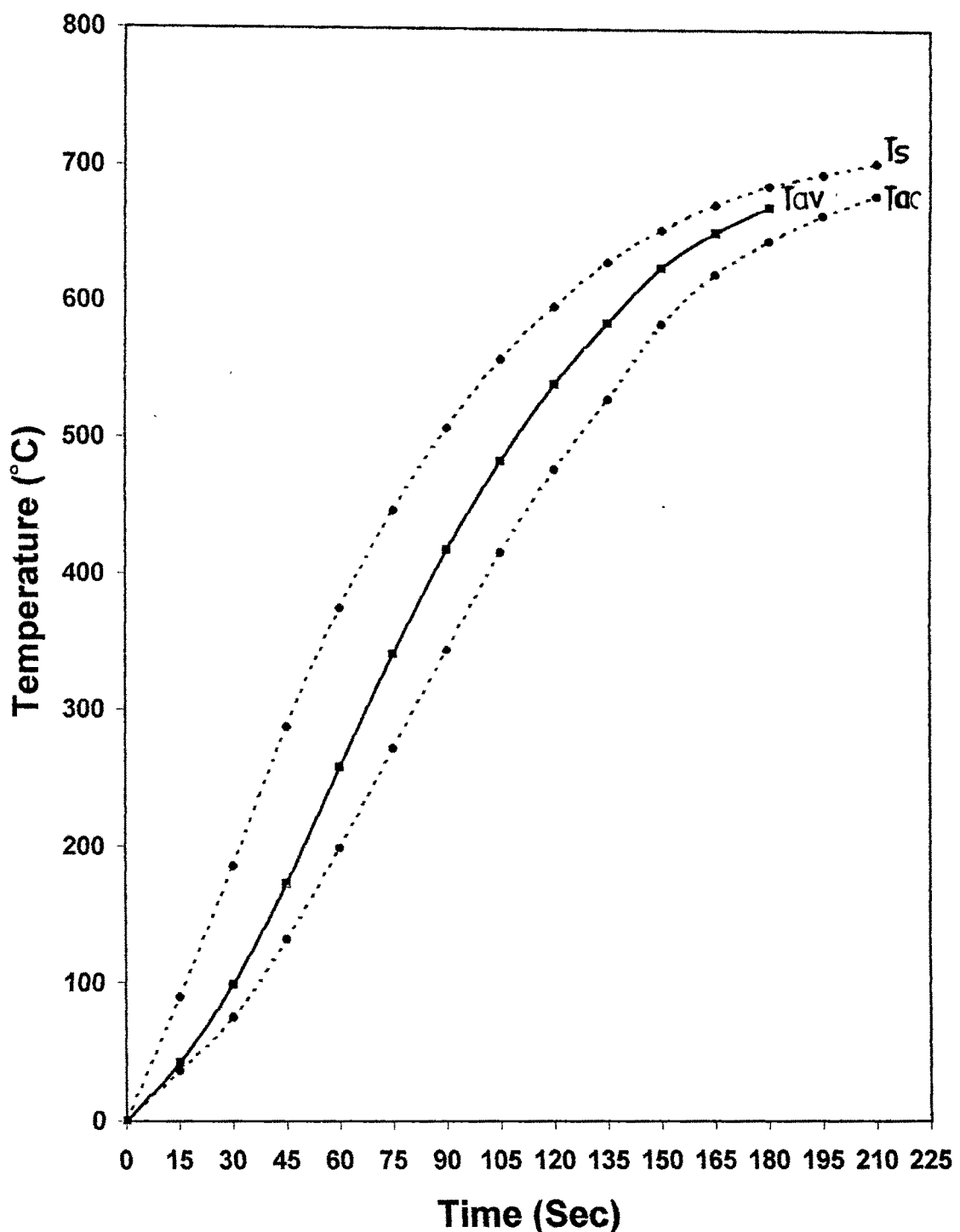


Fig. 4.29 Rise in surface, centre and average temperature in pelletized pellet with time.(Size= 0.6283cm&Porosity=28.08%)

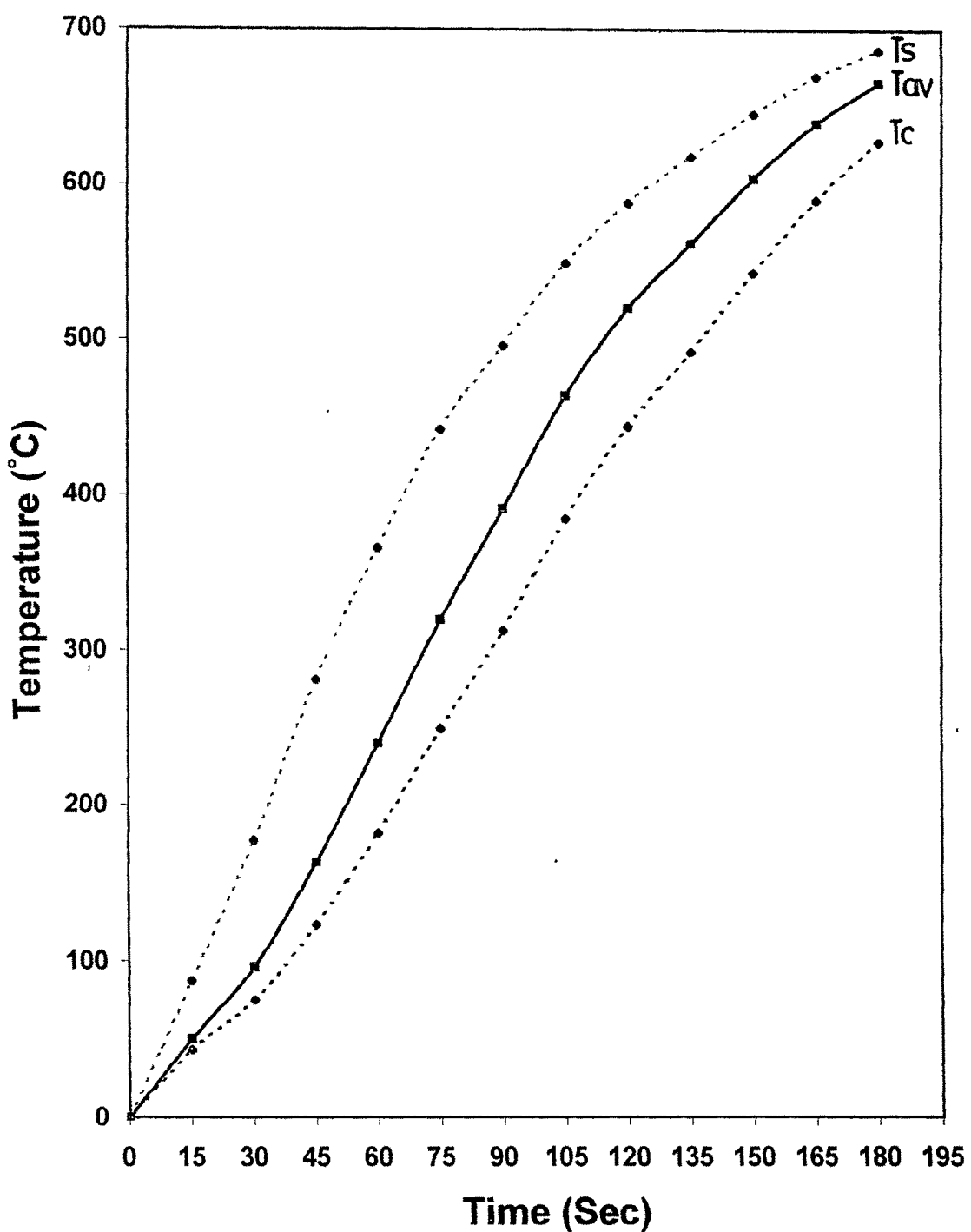


Fig. 4.30 Rise in surface, centre and average temperature in pelletized pellet with time.(Size=0.6294cm&Porosity=32.17%)

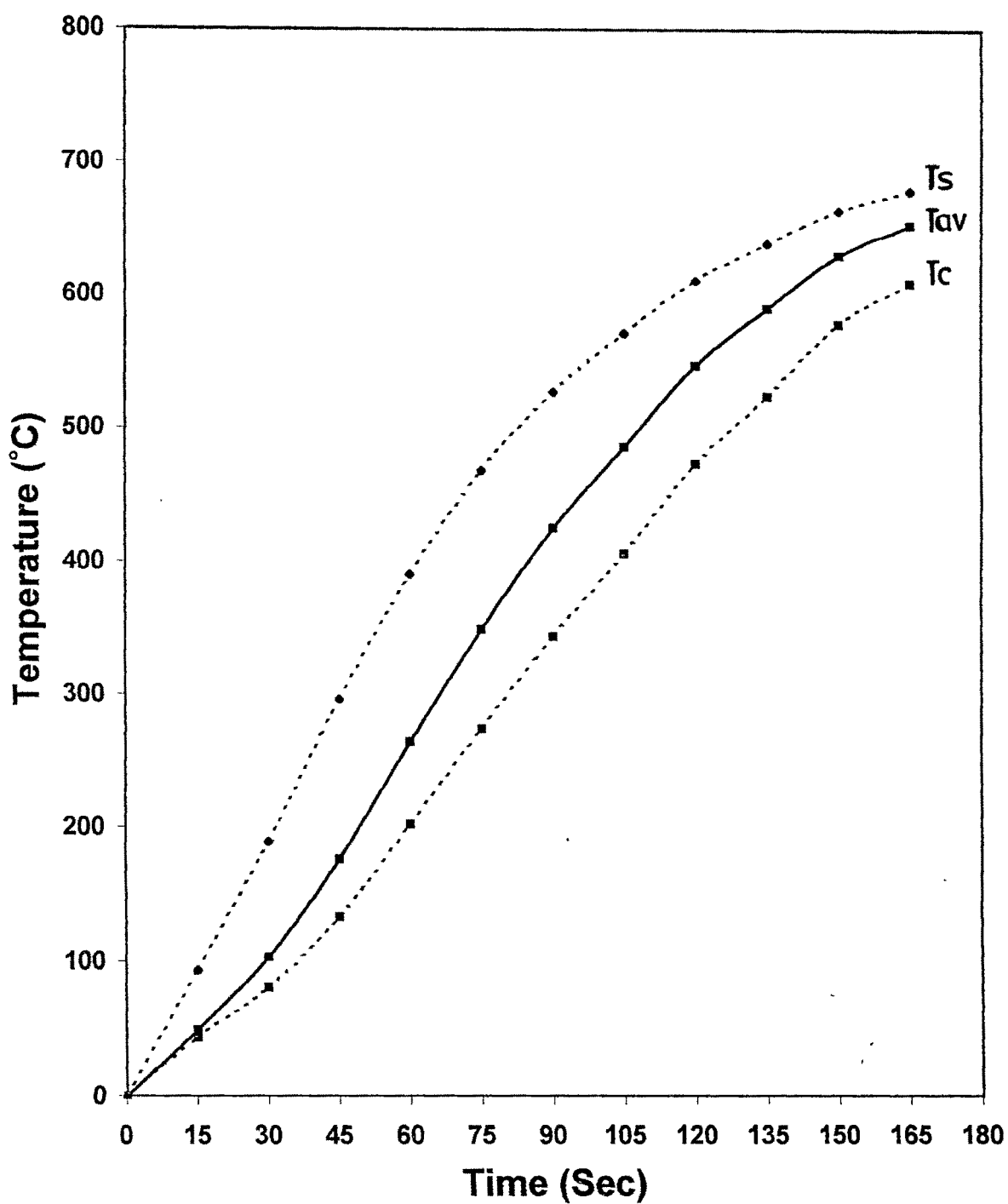


Fig. 4.31 Rise in surface, centre and average temperature in pelletized pellet with time.(Size= 0.6294cm& Porosity=32.17%)

How different from U.S.A?

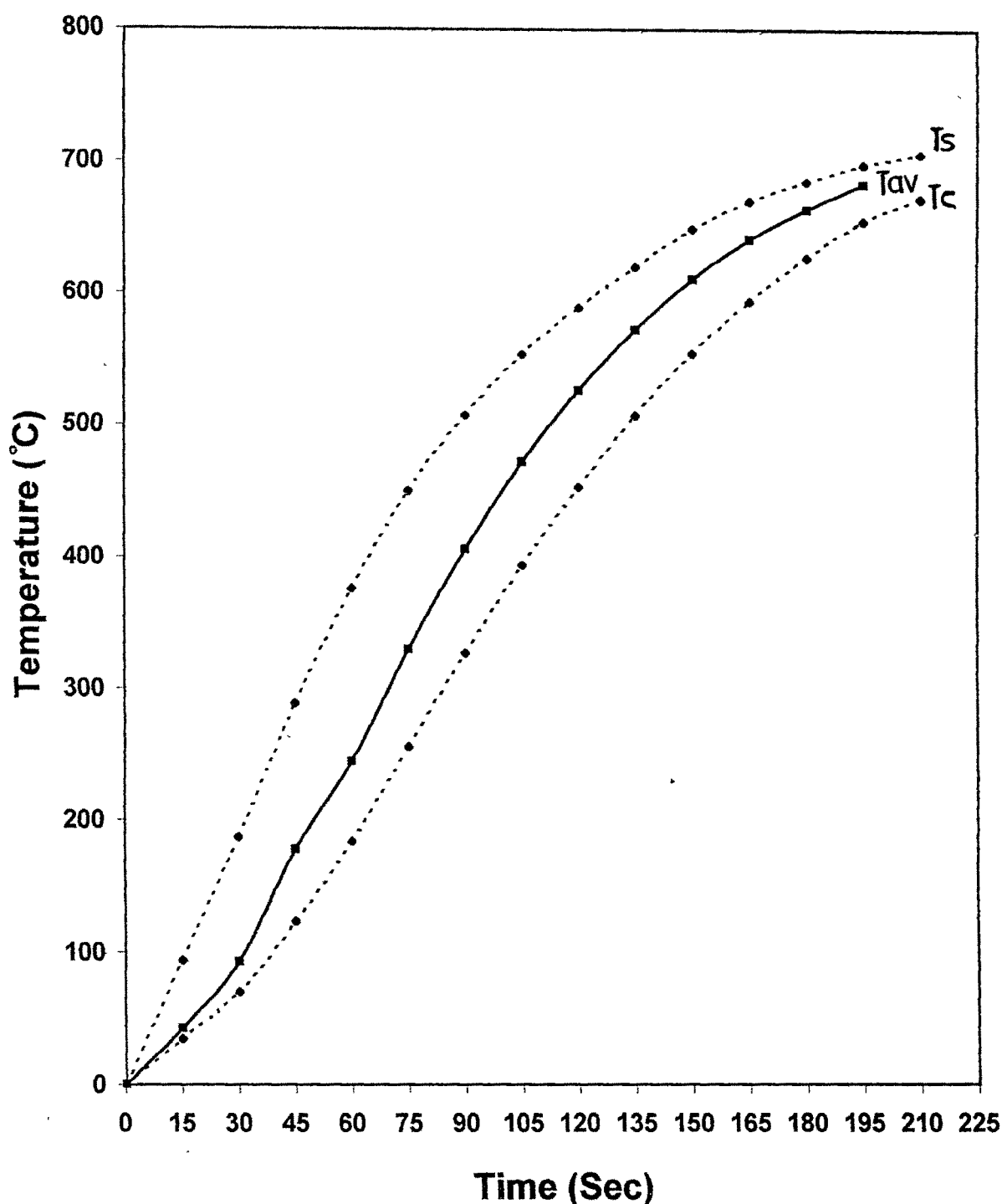


Fig. 4.32 Rise in surface, centre and average temperature in pelletized pellet with time. (Size=0.6360cm&Porosity=33.54%)

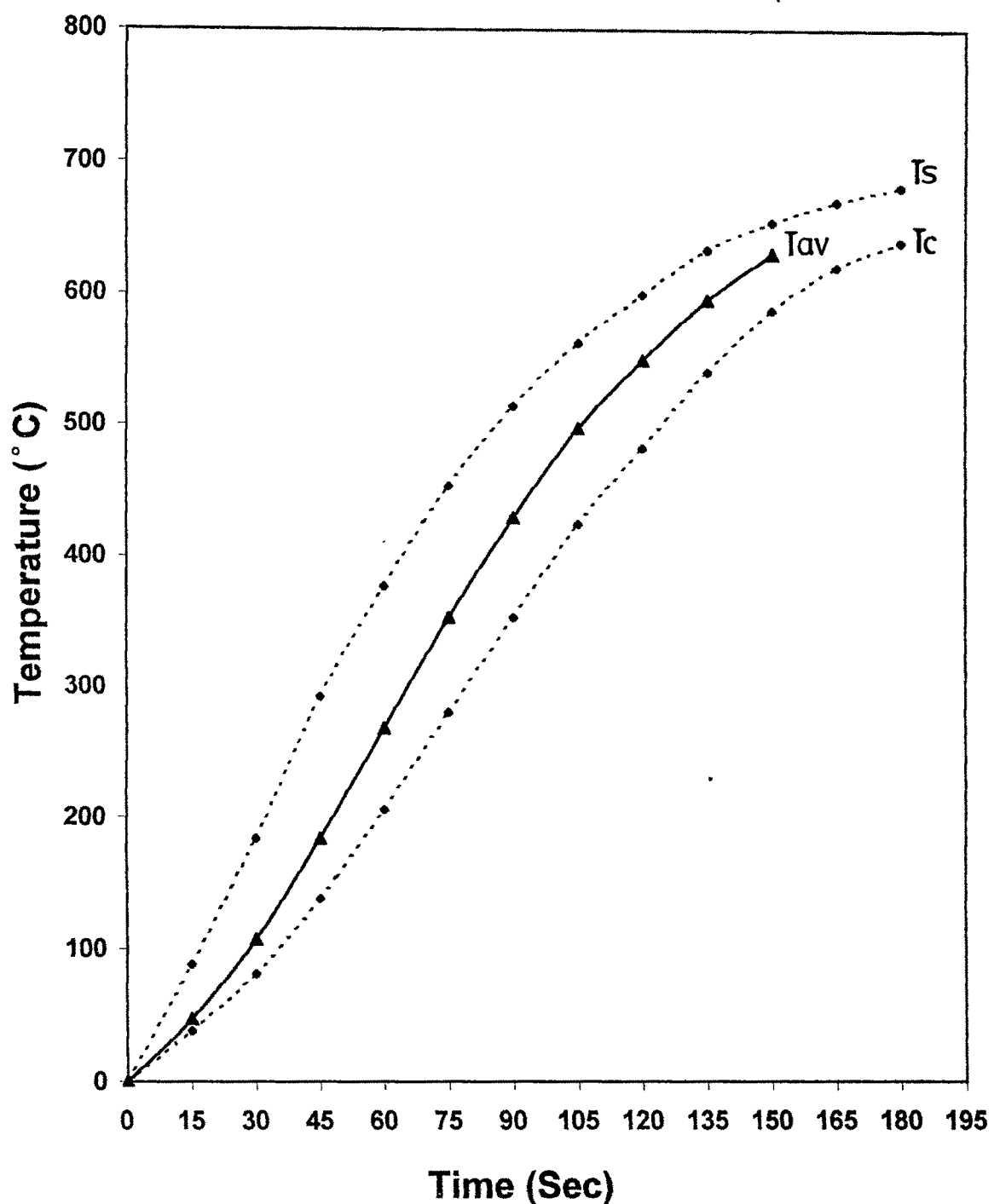


Fig.4.33 Rise in surface, centre and average temperature in pelletized pellet with time.(Size=0.6154&Porosity=34.13%)

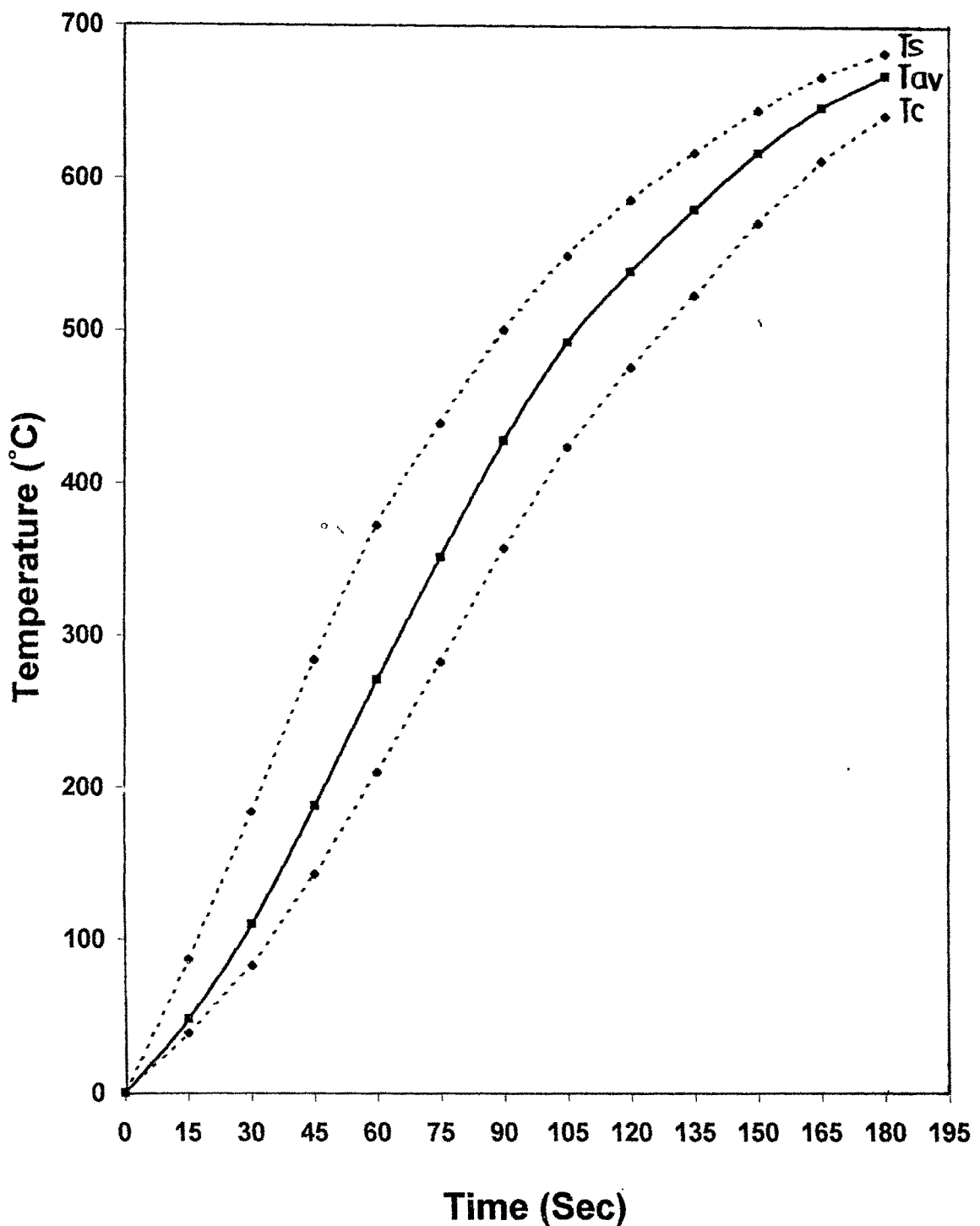


Fig. 4.34 Rise in surface, centre and average temperature in pelletized pelle with time.(Size=0.6154cm&Porosity=34.13%)

See w. (3).

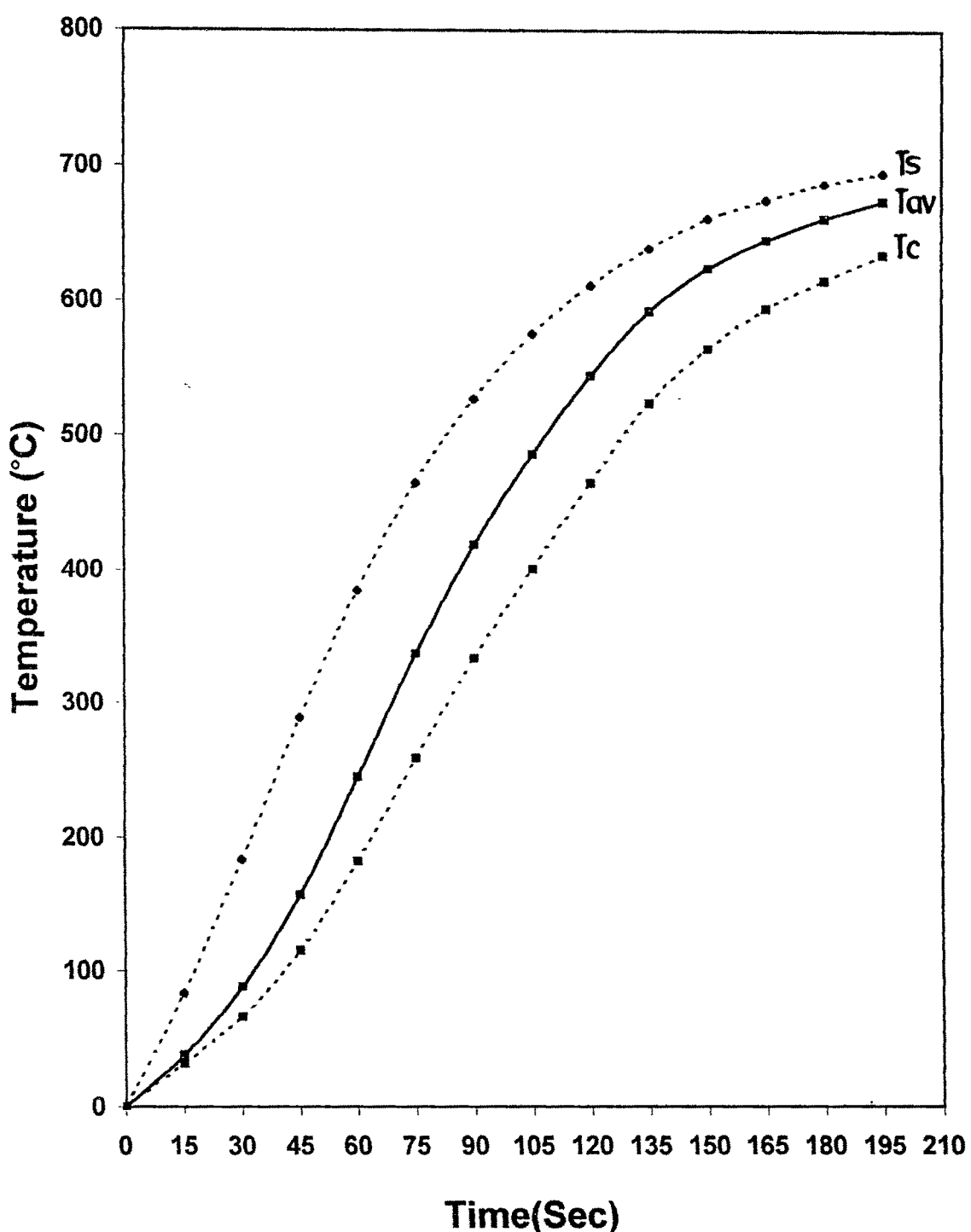


Fig. 4.35 Rise in surface, centre and average temperature in pelletized pellet with time. (Size= 0.6839cm&Porosity=34.51%)

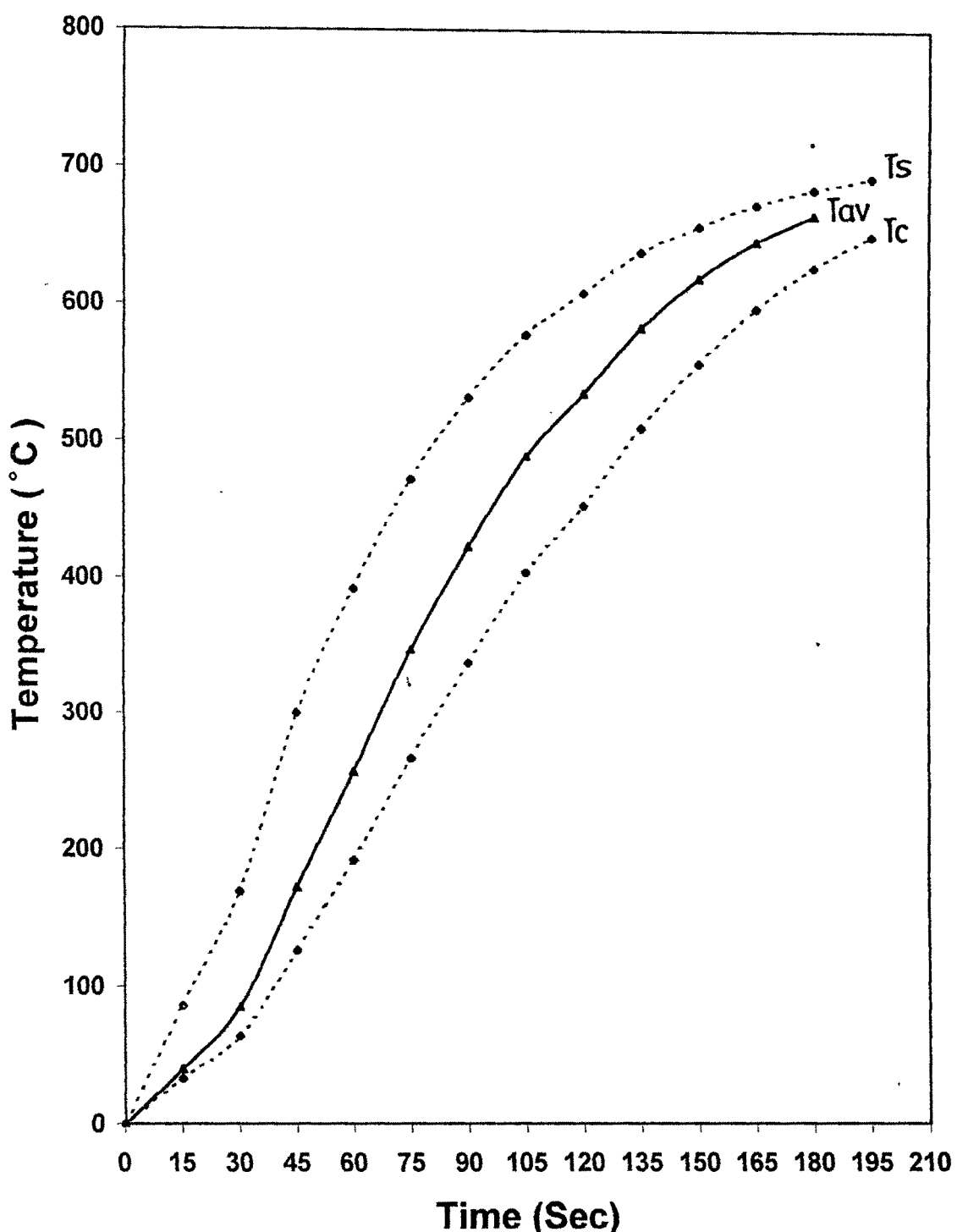


Fig. 4.36 Rise in surface, centre and average temperature in pelletized pellet with time. (Size=0.6921cm&Porosity=35.36%)

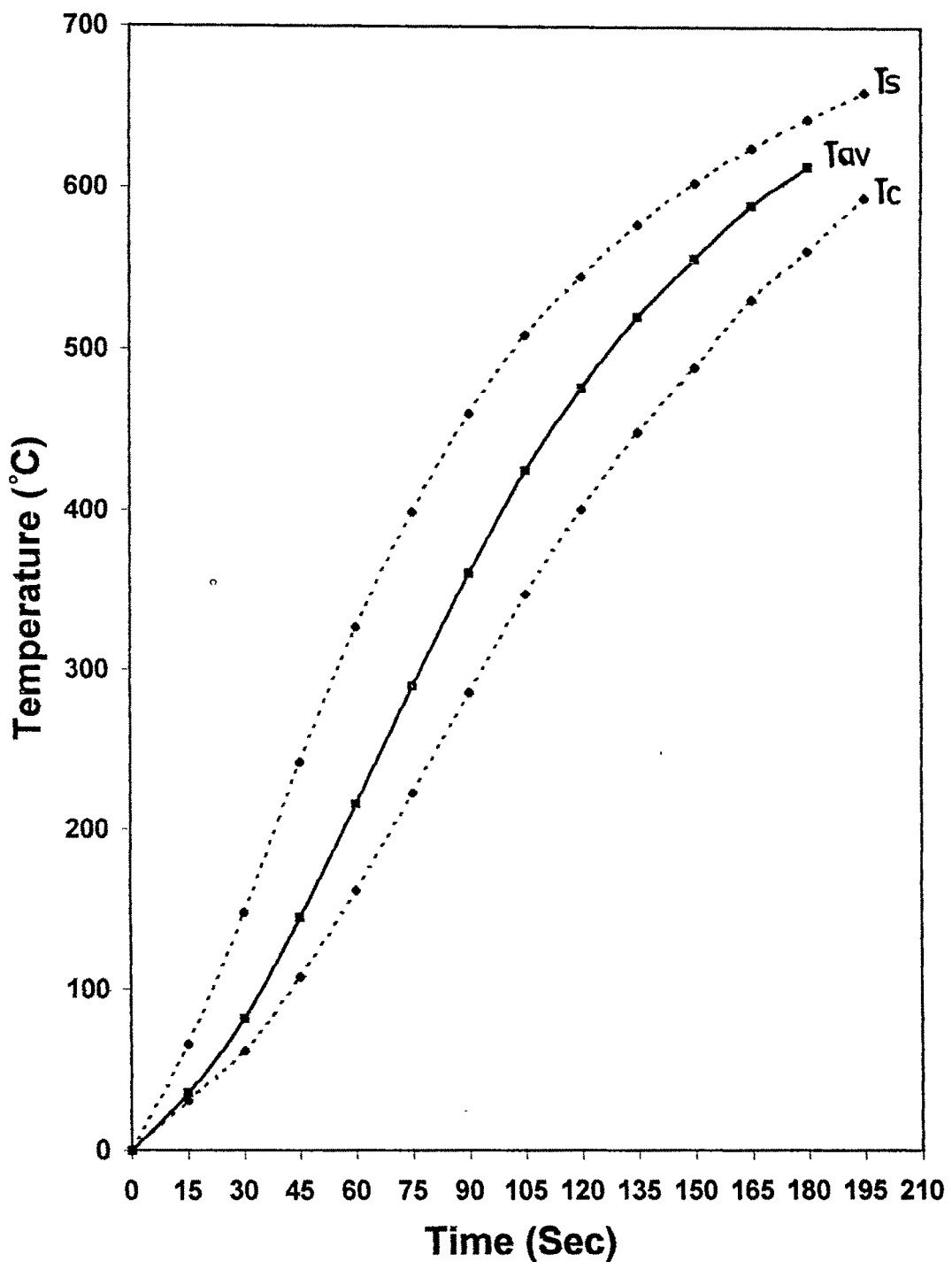


Fig. 4.37 Rise in surface, centre and average temperature in pelletized pellet with time.(Size=0.6921cm&Porosity= 35.65%)

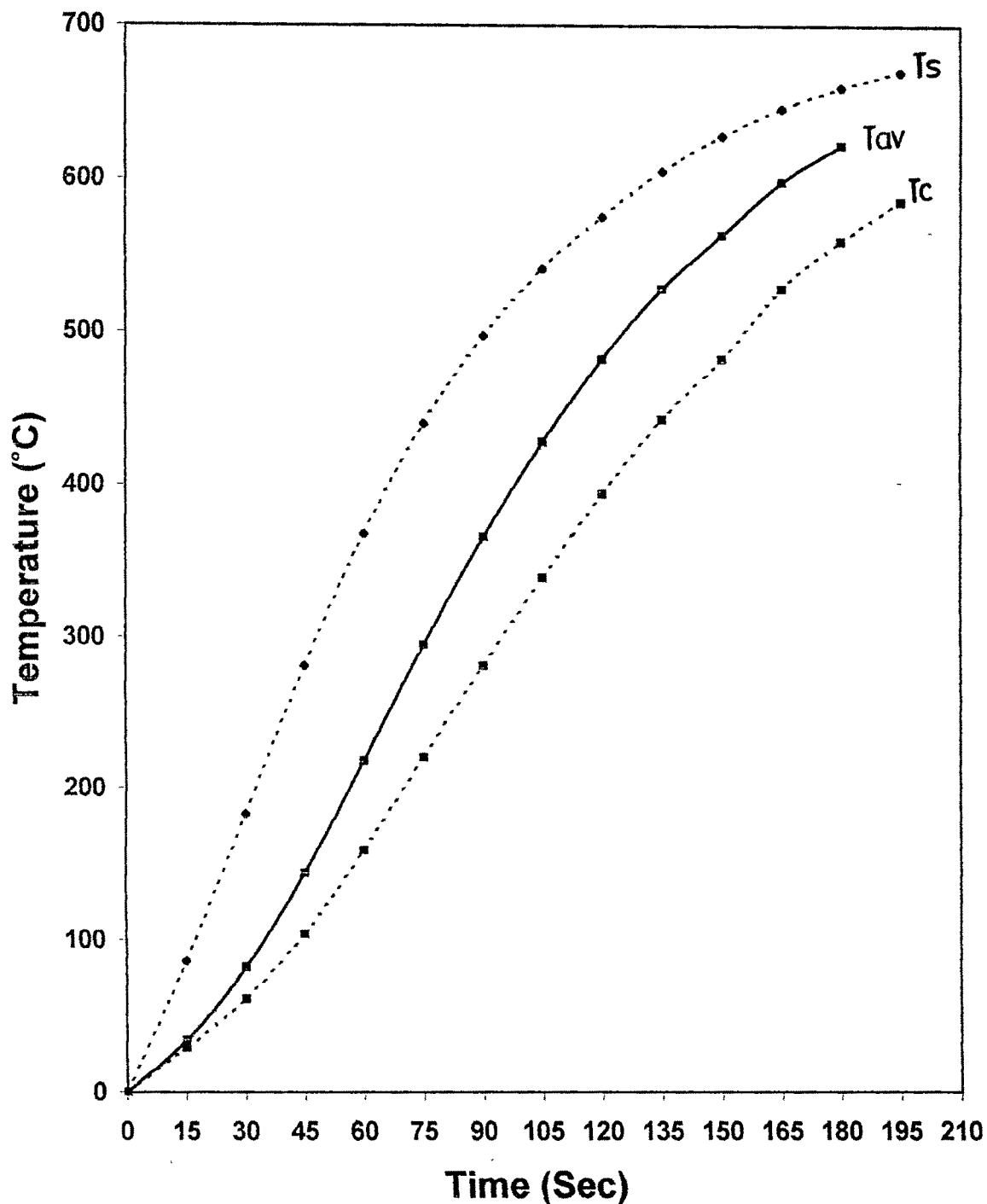


Fig. 4.38 Rise in surface, centre and average temperature in pelletized pellet with time.(Size=0.7863cm&Porosity=38.76%)

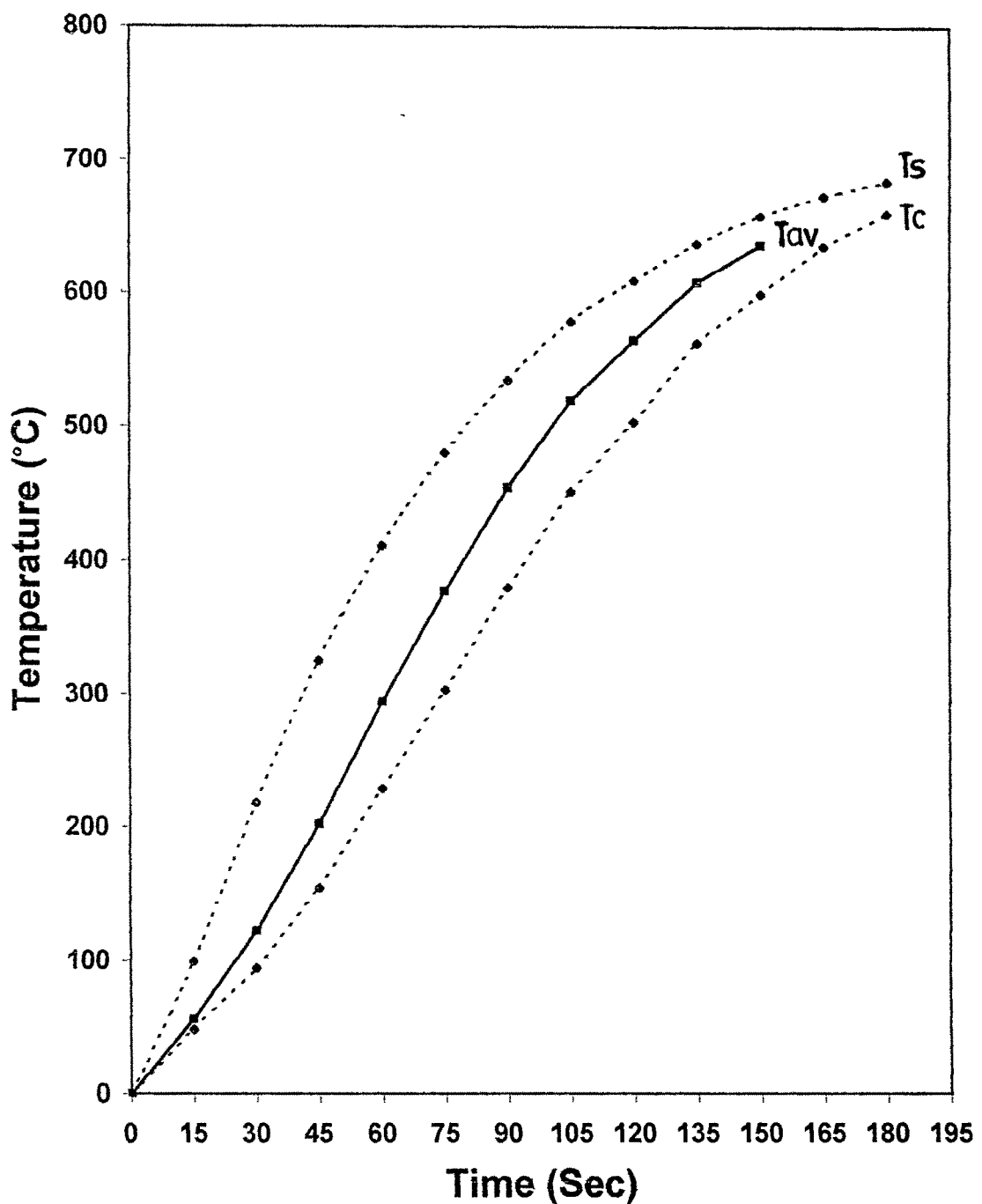


Fig. 4.39 Rise in surface, centre and average temperature in hand rolled pellet with time. (Size= 0.5672cm & Porosity=28.36%)

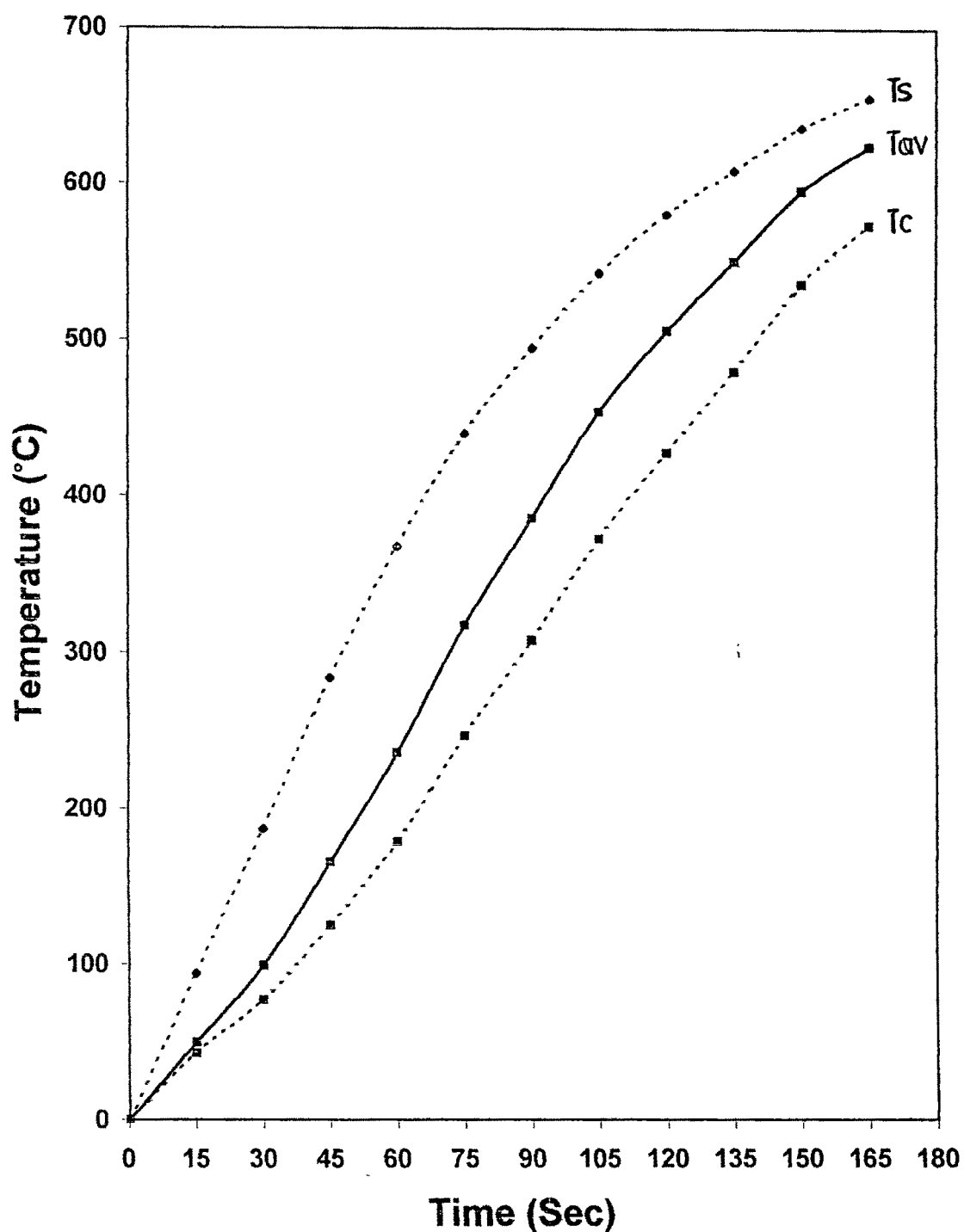


Fig.4.40 Rise in surface, centre and average temperature in hand rolled pellet with time. (Size=0.6490cm & Porosity =29.51%)

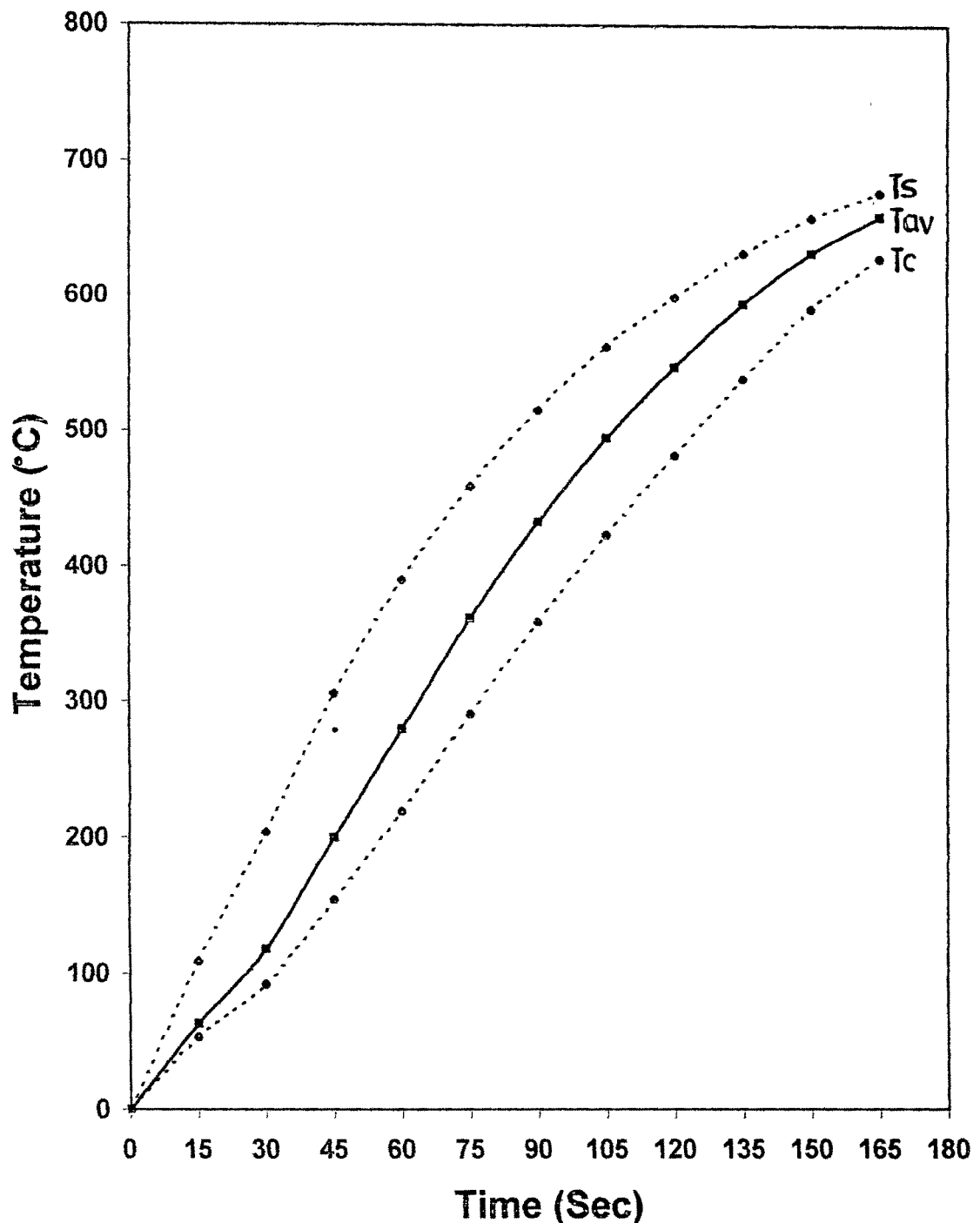


Fig.4.41 Rise in surface, centre and average temperature in hand rolled pellet with time.(Size=0.5756cm& Porosity=30.44%)

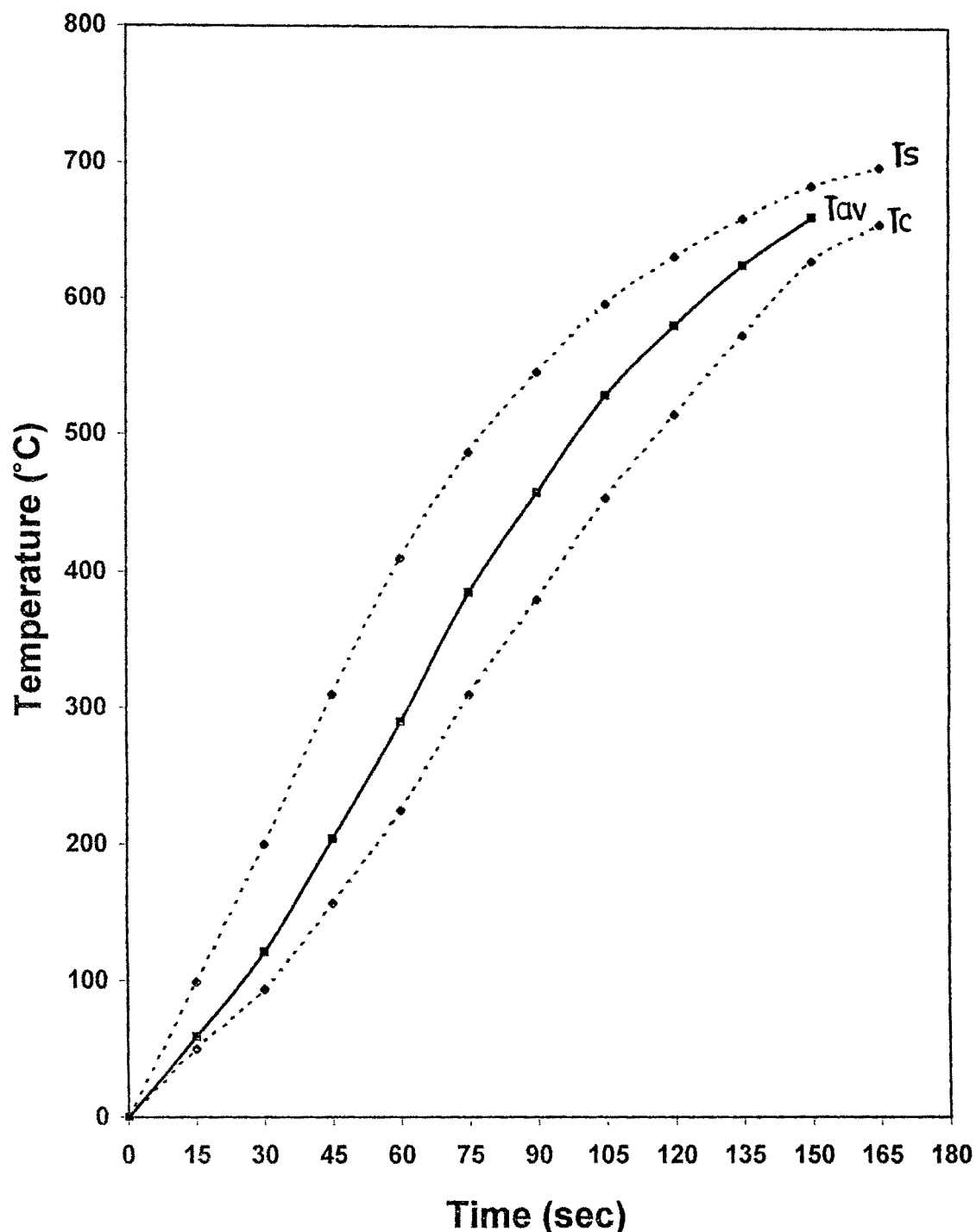


Fig. 4.42 Rise in surface, centre and average temperature in hand rolled pellet with time. (Size= 0.5756cm & Porosity=30.44%)

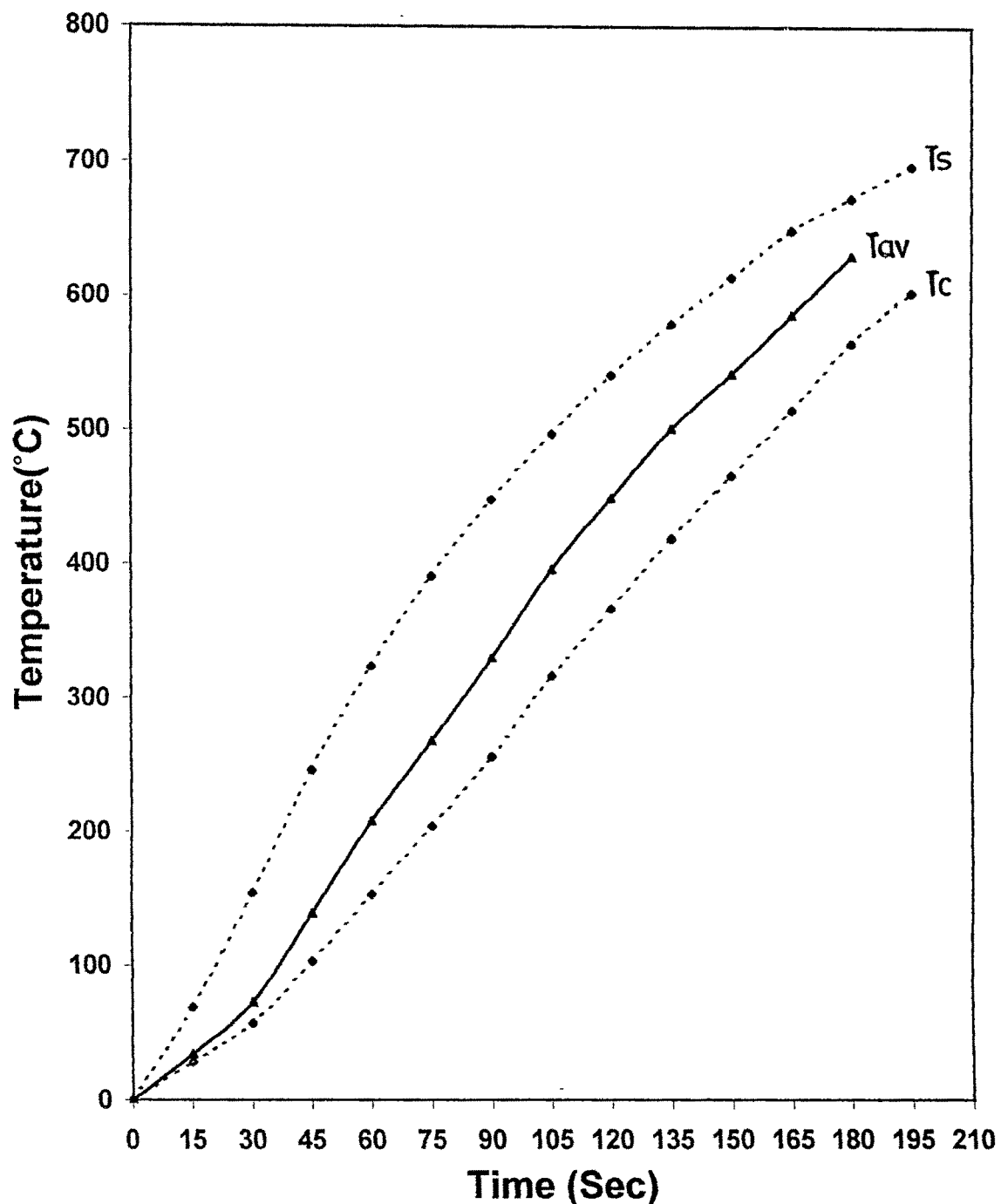


Fig4.43 Rise in surface, centre and average temperature in hand rolled pellet with time. (Size=0.6690cm&Porosity=34.96%)

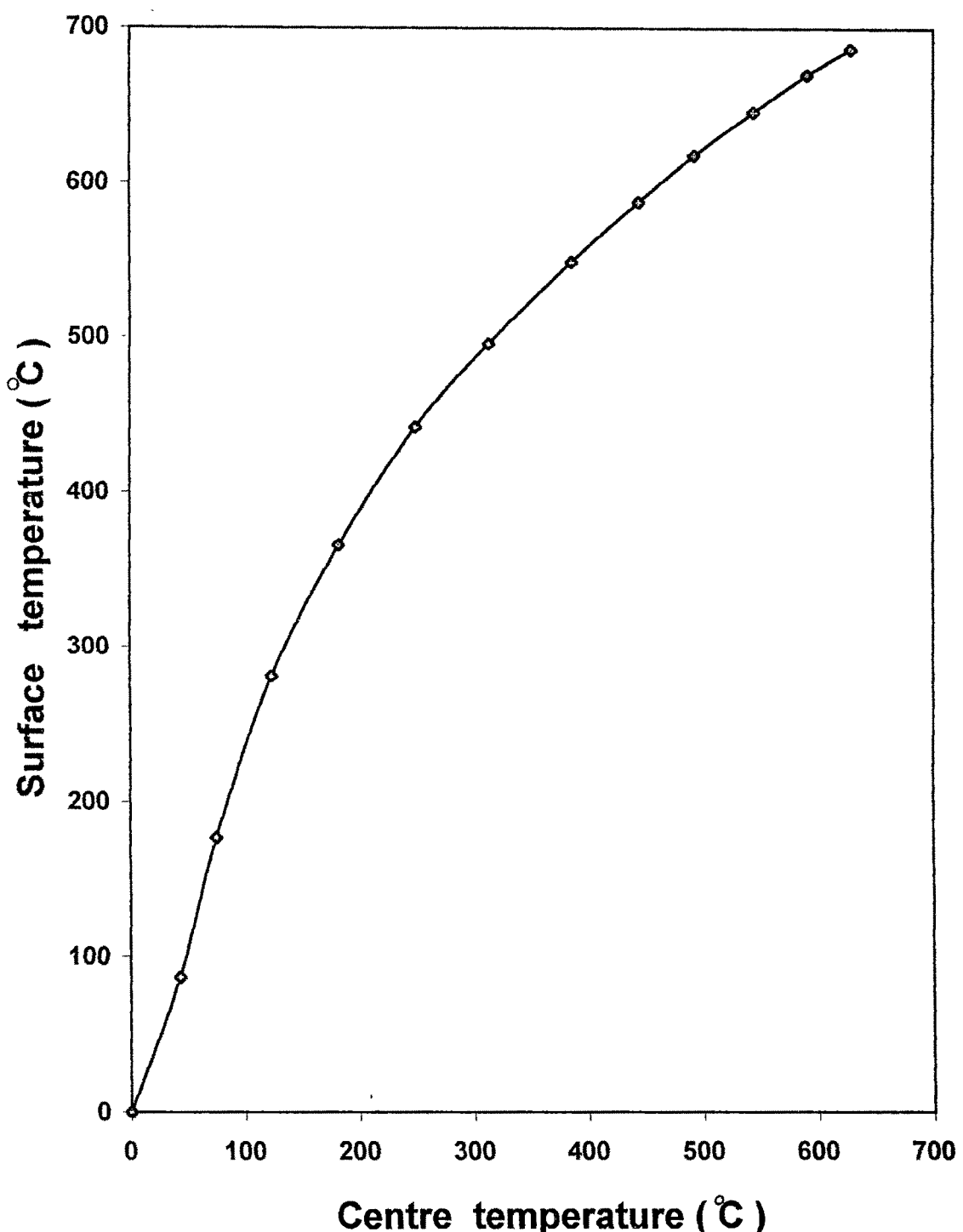


Fig. 4.44 Relationship between surface temperature( $T_s$ ) and centre temperature ( $T_c$ ). ( Pelletized pellet)  
(Size=0.6294cm&Porosity=32.17%)

Validity of the equation (4.11) in the present work was tested by plotting a curve between  $-\ln((T_s - T_c)/(T_s - T_0))$  with time (t) for one case and is represented in figure 4.45. The linear plot confirms the suitability of the expression for most of the region of heating, except at final stages when 'Tc' approaches 'Ts' and the curve tends to be asymptotic. The system takes about 30 to 45 seconds to stabilize depending on pellet size. A similar type of expression correlating temperature of a volume element at a radial distance 'r' can be envisaged as:

$$T_r = T_s (1 - e^{-k't}) + T_0 e^{-k't} \quad (4.13)$$

Where  $k'$  is another parameter. Relation between  $k$  and  $k'$  is necessary for further analysis of the results and needs to be evaluated.

Taking

$$K' = k(R/R-r)^n \quad (4.14)$$

here 'R' is the radius of the pellet, Eq.(4.13) modifies to

$$T_r = T_s (1 - e^{-k t (R/R(r))})^n + T_0 e^{-k t (R/(R-r))}^n \quad (4.15)$$

The above equation satisfies our boundary conditions for any value of 'n'. The value of 'n' in the present case was determined experimentally. The temperature at surface and at half-radial distance  $r=R/2$  were measured during heating of a pellet when exposed to furnace. Subsequently for the same pellet, a hole up to half radius was extended to centre and 'Ts' and 'Tc' were recorded. Two runs were taken to check reproducibility in each case. Pure iron oxide pellet was preferred for this run. Figure 4.46 represents the variation of temperature at surface, half radius and at

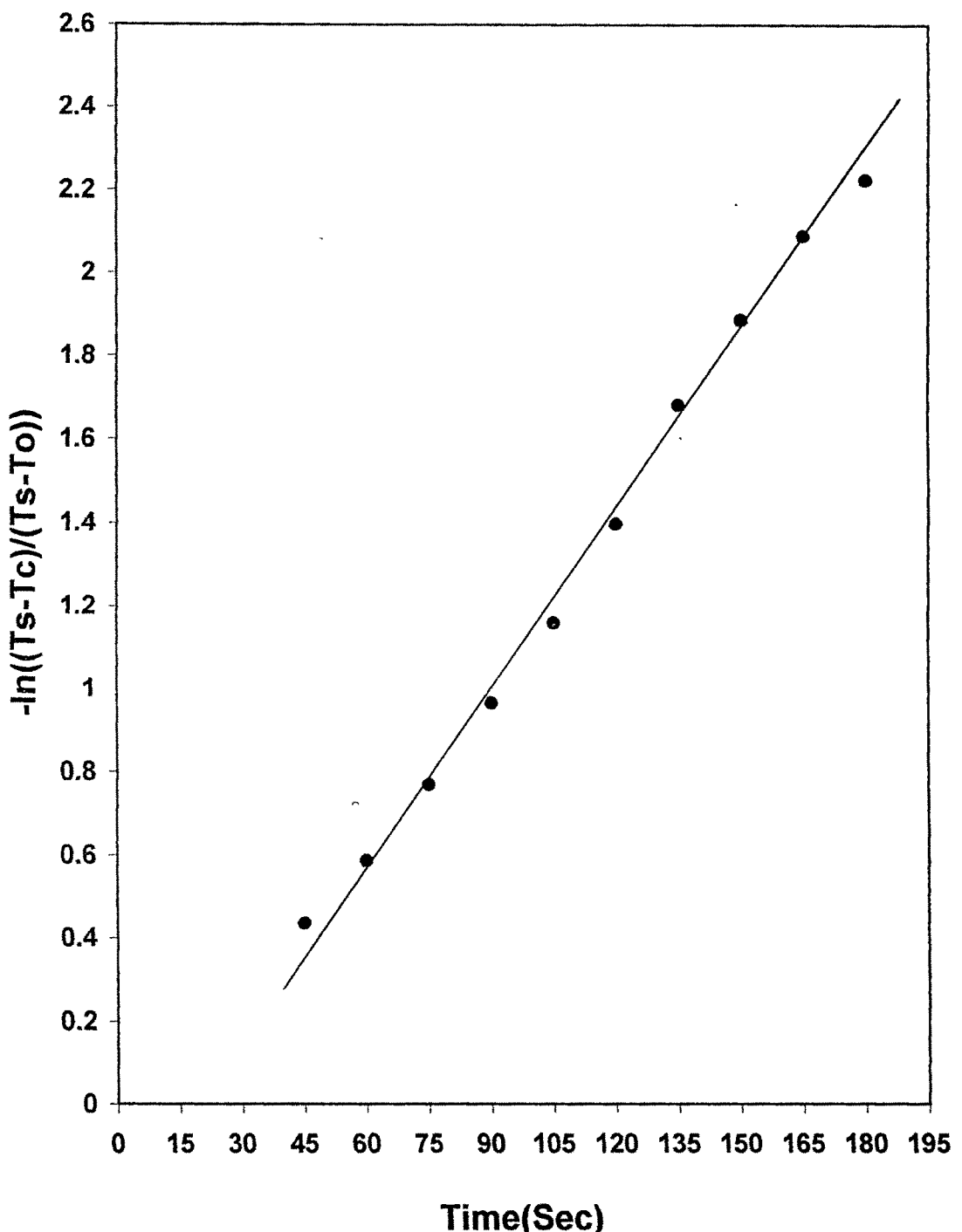


Fig. 4.45 Validity of equation (4.12 ) in case of pelletized pellet.  
(Values of parameter k.)  
(Pellet size=0.6839cm&Porosity=34.51%)

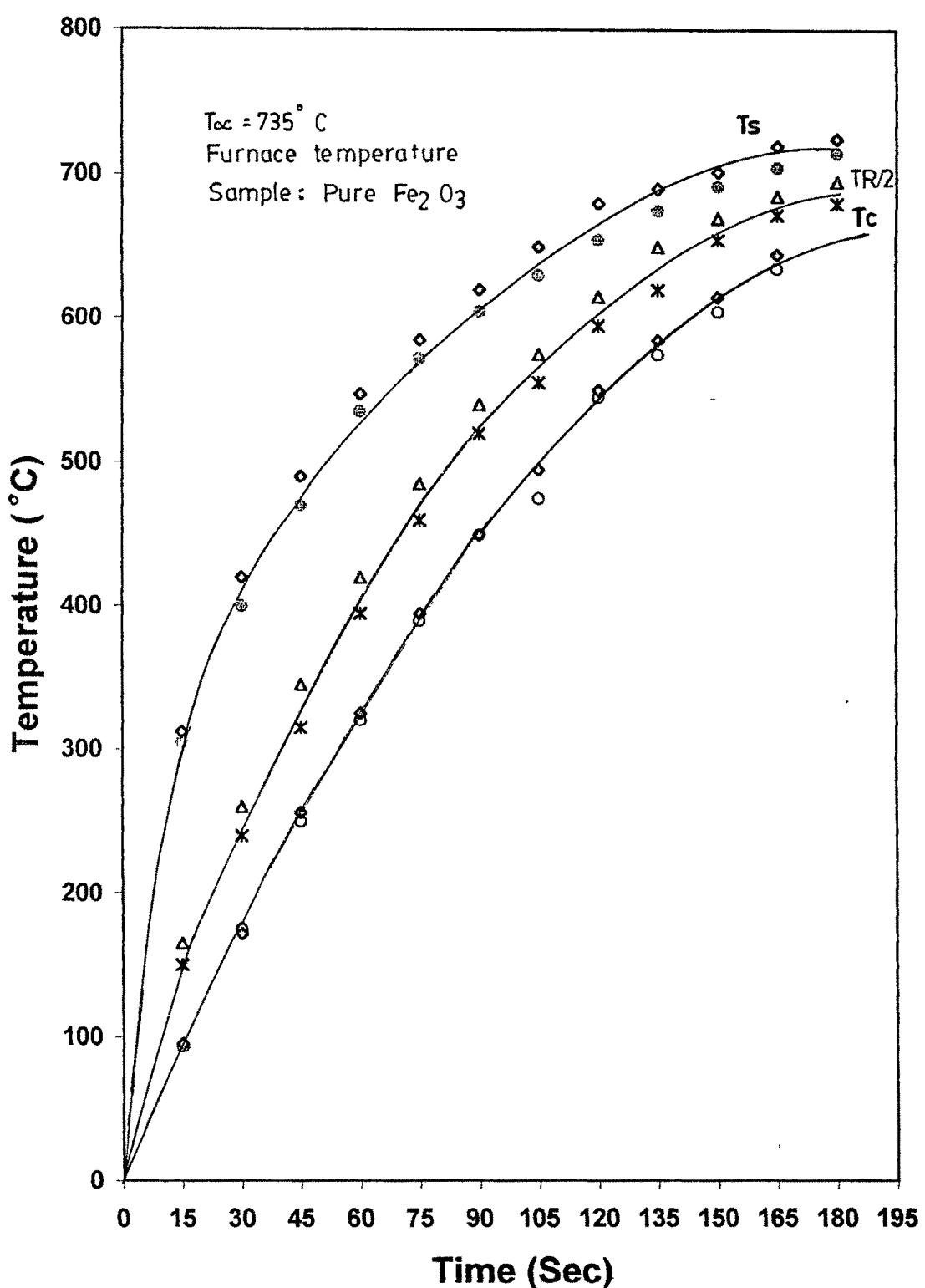


Fig.4.46 Rise in surface, half radial and centre temperature with time.

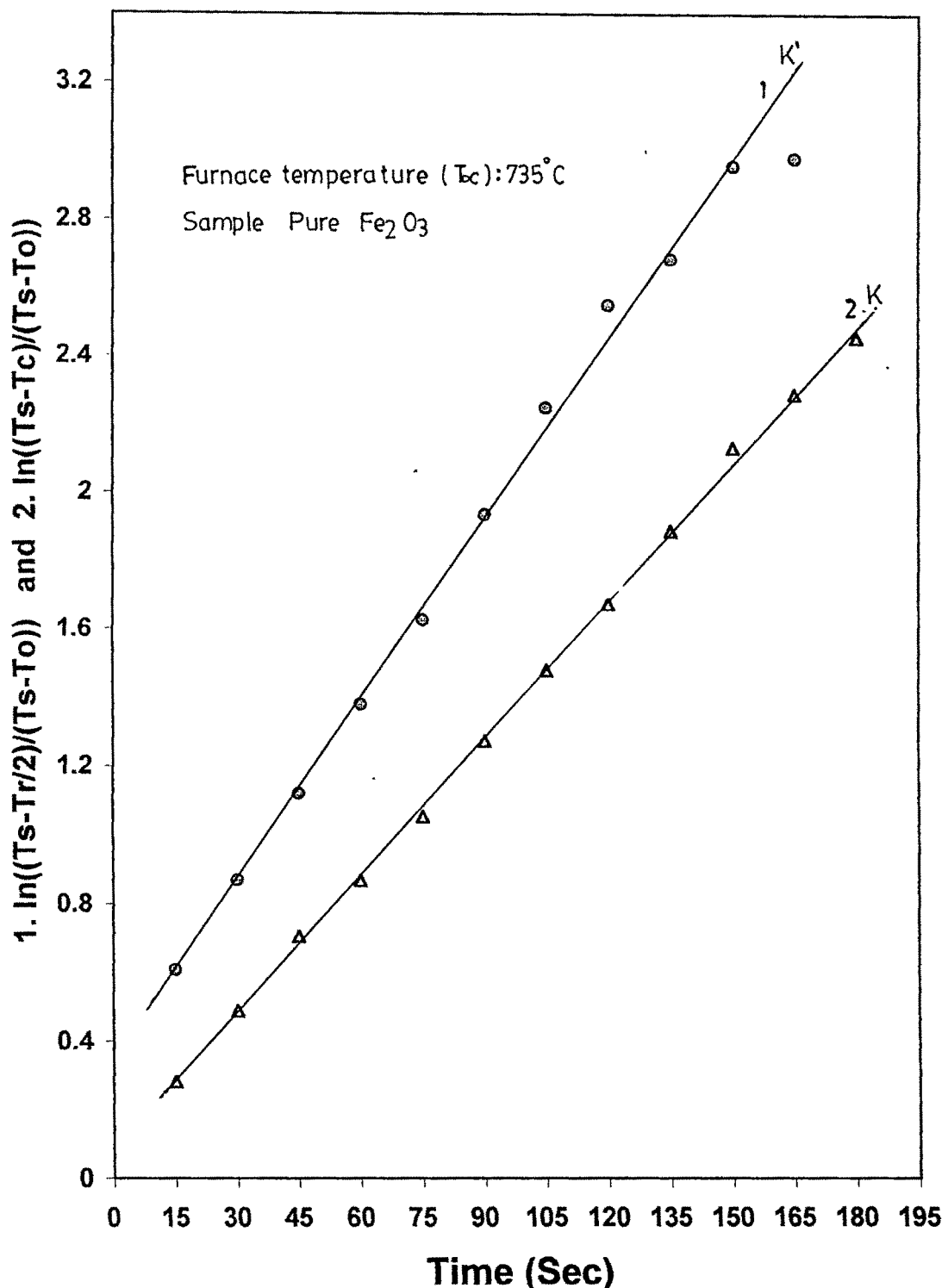


Fig.4.47 Calculation of parameter  $k$  and  $k'$ .  
(Pellet size=0.6550cm.&  $T_{so}=735^\circ\text{C}$ )

centre of the iron oxide pellet with time. The parameter  $k'$  and  $k$  were evaluated by plotting  $-\ln((Ts-Tr)/2)/(Ts-To)$  and  $\ln((Ts-Tc)/(Ts-To))$  Vs time ( $t$ ) for this pellet. The results are indicated in figure 4.47. The ratio between the slopes of these two linear plot  $k'/k$  was found to be 1.238 and the value of 'n' in Equation (4.15) as 0.3. Thus the expression modifies to

$$Tr = Ts \left(1 - e^{-kt(R/(R-r))}\right)^n + To e^{-kt(R/(R-r))} \quad (4.16)$$

On simplification

$$Tr = Ts - (Ts - To) e^{-kt(R/(R-r))^{0.3}} \quad (4.17)$$

Ray<sup>62</sup> reported that the parameter 'k' is not a constant but may vary with process conditions. In view of the above the temperature 'Tr' is calculated with instantaneous 'k' value at any time ( $t$ ). The temperature of elements of 1mm thickness and with radial distance 'r' equal to (R-0.05), (R-0.15), (R-0.25)....are calculated using equation (4.17) for various time intervals. The results of various sets are indicated in figure 4.48 to 4.59 which in fact, indicate the temperature profile within pellet at various intervals. The average temperature of pellet at an instant was further calculated by using an equation.<sup>63</sup>

$$T_{av} = \frac{\int_0^R 4\pi r^2 Tr dr}{\int_0^R 4\pi r Tr dr} \quad (4.18)$$

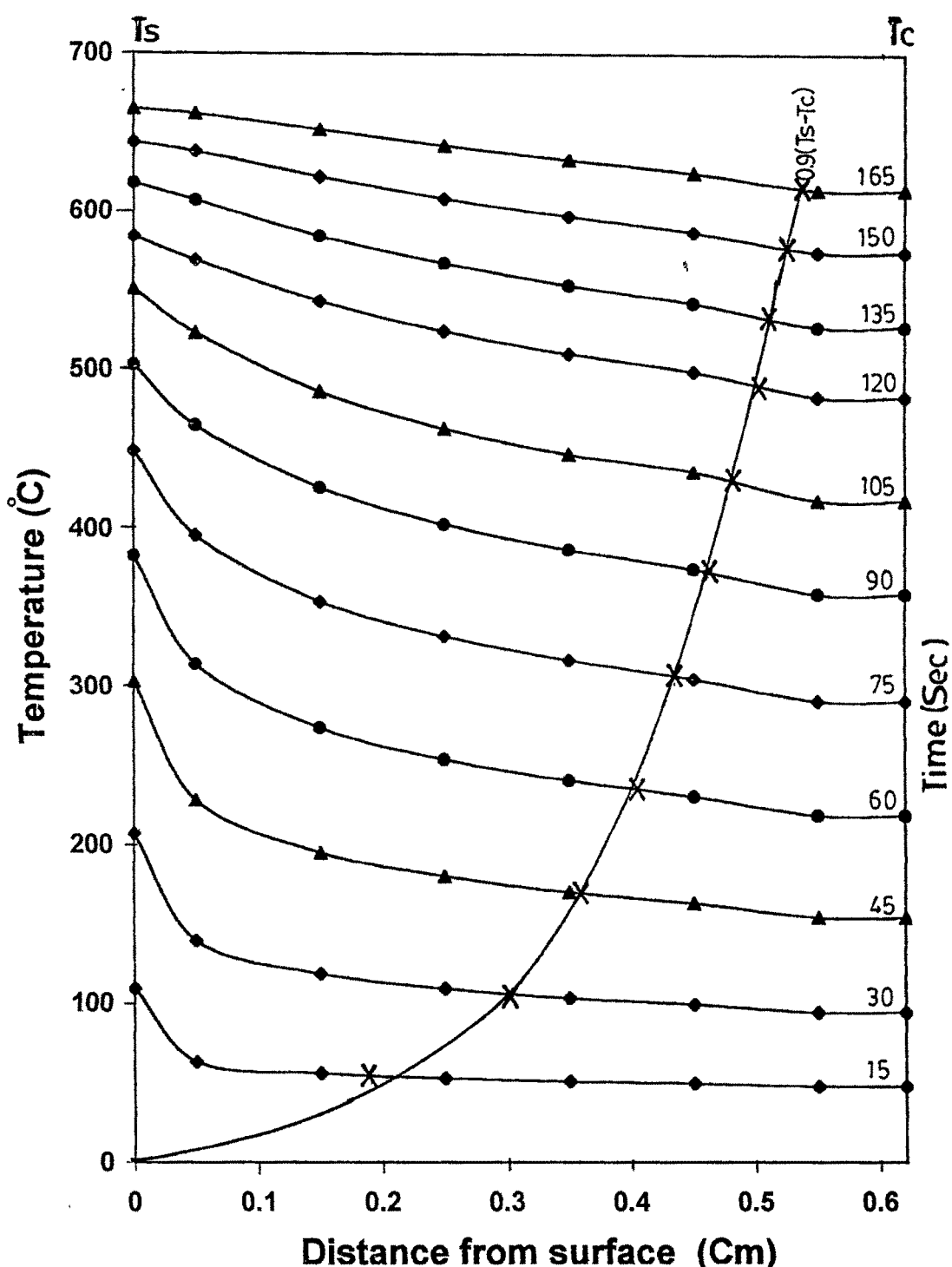
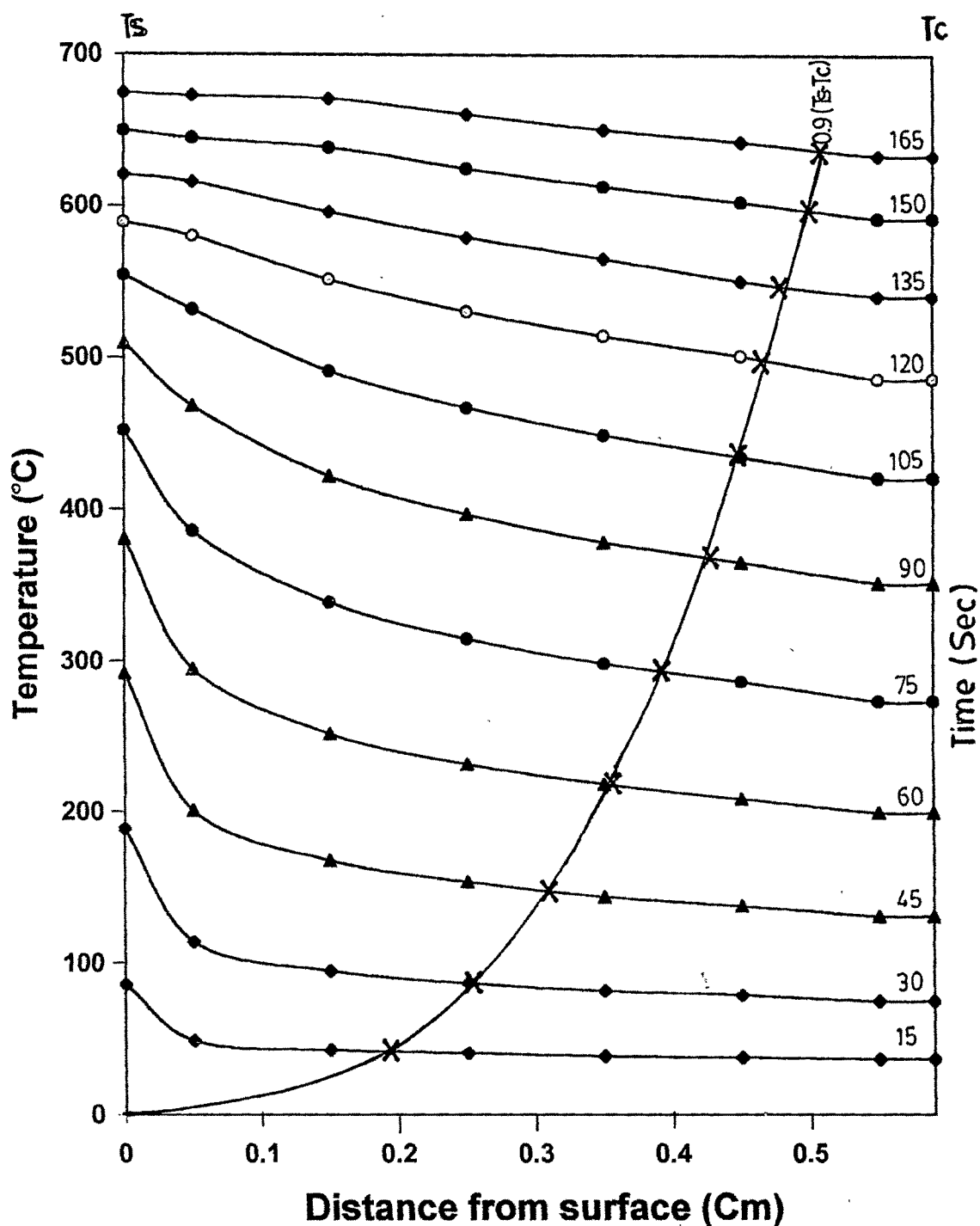
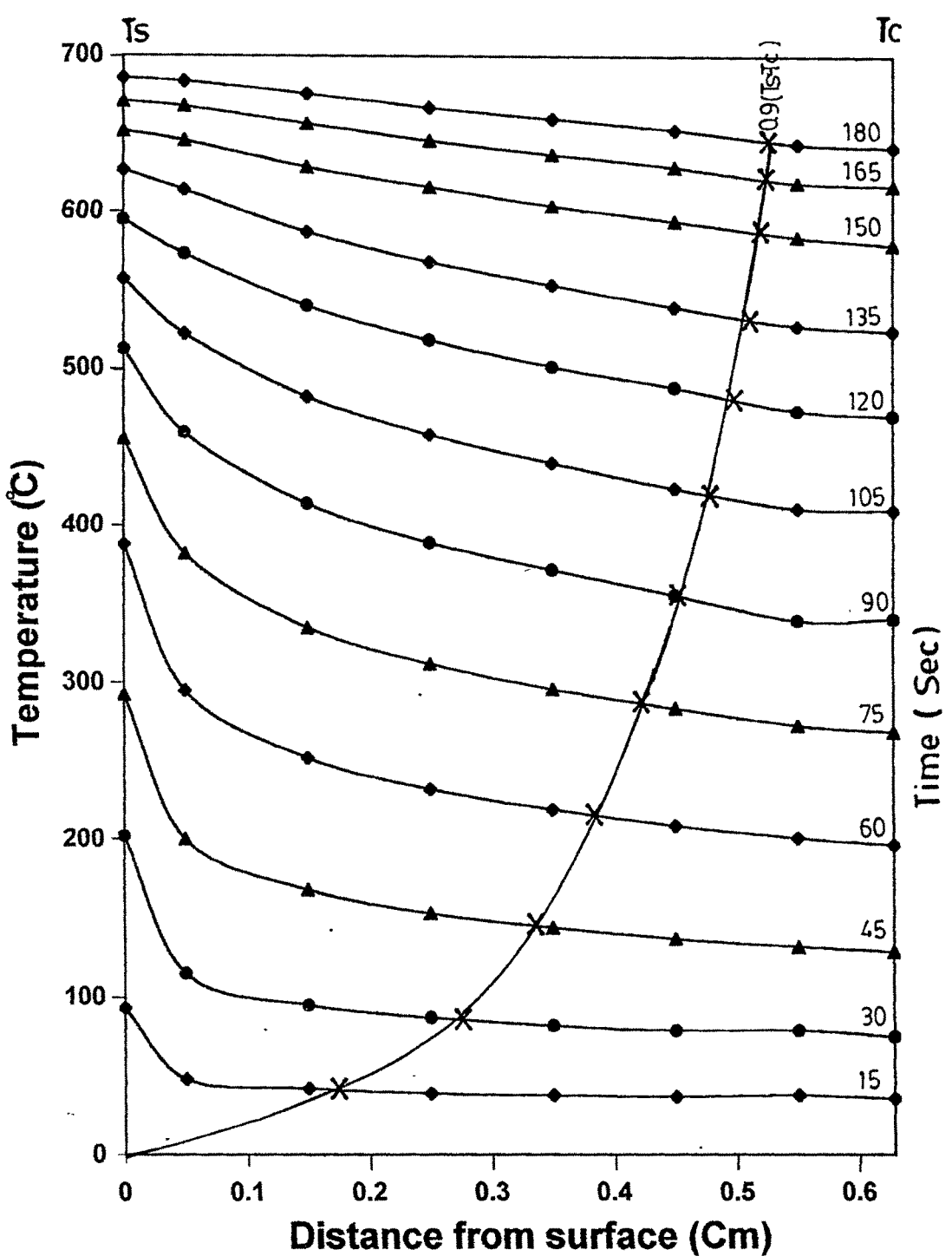


Fig. 4.48 Change in temperature profile and movement of heat front with time (Pelletized pellet).  
(Pellet size=0.6146cm&Porosity=24.27%)



**Fig.4.49 Change in temperature profile and movement of heat front with time (Pelletized pellet).**  
**(Pellet size=0.5854cm&Porosity=25.87%)**



**Fig. 4.50 Change in temperature profile and movement of heat front with time (Pelletized pellet).**  
 (Pellet size=0.6283cm&Porosity=28.08%)

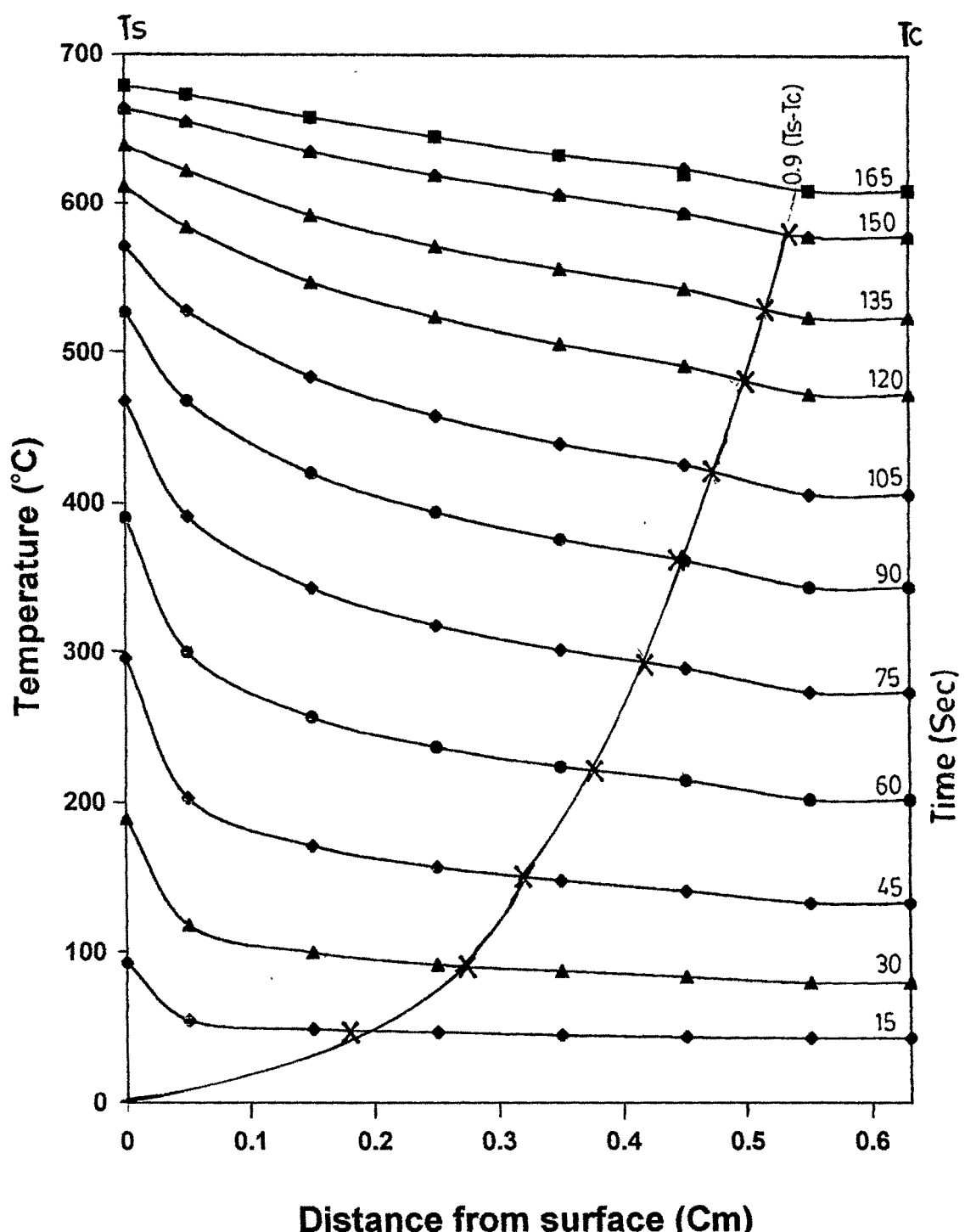


**Fig.4.51** Change in temperature profile and movement of heat front with time (Pelletized pellet).  
 (Pellet size=0.6294cm&Porosity=32.17%)

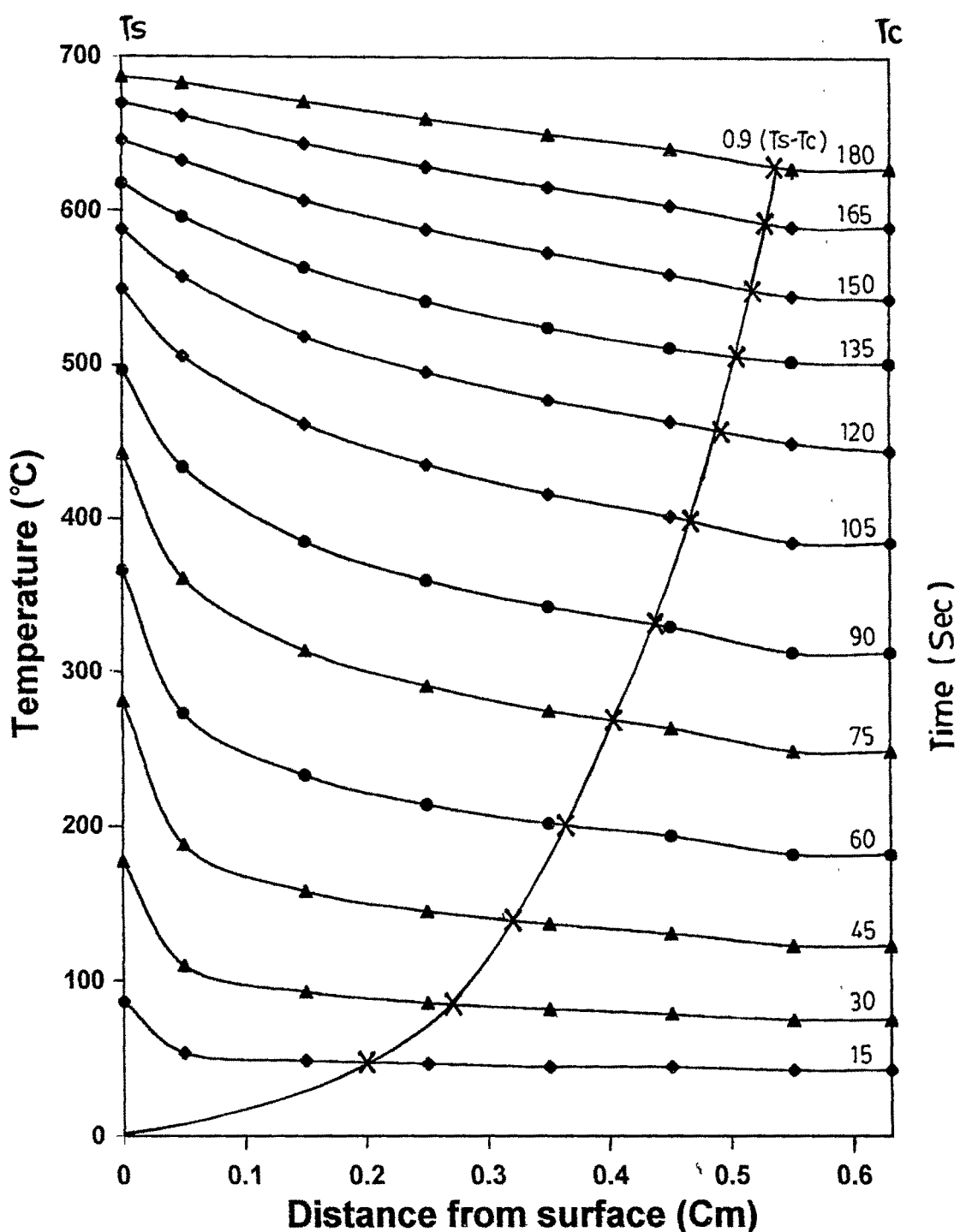


Fig.4.52 Change in temperature profile and movement of heat front with time (Pelletized pellet).  
(Pellet size=0.6294cm&Porosity=32.17%)

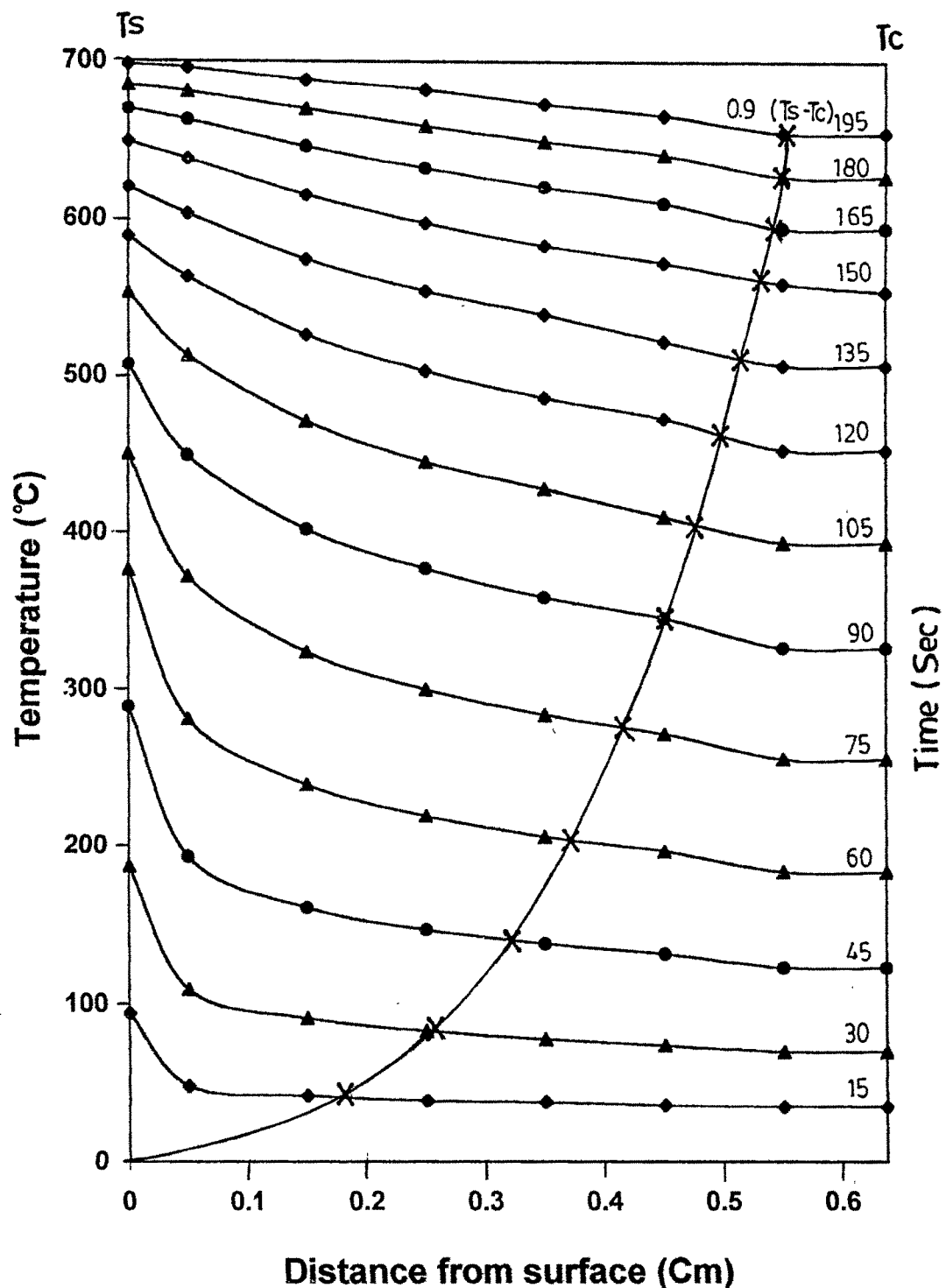
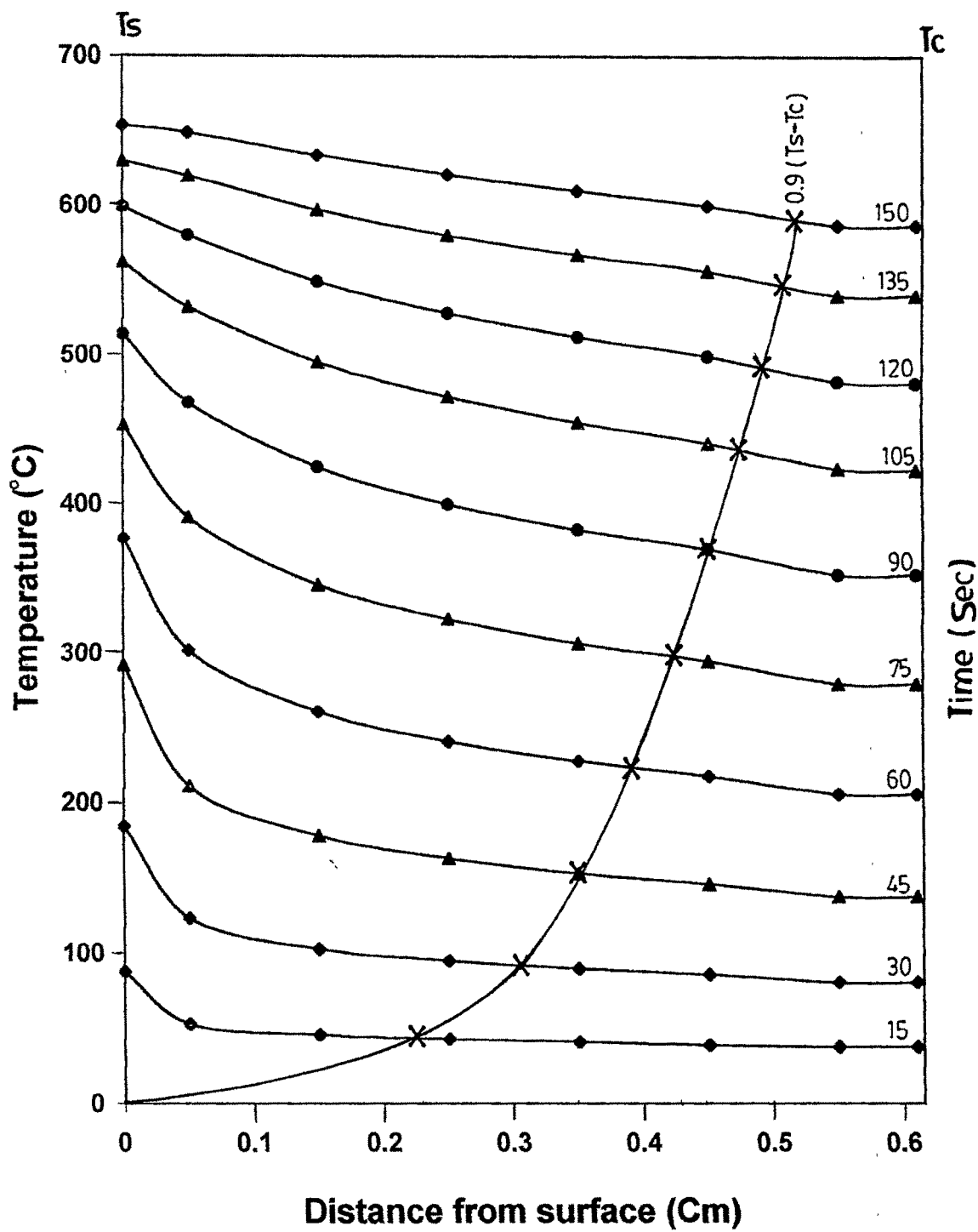
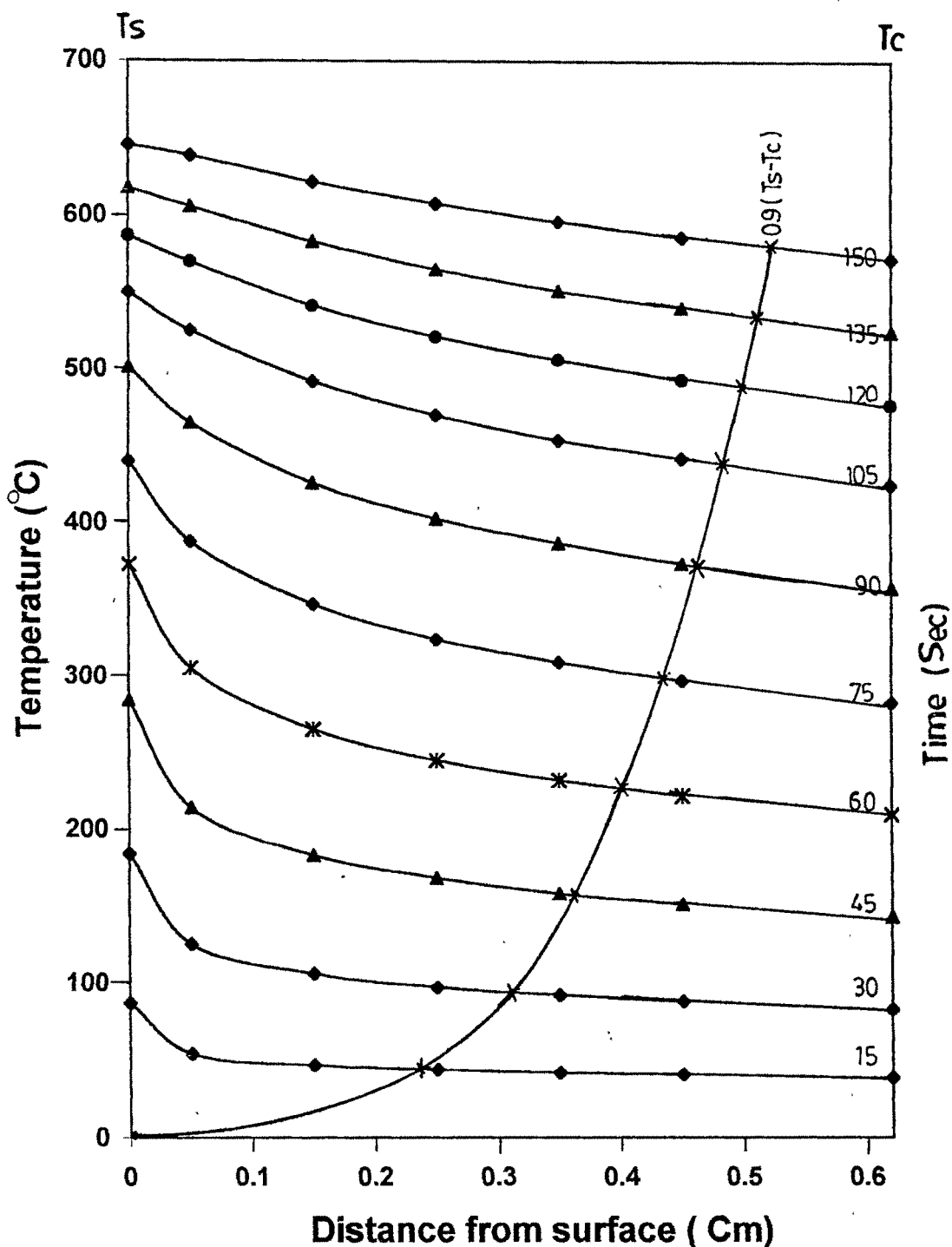


Fig. 4.53 Change in temperature profile and movement of heat front with time (Pelletized pellet).  
 ( Pellet size=0.6360cm&Porosity=33.54%)



**Fig. 4.54 Change in temperature profile and movement of heat front with time (Pelletized pellet).**  
**(Pellet size=0.6154cm&Porosity=34.13%)**



**Fig. 4.55 Change in temperature profile and movement of heat front with time (Pelletized pellet).**  
**(Pellet size=0.6154cm&Porosity=34.13%)**

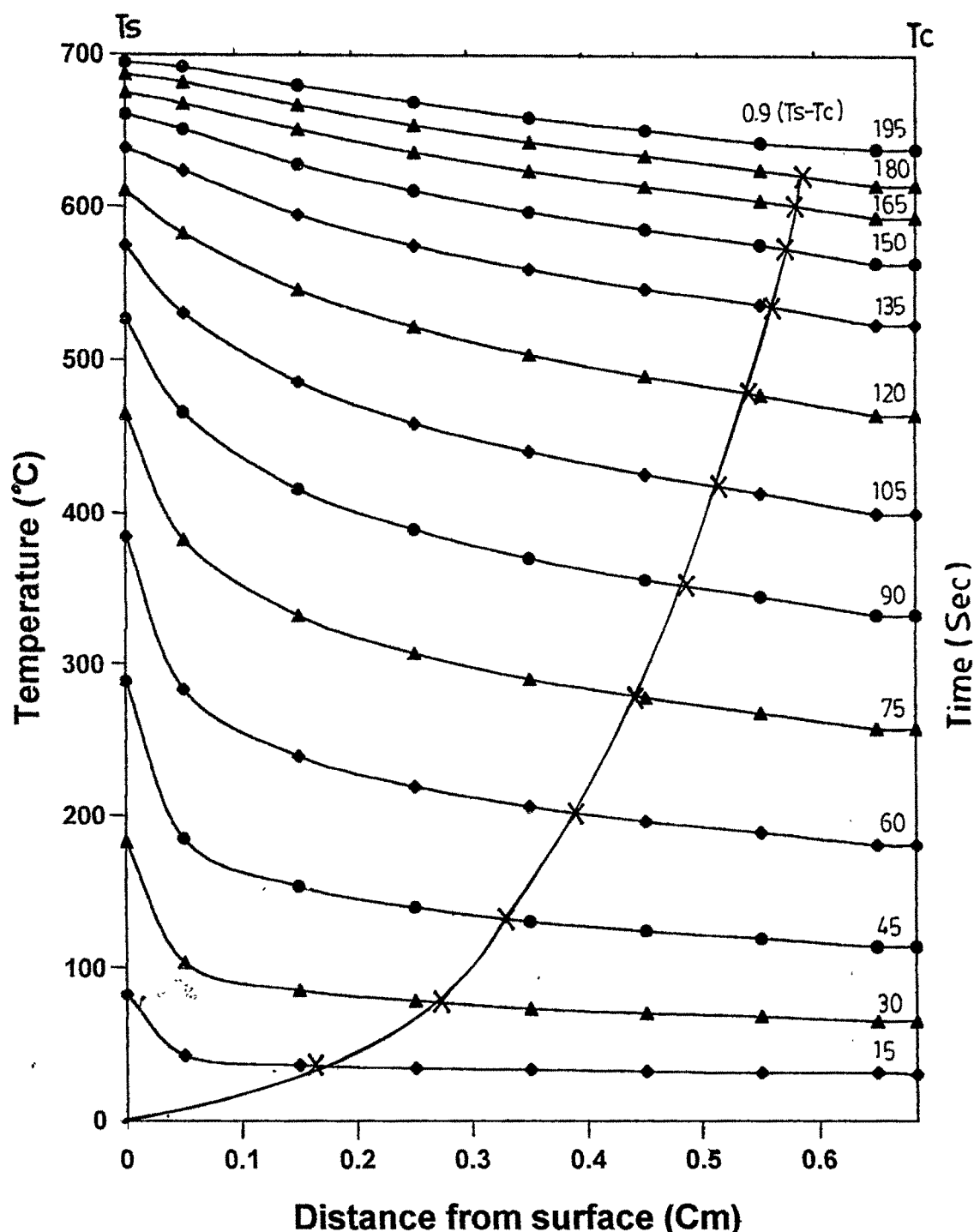


**Fig. 4.56 Change in temperature profile and movement of heat front with time (Pelletized pellet).**  
 (Pellet size=0.6839cm&Porosity=34.51%)

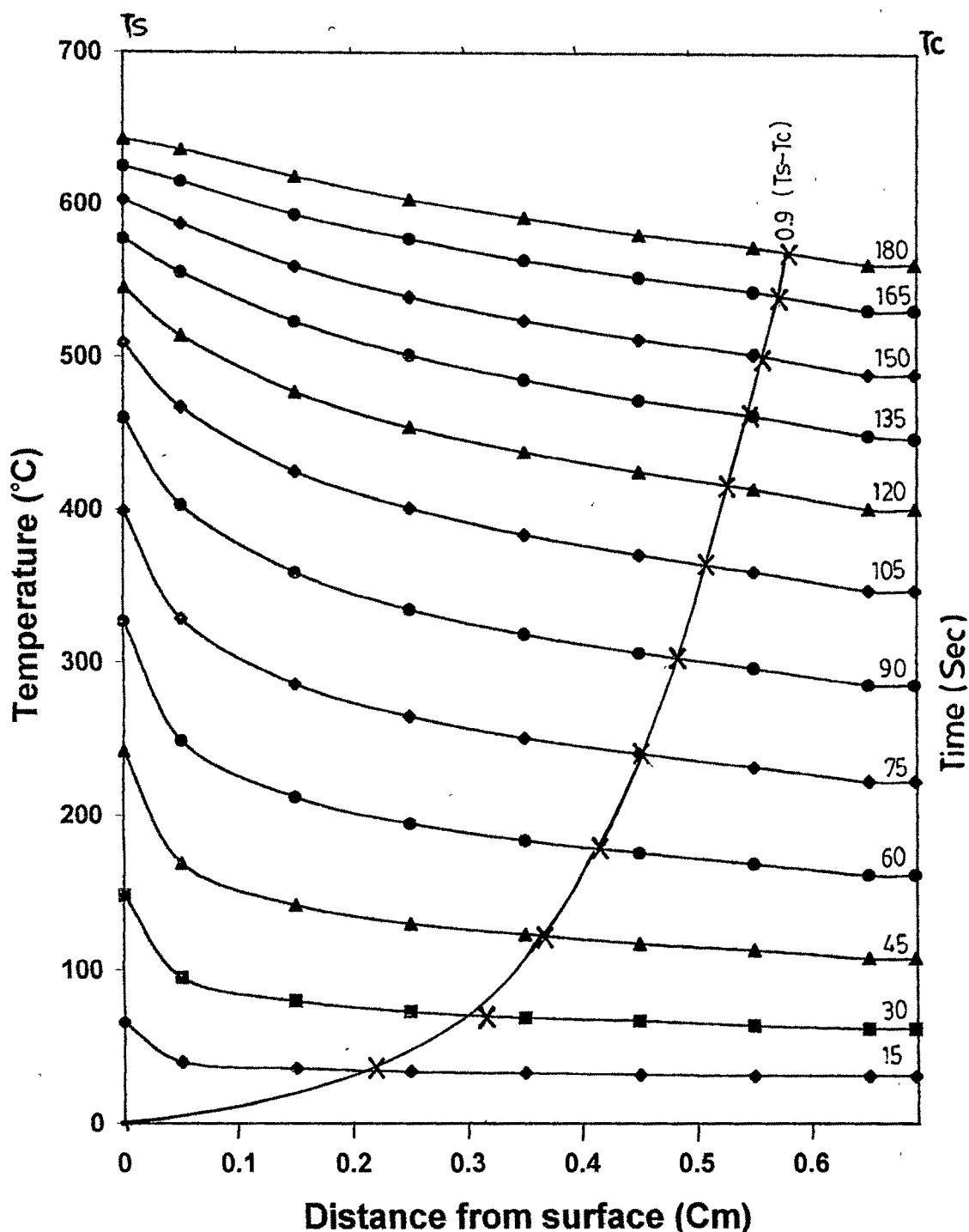
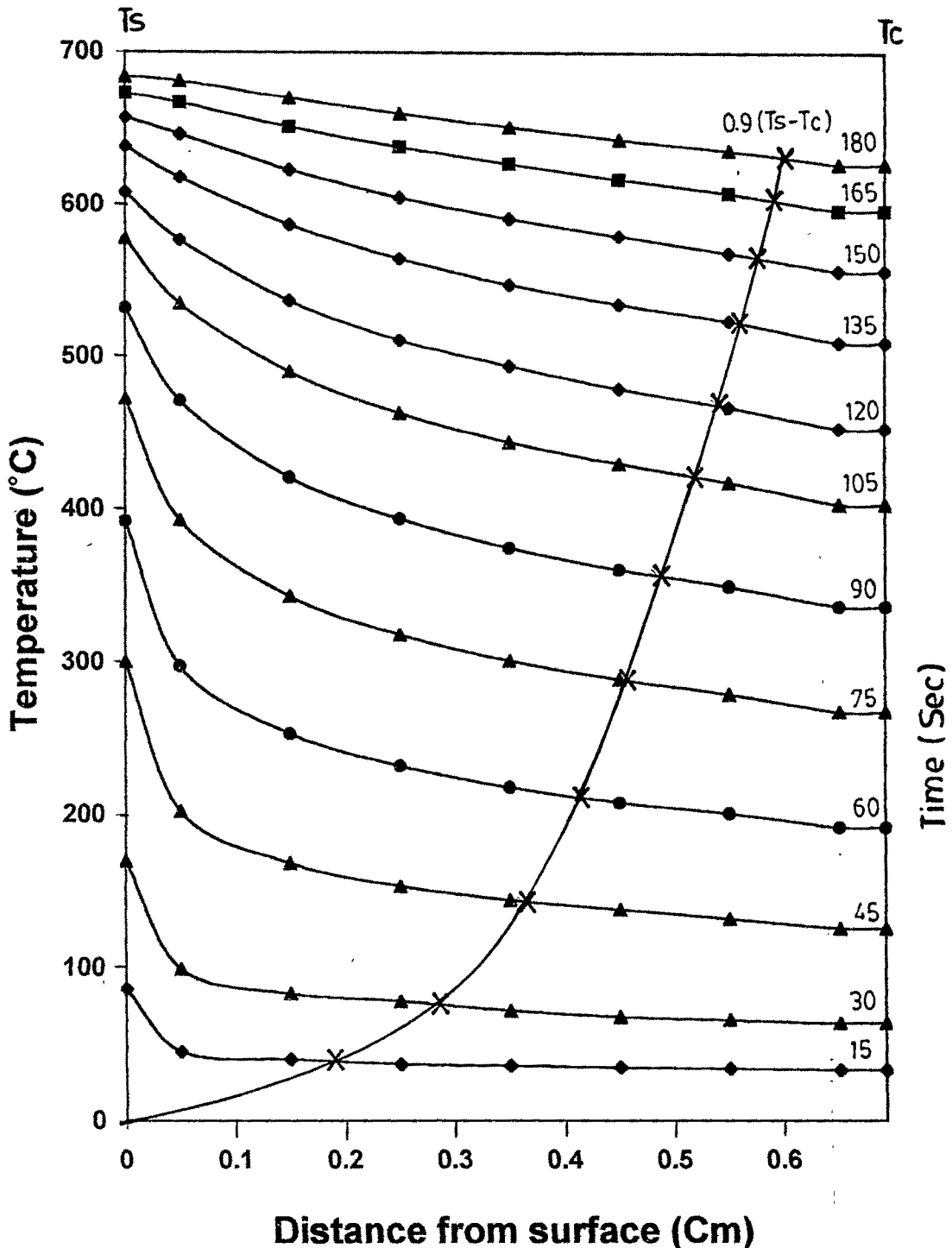


Fig.4.57 Change in temperature profile and movement of heat front with time (Pelletized pellet).  
( Pellet size= 0.6921cm&Porosity=35.65 %)



**Fig. 4.58 Change in temperature profile and movement of heat front with time (Pelletized pellet).**  
**(Pellet size= 0.6921cm&Porosity=35.36%)**

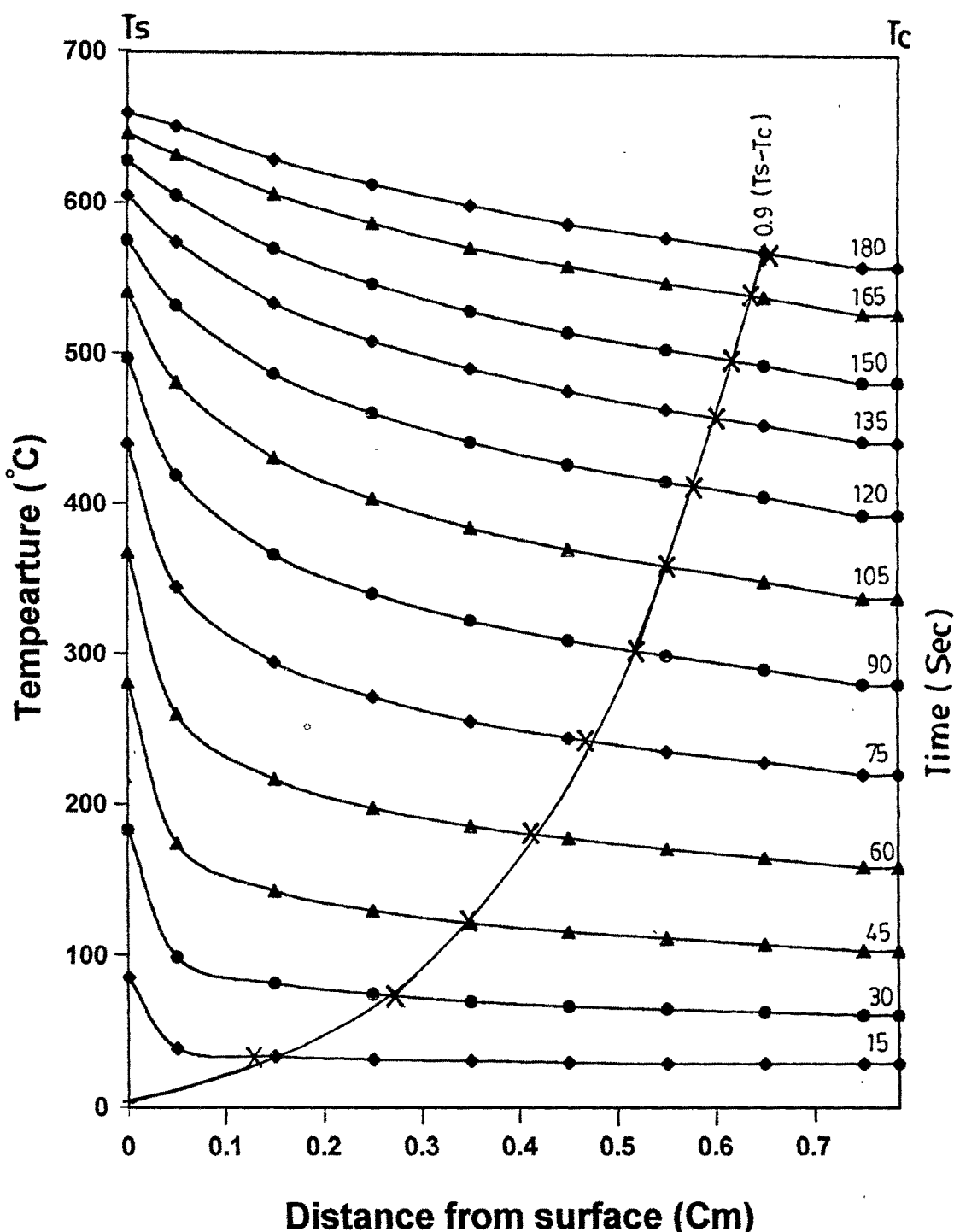


Fig. 4.59 Change in temperature profile and movement of heat front with time (Pelletized pellet).  
(Pellet size=0.7863cm&Porosity=38.76%)

and substituting the value of 'Tr' from eq. (4.17) further integration. The calculated value of 'Tav' with time is plotted in figures 4.27 to 4.38 and 4.39 to 4.43 along with Ts & Tc. One sample calculation for 'Tav' for pellet of size 0.5759cm and porosity 14.29 % is presented in table No. 4.8 (A, B).

#### 4.2.1 Calculation of thermal diffusivity by heat balance.

The heat balance at the surface of pellet dictate that amount of heat passing through the pellet surface inside is utilised in heating the pellet.

Thus.

$$KA \frac{dT}{dr} = V \rho C \frac{Tav}{dt} \quad (4.19)$$

Where, K= thermal conductivity of pellet( $\text{Wm}^{-1}\text{K}^{-1}$ )

V= volume( $\text{m}^3$ )

$\rho$ = density.( $\text{Kg/m}^3$ )

C=heat capacity, ( $\text{J.Kg}^{-1}\text{K}^{-1}$ )

A= surface area of pellet.( $\text{m}^2$ )

Re arranging Eq. (4.19)

$$\frac{dTav}{dt} = [(K.A)/(V.\rho.C)].\frac{dT}{dr} \quad (4.20)$$

Substituting for  $K/\rho C$  as ' $\alpha$ ' and  $A/V$  as  $3/R$  for spherical geometry.

$$\frac{dTav}{dt} = (3\alpha/R).\frac{dT}{dr} \quad (4.21)$$

and

$$\alpha = (R/dTav/dt) / (3dT/dr) \quad (4.22)$$

Table No.4.8(A)

**Average temperature calculation of pellet (Tav)**

Pressed pellet. Pellet size=0.5759cm Porosity=14.29%

Time (Sec) ↓	Element Temperature (Tr) ( °C)				
	0.05	0.15	0.25	0.35	0.45
(R-r)Cm→					
15	49.72	43.67	41.3	39.89	38.9
30	141.91	117.35	107.06	100.72	96.22
45	249.89	208.13	189.81	178.25	169.91
60	361.89	310.77	286.22	270.18	258.38
75	449.59	397.64	370.59	352.28	338.51
90	518.66	469.9	442.52	423.38	408.67
105	575.47	534.2	508.84	490.37	475.81
120	617.11	584.95	563.12	546.49	533.01
135	647.56	622.48	603.92	589.2	576.97
150	675.82	655.96	640.09	627.05	615.96
165	642.65	677.19	663.9	652.6	642.78
180	702.61	693.34	684.22	675.94	668.47
195	715.35	708.02	700.36	693.19	686.59

Table No.4.8(B)

**Average temperature calculation of pellet (Tav)**Pressed pellet. Pellet size=0.5759cm Porosity=14.29%  $r^3/2=0.06365782$ (Denominator)

$$Tav = \frac{4\pi \int_0^R r^2 dr Tr}{4\pi \int_0^R r^2 dr}$$

Time (Sec) ↓ $r^2 dr$	$r^2 dr Tr$					$\Sigma r^2 dr Tr$ Numerator	Tav (°C)
	1	2	3	4	5		
	0.027657	0.018139	0.010621	0.005103	0.001585		
15	1.3752	0.79203	0.4387	0.2036	0.06166	2.87119	45.09641
30	3.9248	2.1287	1.1371	0.5139	0.1525	7.85704	123.4068
45	6.8955	3.7752	2.016	0.9096	0.2693	13.86559	217.7802
60	10.0088	5.6372	3.0399	1.3786	0.4095	20.47404	321.5759
75	12.3468	7.2131	3.9362	1.7977	0.5366	25.8304	405.7051
90	14.3446	8.5236	4.7001	2.1605	0.6477	30.3766	477.1104
105	15.9157	9.6899	4.54045	2.5023	0.7542	34.2667	538.2098
120	17.0674	10.6103	5.9809	2.7887	0.8448	37.2921	585.7292
135	17.9096	11.2911	6.4142	3.0067	0.9145	39.5361	620.9743
150	18.6912	11.8985	6.7984	3.1998	0.9763	41.5642	652.829
165	19.083	12.1568	6.4492	3.2718	0.9985	42.4593	666.8877
180	19.4322	12.5763	7.267	3.4494	1.0595	43.7844	687.7009
195	19.7845	12.8428	7.4385	3.5374	1.0883	44.6915	701.9472

The thermal diffusivity ( $\alpha$ ) can be evaluated for known values of  $(dT_{av}/dt)$  and  $(dT/dr)$ . The value of  $(dT_{av}/dt)$  for various time interval, can be evaluated from 'T<sub>av</sub>' values indicated in figures 4.27 to 4.38 and 4.39 to 4.43. The slope  $(dT_{av}/dt)$  at an instant was calculated by taking reading of 'T<sub>av</sub>' for points one stage ahead and one stage behind and dividing the difference by 30 (Sec). Evaluation of  $dT/dr$  is difficult and requires certain assumptions. Many expressions relating  $dT/dr$  with heat transfer parameter ' $\alpha$ ' for different boundary conditions are available in literature <sup>44</sup>. These expression are not useful in present case as the basic aim is to evaluate ' $\alpha$ ' through  $dT/dr$ . From figures 4.48 to 4.64 it is evident that the depth of major temperature fall from T<sub>s</sub> to T<sub>c</sub>, changes with time of exposure. Initially the heat front is concentrated at narrow depth near surface and with time it penetrates inside. In present study 90% of temperature fall from 'T<sub>s</sub>' to 'T<sub>c</sub>' is assumed major change and the depth at which it occur is calculated by equation (4.17) to calculate  $dT/dr$ . Subsequently the values of ' $\alpha$ ' were calculated. The calculations are shown in table 4.9 to 4.20 for pelletized pellets and 4.21 to 4.25 for hand rolled pellets. The average of best (middle) 7 to 8 readings is considered to calculate average thermal diffusivity. The thermal conductivities are calculated by taking the true heat capacity values <sup>52</sup> of iron oxide at 700°C as 1.047kJ/kg.K as indicated in chapter 2. The average value of ' $\alpha$ ' for pelletized pellet with their other physical properties is indicated in table 4.26 and same for hand rolled pellet in table 4.27.

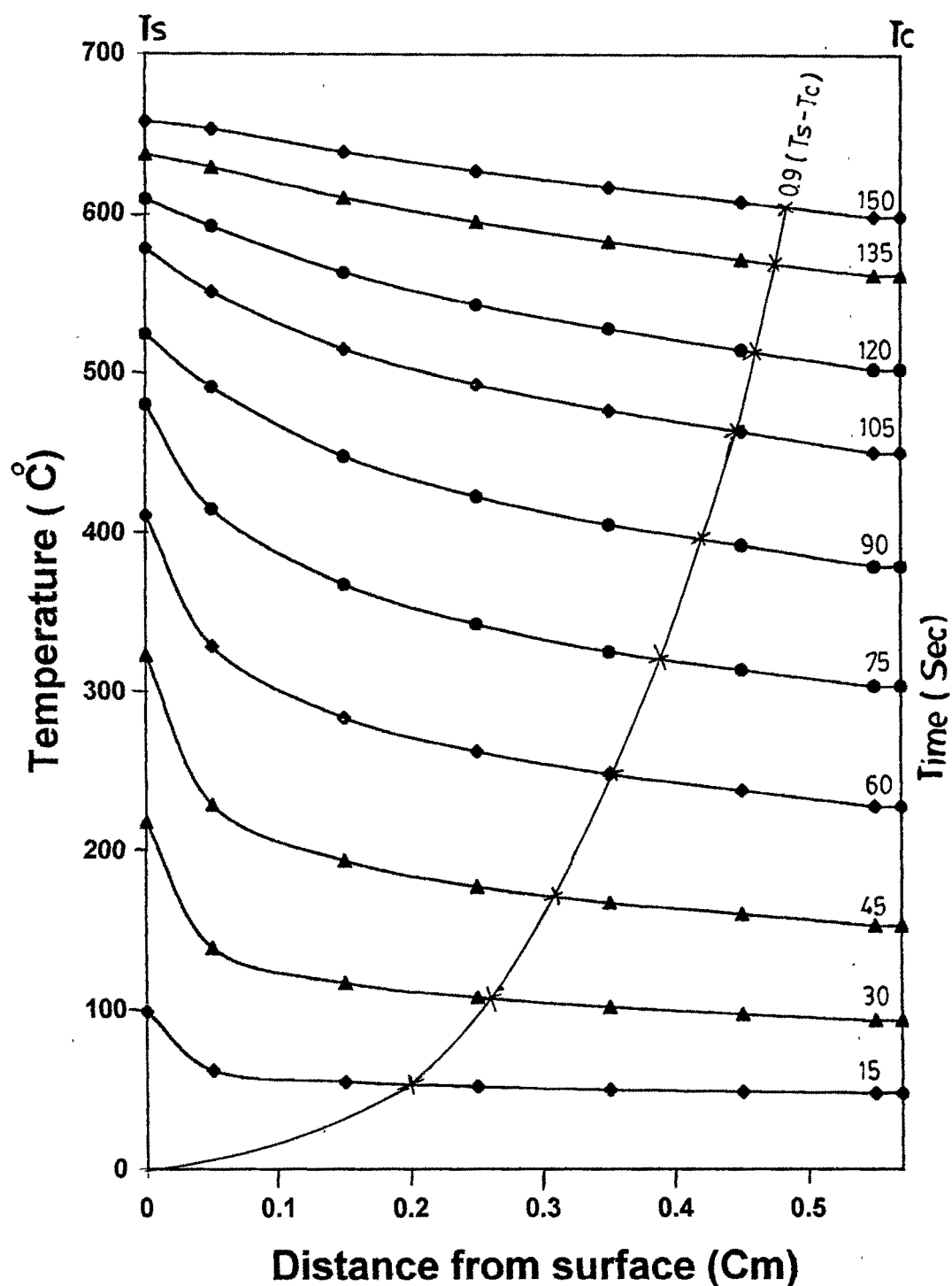


Fig. 4.60 Change in temperature profile and movement of heat front with time (Hand rolled pellet).  
(Pellet size=0.5672cm&Porosity=28.36%)

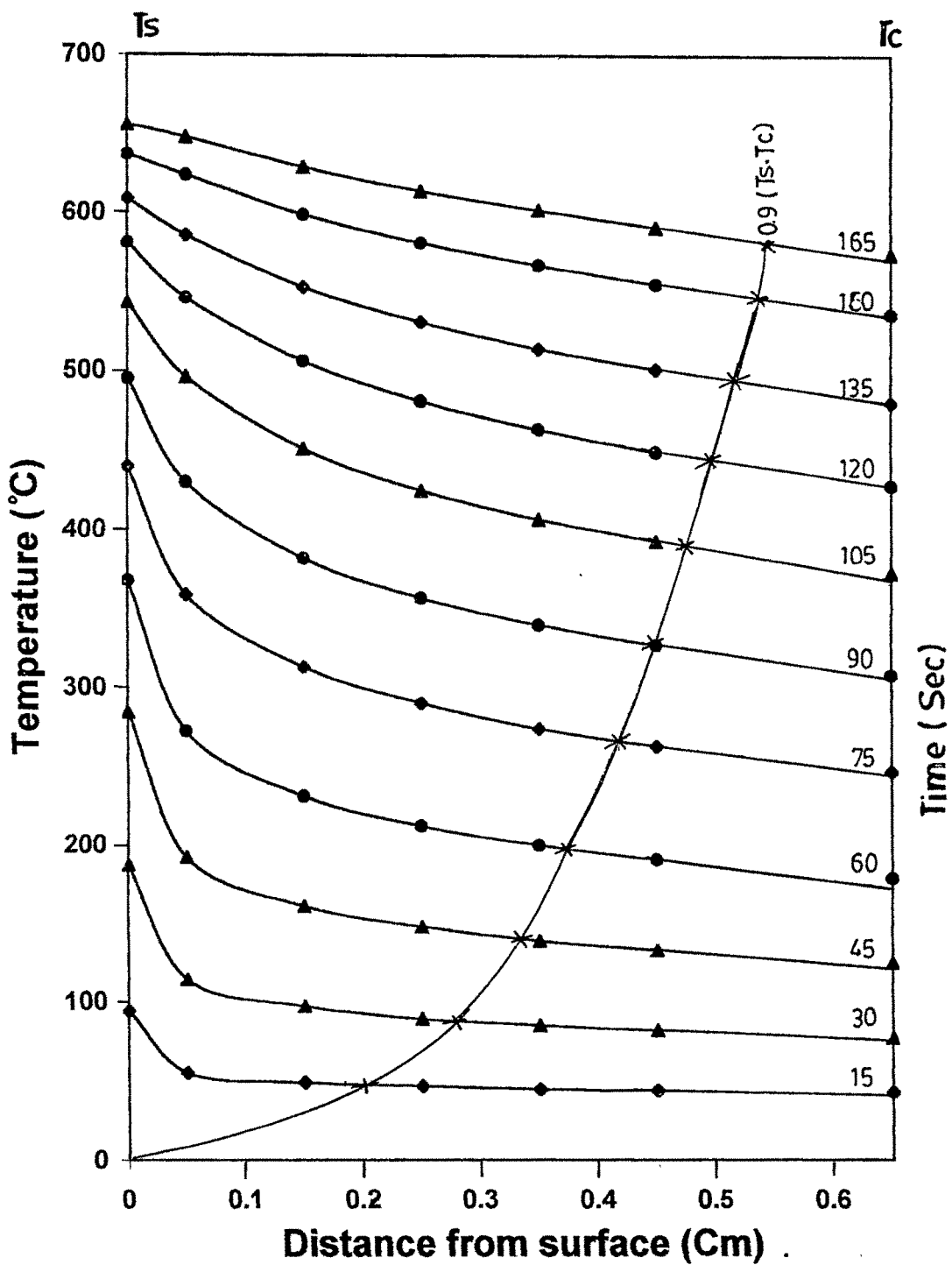
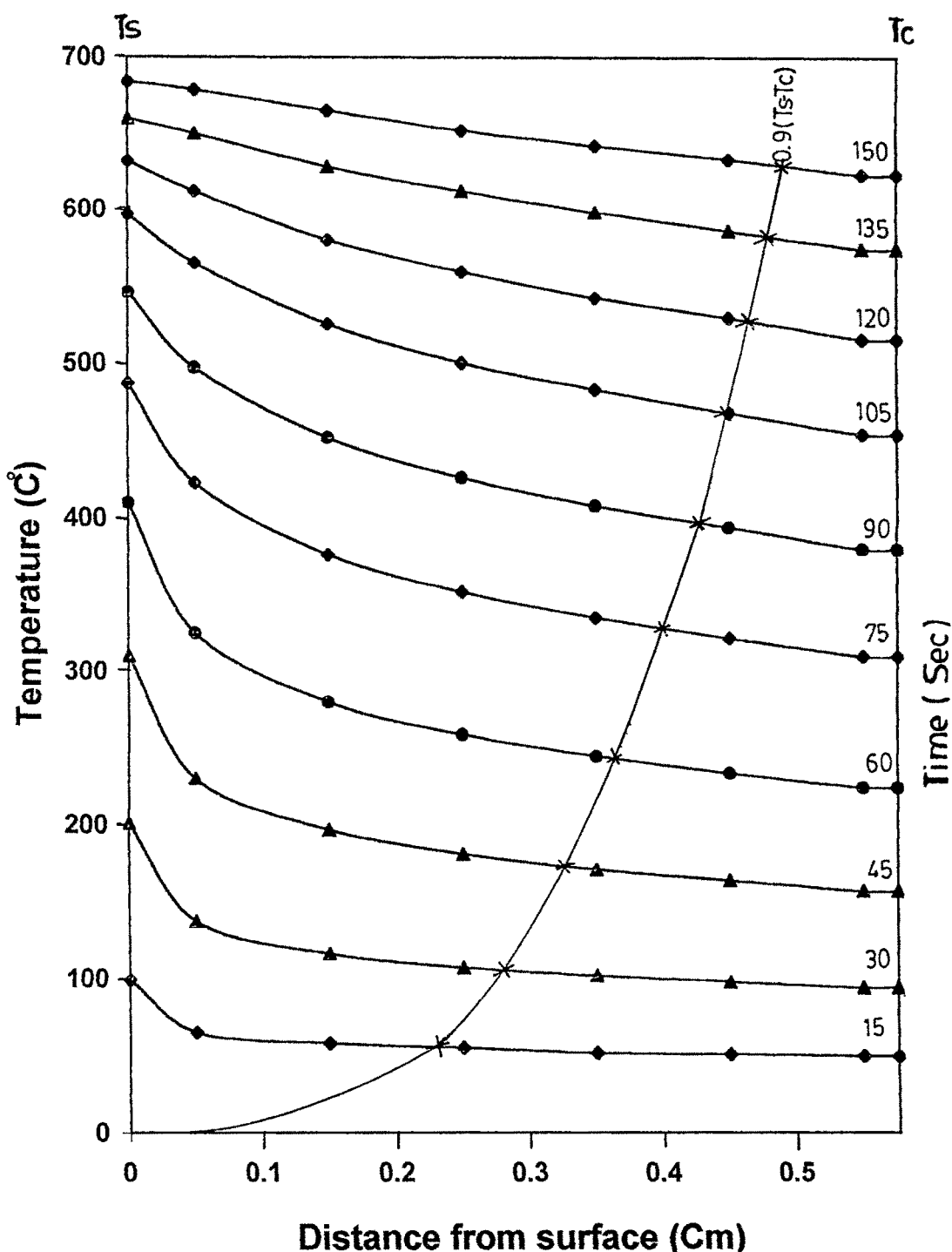


Fig. 4.61 Change in temperature profile and movement of heat front with time (Hand rolled pellet).  
(Pellet size=0.6490cm & Porosity=29.51%)



**Fig. 4.62 Change in temperature profile and movement of heat front with time (Pelletized pellet).**  
**(Pellet size=0.5756cm&Porosity=30.44%)**

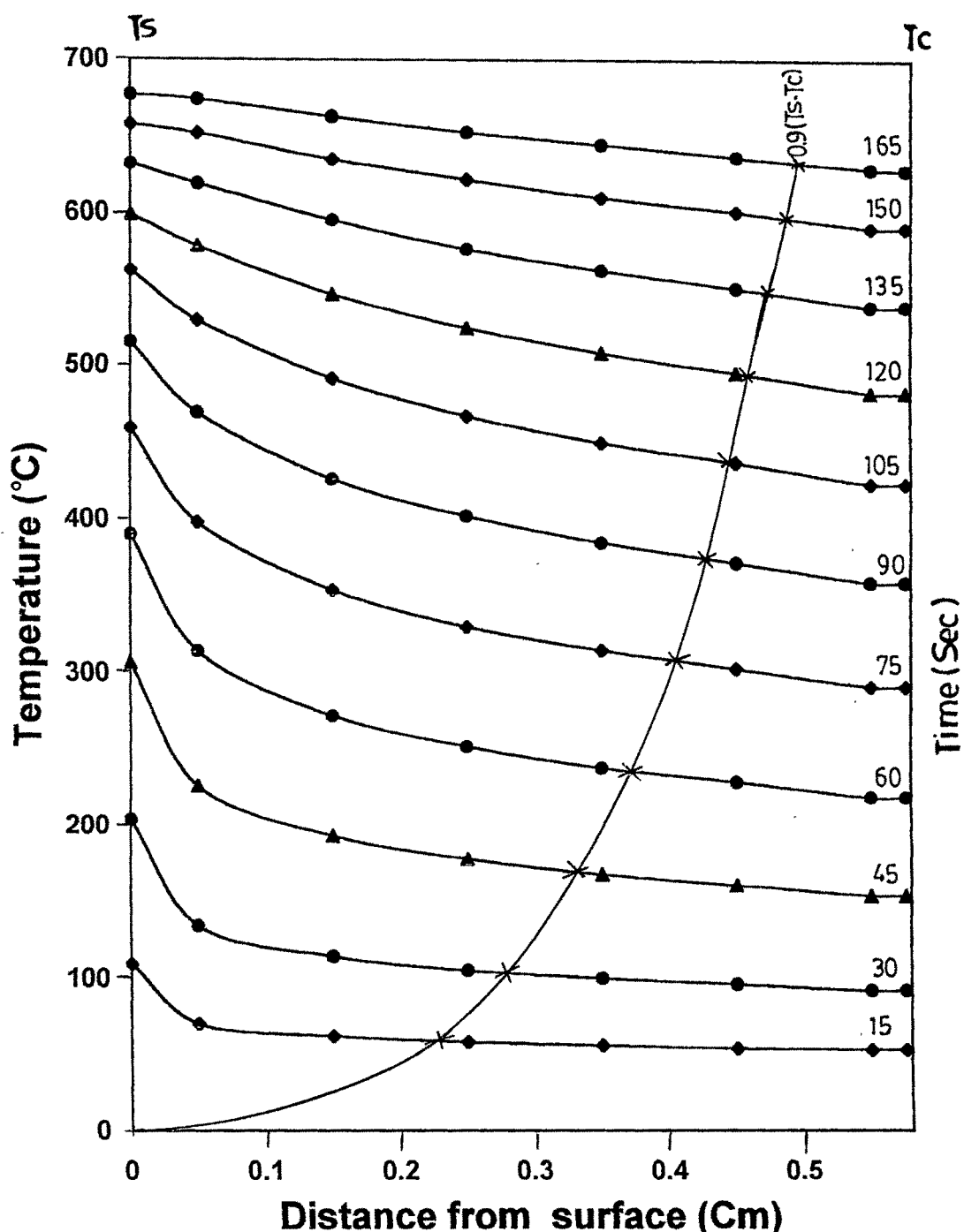
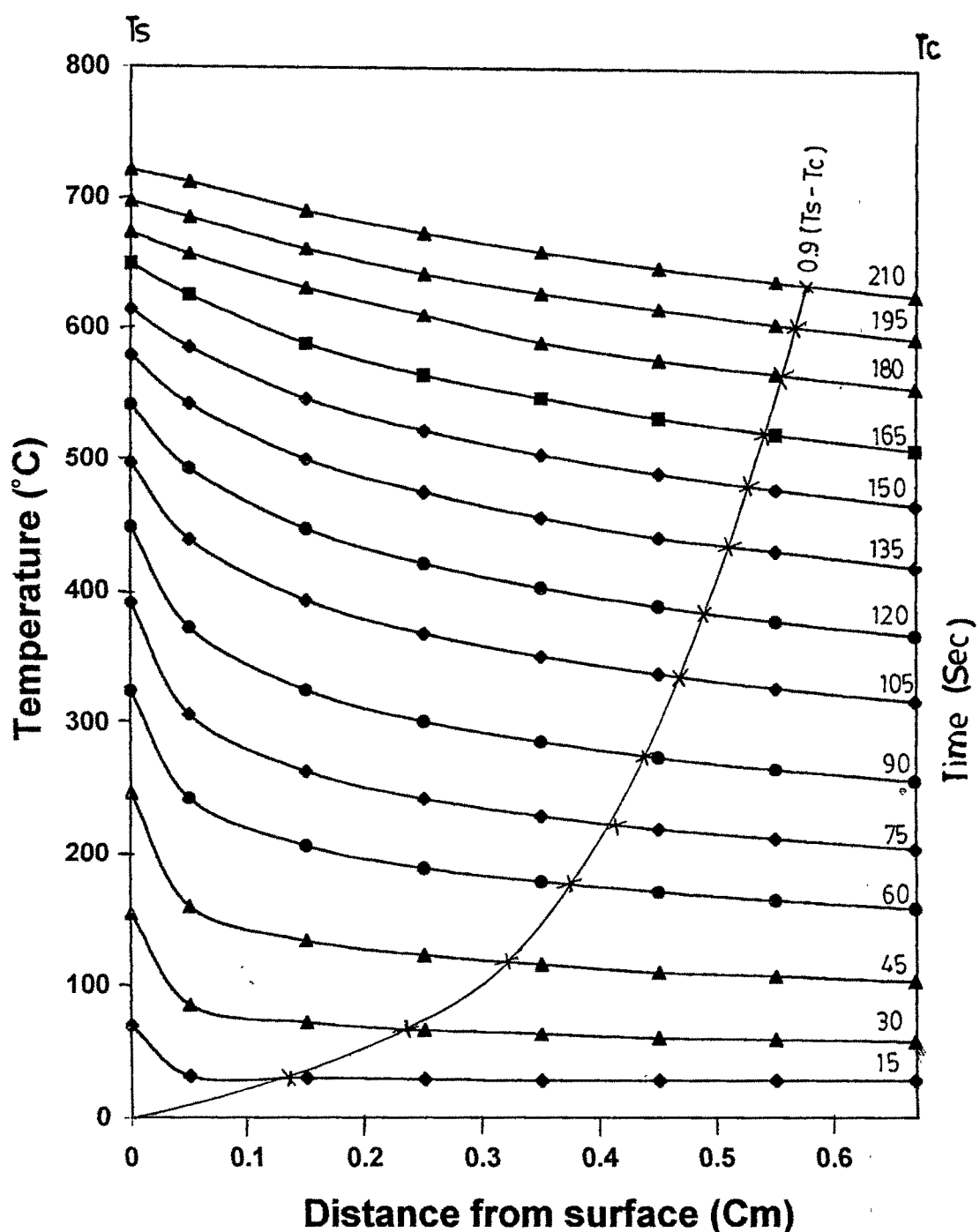


Fig. 4.63 Change in temperature profile and movement of heat front with time (Hand rolled pellet).  
(Pellet size=0.5756cm&Porosity=30.44%)



**Fig. 4.64 Change in temperature profile and movement of heat front with time (Hand rolled pellet).**  
**(Pellet size=0.6690cm&Porosity=34.96%)**

Table No. 4.9

## Calculation of Thermal Diffusivity

$\hat{\alpha}_C = ((dTav/dt)xR) / (3x(\alpha T/dr))$   
 Sample: Iron ore pelletized pellet. Radius=0.6146cm. Density=3650Kg/m<sup>3</sup> Porosity=24.27%.  $T_0=30^\circ\text{C}$

Time (Sec)	$T_s-T_0$ (°C)	$T_s-T_c$ (°C)	$0.9(T_s-T_c)$ (°C)	$k$ (-)	Distance from surface for 0.9( $T_s-T_c$ ) temp.drop (Cm)	$dT/dr$ (°C/Cm)	$T_{av}$ (°C)	$dTav/dt$ (°C/Sec)	Thermal Diffusivity $\times 10^{-7} \text{ m}^2/\text{Sec}$
15	79	61	54.9	0.0172383	0.1966984	279.1075	57.2778		
30	177	113	101.7	0.0149587	0.3042918	334.2187	121.8989	4.78183	2.931
45	273	149	134.1	0.0134561	0.3600518	372.4464	200.7326	5.26912	2.898
60	353	164	147.6	0.0127767	0.4000986	368.9091	279.9726	5.30574	2.946
75	419	158	142.2	0.0130037	0.436604	325.6956	359.9048	4.9885896	3.138
90	473	144	129.6	0.0132142	0.4631314	279.8341	429.6301	4.1234573	3.019
105	516	132	118.8	0.0129839	0.4795469	247.7339	483.6085	3.87741	3.206
120	558	101	90.9	0.0142437	0.503505	180.5345	545.9524	3.274681	3.716
135	588	91	81.9	0.0138212	0.511762	160.0353	581.8489	2.403037	3.076
150	614	70	63	0.0144767	0.524816	120.0421	618.0435	2.16412	3.693
165	635	51	45.9	0.0152836	0.5362116	85.60054	646.7725		
								Avg=3.143x10 <sup>-7</sup>	

Table No. 4.10

**Calculation of Thermal Diffusivity**  
 $\alpha = ((dTav/dt)xR) / (3x (dT/dr))$

Sample: Iron ore pelletized pellet. Radius=0.5854cm. Density=3521Kg/m<sup>3</sup> Porosity=25.87%. To=22°C

Time (Sec)	Ts-To (°C)	Ts-Tc (°C)	0.9(Ts-Tc) (°C)	k (-)	Distance from surface for 0.9(Ts-Tc) temp.drop (Cm)	dT/dr (°C/Cm)	Tav (°C)	dTav/dt (°C/Sec)	Thermal Diffusivity x10 <sup>-7</sup> m <sup>2</sup> /Sec)
15	64	49	44.1	0.0178042	0.193216	228.2419	44.5251		
30	166	113	101.7	0.0128199	0.261177	389.3911	99.3705	4.36106	2.185
45	271	162	145.8	0.0114338	0.314604	463.4397	175.357	5.393049	2.27
60	361	183	164.7	0.0113232	0.36203	454.9347	261.1619	5.73635	2.46
75	435	183	164.7	0.0115448	0.39923	412.5441	347.4475	5.59211	2.645
90	497	167	150.3	0.0121177	0.43047	349.1532	428.9253	4.91559	2.747
105	543	144	129.6	0.0126409	0.453806	285.5895	494.9151	4.11969	2.815
120	582	118	106.2	0.0132982	0.473036	224.50723	552.5161	3.32569	2.89
135	609	91	81.9	0.0140811	0.48905	167.4675	594.6859	2.75578	3.211
150	640	70	63	0.0147532	0.50133	125.6573	635.2895	2.38326	3.7
165	663	52	46.8	0.0154275	0.5113808	91.51693	666.1838	1.64413	3.505
180	677	38	34.2	0.0160005	0.51932937	65.85416	684.6138		
								Avg=2.920x10 <sup>-7</sup>	

Table No. 4.11

## Calculation of Thermal Diffusivity

$$\alpha C = \frac{((dTav/dt) \times R)}{(3 \times (dT/dr))}$$

Radius=0.6283cm. Density=3416Kg/m<sup>3</sup> Porosity=28.08%. To=22°C

Sample: Iron ore pelletized pellet.

Time (Sec)	Ts-To *(°C)	Ts-Tc (°C)	0.9(Ts-Tc) (°C)	K (-)	Distance from surface for 0.9(Ts-Tc) temp.drop (Cm)	dT/dr (°C/Cm)	Tav (°C)	dTav/dt (°C/Sec)	Thermal Diffusivity $\times 10^7$ m <sup>2</sup> /Sec)
15	69.6	56.1	50.49	0.0143752	0.1668076	302.6841	42.7815		
30	172.25	120	108	0.0120485	0.2678323	403.23739	99.1141	4.349827	2.259
45	268	161	144.9	0.011324	0.3358086	431.4957	173.2763	5.3208136	2.583
60	359.25	184.75	166.28	0.0110836	0.3848773	432.04681	258.7385	5.608513	2.719
75	429	182.75	164.48	0.0113778	0.426257	385.8706	341.5317	5.318893	2.887
90	487.25	168.5	151.65	0.0117982	0.458361	330.8527	418.3053	4.743797	3.003
105	534.75	149	134.1	0.012171	0.4824687	277.9458	483.8456	4.03836	3.043
120	573.5	126	113.4	0.0126289	0.5021794	225.8157	539.4561	3.36998826	3.125
135	605.5	104	93.6	0.0130494	0.517704	180.7983	584.9421	2.860497	3.313
150	630.75	73.75	66.38	0.0143082	0.5355983	123.9362	625.271	2.222576	3.756
165	649.25	54.75	49.28	0.0149881	0.5467946	90.1253	651.6194	1.4928763	3.469
180	664	44.5	40.05	0.0150155	0.5531094	72.4088	670.0573		

\* Average of two readings.

$$\text{Avg} = 2.95 \times 10^7$$

Table No. 4.12

## Calculation of Thermal Diffusivity

$\alpha_C = ((dTav/dt) \times R) / (3x(dT/dr))$

Sample: Iron ore pelletized pellet. Radius=0.6294cm. Density=3154Kg/m<sup>3</sup>. Porosity=32.17%.  $T_0=30^\circ\text{C}$

Time (Sec)	$T_s-T_0$ ( $^\circ\text{C}$ )	$T_s-T_c$ ( $^\circ\text{C}$ )	$0.9(T_s-T_c)$ ( $^\circ\text{C}$ )	$k$ (-)	Distance from surface for $0.9(T_s-T_c)$ temp. drop (cm)	$dT/dr$ ( $^\circ\text{C}/\text{cm}$ )	$T_{av}$ ( $^\circ\text{C}$ )	$dTav/dt$ ( $^\circ\text{C}/\text{sec}$ )	Thermal Diffusivity $\times 10^7$ ( $\text{m}^2/\text{sec}$ )
15	57	44	39.6	0.0172574	0.2016481	196.38171	49.6574	3.78431	2.339
30	147	102	91.8	0.0121819	0.2705253	339.3397	96.2549	4.7759	2.238
45	251	158	142.2	0.0102857	0.3177095	447.5786	163.1868	5.2394	2.441
60	336	184	165.6	0.0100362	0.3677056	450.3602	239.5317	5.04267	2.485
75	412	193	173.7	0.0101111	0.407937	425.801	320.3682	4.79066	2.69
90	466	183	164.7	0.0103855	0.4408578	373.5898	390.8117	4.29694	2.871
105	519	164	147.6	0.0109717	0.4701412	313.9482	464.0881	3.27733	2.601
120	558	144	129.6	0.0112878	0.490319	264.3177	519.7199	2.81346	2.628
135	588	126	113.4	0.0114107	0.5048377	224.6266	562.4079	1.78.2469	3.034
150	616	103	92.7	0.0119234	0.520065	134.88564	604.1238	2.5778	3.192
165	640	80	72	0.0126026	0.5337855	134.88564	639.7418	2.05208	
180	657	59	53.1	0.0133897	0.54574	97.29908	665.6863		
Avg=2.686x10 <sup>-7</sup>									

Table No. 4.13

## Calculation of Thermal Diffusivity

$$\infty = ((dTav/dt)xR) / (3x(dT/dr))$$

Sample: Iron ore pelletized pellet. Radius=0.6294cm. Density=3154Kg/m<sup>3</sup> Porosity=32.17%. To=30°C

Time (Sec)	Ts-To (°C)	Ts-Tc (°C)	0.9(Ts-Tc) (°C)	k (-)	Distance from surface for 0.9(Ts-Tc) temp. drop (Cm)	dT/dr (°C/Cm)	Tav (°C)	dTav/dt (°C/Sec)	Thermal Diffusivity x10 (m <sup>2</sup> /Sec)
15	63	50	45	0.0154074	0.1799553	250.0621	49.8436	4.218143	2.5
30	159	109	98.1	0.0125852	0.2770917	354.0344	103.3648	5.361523	2.521
45	266	163	146.7	0.0108832	0.3287314	446.2609	176.3879	5.765249	2.726
60	360	188	169.2	0.0108277	0.3813746	443.6583	264.2105	5.36409	2.704
75	438	194	174.6	0.0108581	0.4195557	416.1545	349.3454	4.586426	2.633
90	497	183	164.7	0.0111011	0.4505913	365.5197	425.1332	4.085766	2.737
105	541	165	148.5	0.0113092	0.474083	313.2362	486.9382	3.45004	2.898
120	581	138	124.2	0.0119791	0.4971934	249.8021	547.7062	2.7730756	2.884
135	609	115	103.5	0.0123473	0.5130961	201.7165	590.4394	2.0918226	3.007
150	634	86	77.4	0.0133181	0.5302987	145.9554	630.8985	116.7704	7
165	649	70	63	0.0134965	0.5395202	Avg=2.763x10	653.1941		

Table No. 4.14

## Calculation of Thermal Diffusivity

 $\infty = ((dTav/dt) \times R) / (3 \times (dT/dr))$   
 Radius=0.6360cm. Density=3057Kg/m<sup>3</sup> Porosity=33.54% To=20°C

Time (Sec)	Ts-To (°C)	Ts-Tc (°C)	0.9(Ts-Tc) (°C)	k (-)	Distance from surface for 0.9(Ts-Tc) temp. drop (Cm)	dT/dr (°C/Cm)	Tav (°C)	dTav/dt (°C/Sec)	Thermal Diffusivity $\times 10^7$ (m <sup>2</sup> /Sec)
15	74	59	53.1	0.0151018	0.1780537	298.22463	43.0461		
30	167	117	105.3	0.0118606	0.2679049	393.04992	93.9607	4.5137	2.435
45	269	166	149.4	0.0107271	0.3293379	453.63743	178.457	5.04461	2.358 ✓
60	356	192	172.8	0.0102905	0.3761525	459.38814	245.2991	5.0609	2.336 ✓
75	430	194	174.6	0.0106123	0.4202249	415.99118	330.2855	5.3802	2.742 ✓
90	487	180	162	0.0110589	0.4547622	356.2301	406.7048	4.7524	2.828 ✓
105	533	159	143.1	0.0115201	0.481446	297.2296	472.8597	3.9938	2.849 ✓
120	569	136	122.4	0.0119268	0.501901	243.8728	526.5178	3.3164	2.883 ✓
135	600	113	101.7	0.0123669	0.5183	196.0935	572.3514	2.8323	3.062 ✓
150	629	95	85.5	0.0126017	0.5308062	161.0757	611.4863	2.3091	3.039 ✓
165	650	76	68.4	0.0130075	0.5421	126.176	641.6258	1.7536	2.946 ✓
180	665	58	52.2	0.0135519	0.5523846	94.4994	664.0947	1.4065	3.155
195	678	43	38.7	0.0141433	0.5612822	68.9493	683.8213		
								Avg=2.783x10 <sup>-7</sup>	

Table No. 4.15

## Calculation of Thermal Diffusivity

$$\infty = \frac{((dTav/dt) \times R)}{(3 \times (dT/dr))}$$

Sample: Iron ore pelletized pellet. Radius=0.6154cm. Density=3030Kg/m<sup>3</sup> Porosity=34.13%. To=20°C

Time (Sec)	Ts-To (°C)	Ts-Tc (°C)	0.9(Ts-Tc) (°C)	K (-)	Distance from surface for 0.9(Ts-Tc) temp.drop (Cm)	dT/dr (°C/Cm)	Tav (°C)	dTau/dt (°C/Sec)	Thermal Diffusivity $\times 10^7$ (m <sup>2</sup> /Sec)
15	68	50	45	0.0204989	0.2304656	195.2569	46.9143	3.152	
30	164	103	92.7	0.0155045	0.3115831	297.5129	107.2377	4.571293	
45	272	154	138.6	0.0126411	0.3492728	396.8245	184.0531	5.3544306	2.768 ✓
60	357	171	153.9	0.0122678	0.393997	390.6184	267.8706	5.620292	2.951 ✓
75	433	173	155.7	0.0122326	0.4283305	363.5043	352.6619	5.386256	3.039 ✓
90	494	161	144.9	0.012457	0.4561721	317.6433	429.4582	4.810383	3.107 ✓
105	542	138	124.2	0.0130286	0.4805502	258.4537	496.9734	3.96927	3.15 ✓
120	579	117	105.3	0.013326	0.4974853	211.6645	548.5369	3.26004	3.159 ✓
135	610	90	81	0.0141751	0.5147098	157.3702	594.7747	2.699647	3.519
150	634	67	60.3	0.0149823	0.5282317	114.1545	629.5258		
								Avg=3.03 x10 <sup>-7</sup>	

Table No. 4.16

**Calculation Of Thermal Diffusivity**

$$\infty = ((dTav/dt) \times R) / (3 \times (dT/dr))$$

Sample: Iron ore pelletized pellet. Radius=0.6154cm. Density=3030Kg/m<sup>3</sup>

T<sub>s</sub>-T<sub>o</sub>=34.13%. T<sub>o</sub>=20°C

Time (Sec)	T <sub>s</sub> -T <sub>o</sub> (°C)	T <sub>s</sub> -T <sub>c</sub> (°C)	0.9(T <sub>s</sub> -T <sub>c</sub> ) (°C)	k (-)	Distance from surface for 0.9(T <sub>s</sub> -T <sub>c</sub> ) temp. drop (Cm)	dT/dr (°C/Cm)	T <sub>av</sub> (°C)	dTav/dt (°C/Sec)	Thermal Diffusivity $\times 10^7$ m <sup>2</sup> /Sec)
15	67	48	43.2	0.0222327	0.2464384	175.2973	48.1819		
30	164	101	90.9	0.0161582	0.3194752	284.5291	109.5951	4.673533	3.369
45	264	141	126.9	0.0139375	0.36667401	346.0216	188.3879	5.38057	3.189
60	353	163	146.7	0.0128786	0.4018953	365.0204	271.0122	5.4512466	3.063
75	420	157	141.3	0.0131201	0.43844313	322.2853	351.9253	5.2714166	3.355
90	481	143	128.7	0.013478	0.46662067	276.0578	429.1547	4.69855	3.491
105	530	125	112.5	0.0137577	0.48666762	231.1599	492.8818	3.70217	3.285
120	567	110	99	0.0136657	0.500055	197.9782	540.2198	2.92287	3.028
135	598	94	84.6	0.0137059	0.5116661	165.3463	580.5679	2.60778	3.235
150	626	74	66.6	0.0142352	0.5241186	127.07062	618.4532	2.26008	3.649
165	648	55	49.5	0.0149488	0.535305	92.47078	648.3703	1.696523	3.763
180	664	41	36.9	0.0154706	0.5437445	67.86276	669.3489		
							Avg=3.235x10 <sup>-7</sup>		



Table No. 4.17

**Calculation of Thermal Diffusivity**

$$\alpha_c = \frac{(dT_{av}/dt) \times R}{(3 \times (dT/dr))}$$

Sample: Iron ore pelletized pellet.  
Radius=0.6839cm.  
Density=29141Kg/m<sup>3</sup>  
Porosity=34.51%.

To=20°C

Time (Sec)	T <sub>s</sub> -T <sub>o</sub> (°C)	T <sub>s</sub> -T <sub>c</sub> (°C)	0.9(T <sub>s</sub> -T <sub>c</sub> ) (°C)	k (-)	Distance from surface for 0.9(T <sub>s</sub> -T <sub>c</sub> ) temp. drop (Cm)	dT/dr (°C/Cm)	T <sub>av</sub> (°C)	dT <sub>av</sub> /dt (°C/Sec)	Thermal Diffusivity x10 <sup>7</sup> (m <sup>2</sup> /Sec)
15	63	51.5	46.35	0.0134368	0.1683565	275.3088	37.9341	4.00022	2.361
30	163	117	105.3	0.0110525	0.2726067	386.2708	88.9481	5.21275	2.521
45	269	174	156.6	0.0096812	0.332223	471.3701	157.9406	2.942	2.942
60	365	203	182.7	0.0097781	0.3943644	463.2771	245.3307	5.7949	3.178
75	445	206	185.4	0.0102693	0.4460486	415.6498	337.2914	3.178	3.178
90	507	193	173.7	0.0107313	0.4842825	358.6749	419.1757	4.9797	3.165
105	555	174	156.6	0.0110467	0.5118204	305.9667	486.6831	4.1755	3.111
120	591	146	131.4	0.0116517	0.5368039	244.7821	544.4413	3.5153	3.274
135	619	115	103.5	0.0124679	0.5585891	185.2882	592.1407	2.6556	3.267
150	641	97	87.3	0.0125887	0.5706664	152.979	624.1093	1.792	2.67
165	655	81	72.9	0.0126677	0.58048293	125.5851	645.9009	1.26111	2.289
180	667	72	64.8	0.0123673	0.5861951	110.5434	661.9427	0.951713	Avg=3.016x10 <sup>-7</sup>

Table No. 4.18

**Calculation of Thermal Diffusivity**  
 $\infty_c = ((dTav/dt)xR) / (3x(dT/dr))$   
 Sample: Iron ore pelletized pellet. Radius=0.6921cm. Density=2812Kg/m<sup>3</sup> Porosity=35.36%. To=20°C

Time (Sec)	T <sub>s</sub> -T <sub>o</sub> (°C)	T <sub>s</sub> -T <sub>c</sub> (°C)	0.9(T <sub>s</sub> -T <sub>c</sub> ) (°C)	k (-)	Distance from surface for 0.9(T <sub>s</sub> -T <sub>c</sub> ) temp. drop (Cm)	dT/dr (°C/Cm)	T <sub>av</sub> (°C)	dTav/dt (°C/Sec)	Thermal Diffusivity $\times 10^7$ (m <sup>2</sup> /Sec)
15	65.5	52.5	47.25	0.0147491	0.1889362	250.08442	40.122	4.4015	3.046
30	149	105.5	94.95	0.0115078	0.2848328	333.3534	84.9447		3.004 ✓
45	280	174	156.6	0.0105718	0.35552633	440.7998	172.1674	5.7406	
60	372	200	180	0.0103429	0.4103467	438.6534	257.1639	5.8242	3.063 ✓
75	452	204.5	184.05	0.0105748	0.4566611	403.0341	346.8947	5.5318	3.166 ✓
90	512	195	175.5	0.0107258	0.4900078	358.1576	423.1191	4.7697	3.072 ✓
105	558	174	156.6	0.0110981	0.518632	301.9482	489.9863	3.7425	2.859 ✓
120	588	155	139.5	0.0111108	0.5371075	259.7245	535.3934	3.1176	2.769 ✓
135	617.5	127.5	114.75	0.0116856	0.5579181	205.6753	583.5154	2.7725	3.11 ✓
150	637	100	90	0.0123439	0.5754945	156.3872	618.5691	2.0873	3.079 ✓
165	653	76	68.4	0.0130354	0.5901129	115.91	646.1345	1.5467	3.078 ✓
180	664	57	51.3	0.0136402	0.601652	85.2652	664.9701		
Avg=3.062x10 <sup>-7</sup>									

Table No. 4.19

## Calculation of Thermal Diffusivity

$$\infty = \frac{((dTav/dt)xR)}{(3x(dT/dr))}$$

Radius=0.6921cm. Density=2812Kg/m<sup>3</sup>. Porosity=35.65%. To=20°C

Time (Sec)	T <sub>s</sub> -T <sub>o</sub> (°C)	T <sub>s</sub> -T <sub>c</sub> (°C)	0.9(T <sub>s</sub> -T <sub>c</sub> ) (°C)	k (-)	Distance from surface for 0.9(T <sub>s</sub> -T <sub>c</sub> ) temp. drop (Cm)	dT/dr (°C/Cm)	Tav (°C)	dTav/dt (°C/Sec)	Thermal Diffusivity x10 <sup>-7</sup> (m <sup>2</sup> /Sec)
15	46	35.4	31.86	0.0174619	0.2242577	142.0687	36.1903		
30	128	86	77.4	0.0132561	0.3161845	244.7998	81.6704	3.6351	3.426
45	222	134	120.6	0.0112186	0.367934	327.7762	145.2441	4.4697	3.146 ✓
60	307	165	148.5	0.0103483	0.4104469	361.8008	215.763	4.8173	3.072 ✓
75	379	176	158.4	0.0102273	0.4506469	351.4947	289.7631	4.8386	3.176 ✓
90	440	174	156.6	0.0103018	0.483555	323.8515	360.9226	4.5212	3.221 ✓
105	489	161	144.9	0.0105805	0.511677	283.1865	425.3995	3.8471	3.134 ✓
120	525	144	129.6	0.0107799	0.5331133	243.1003	476.3358	3.1677	3.006 ✓
135	557	128	115.2	0.0108928	0.5495263	209.6351	520.4311	2.6458	2.912 ✓
150	583	114	102.6	0.0108799	0.5618223	182.62	555.7109	2.2852	2.887 ✓
165	605	94	84.6	0.0112844	0.5760752	146.8558	588.9889	1.911	3.002 ✓
180	623	82	73.8	0.0112657	0.5845758	126.2492	613.0398		
								Avg=3.02 x10 <sup>-7</sup>	

Table No. 4.20

## Calculation of Thermal Diffusivity

 $\infty C = \frac{(dTav/dt) \times R}{(3x (dT/dr))^3}$   
 Radius=0.7863cm. Density=2654Kg/m<sup>3</sup> Porosity=38.70%. To=20°C

Time (Sec)	Ts-To (°C)	Ts-Tc (°C)	0.9(Ts-Tc) (°C)	k (-)	Distance from surface for 0.9(Ts-Tc) temp.drop (cm)	dT/dr (°C/Cm)	Tav (°C)	dTav/dt (°C/Sec)	Thermal Diffusivity $\times 10^7$ (m <sup>2</sup> /Sec)
15	66	57	51.3	0.0097735	0.1292998	396.75235	34.4419		
30	163	122	109.8	0.0096576	0.2796217	392.67338	82.7596	3.66963	2.449
45	261	177	159.3	0.0086304	0.3532627	450.9392	144.5309	4.52751	2.632
60	348	209	188.1	0.0084978	0.4203962	447.4351	218.5848	5.0344	2.949
75	420	219.5	197.55	0.0086521	0.4761859	414.8589	295.5629	4.9139	3.104
90	477	216	194.4	0.0088026	0.518592	374.8611	366.0018	4.42649	3.095
105	521	202	181.8	0.0090236	0.5532737	328.5895	428.3575	3.8862	3.099
120	555	181	162.9	0.0093372	0.5827451	279.53903	482.5856	3.32677	3.119
135	585	162.5	146.25	0.0094884	0.6041702	242.06754	528.1578	2.69126	2.914
150	608	146	131.4	0.0095104	0.6200497	211.9184	563.3233	2.35007	2.907
165	626	118	106.2	0.0101131	0.6411342	165.64402	598.6598	1.95662	3.096
180	640	101	90.9	0.0102575	0.6535098	139.0951	622.025		
								Avg=2.991x10 <sup>-7</sup>	

Table No. 4.21

## Calculation of Thermal Diffusivity

$$\alpha = \frac{((dTav/dt) \times R)}{(3x(dT/dr))}$$

Sample: Iron oxide hand rolled pellet. Radius=0.5672cm. Density=3453Kg/m<sup>3</sup> Porosity=28.36% T<sub>0</sub>=30°C

Time (Sec)	T <sub>s</sub> -T <sub>0</sub> (°C)	T <sub>s</sub> -T <sub>c</sub> (°C)	0.9(T <sub>s</sub> -T <sub>c</sub> ) (°C)	k (~)	Distance from surface for 0.9(T <sub>s</sub> -T <sub>c</sub> ) temp. drop (Cm)	dT/dr (°C/Cm)	T <sub>av</sub> (°C)	dTav/dt (°C/Sec)	Thermal Diffusivity x10 <sup>7</sup> (m <sup>2</sup> /Sec)
15	69	51	45.9	0.0201521	0.2093377	219.2629	56.7583	4.8626	2.202
30	188	124	111.6	0.013872	0.2673201	417.4747	122.4484		2.254 ✓
45	293	169	152.1	0.0122283	0.3163193	480.8432	202.6375		2.446 ✓
60	381	182	163.8	0.0123132	0.3636966	450.3754	294.4321	5.8268	
75	450	177	159.3	0.0124413	0.3970661	401.1927	377.4418	5.3475	2.52 ✓
90	504	154	138.6	0.01311736	0.4270608	324.5434	454.858	4.7468	2.765 ✓
105	548	127	114.3	0.0139247	0.449789	254.1199	519.8446	3.6495	2.715 ✓
120	579	106	95.4	0.0141488	0.4640593	205.5772	564.3428	2.9548	2.717 ✓
135	607	75	67.5	0.0154892	0.4814744	140.1944	608.4877	2.4037	3.242
150	628	59	53.1	0.0157666	0.4905015	108.2565	636.4536		
								Avg=2.569x10 <sup>-7</sup>	

Table No. 4.22

## Calculation of Thermal Diffusivity

$$\infty = \frac{((dT/dt)xR)}{(3x(dT/dr))} \quad (3x(dT/dr))^3$$

Sample: iron oxide hand rolled pellet. Radius=0.6490cm. Density=3278Kg/m<sup>3</sup> Porosity=29.50% T<sub>0</sub>=30°C

Time (Sec)	T <sub>s</sub> -T <sub>0</sub> (°C)	T <sub>s</sub> -T <sub>c</sub> (°C)	0.9(T <sub>s</sub> -T <sub>c</sub> ) (°C)	k (-)	Distance from surface for 0.9(T <sub>s</sub> -T <sub>c</sub> ) temp.drop ( Cm)	dT/dr ( °C/Cm)	T <sub>av</sub> ( °C)	dT <sub>av</sub> /dt ( °C/Sec)	Thermal Diffusivity x10 <sup>-7</sup> m <sup>2</sup> /Sec
15	64	51	45.9	0.0151372	0.1821459	251.9958	49.94		
30	157	110	99	0.0118588	0.2733501	362.1729	98.5763	3.8717	2.313
45	254	159	143.1	0.0104096	0.3300313	433.5952	166.0909	4.5768	2.283 ✓
60	338	189	170.1	0.0096883	0.3724812	456.6658	236.8799	5.0786	2.406 ✓
75	410	193	173.7	0.0100462	0.4195354	414.0294	318.449	4.9924	2.609 ✓
90	465	187	168.3	0.0101214	0.450606	373.4971	386.6531	4.5188	2.617 ✓
105	513	170	153	0.0105188	0.4790038	319.4129	454.0123	4.0006	2.71 ✓
120	551	153	137.7	0.0106775	0.4987122	276.1112	506.6707	3.2577	2.552 ✓
135	579	129	116.6	0.0111221	0.5176801	224.2698	551.7428	2.9939	2.888 ✓
150	607	101	90.9	0.0119561	0.5365457	169.4171	596.488	2.4481	3.126 ✓
165	626	82	73.8	0.012319	0.5483898	134.5758	628.1857		
								Avg=2.649x10 <sup>-7</sup>	

Table No. 4.23

**Calculation of Thermal Diffusivity**  
 $\infty = \frac{(\partial T_{av}/\partial t) \times R}{(3 \times (\partial T/\partial r))}$   
 Sample: Iron oxide hand rolled pellet.  
 Radius=0.5756cm. Density=3340Kg/m<sup>3</sup> Porosity=30.44%  $T_0=30^\circ C$

Time (Sec)	$T_s-T_0$ (°C)	$T_s-T_c$ (°C)	$0.9(T_s-T_c)$ (°C)	k (-)	Distance from surface for 0.9( $T_s-T_c$ ) temp. drop	$\partial T/\partial r$ (°C/Cm)	$T_{av}$ (°C)	$\partial T_{av}/\partial t$ (°C/Sec)	Thermal Diffusivity $\times 10^7$ m <sup>2</sup> /Sec)
15	79	56	50.4	0.0229397	0.2362787	213.3074	63.8522		
30	174	112	100.8	0.0146852	0.28164546	357.8968	118.9707	4.559985	2.445
45	276	152	136.8	0.013256	0.33470308	408.7207	200.6516	5.39486	2.533
60	360	171	153.9	0.0124073	0.3702472	415.6682	280.8165	5.37831	2.478
75	429	168	151.2	0.0124999	0.4035858	374.6415	362.0007	5.07563	2.599
90	485	156	140.4	0.0126033	0.4280973	327.9628	433.0853	4.44554	2.6
105	532	139	125.1	0.0127825	0.44741699	279.6049	495.3683	3.81676	2.619
120	569	117	105.3	0.0131809	0.464665	226.8094	547.8712	3.29967	2.791
135	602	94	84.6	0.0137553	0.4788839	176.66017	594.3589	2.832626	3.076
150	628	68	61.2	0.0148202	0.49327349	124.0701	632.8502	2.168159	3.353
165	647	49	44.1	0.0156396	0.50372017	87.547707	659.4036		
								Avg=2.671x10 <sup>-7</sup>	

Table No. 4.24

**Calculation of Thermal Diffusivity**  
 $\infty = ((dTav/dt) \times R) / (3 \times (dT/dr))$   
 Sample: Iron oxide hand rolled pellet. Radius=0.5756cm. Density=3340Kg/m<sup>3</sup> Porosity=30.44% T<sub>0</sub>=30 °C

Time (Sec)	T <sub>s</sub> -T <sub>0</sub> (°C)	T <sub>s</sub> -T <sub>c</sub> (°C)	0.9(T <sub>s</sub> -T <sub>c</sub> ) (°C)	k (-)	Distance from surface for 0.9(T <sub>s</sub> -T <sub>c</sub> ) temp. drop (Cm)	dT/dr (°C/Cm)	T <sub>av</sub> (°C)	dTav/dt (°C/Sec)	Thermal Diffusivity $\times 10^7$ (m <sup>2</sup> /Sec)
15	69	49	44.1	0.0228191	0.23536782	187.4145	59.4145		
30	170	106	95.4	0.0157176	0.293522928	324.38787	121.1748	4.833773	2.86 ✓
45	280	153	137.7	0.0134341	0.336882493	408.75125	204.4282	5.632705	2.647 ✓
60	380	185	166.5	0.01199692	0.365065933	456.0832	290.156	6.031753	2.537 ✓
75	457	177	159.3	0.0126471	0.4051725	393.16781	385.3808	5.62282	2.744 ✓
90	516	166	149.3	0.0126013	0.4280746	349.00776	458.8406	4.8024273	2.64 ✓
105	567	143	128.7	0.0131192	0.450221573	285.8584	529.4535	4.1011206	2.753 ✓
120	602	117	105.3	0.0136567	0.4676071	225.18905	581.8742	3.2468106	2.766 ✓
135	630	86	77.4	0.0147509	0.48471379	159.68225	626.8579	2.6662046	3.204
150	654	61	54.9	0.0158149	0.497979744	110.24528	661.8603		
								Avg=2.707x10 <sup>-7</sup>	

Table No. 4.25

## Calculation of Thermal Diffusivity

$\alpha_C = \frac{((dT_{av}/dt) \times R)}{(3 \times (dT/dr))}$        $R = 0.6690 \text{ cm.}$        $Density = 2973 \text{ Kg/m}^3$        $\text{Porosity} = 34.95\%$        $T_0 = 25^\circ\text{C}$

Sample: Iron oxide hand rolled pellet.

Time (Sec)	Ts-To (°C)	Ts-Tc (°C)	0.9(Ts-Tc) (°C)	K (-)	Distance from surface for 0.9(Ts-Tc) temp.drop (Cm)	dT/dr (°C/Cm)	Tav (°C)	dTav/dt (°C/Sec)	Thermal Diffusivity $\times 10^7$ [m <sup>2</sup> /Sec]
15	44	41	36.9	0.0047078	0.0318912	372.2758	29.7966	3.65396	2.189
30	129	97	87.3	0.0095033	0.2345035	396.2165	73.5867	4.154	2.574
45	221	143	128.7	0.0096737	0.3248224	382.3843	210.8068	4.28998	2.502
60	299	165	148.5	0.0099083	0.3883528	408.8711	268.1148	3.9743	2.168
75	366	187	168.3	0.008954	0.4116232	392.146	330.0353	4.2676	2.427
90	423	192	172.8	0.008776	0.4406522	342.1908	396.1431	3.9765	2.591
105	472	180	162	0.009181	0.4734363	318.6371	449.3303	3.4823	2.437
120	516	174	156.6	0.0090587	0.4914834	282.3686	500.6135	3.1157	2.461
135	554	160	144	0.0091998	0.5099718	254.3968	542.8027	2.8763	2.521
150	589	148	133.2	0.009208	0.5235914	238.3009	586.902	2.9229	2.735
165	624	141	126.9	0.0090144	0.53252	175.7761	630.4896	2.3378	2.966
180	648	108	97.2	0.0099542	0.5529771	168.02057	657.0361	Avg=2.491x10 <sup>-7</sup>	
195	672	104	93.6	0.00956855	0.55707465				

**Table No.4.26**  
**Variation of thermal diffusivity/conductivity with porosity (Iron ore pelletized pellet)**

Serial No.	Weight of Pellet (gram)	Size (cm)	Volume (cm <sup>3</sup> )	Density (Kg/m <sup>3</sup> )	Firing treatment (°C)	True density (Kg/m <sup>3</sup> )	Theoretical Volume (Cm <sup>3</sup> )	Porosity (%)	Ratio of specific volume	Thermal diffusivity (m <sup>2</sup> /sec)	Thermal conductivity (W/mK)
1	3.5496	0.6146	0.9724476	3650	1275	(4820)	24.27	0.736432	1.3205	$3.143 \times 10^{-7}$	1.201
2	2.9585	0.5854	0.840324	3521	1250	(4750)	25.87	0.622842	1.3492	$2.920 \times 10^{-7}$	1.076
3	3.5496	0.6283	1.03894	3416	1250	(4750)	28.08	0.747284	1.3903	$2.950 \times 10^{-7}$	1.055
4	3.2939	0.6294	1.044405	3154	1215	(4650)	32.17	0.708366	1.4744	$2.686 \times 10^{-7}$	0.887
5	3.2939	0.6294	1.044405	3154	1215	(4650)	32.17	0.708366	1.4744	$2.763 \times 10^{-7}$	0.9124
6	3.2939	0.636	1.077606	3057	1200	(4600)	33.54	0.716065	1.5049	$2.783 \times 10^{-7}$	0.8907
7	2.9585	0.6154	0.97625	3030	1200	(4600)	34.13	0.643152	1.5179	$3.03 \times 10^{-7}$	0.9616
8	2.9585	0.6154	0.97625	3030	1200	(4600)	34.13	0.643152	1.5179	$3.235 \times 10^{-7}$	1.027
9	3.9043	0.6839	1.33988	2914	1120	(4450)	34.51	0.877371	1.5272	$3.016 \times 10^{-7}$	0.9217
10	3.9043	0.6921	1.3886572	2812	0950	(4350)	35.36	0.893432	1.5543	$3.062 \times 10^{-7}$	0.9015
11	3.9043	0.6921	1.3886572	2812	1030	(4370)	35.65	0.89754	1.5472	$3.020 \times 10^{-7}$	0.8891
12	5.45	0.7863	2.036355	2676	1030	(4370)	38.76	1.2471395	1.6328	$2.991 \times 10^{-7}$	0.838

**Table No.4.27 Variation of thermal diffusivity/conductivity with porosity. ( Iron oxide hand rolled pellet)**

Serial No.	Weight of Pellet (gram)	Size (cm)	Volume (cm <sup>3</sup> )	Density (Kg/m <sup>3</sup> )	Firing treatment (°C)	True density (Kg/m <sup>3</sup> )	Porosity (%)	Theoretical volume (Cm <sup>3</sup> )	Ratio of specific volume	Thermal diffusivity (m <sup>2</sup> /sec)	Thermal conductivity (W/mK)
1	2.6393	0.5672	0.764359	3453	1275 (4820)	0.547573	28.36	0.547573	1.3959	2.569x10 <sup>-7</sup>	0.9288
2	3.753	0.649	1.145045	3278	1225 (4650)	0.807097	29.50	0.807097	1.4187	2.649x10 <sup>-7</sup>	0.9092
3	2.6393	0.5756	0.798823	3304	1250 (4750)	0.555642	30.44	0.555642	1.4377	2.671x10 <sup>-7</sup>	0.924
4	2.6393	0.5756	0.798823	3304	1250 (4750)	0.555642	30.44	0.555642	1.4377	2.707x10 <sup>-7</sup>	0.9364
5	3.753	0.669	1.254201	2992	1200 (4600)	0.815869	34.95	0.815869	1.5373	2.491x10 <sup>-7</sup>	0.7803

#### 4.2.2 Model fitting:

A simple expression for effective thermal conductivity of iron ore pellet to its porosity is useful in solving the heat transfer problems. Many expression used for an agglomerates are listed by Akiyama and co-workers. They explained their results by applying unit cell model originally proposed by Luikov.<sup>49</sup> In the present investigation attempts were made to correlate the effective thermal conductivity observed and voids fraction 'e', by different model equations indicated in chapter 2 of this text. The radiative heat transfer within pore is neglected in these equations as mentioned earlier. The equations tried are,

$$(a) \quad Ke = e.Kg + (1-e) Ks \quad (4.22) \quad \text{Ref}$$

$$(b) \quad Ke = (e/kg + (1-e) / Ks)^{-1} \quad (4.23) \quad \text{Ref}$$

$$(c) \quad Ke = Ks^{1-e} \cdot Kg^e \quad (4.24)$$

$$(d) \quad Ke/Ks = ((1-2e(P-1)/(2P+1)) / ((1+e(P-1)/(2P+1))) \quad (4.25) \quad \text{Ref}$$

$$(e) \quad Ke/Ks = (e^{2/3} + P(1-e^{2/3})) / (e^{2/3} - e + P(1-e^{2/3}) + e) \quad (4.26) \quad \text{Ref}$$

Where,

$K_s$  = thermal conductivity of pellet with zero porosity.

$K_g$  = thermal conductivity of gas in pore.

$P = K_s/kg$

Dry diffusent  
exp. res. see Fig.

Figure 4.65 indicates the experimental points of thermal conductivities with porosity of the pellets, along with calculated values of effective thermal conductivity by equation (4.25) and (4.26). The variation of 'Ke' with porosity computed by equation (4.22) and (4.23) is too low and that by equation (4.24) is too

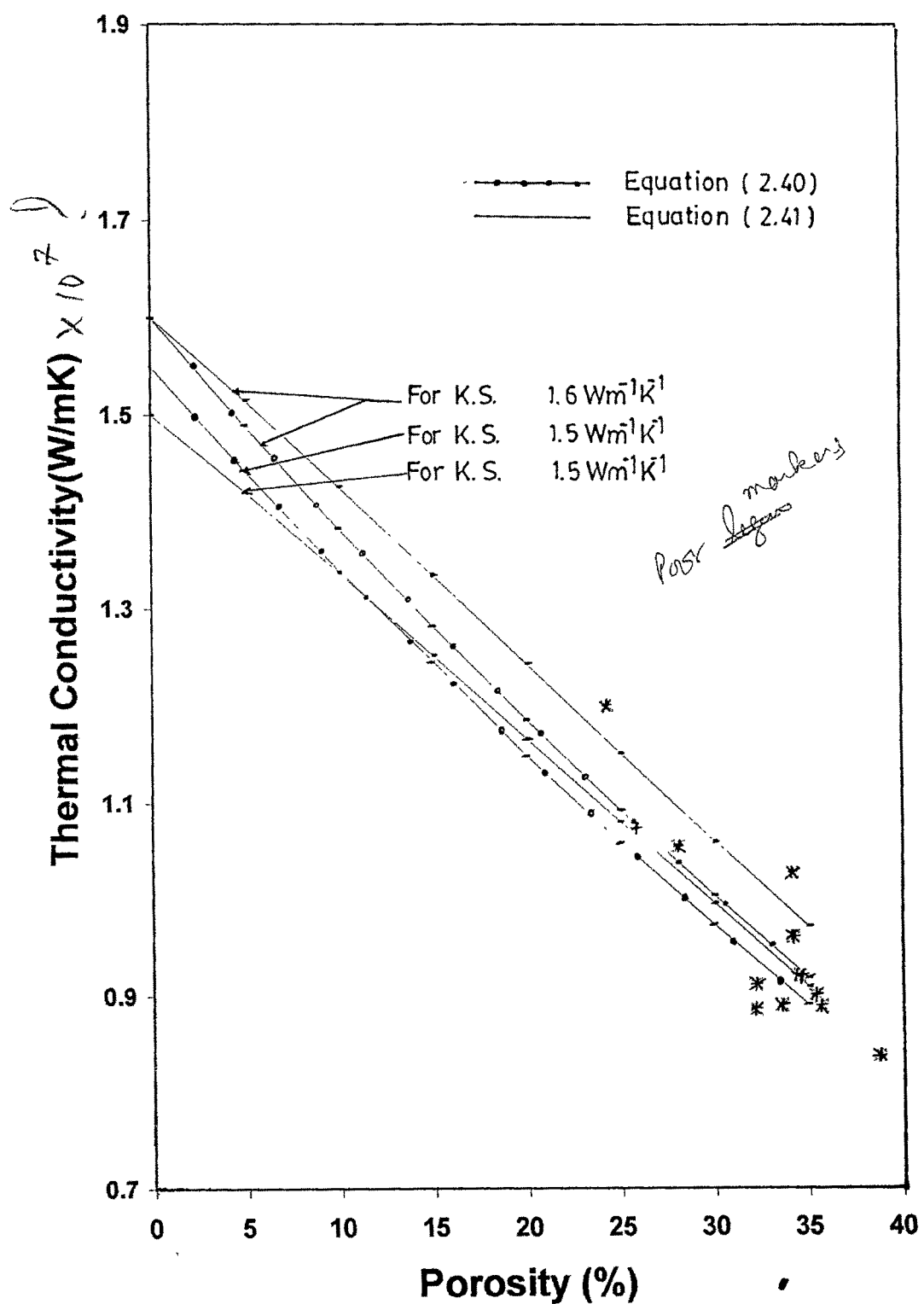


Fig.4.65 Effect of porosity on thermal conductivity.  
(Pelletized pellets).

high to explain present experimental values. However it could be noticed from the figure that values computed by equation (4.25) and (4.26) fit in satisfactorily for 'K<sub>s</sub>' values of 1.55 to 1.60 Wm<sup>-1</sup>K<sup>-1</sup> for equation (4.25) and (4.26), respectively. The thermal conductivity of air for these calculations was taken as <sup>64</sup> 0.068 Wm<sup>-1</sup>K<sup>-1</sup>. Equation (4.25) is a better fit out of the two equations. It could also be observed that the present experimental values of effective thermal conductivities increase more sharply with the decrease in porosity than those predicted by these models. This aspect motivated us to analyse the results further by using basic sintering equation available in literature.

The process of sintering of fine powders was widely investigated in powder metallurgy and discussed in chapter 2. Various mechanisms were proposed and activation energies calculated. The sintering behaviour of iron oxide was in specific reported by Misra, <sup>wk</sup> Seshadri<sup>34</sup> and Wynnyckj<sup>15</sup>. The representation of densification of pellet with parameters which approach '1' on sintering to theoretical density were used to interpret sintering kinetics. Use of volume ratio by Tikkannen to explain sintering of metal powders and by Wynnyckj for sintering of iron ore pellets is reported in literature. With the same logic, an attempt has been made in present investigation to correlate the thermal conductivity to ratio of volume of pellet to its volume at zero porosity. The results for iron ore pellets and pure oxide pellets are indicated in Figure 4.66. The extrapolation of the plot to ratio of '1' will lead to the value of 'K<sub>s</sub>'. The log/log plot for same results is indicated in figure 4.67 and the intercept value are calculated by least square method for iron ore is 1.75 Wm<sup>-1</sup>K<sup>-1</sup> at 700°C. The results are compared with pure iron oxide pellets.

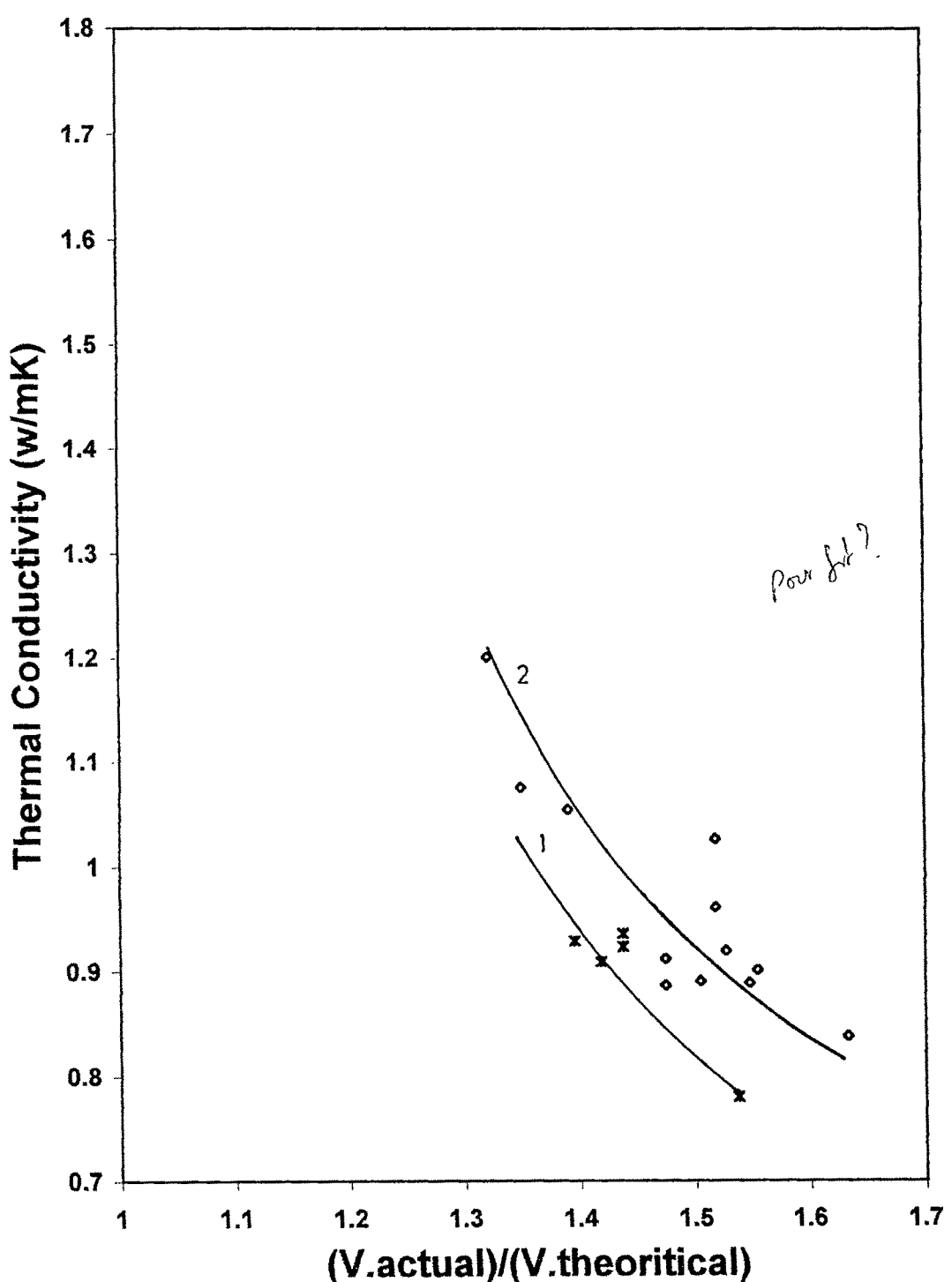


Fig. 4.66 Plot between thermal conductivity and volume ratio.  
 (1) Hand rolled pellet (2) Pelletized pellet

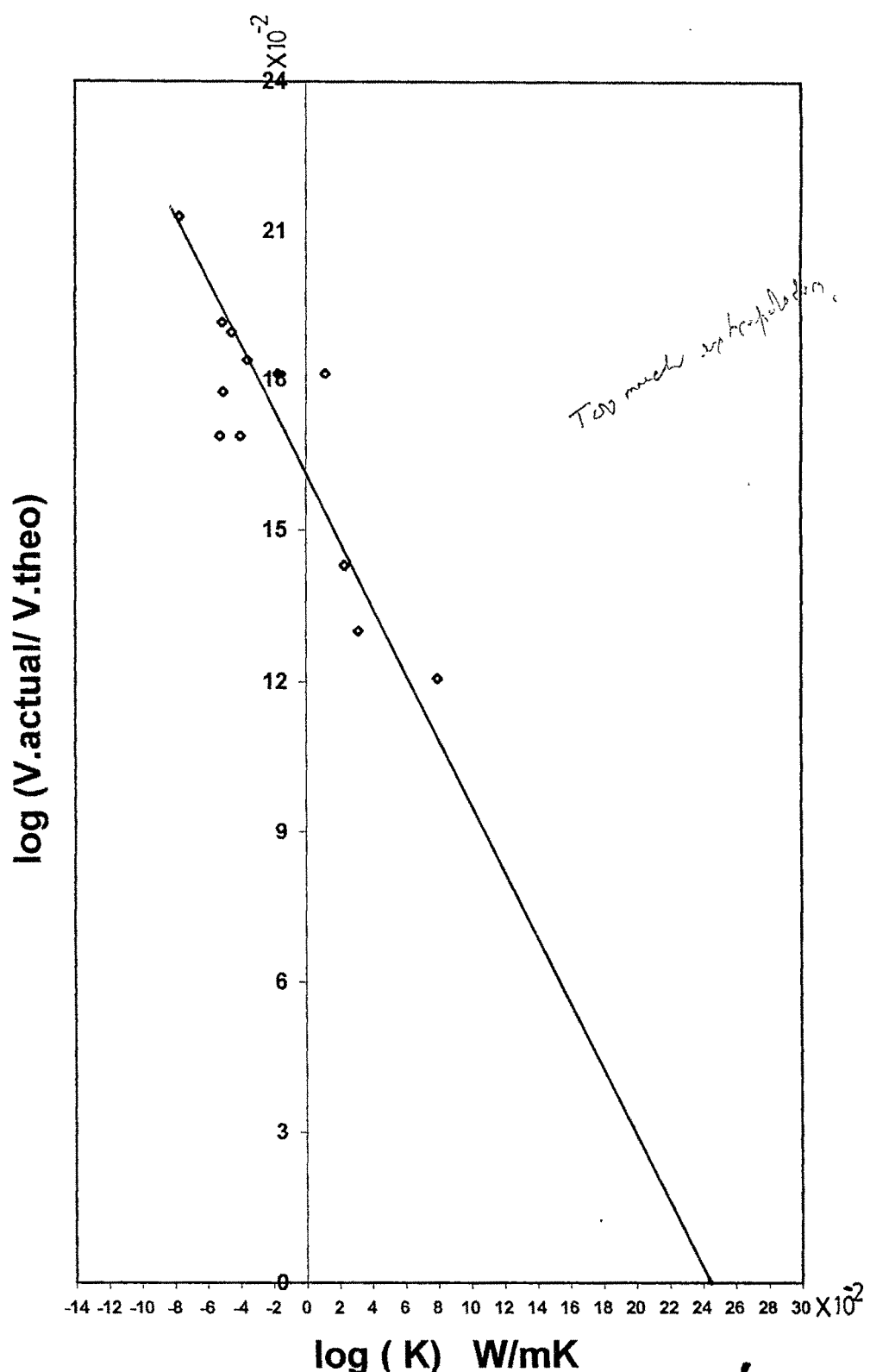


Fig. 4.67 log-log plot between thermal conductivity and volume ratio (Pelletized pellet).

An attempts were made to prepare pellets with low porosity to assess the validity range of the model equation and are discussed below.

#### **4.2.3 Thermal diffusivity and conductivity of pressed pellet with low porosity**

Method used to measure the thermal diffusivity and conductivity of pressed pellet was similar to one mentioned for pelletized pellet, Figure 4.68 to 4.83 indicate the values of 'Ts', 'Tc' and 'Tav' with time. Figure 4.84 indicate the relationship between surface temperature 'Ts' and centre temperature 'Tc' for a specific time 't'. Figure 4.85 indicates the validity of equation (4.12). The thermal profile within pellet in this case is indicated in figure 4.86 to 4.101. The tables from 4.28 to 4.43 indicate the calculation of thermal diffusivity. The average value of ' $\alpha$ ' and corresponding thermal conductivity for these pellets with their other physical properties is indicated in table 4.44. The variation of thermal conductivity and diffusivity of pellet with porosity is plotted in figure 4.102 and 4.103 respectively. The results indicate that the effective thermal conductivity of the pellet increase with decreasing porosity in the range of 34 to 20% as in case of pelletized pellet. Figures 4.102 and 4.103 indicate that, both thermal diffusivity and conductivity have a maximum value around 20-22% porosity which then decreases with decrease in porosity indicating a deviation from proposed model .

The porosity of pellets control thermal conductivity due to two aspects.

1. Decrease in porosity increases solid/solid contact area and increasing solid state conduction.

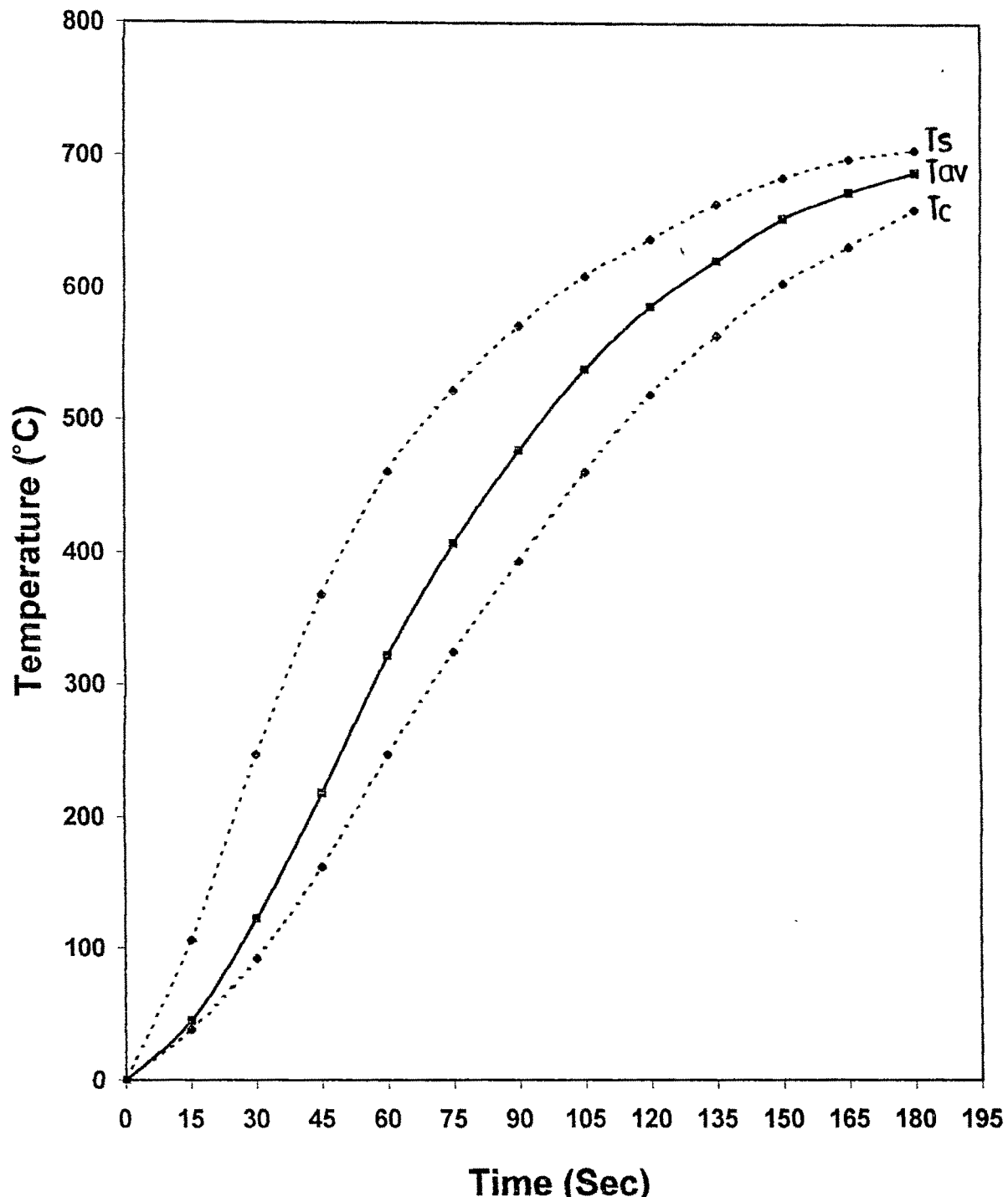


Fig. 4.68 Rise in surface, centre and average temperature in pressed pellet with time.(Size=0.5759cm&Porosity=14.29%)

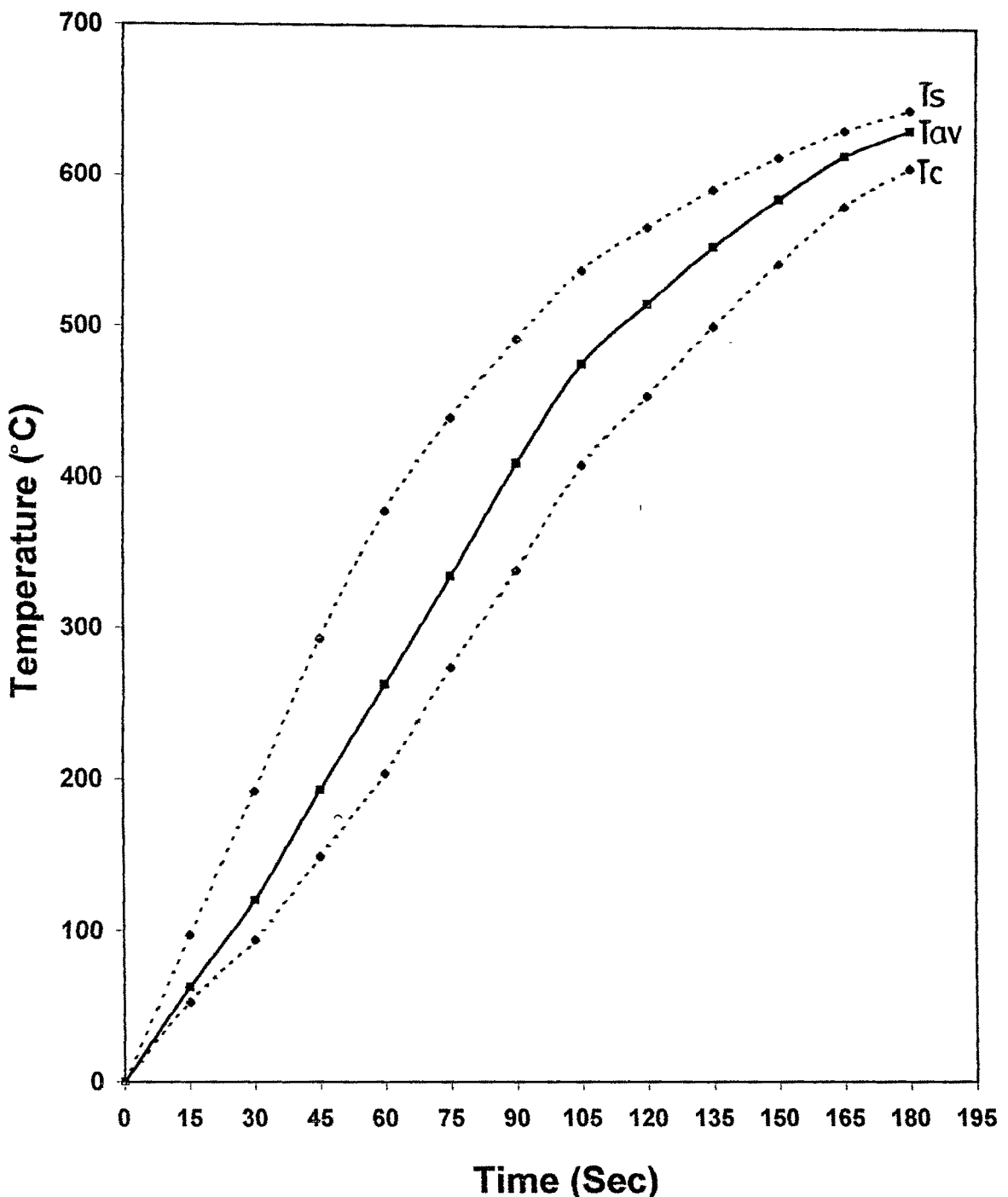


Fig. 4.69 Rise in surface, centre and average temperature in pressed pellet with time. (Size=0.5319cm & Porosity=14.50%)

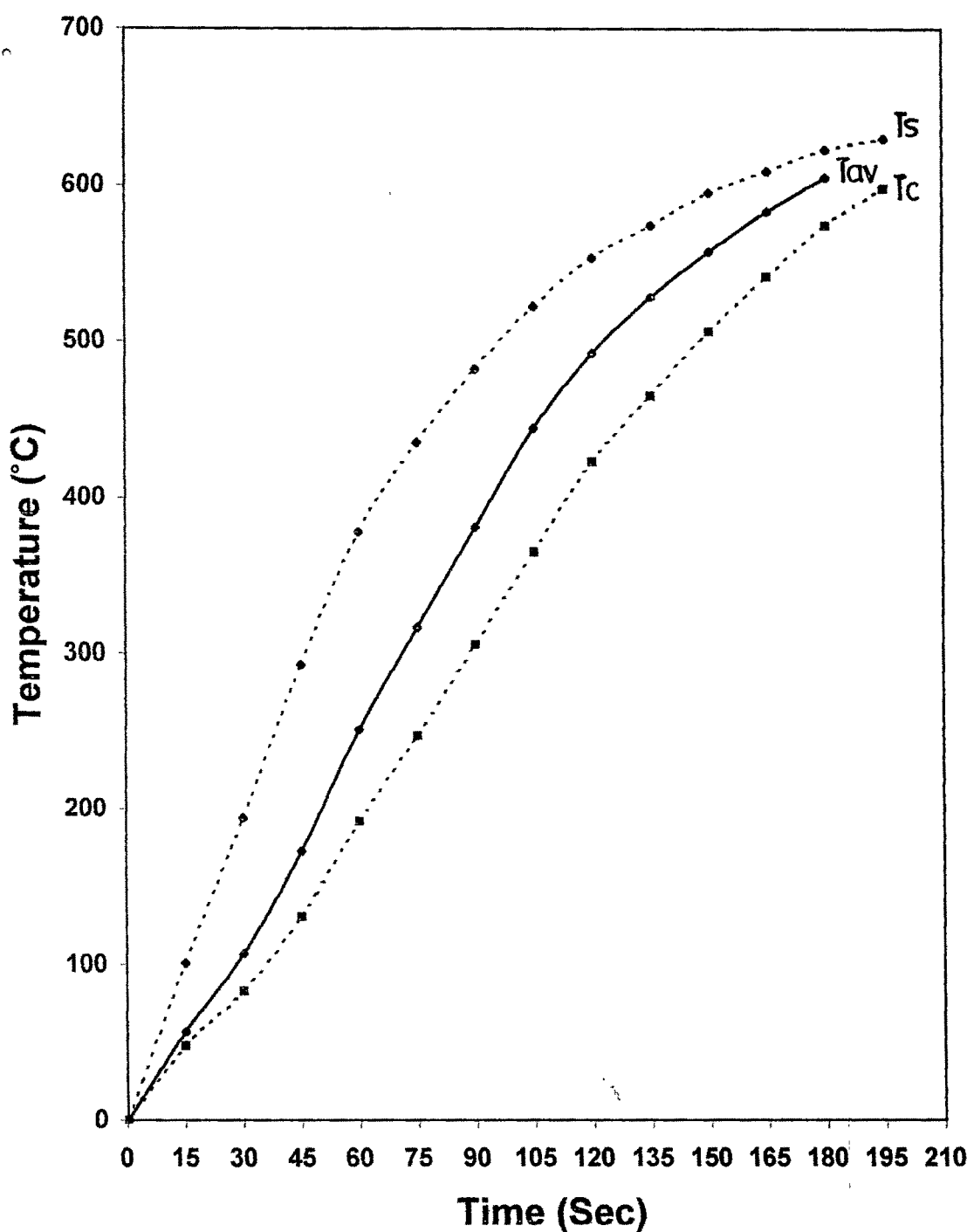


Fig.4.70 Rise in surface, centre and average temperature in pressed pellet with time. ( Size=0.5880cm&Porosity=17.95%)

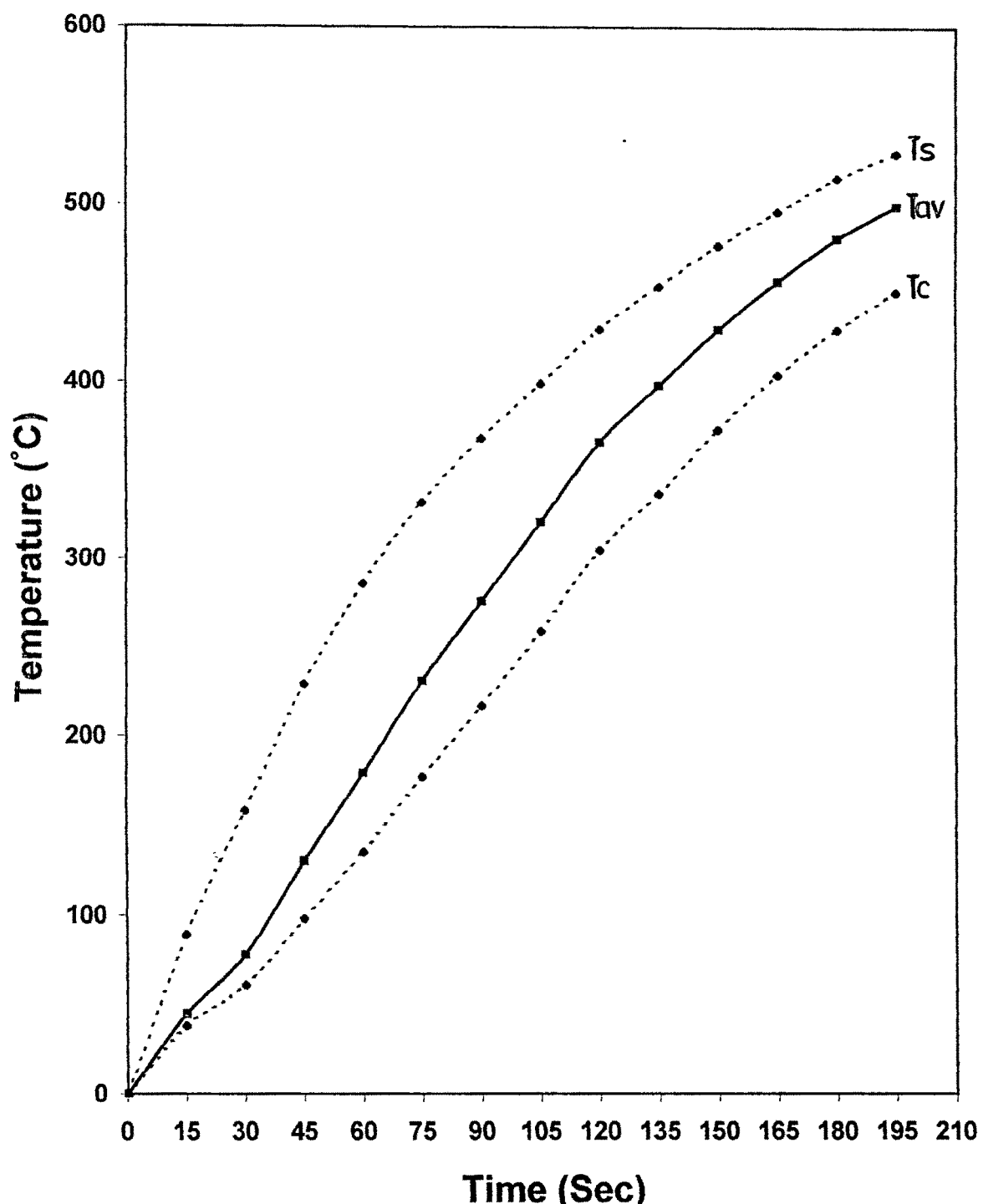


Fig. 4.71 Rise in surface, centre and average temperature in pressed pellet with time.(Size=0.6424cm&Porosity=18.49% )

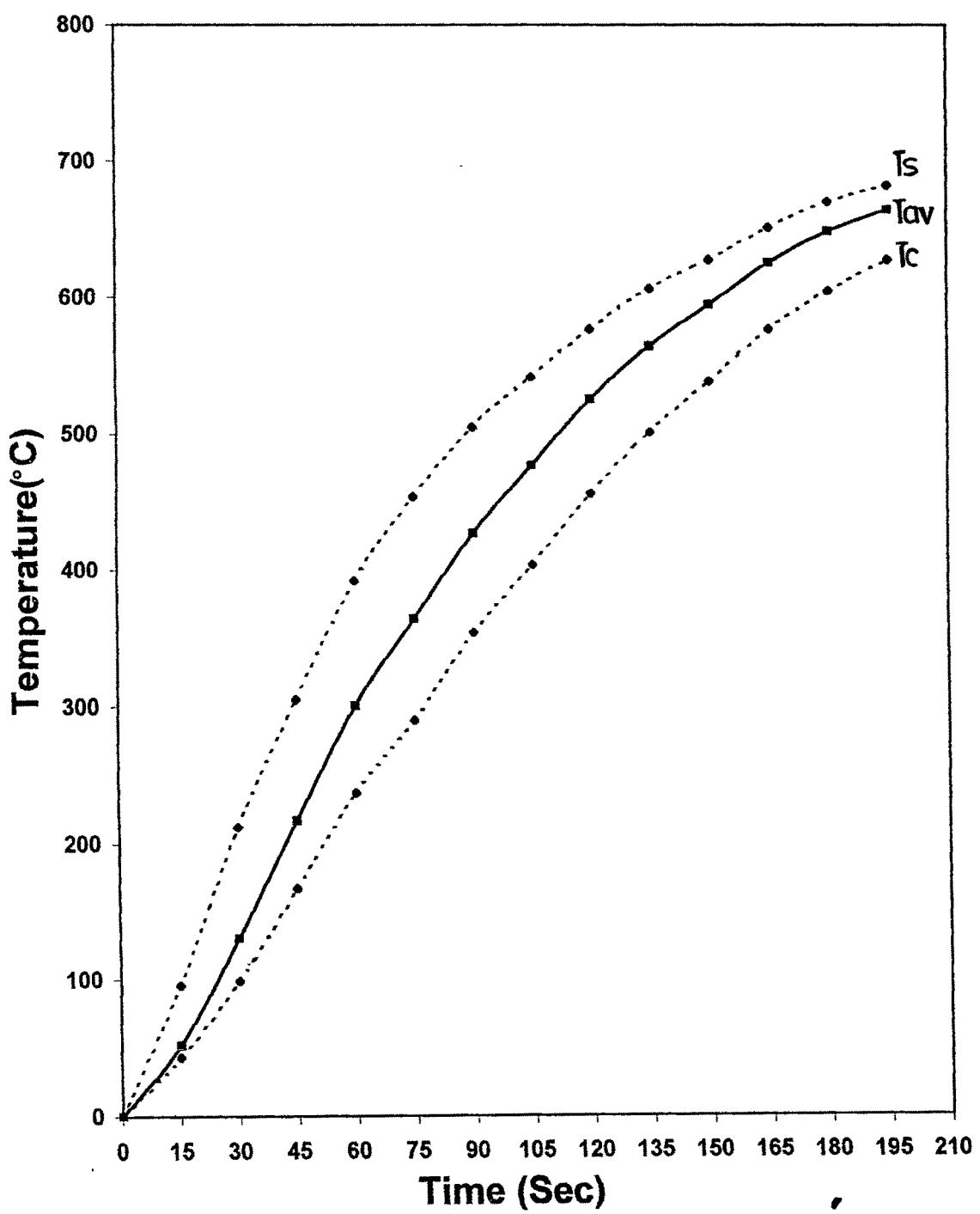


Fig. 4.72 Rise in surface, centre and average temperature in pressed pellet with time.(Size=0.7413cm&Porosity=19.67%)

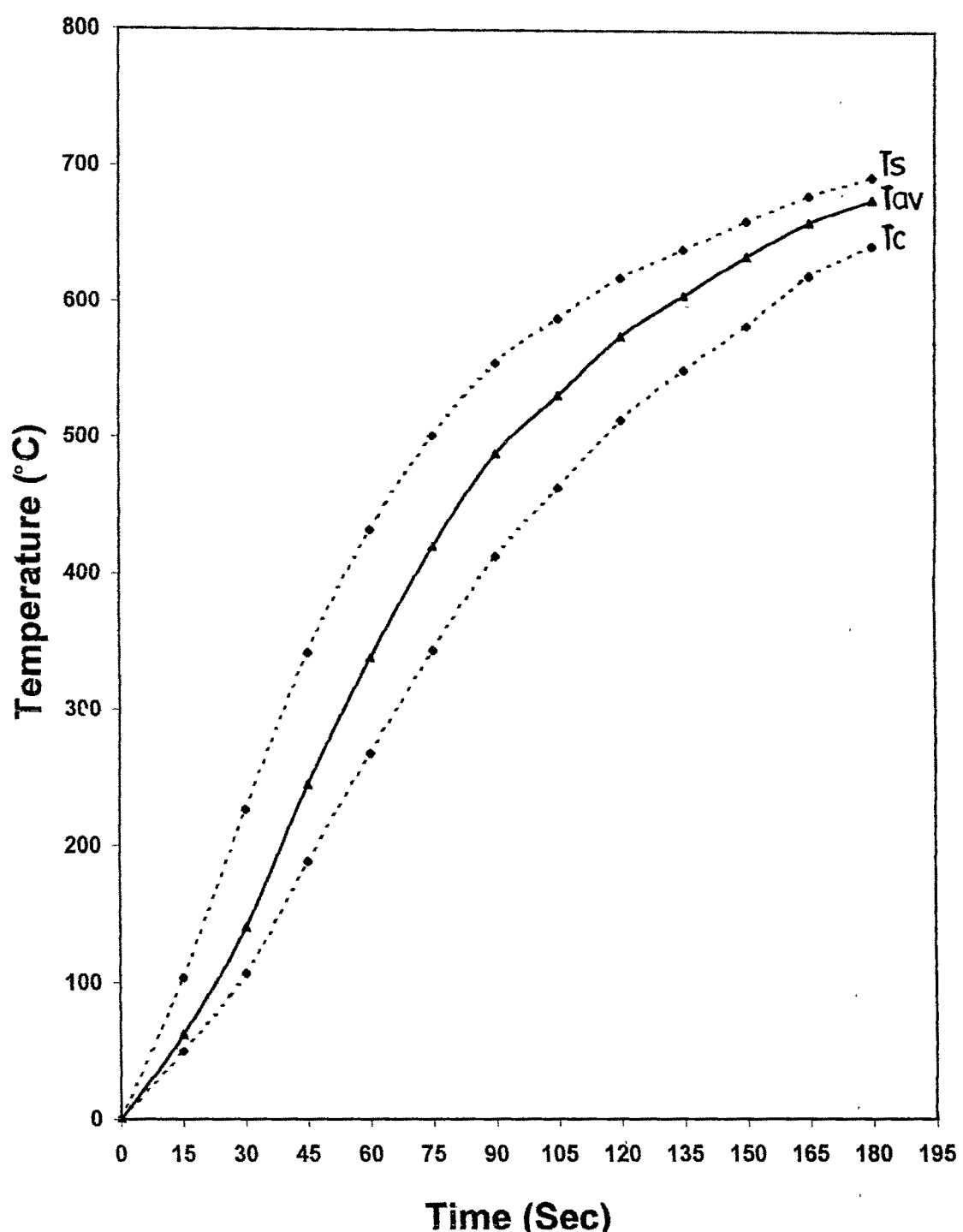


Fig. 4.73 Rise in surface, centre and average temperature in pressed pellet with time.(Size= 0.7155cm&Porosity=19.70%)

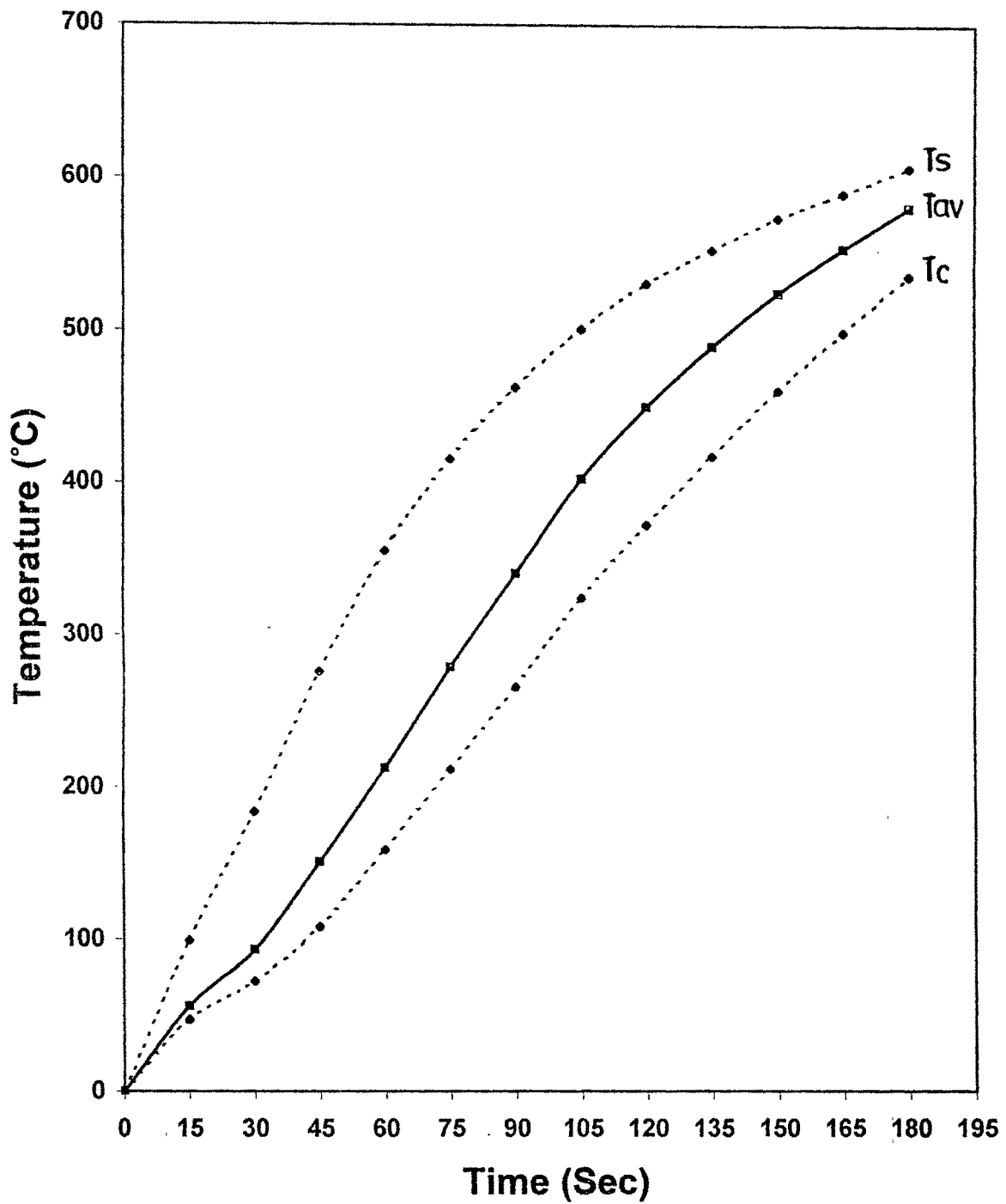


Fig. 4.74 Rise in surface, centre and average temperature in pressed pellet with time. (Size=0.6501cm & Porosity=19.93%)

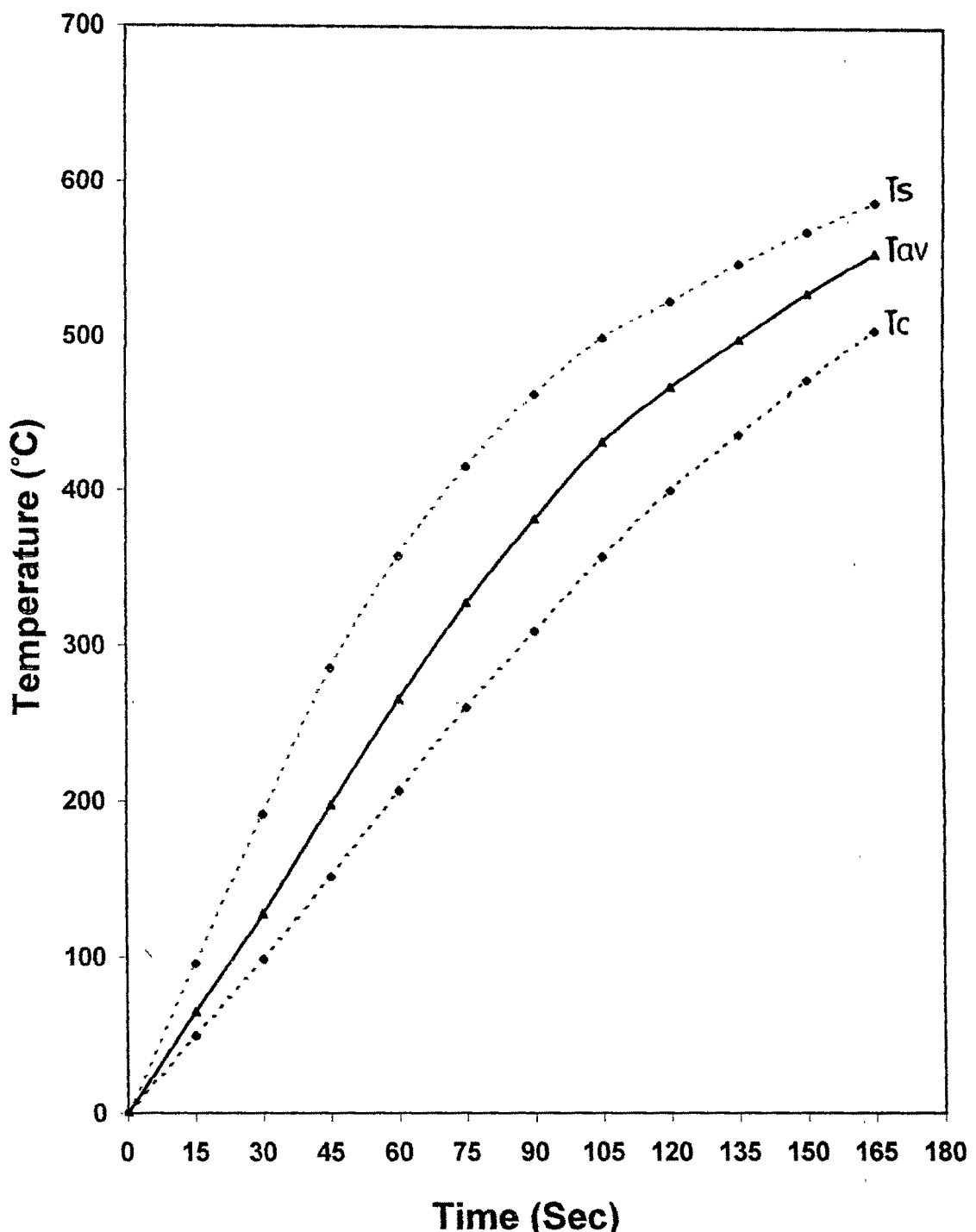


Fig. 4.75 Rise in surface, centre and average temperature in pressed pellet with time.(Size= 0.7219cm&Porosity=20.02%)

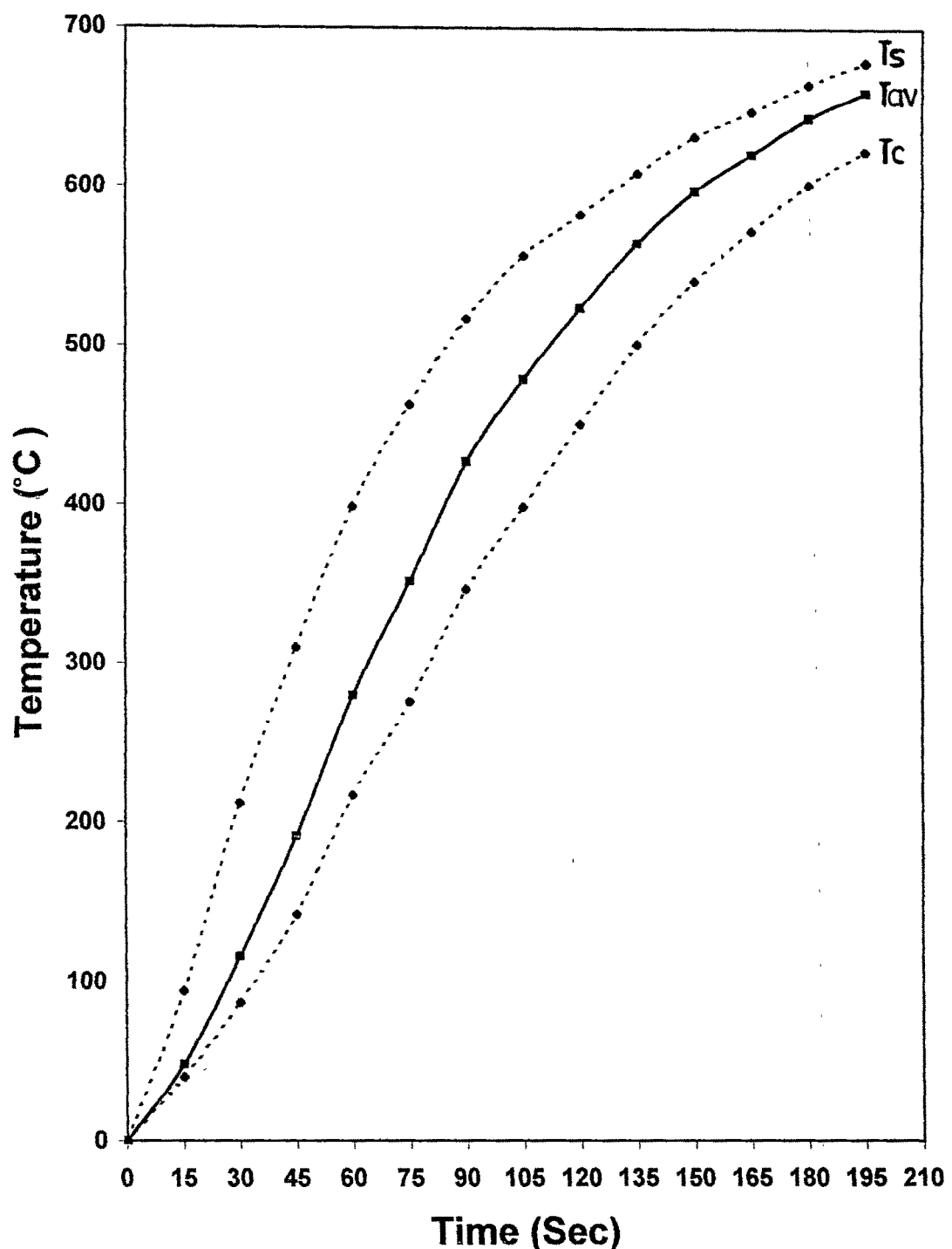


Fig. 4.76 Rise in surface, centre and average temperature in pressed pellet with time. (Size= 0.7122cm&Porosity=21.24%)

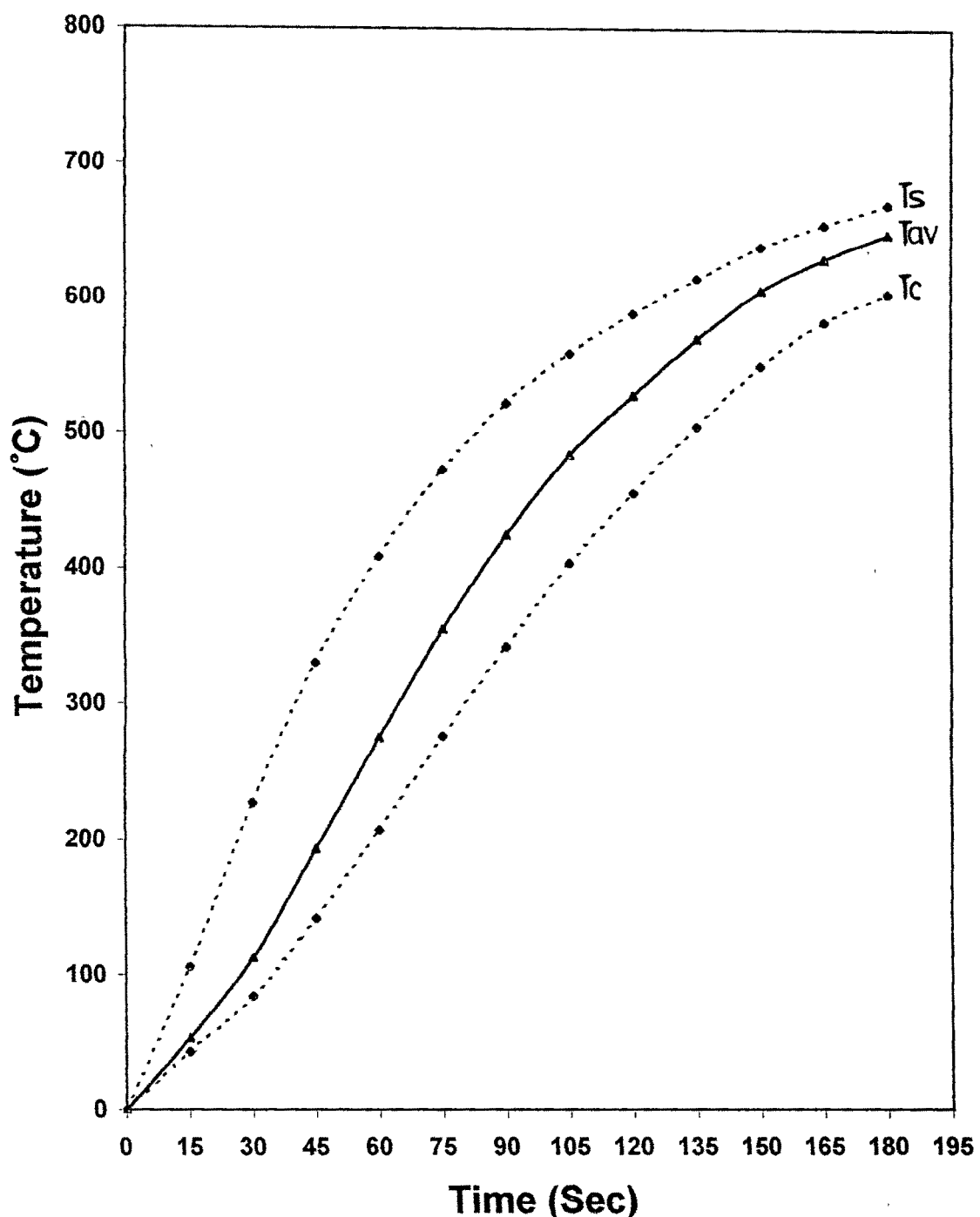


Fig. 4.77 Rise in surface, centre and average temperature in pressed pellet with time.(Size= 0.7543cm & Porosity=22.20%)

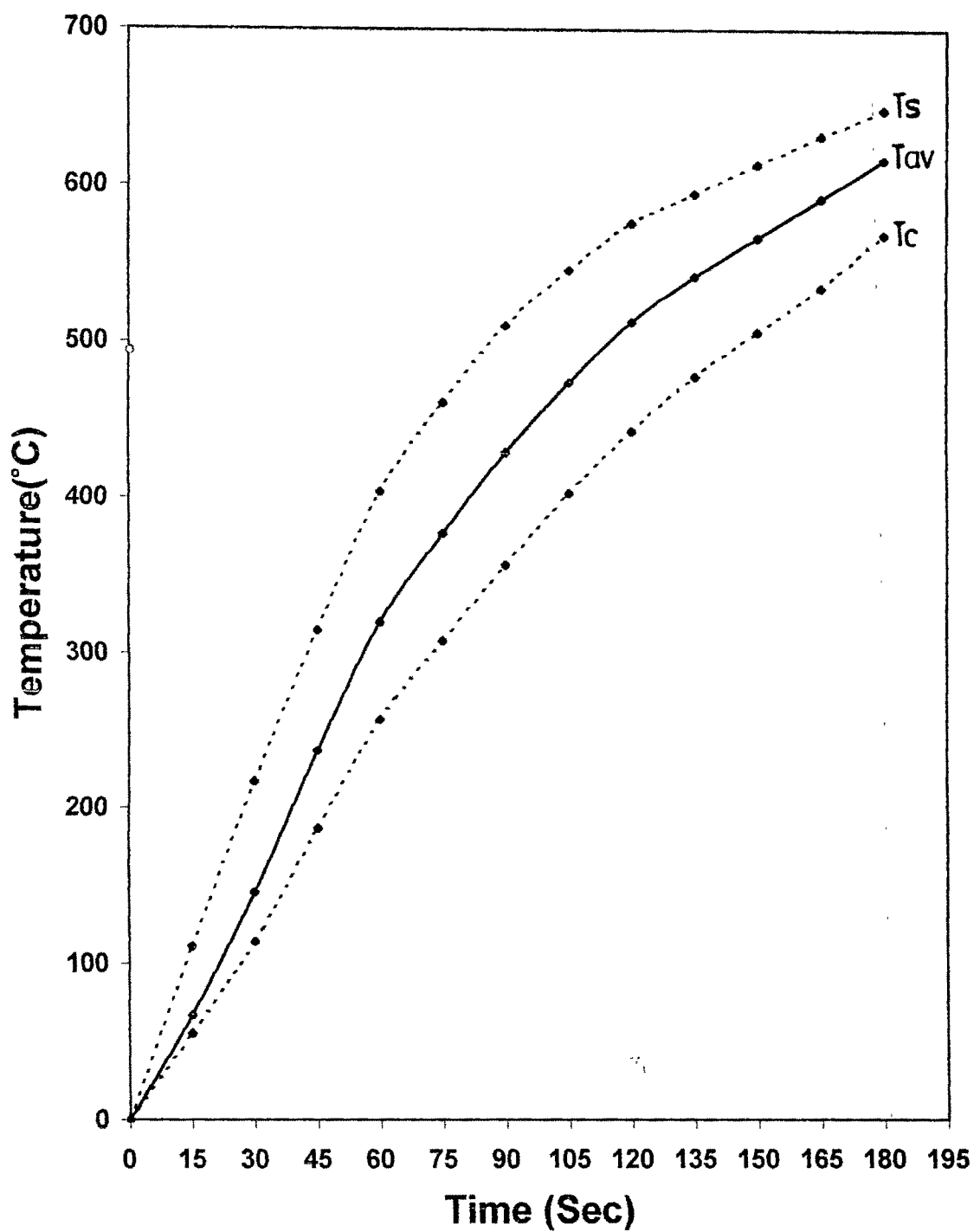


Fig. 4.78 Rise in surface, centre and average temperature in pressed pellet with time. (Size=0.6758cm&Porosity=22.67%)

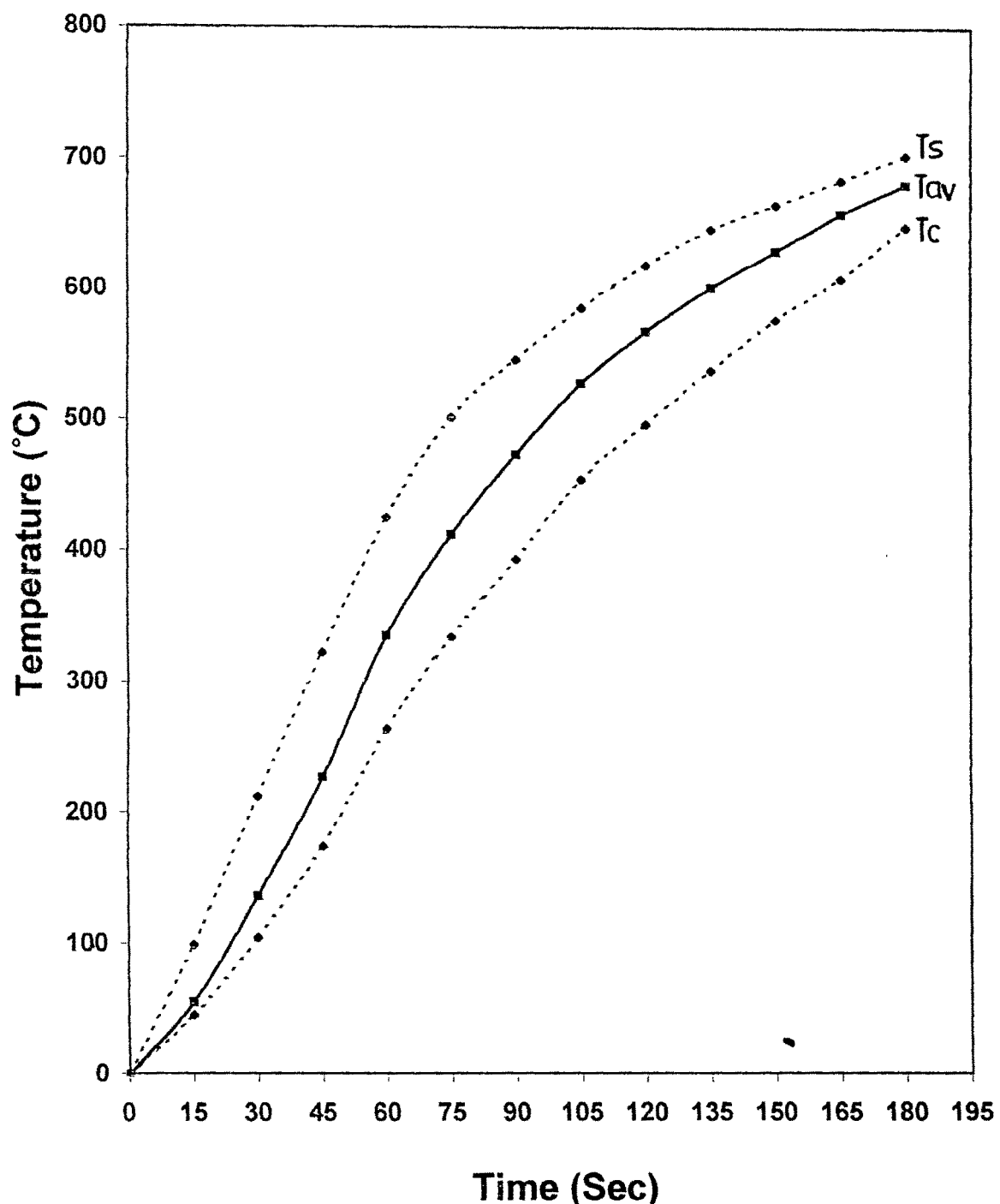


Fig. 4.79 Rise in surface, centre and average temperature in pressed pellet with time.(Size=0.7719cm&Porosity=23.15%)

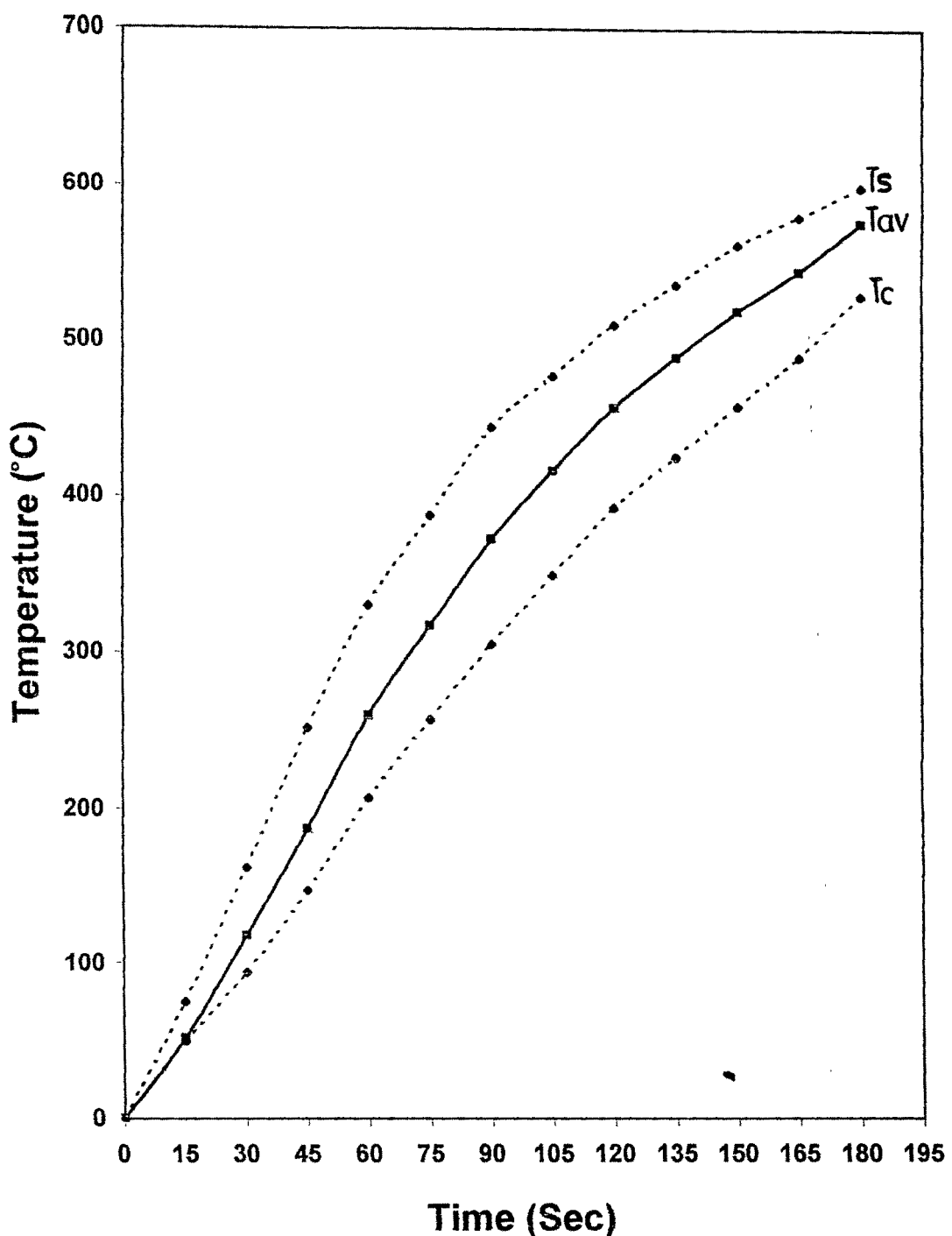


Fig. 4.80 Rise in surface, centre and average temperature in pressed pellet with time.(Size=0.7790cm & Porosity=23.51%)

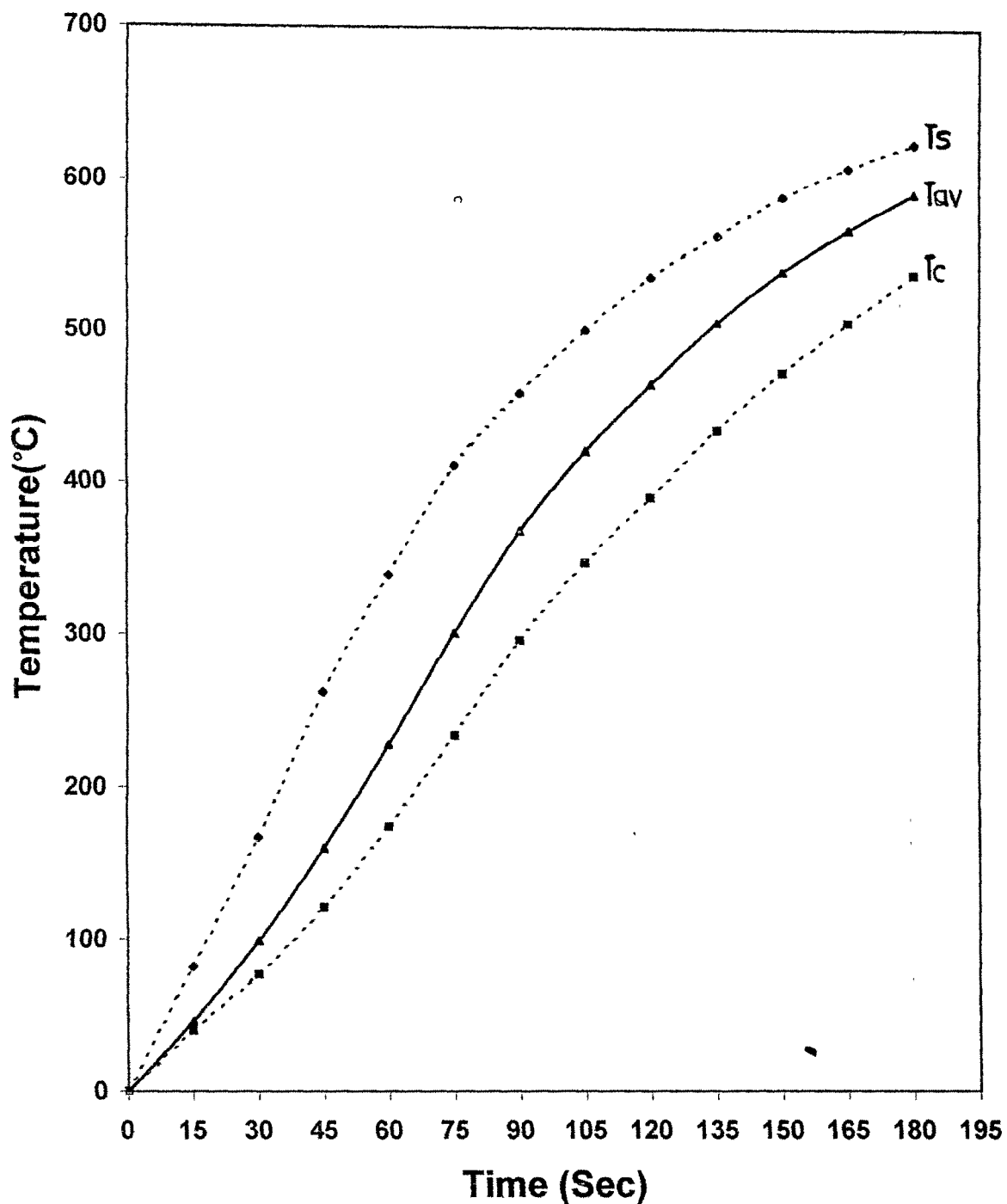


Fig. 4.81 Rise in surface, centre and average temperature in pressed pellet with time. (Size=0.7157cm&Porosity=28.28%)

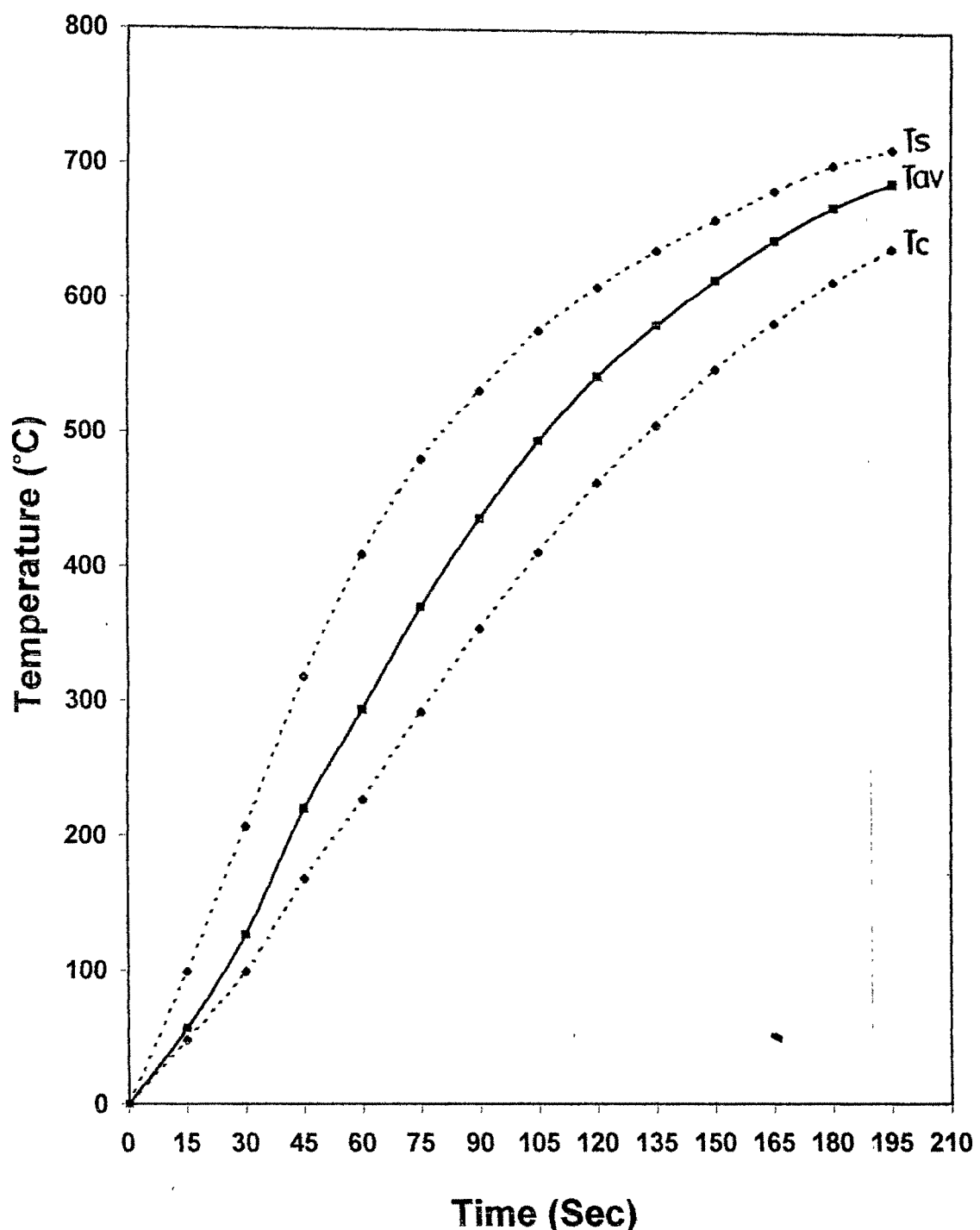


Fig. 4.82 Rise in surface, centre and average temperature in pressed pellet with time. (Size=0.7185cm&Porosity=29.73%)

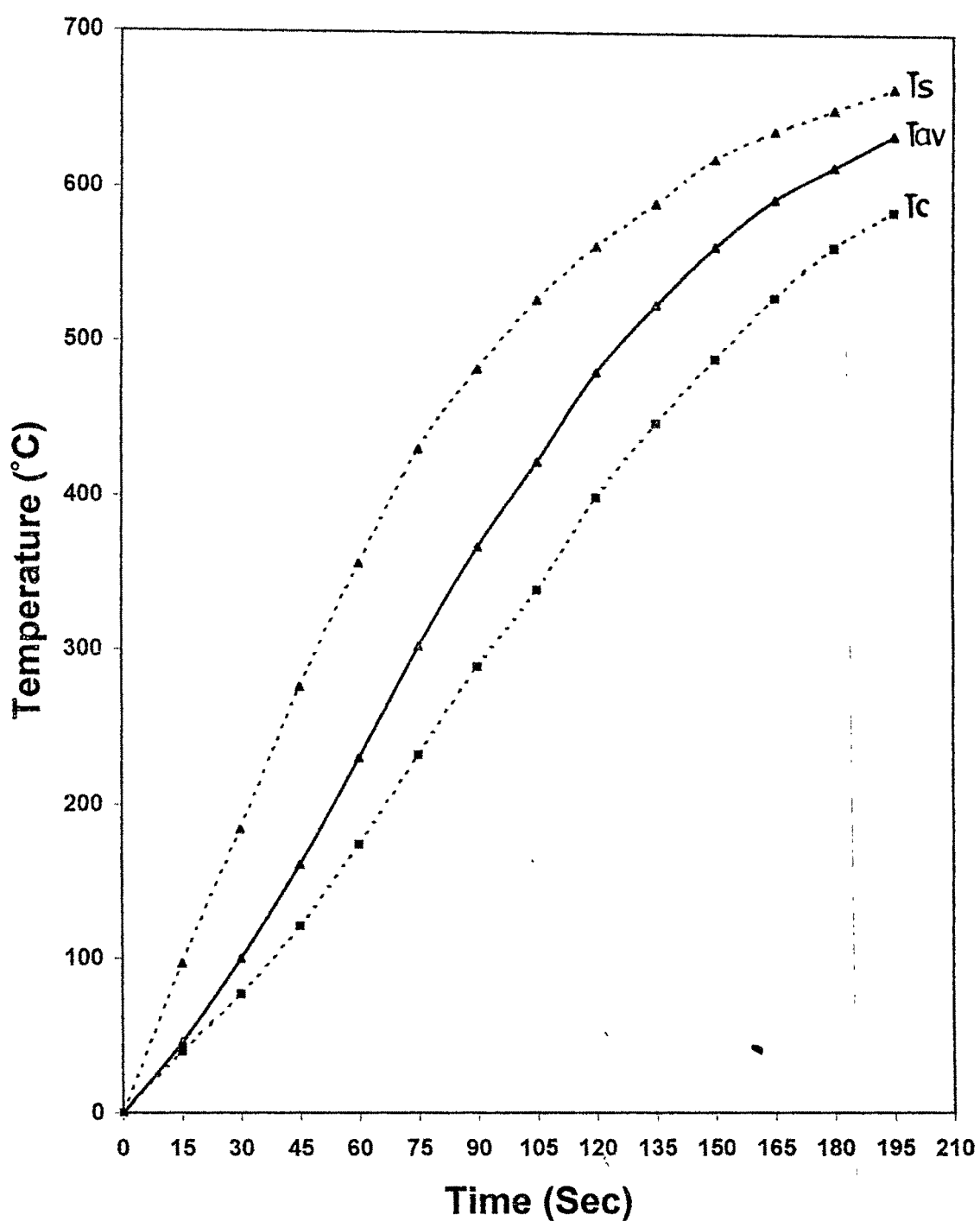


Fig. 4.83 Rise in surface,centre and average temperature in pressed pellet with time.(Size=0.6762cm&Porosity=33.89%)

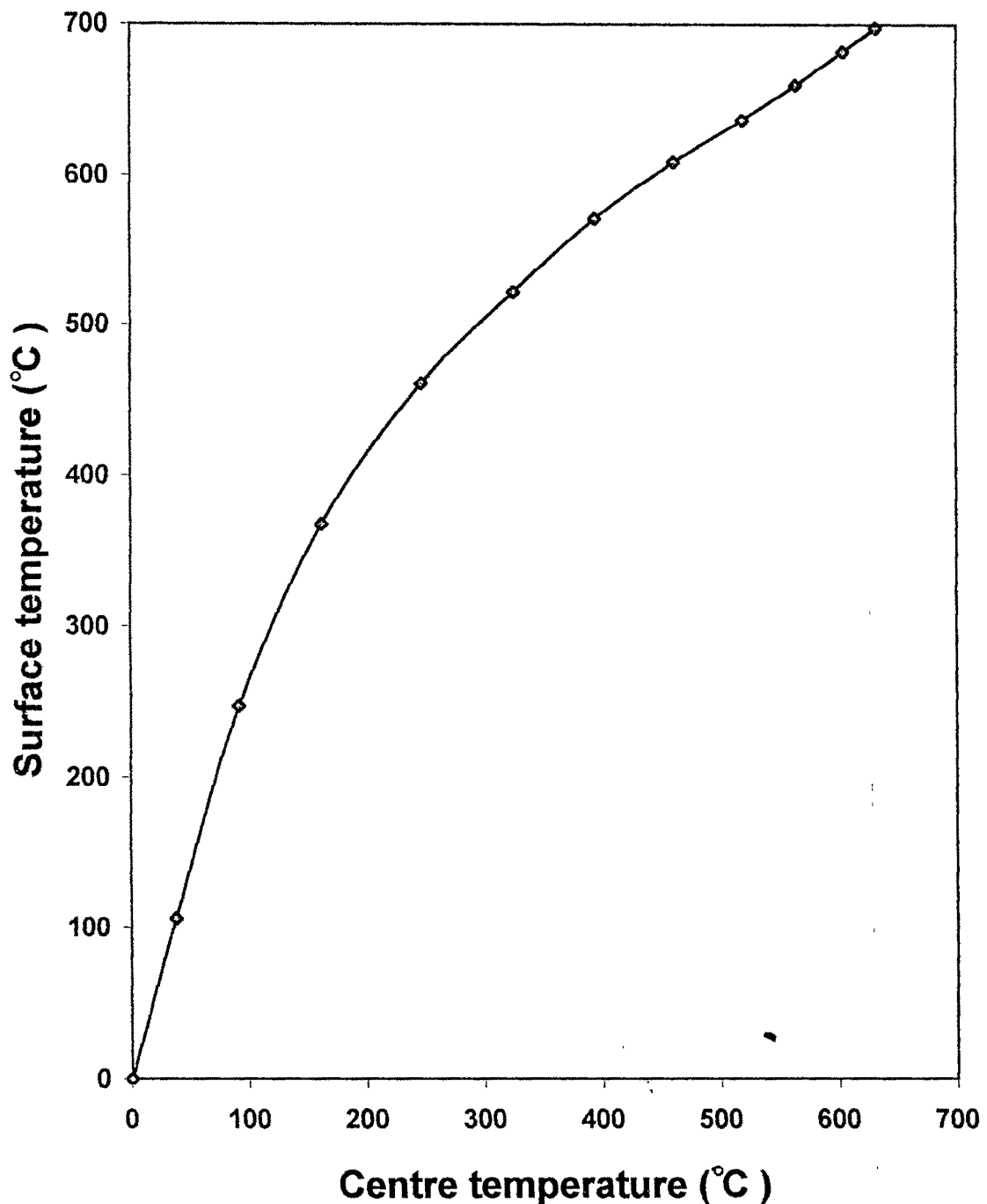


Fig. 4.84 Relationship between surface temperature( $T_s$ ) and centre temperature( $T_c$ ) for pressed pellet.  
(pellet size=0.5759cm&Porosity=14.28%)

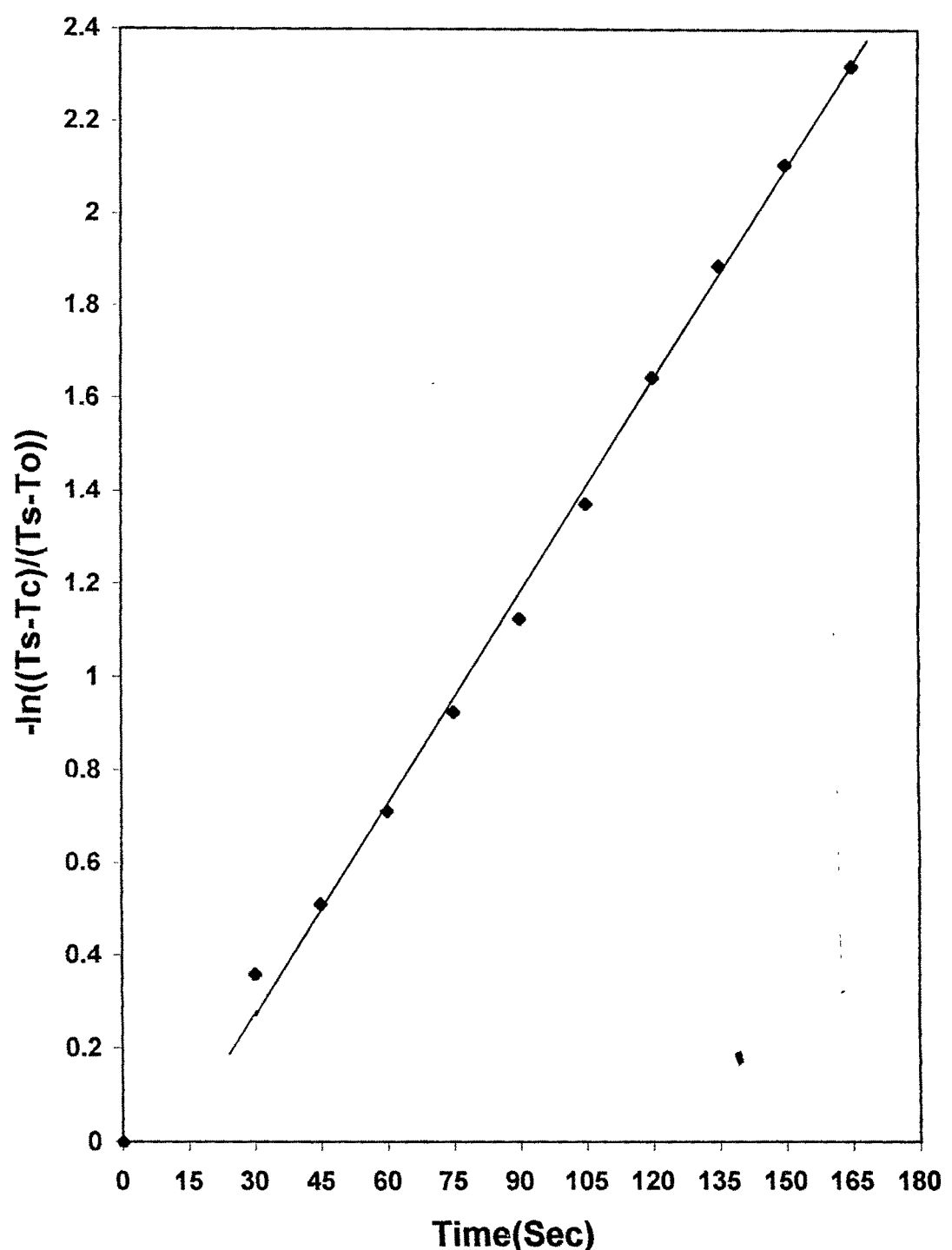
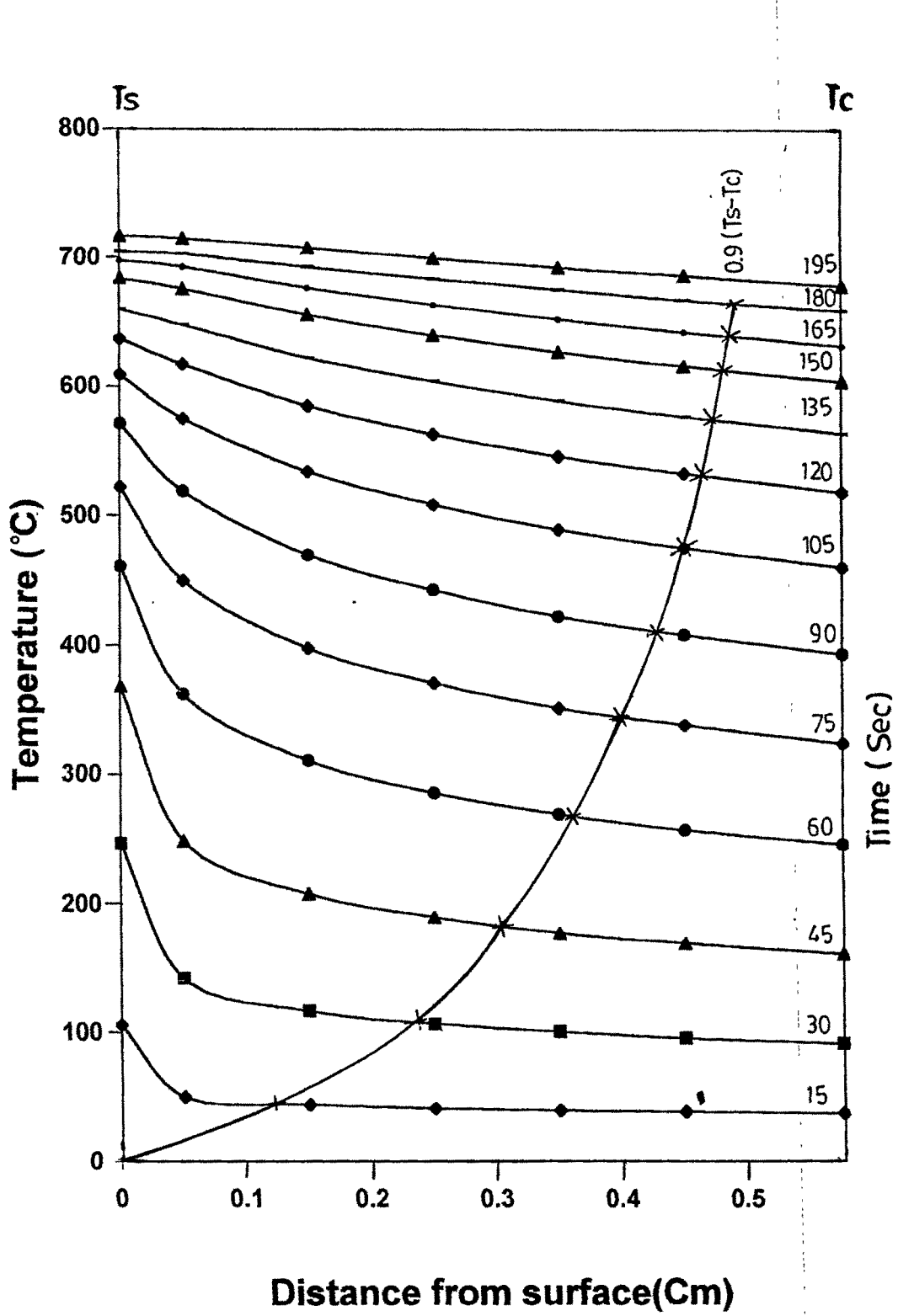
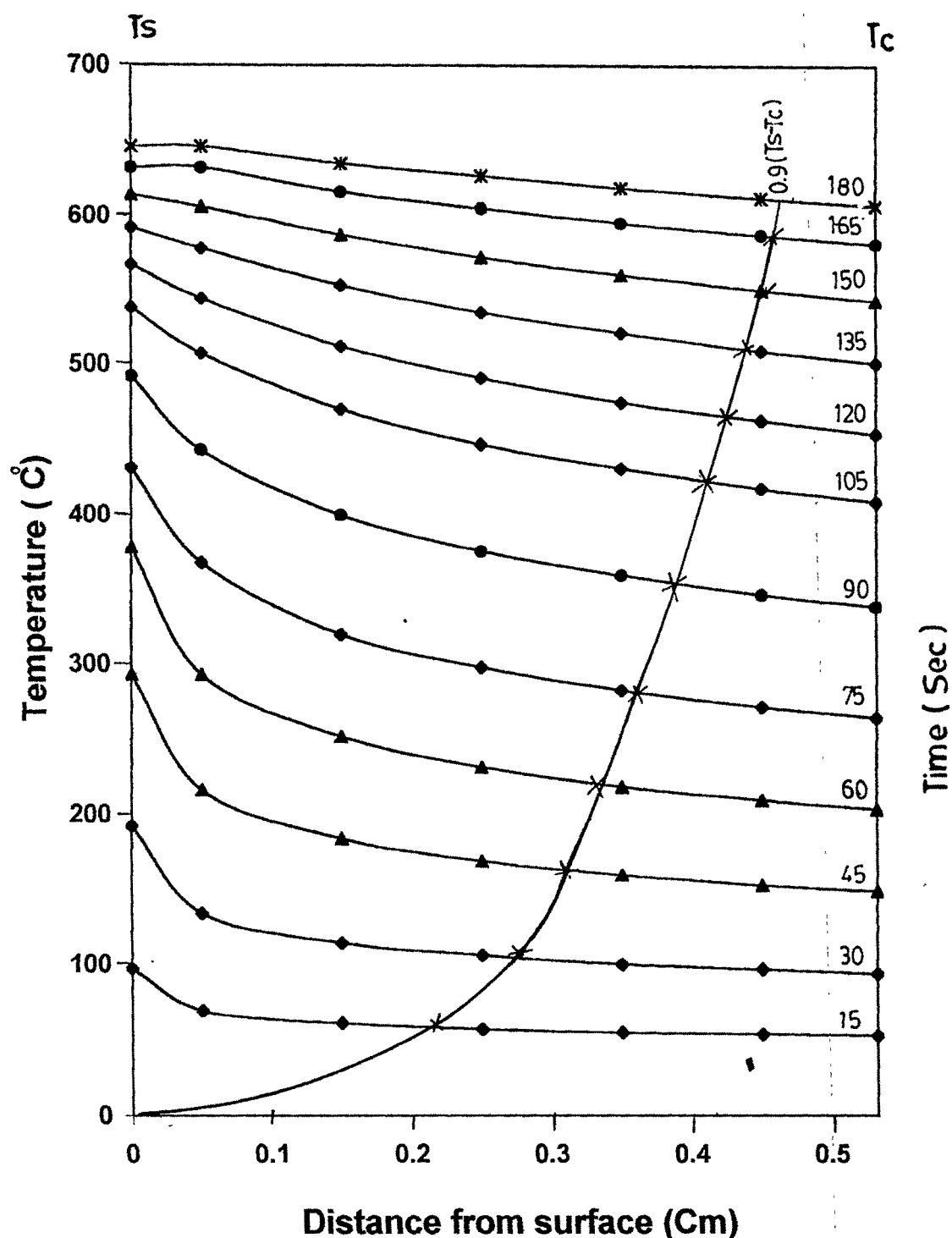


Fig. 4.85 Validity of equation (4.12) in case of pressed pellet  
 (Values of parameter k).  
 (Pellet size= 0.5759cm&Porosity=14.28%)



**Fig.4.86 Change in temperature profile and movement of heat front with time (Pressed pellet).**  
 (pellet size=0.5759cm&Porosity=14.29%)



**Fig. 4.87 Change in temperature profile and movement of heat front with time (Pressed pellet).**  
**(Pellet size=0.5319cm&Porosity=14.50%)**

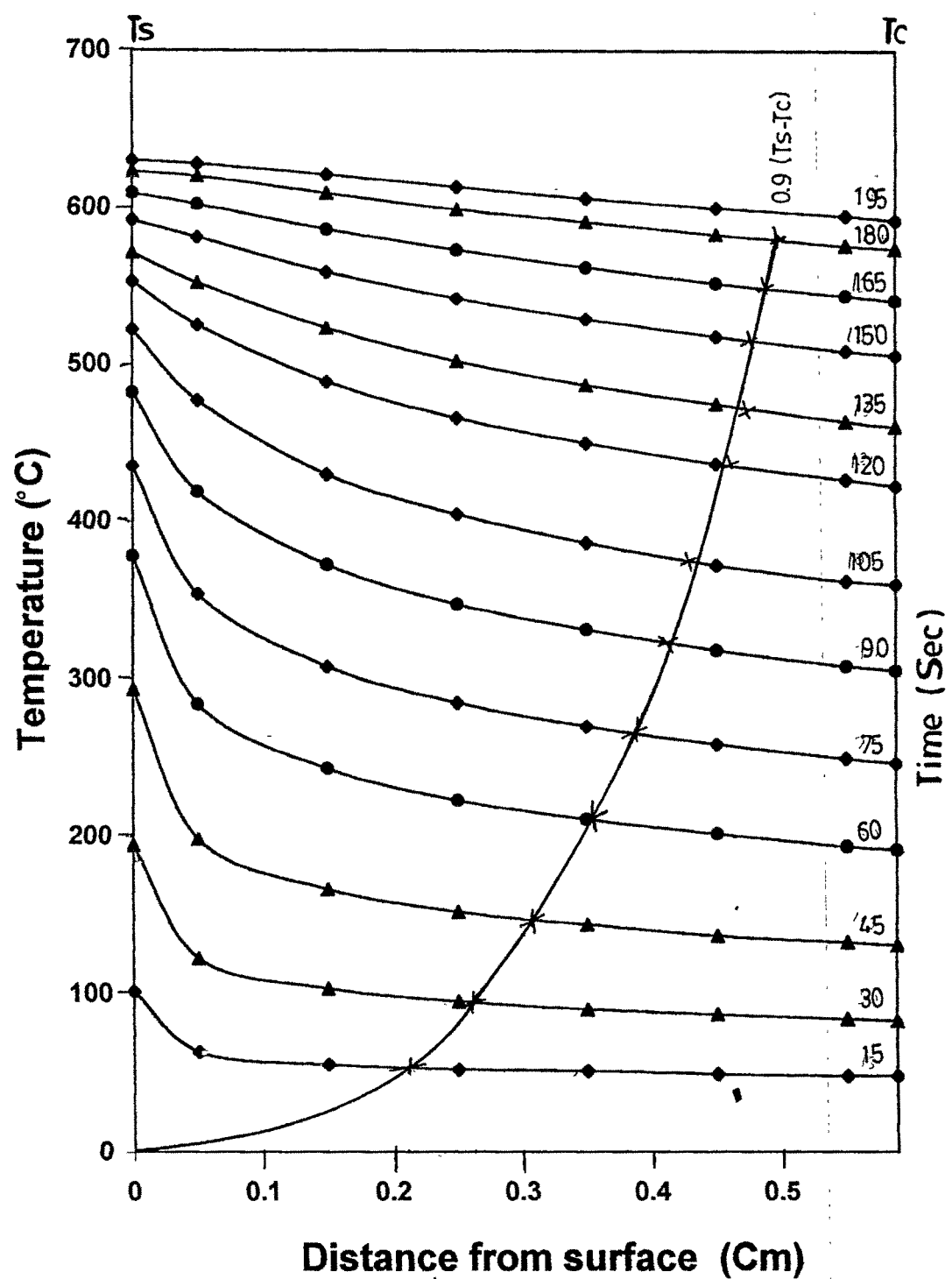


**Fig. 4.88 Change in temperature profile and movement of heat front with time (Pressed pellet).**  
**( Pellet size=0.5880cm&Porosity=17.95%)**

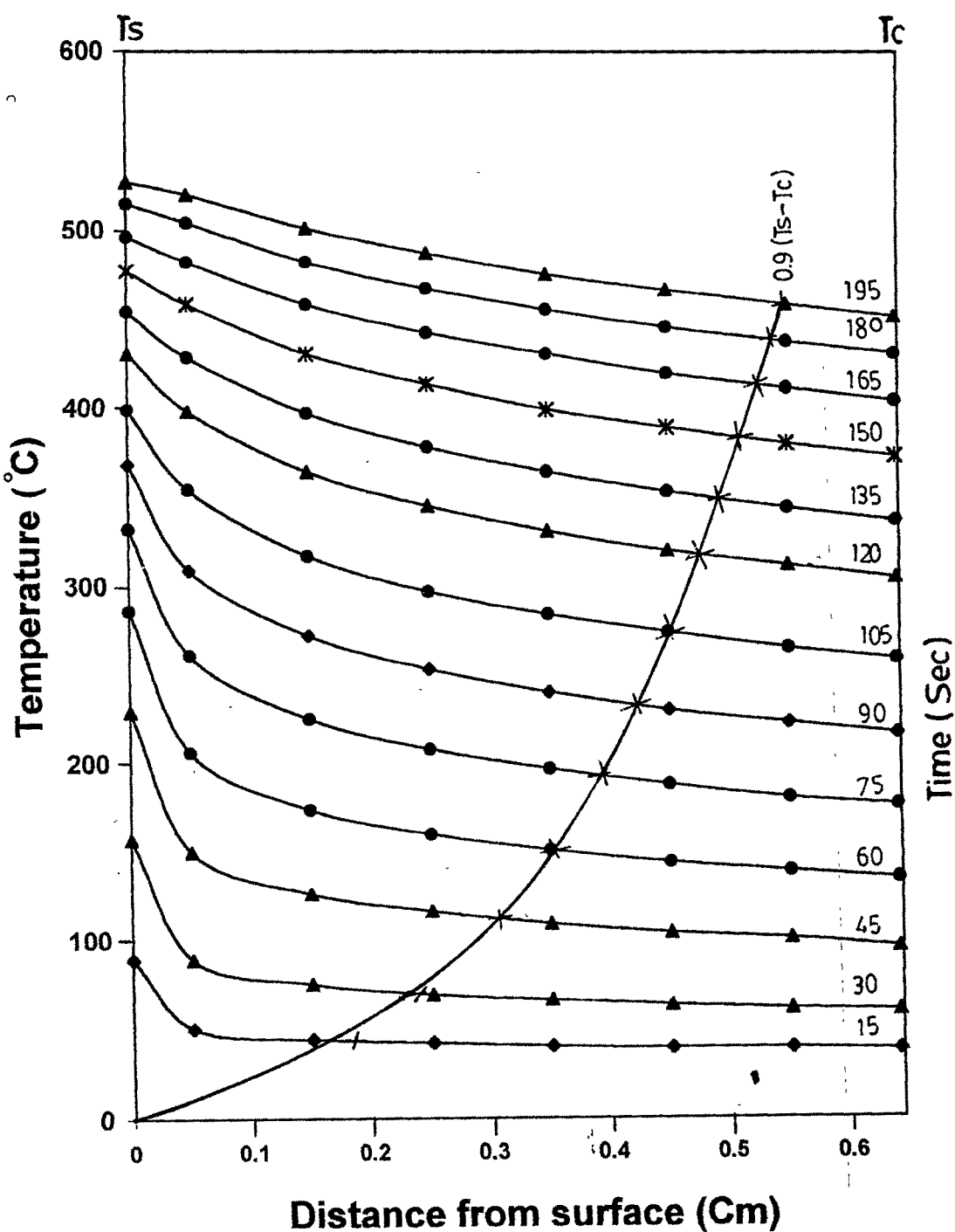


**Fig.4.89 Change in temperature profile and movement of heat front with time (Pressed pellet).**  
**(Pellet size=0.6424cm&Porosity=18.49%)**

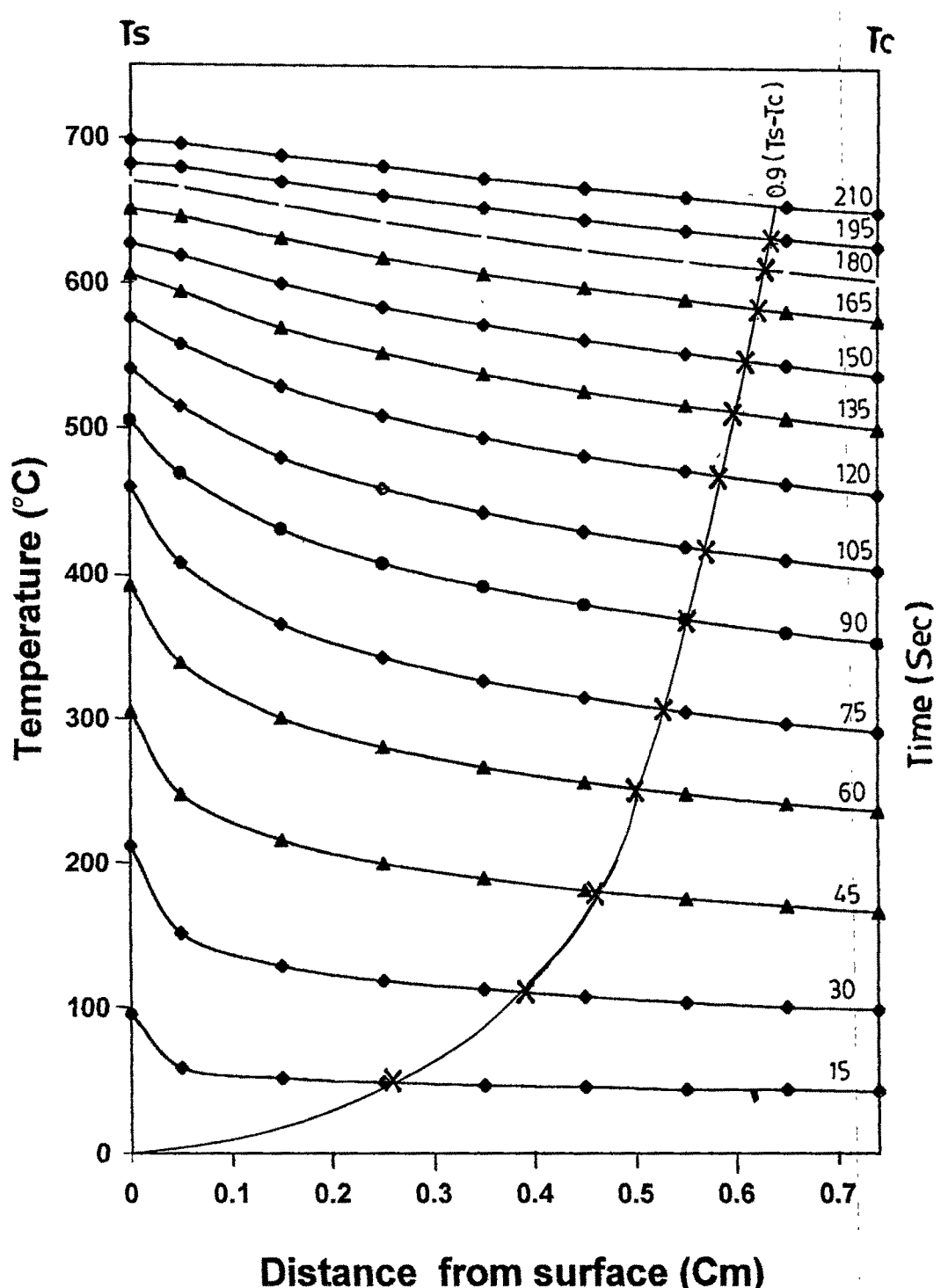


**Fig.4.90 Change in temperature profile and movement of heat front with time (Pressed pellet).**  
 ( pellet size=0.7413cm& Porosity=19.67%)

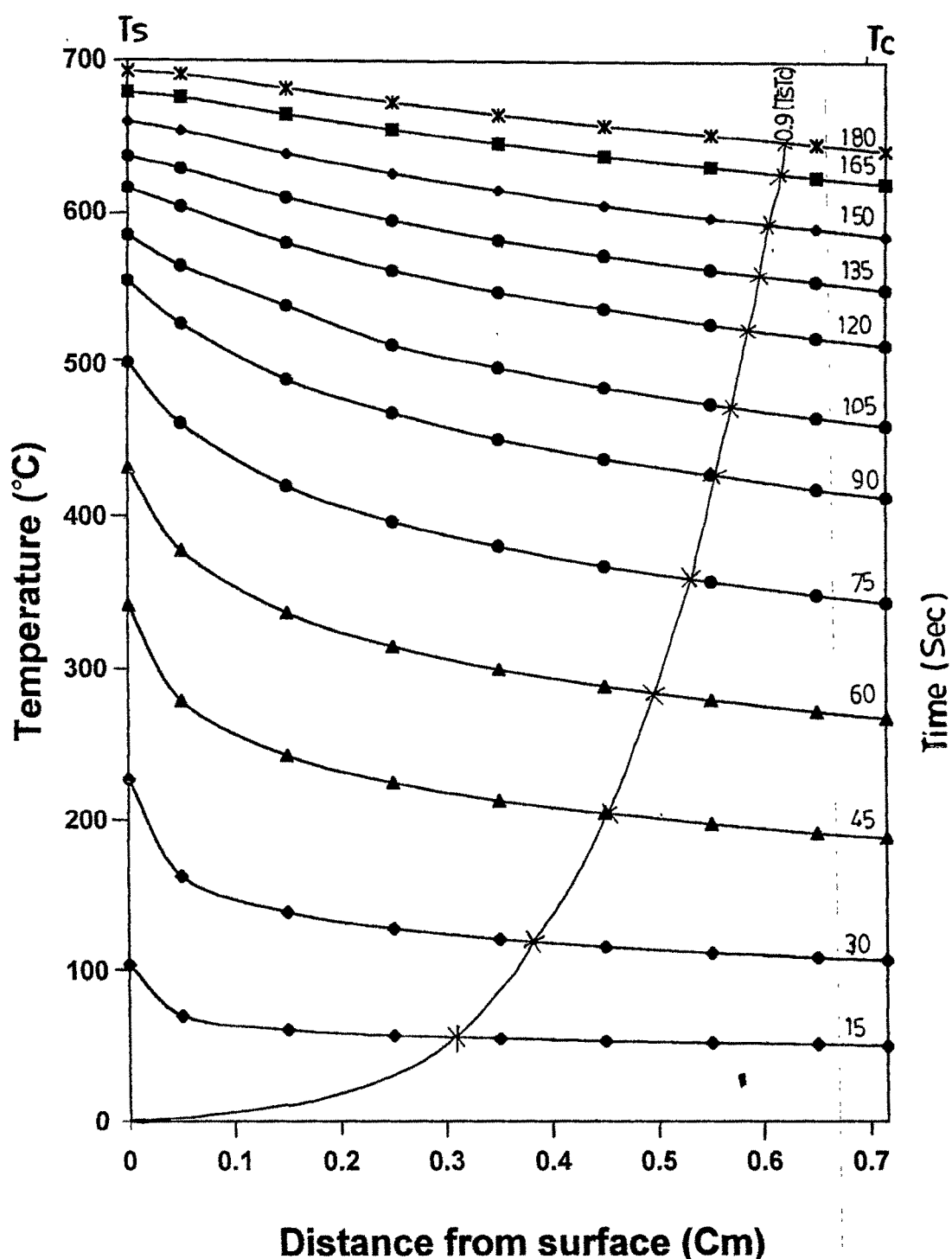


**Fig. 4.91 Change in temperature profile and movement of heat front with time (Pressed pellet).**  
**(Pellet size=0.7155Cm&Porosity=19.70%)**

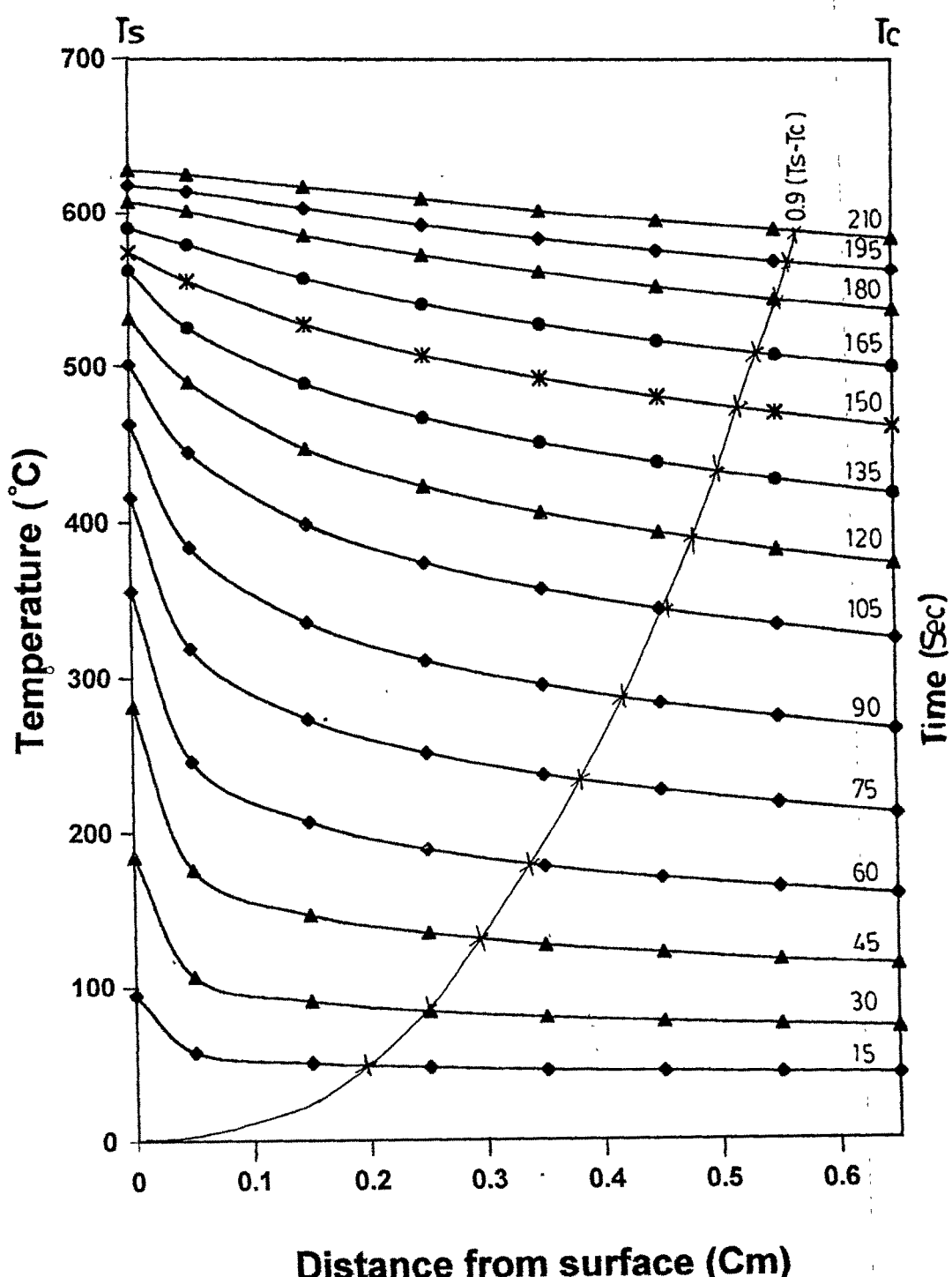


**Fig.4.92 Change in temperature profile and movement of heat front with time (Pressed pellet).**  
 (pellet size=0.6501cm&Porosity=19.93%)

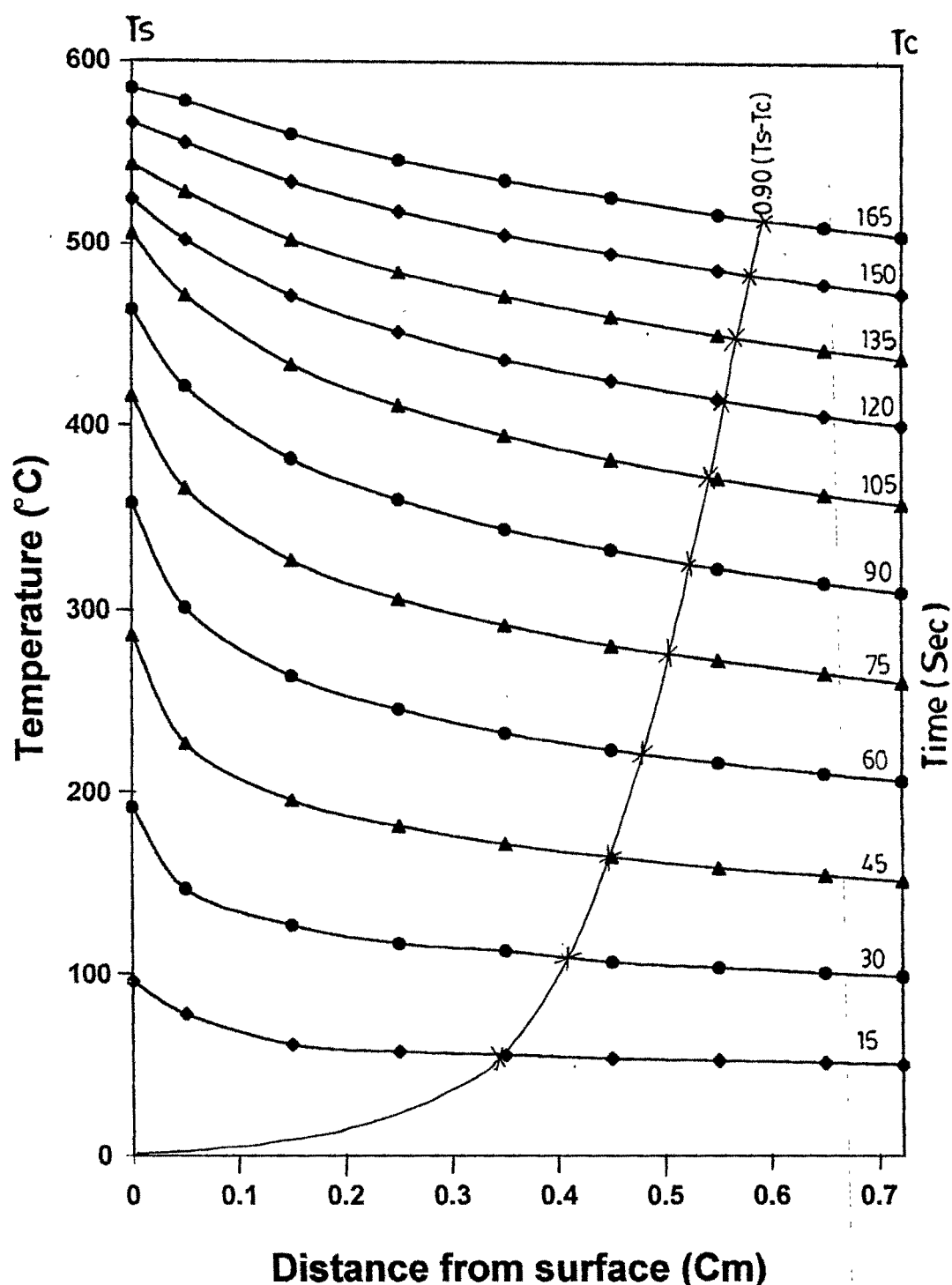


**Fig. 4.93 Change in temperature profile and movement of heat front with time (Pressed pellet).**  
**(Pellet size=0.7219Cm&Porosity=20.02%)**

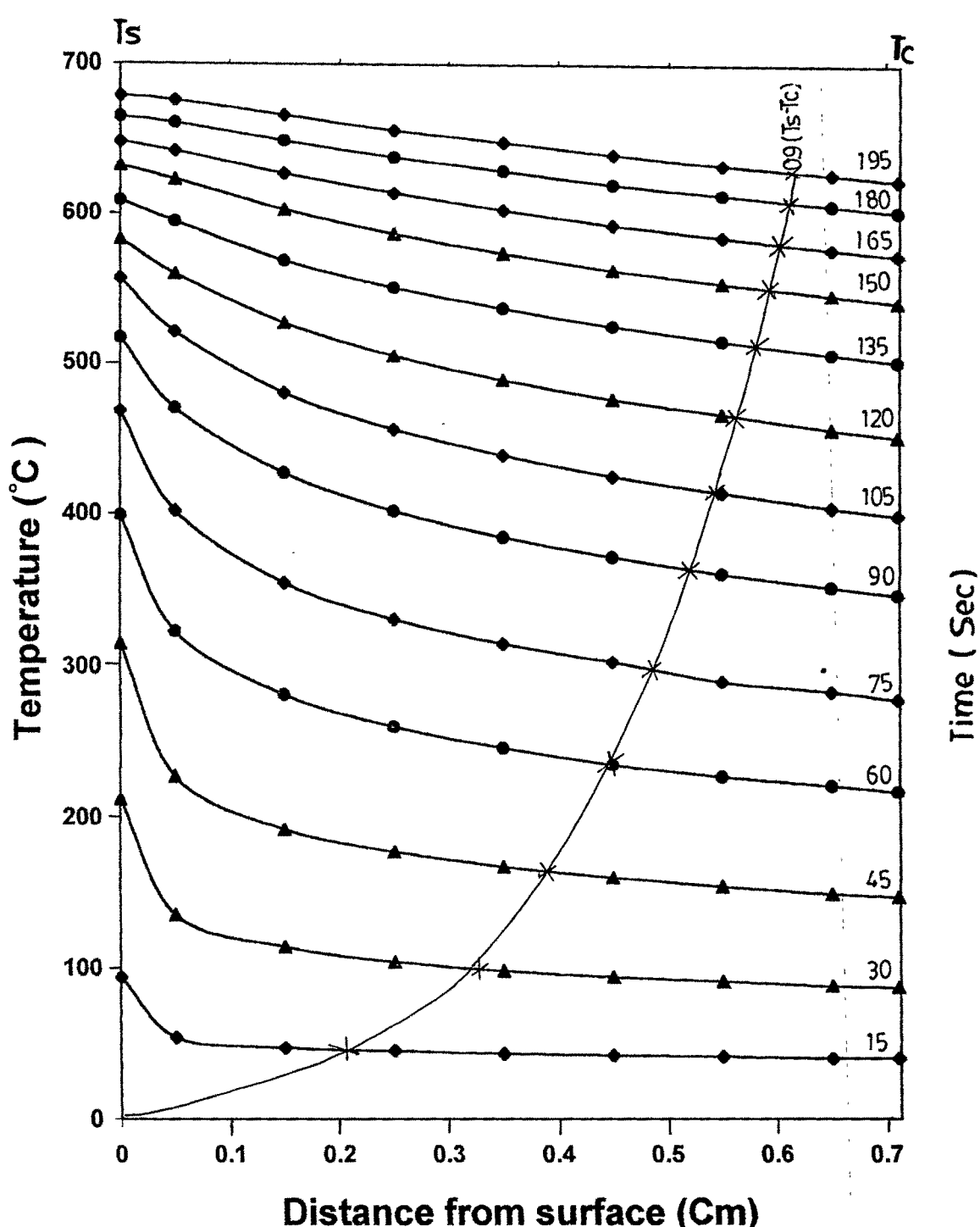
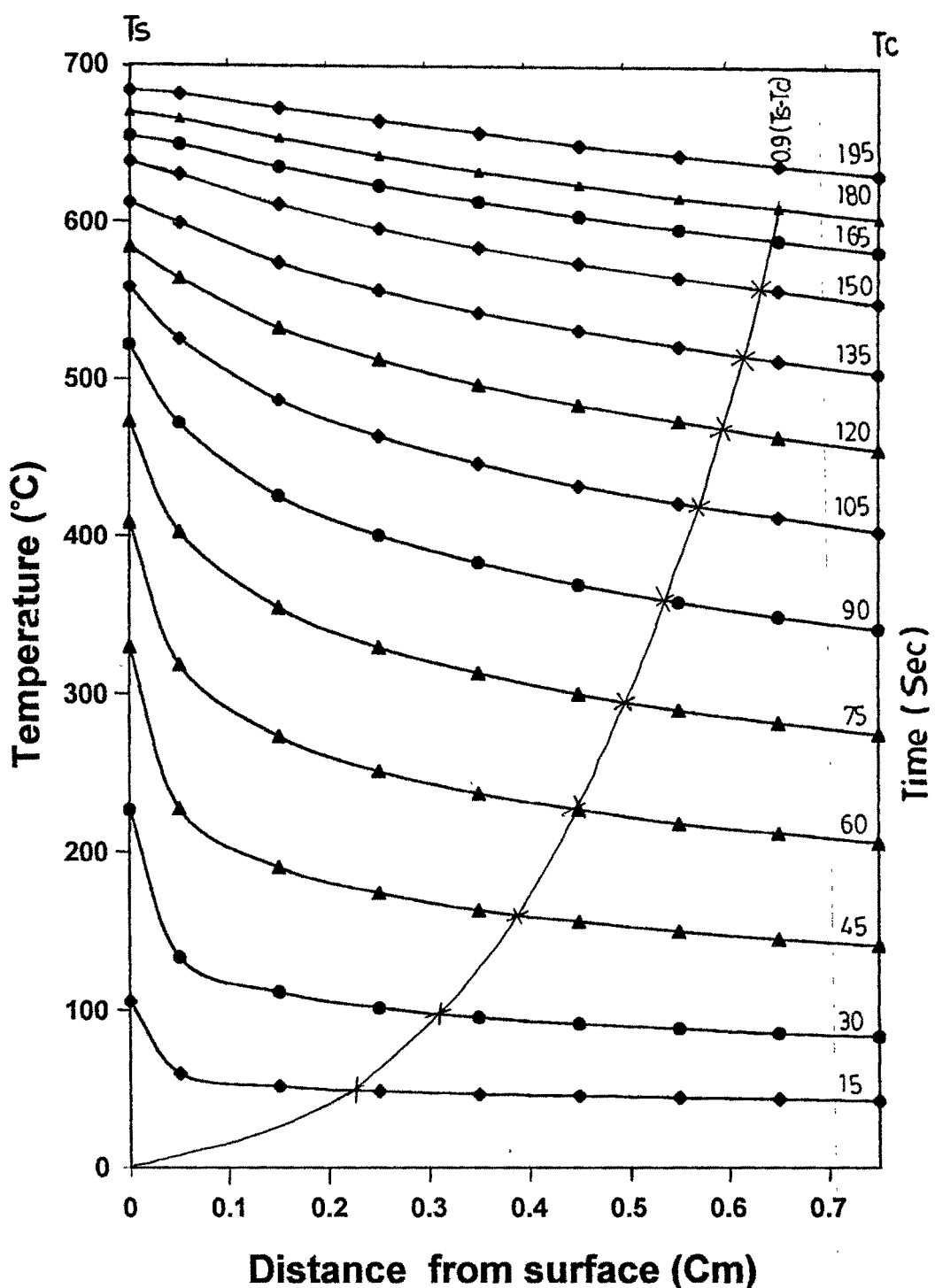
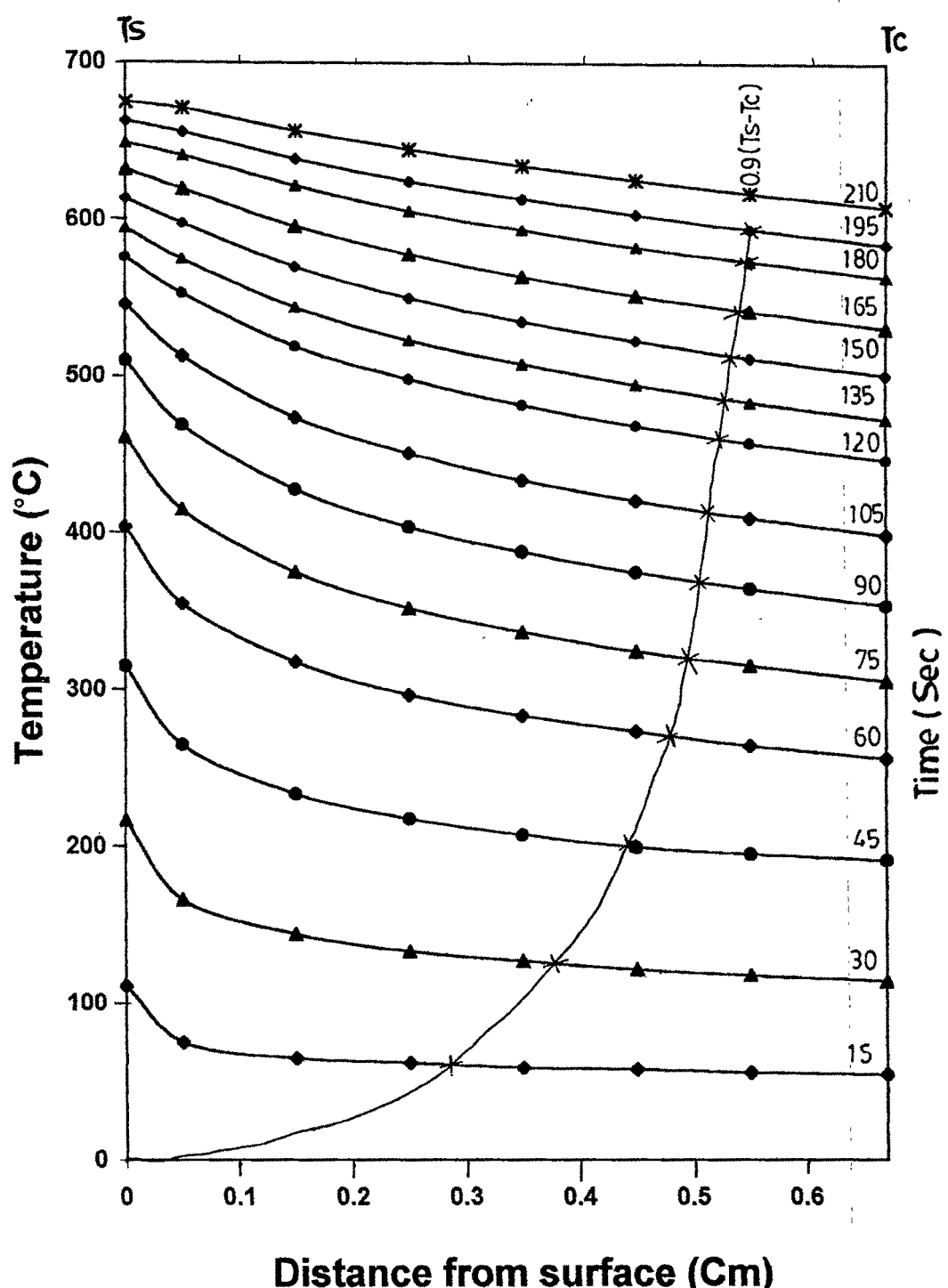


Fig.4.94 Change in temperature profile and movement of heat front with time (Pressed pellet).  
 (Pellet size=0.7122cm & Porosity=21.24%)



**Fig. 4.95 Change in temperature profile and movement of heat front with time (Pressed pellet).**  
**(Pellet size=0.7543cm&Porosity=22.30%)**



**Fig.4.96 Change in temperature profile and movement of heat front with time (Pressed pellet).**  
**(Pellet size=0.6758cm&Porosity=22.67%)**

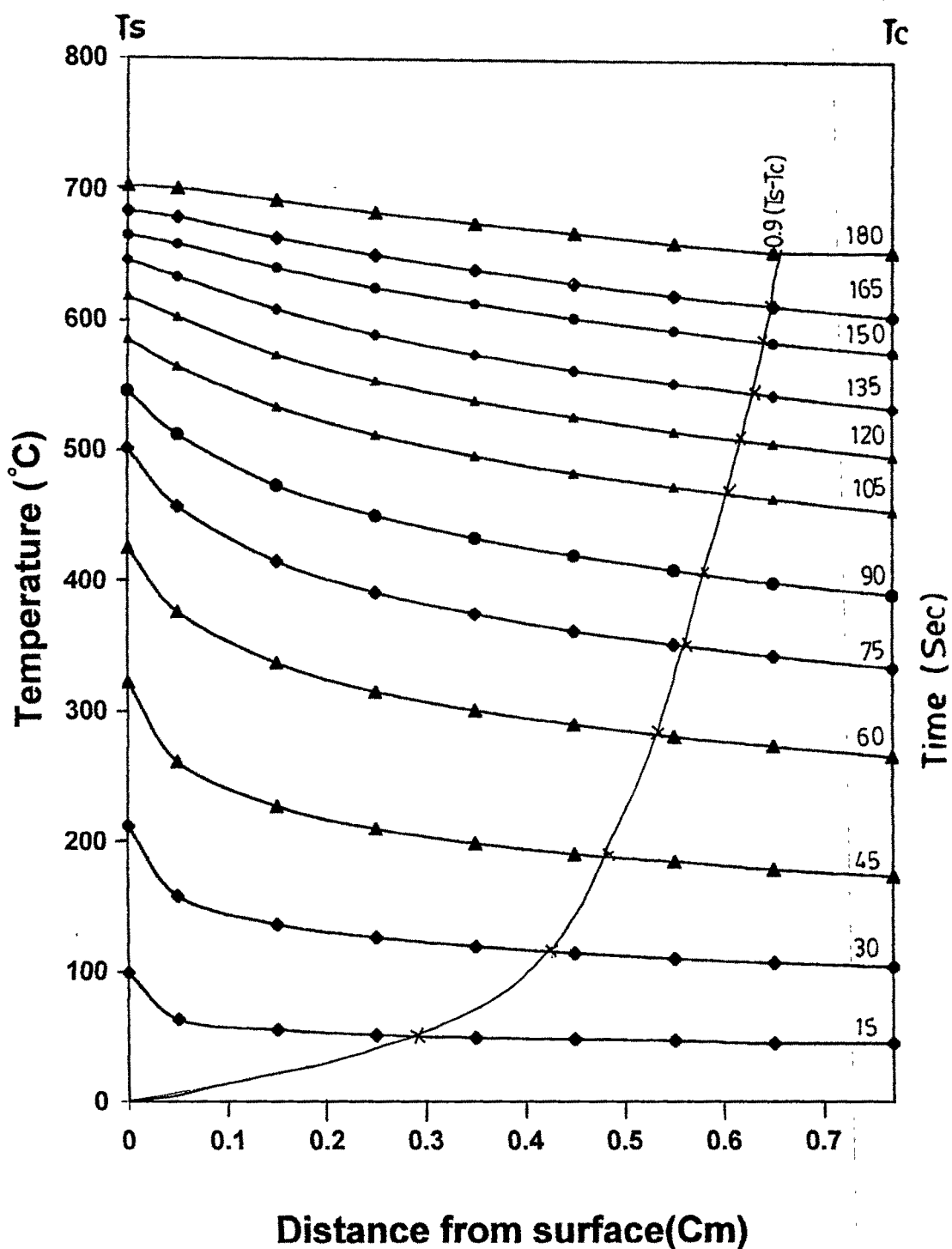


**Fig.4.97 Change in temperature profile and movement of heat front with time (Pressed pellet).**  
**(Pellet size=0.7719cm & Porosity=23.15% P)**

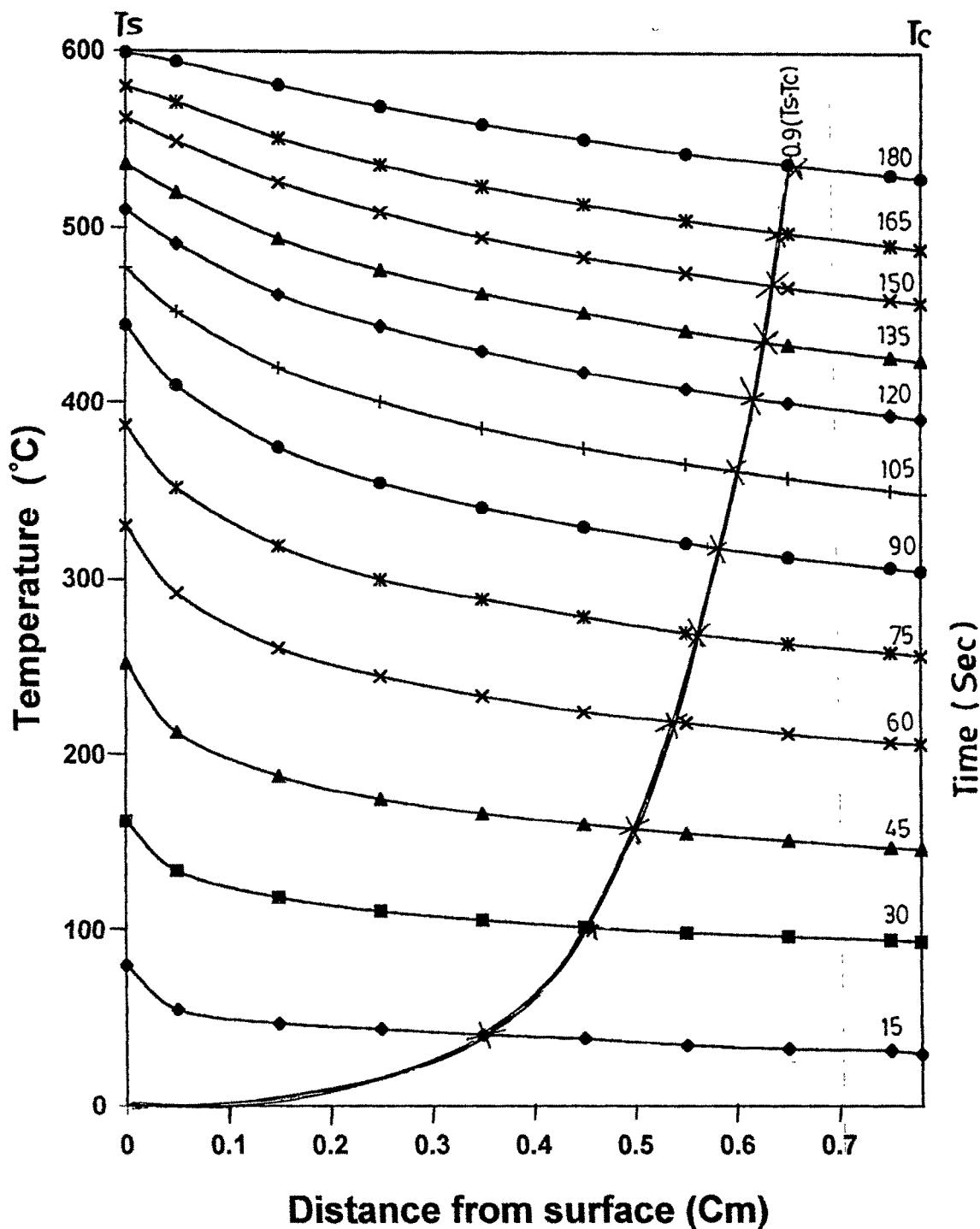
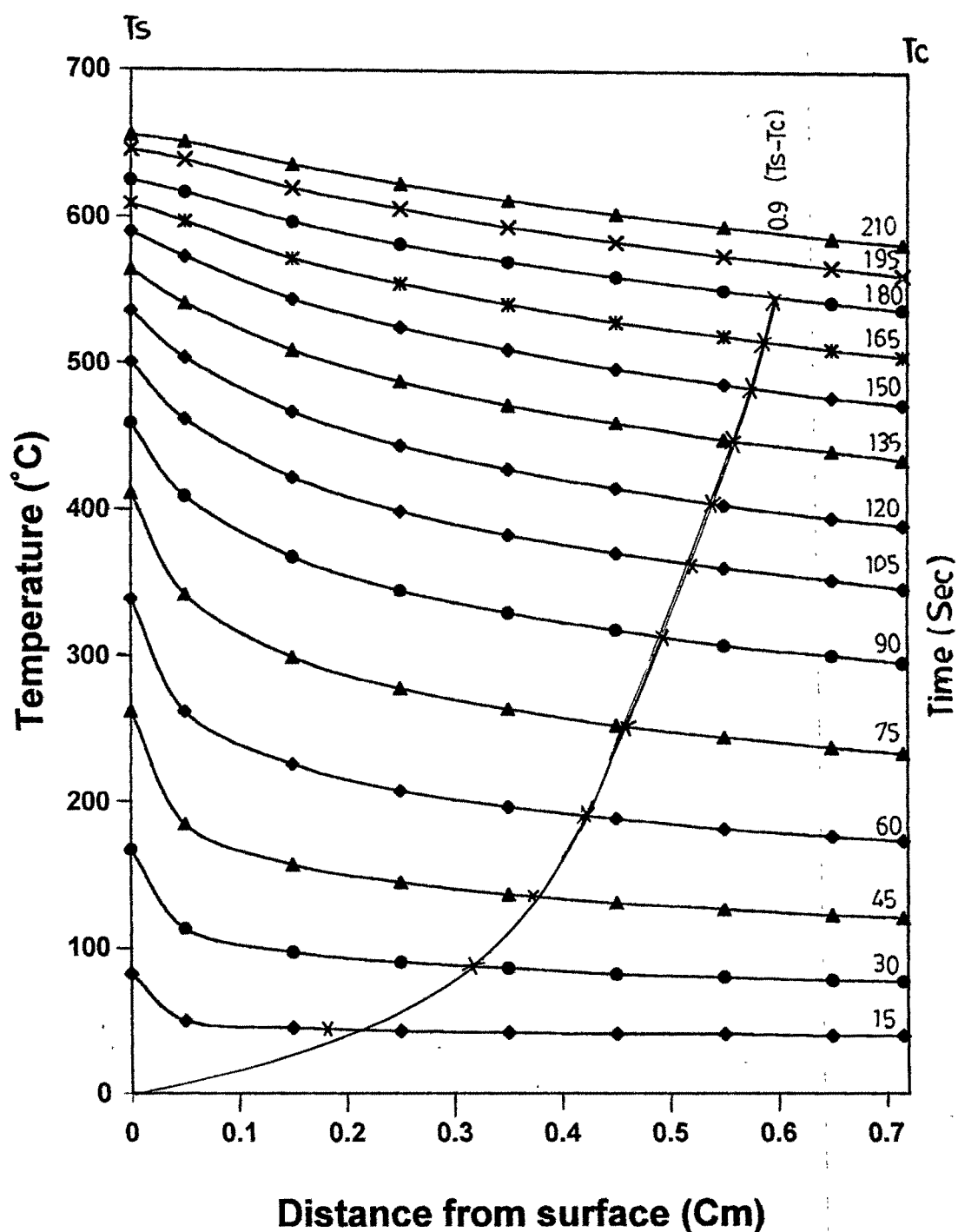


Fig.4.98 Change in temperature profile and movement of heat front with time (Pressed pellet).  
 (Pellet size=0.7790 Cm & Porosity=23.51%)



**Fig. 4. 41 Change in temperature profile and movement of heat front with time (Pressed pellet).**  
**(Pellet size=0.7157cm&Porosity=28.28%)**

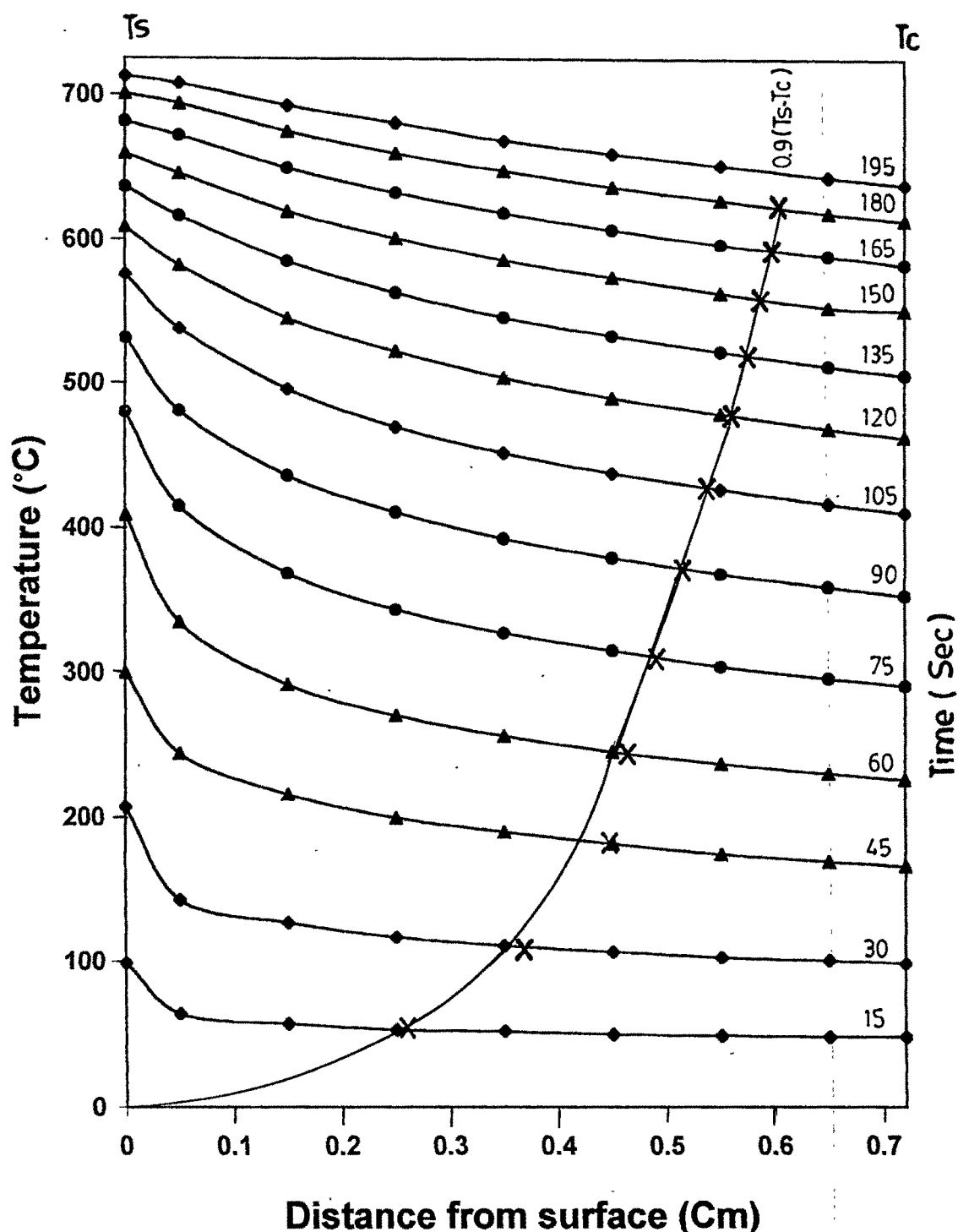
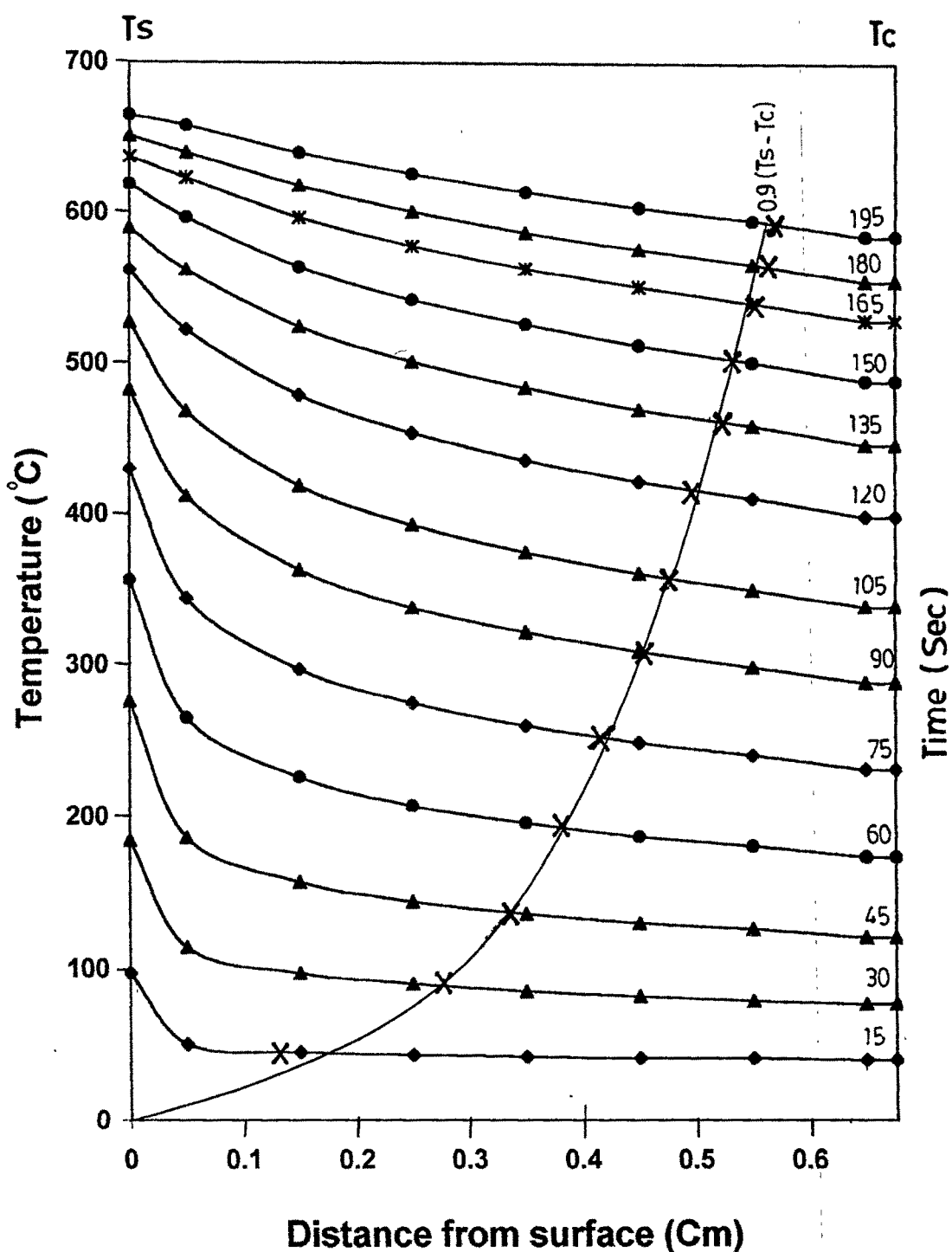


Fig. 4.100 Change in temperature profile and movement of heat front with time (Pressed pellet).  
 (Pellet size=0.7185cm & Porosity=29.73%)



**Fig. 4.101 Change in temperature profile and movement of heat front with time (pressed pellet).**  
**(Pellet size=0.6762cm&Porosity=33.89%)**

Table No. 4.28

## Calculation of Thermal Diffusivity

$$\alpha^2 = ((dT_{av}/dt) \times R) / (3x(dT/dr))$$

Radius(R):=0.5759 cm      Density:=3754Kg/m<sup>3</sup>      Porosity:=14.29%      To:=25 °C

Time (Sec)	T <sub>s</sub> -T <sub>o</sub> (°C)	T <sub>s</sub> -T <sub>c</sub> (°C)	0.9(T <sub>s</sub> -T <sub>c</sub> ) (°C)	K (-)	Distance from surface for 0.9(T <sub>s</sub> -T <sub>c</sub> ) temp.drop (Cm)	dT/dr (°C/Cm)	T <sub>av</sub> (°C)	dT <sub>av</sub> /dt (°C/sec)	Thermal Diffusivity x10 <sup>7</sup> (m <sup>2</sup> /sec)
15	81	68	61.2	0.011663	0.119655	511.4705	45.096	5.75623	1.936
30	222	155	139.5	0.011975	0.244368	570.8603	123.406	6.6058	2.106
45	343	206	185.4	0.01133	0.30793	602.0849	217.783	6.30973	2.286
60	436	214	192.6	0.011861	0.36347	529.8924	321.58	5.18433	2.256
75	497	197	177.3	0.012338	0.40197	441.0777	407.075	4.37123	2.252
90	546	177	159.3	0.012516	0.42747	372.6577	477.1101	3.62566	2.352
105	584	148	133.2	0.013073	0.45006	295.9605	538.212	2.7589	2.335
120	612	118	106.2	0.013717	0.4683	226.7777	585.88	2.23178	2.383
135	635	96	86.4	0.013995	0.480643	179.7592	620.979	1.72996	2.258
150	659	80	72	0.014058	0.489516	147.0841	652.8334	1.16248	1.865
165	673	66	59.4	0.014073	0.496668	119.5941	687.708	0.96913	2.33
180	680	45	40.5	0.015086	0.5073	79.8344	701.952	Avg=2.214x10 <sup>7</sup>	
195	692	38	34.2	0.0148821	0.511358	66.88074			

Table No. 4.29

## Calculation of Thermal Diffusivity

$$\infty = \frac{((dT_{av}/dt) \times R)}{(3 \times (dT/dr))} / \left( \frac{3 \times (dT/dr)}{(3R)} \right)$$

Radius(R)=0.5319Cm      Density=3744.6Kg/m<sup>3</sup>      Porosity:=14.50%      To=30 °C

Time (Sec)	Ts-To (°C)	Ts-Tc (°C)	0.9(Ts-Tc) (°C)	K ( - )	Distance from surface for 0.9(Ts-Tc) temp.drop (Cm)	dT/dr (°C/Cm)	Tav ( °C)	dTav/dt ( °C/sec).	Thermal Diffusivity $\times 10^{-7}$ ( m <sup>2</sup> /Sec )
15	67	44	39.6	0.0280335	0.2524344	156.8725	—	—	—
30	162	98	88.2	0.0167543	0.2820559	312.7039	119.789	4.338267	2.459
45	263	144	129.6	0.0133854	0.3107967	416.9929	193.008	4.7688	2.027
60	348	174	156.6	0.0115525	0.33188171	471.8548	262.853	4.3136	1.621
75	393	166	149.4	0.011491	0.362131	412.5578	322.415	4.88953	2.101
90	462	153	137.7	0.0122792	0.3926488	350.6951	409.539	5.1157	2.586
105	508	129	116.1	0.013054	0.41554957	279.3891	475.887	3.5567	2.252
120	537	113	101.7	0.0129884	0.4276948	237.7863	516.242	2.6114	1.947
135	562	91	81.9	0.0134862	0.4409454	185.7373	554.229	2.334	2.228
150	584	71	63.9	0.0140481	0.452059	141.3532	586.26	2.0103	2.522
165	602	51	45.9	0.0149602	0.4627246	99.195	614.537	1.5257	2.727
180	616	39	35.1	0.0153316	0.4694523	74.768	632.032		
								Avg=2.160x10 <sup>-7</sup>	

Table No. 4.30

## Calculation of Thermal Diffusivity

$$\infty = \frac{(\text{dTav/dt}) \times R}{(3x(\text{dT/dr}))}$$

Sample: Iron ore pressed pellet      Radius(R):=0.5880Cm      Density:=3594Kg/m<sup>3</sup>      Porosity:=17.95%      To=30 °C

Time (Sec)	Ts-To ( °C)	Ts-Tc ( °C)	0.9(Ts-Tc) ( °C)	k ( - )	Distance from surface for 0.9(Ts-Tc) temp. drop (Cm)	dT/dr ( °C/Cm)	Tav ( °C )	dTav/dt ( °C/sec )	Thermal Diffusivity $\times 10^7$ ( m <sup>2</sup> /Sec )
15	71	53	47.7	0.01949253	0.21080479	226.2757	—	—	—
30	164	111	99.9	0.01301121	0.2657268	376.8008	107.2233	3.8821	2.019
45	263	162	145.8	0.01076795	0.3051803	477.7504	173.355	4.8077	1.972
60	348	186	167.4	0.0104409	0.3502147	477.9925	251.454	4.7739	1.958
75	405	188	169.2	0.0102326	0.382951	441.8319	316.572	4.3106	1.912
90	452	176	158.4	0.01047998	0.4131217	383.4221	380.771	3.6926	1.888
105	492	173	155.7	0.00995416	0.4269153	364.7094	427.349	3.7057	1.992
120	523	130	117	0.01160039	0.46105925	253.7635	491.942	3.1909	2.465
135	541	110	99	0.0117995	0.4749571	208.4398	523.078	2.1923	2.062
150	562	86	77.4	0.0125144	0.49014733	157.9117	557.713	1.9894	2.469
165	579	68	61.2	0.0129806	0.50102887	122.14865	583.395	1.5838	2.541
180	593	49	44.1	0.0138521	0.51222296	86.0942	605.223	Avg=2.035x10 <sup>-7</sup>	

Table No. 4.31

**Calculation of Thermal Diffusivity**  
 $\infty = ((dTav/dt) \times R) / (3x(dT/dr))$

Sample: Iron ore pressed Pellet      Radius (R):=0.6424 Cm      Density=3570Kg/m<sup>3</sup>      Porosity=18.49%      To=25 °C

Time (Sec)	Ts-To (°C)	Ts-Tc (°C)	0.9(Ts-Tc) (°C)	k ( - )	Distance from surface for 0.9(Ts-Tc) temp.drop (Cm)	dT/dr (°C/Cm)	Tav (°C)	dTav/dt (°C/sec)	Thermal Diffusivity $\times 10^7$ (m <sup>2</sup> /Sec)
15	64	51	45.9	0.0151372	0.1802934	254.585	44.9815	-	-
30	132	97	87.3	0.0102697	0.2409834	362.2656	77.6066	2.84654	1.683
45	204	131	117.9	0.0098427	0.315412	373.7967	130.3777	3.38599	1.939~
60	261	151	135.9	0.0091207	0.3572	380.4591	179.1863	3.3404	1.88~
75	307	155	139.5	0.0091123	0.39833124	350.211	230.5884	3.2389	1.98~
90	343	151	135.9	0.009116	0.429442465	316.4699	276.3555	3.0101	2.037~
105	374	140	126	0.0093582	0.457456	275.4363	320.89	3.0039	2.335~
120	405	125	112.5	0.0097964	0.4825501	233.1364	366.4715	2.5625	2.354~
135	429	117	105.3	0.0096243	0.4953683	212.5691	397.764	2.1325	2.148~
150	452	104	93.6	0.0097953	0.5099807	183.5364	430.4451	1.9845	2.315~
165	471	92	82.8	0.0098974	0.5215529	158.7567	457.2994	1.6744	2.258~
180	490	85	76.5	0.009732	0.5287599	144.6781	480.6781	1.3771	2.038~
195	504	78	70.2	0.0095686	0.534925	131.2334	498.6125	Avg=2.129x10 <sup>7</sup>	

Table No. 4.32

## Calculation of Thermal Diffusivity

$$\alpha = \frac{(dTav/dt)R}{(3x(dT/dr))} / (3x(dt/dr))$$

Radius(R):=0.7413 Cm      Density=3695.2Kg/m<sup>3</sup>      Porosity 19.67%      To=25 °C

Time (Sec)	Ts-To (°C)	Ts-Tc (°C)	0.9(Ts-Tc) (°C)	K (-)	Distance from surface for 0.9(Ts-Tc) temp.drop (Cm)	dT/dr (°C/Cm)	Tav (°C)	dTav/dt (°C/sec)	Thermal Diffusivity x10 <sup>-7</sup> (m <sup>2</sup> /Sec)
15	71	53	47.7	0.0194925	0.2657632	179.4831	52.372	—	—
30	187	113	101.7	0.01679069	0.3935885	258.3917	130.615	5.482066	5.243
45	280	138	124.2	0.01572302	0.4667004	266.1236	216.834	5.682533	5.276
60	367	155	139.5	0.0143656	0.5047127	276.3949	301.091	4.75066	4.247
75	429	168	151.2	0.0124949	0.5197674	290.8994	359.354	4.255696	3.616
90	480	151	135.9	0.01285007	0.5543393	245.1567	428.8	3.9201	3.951
105	516	137	123.3	0.0126297	0.5745278	214.611	476.957	3.1926	3.676
120	551	120	108.1	0.01270203	0.5932467	182.0491	524.578	2.90593	3.944
135	581	105	94.5	0.01267252	0.6074027	155.5805	564.135	2.3097	3.668
150	602	89	80.1	0.0127441	0.6119901	129.2142	593.869	2.02	3.863
165	626	75	67.5	0.01285977	0.6307234	107.02	624.736	1.7959	4.147
180	645	66	59.4	0.01266442	0.6376545	93.1539	647.748	1.3133	3.484
195	657	55	49.5	0.01271975	0.6453141	76.7068	664.134	Avq=3.844x10 <sup>-7</sup>	

Table No. 4.33

**Calculation of Thermal Diffusivity**  
 $\alpha_C = ((dTav/dt) \times R) / (3x(dT/dr))$   
 Sample: Iron ore pressed pellet      Radius (R):=0.7155 Cm      Density=3573Kg/m<sup>3</sup>      Porosity:=19.70%      To:=25 C

Time (Sec)	Ts-To (°C)	Ts-Tc (°C)	0.9(Ts-Tc) (°C)	K (-)	Distance from surface for 0.9(Ts-Tc) temp.drop (Cm)	dT/dr (°C/Cm)	Tav (°C)	dTav/dt (°C/sec)	Thermal Diffusivity x10 <sup>-7</sup> (m <sup>2</sup> /Sec)
15	79	54	48.6	0.0253643	0.31675679	153.4	61.90826	-	-
30	202	120	108	0.0173592	0.3871532	278.9593	141.30289	6.10903	8.142
45	317	153	137.7	0.0161881	0.4560954	301.9105	245.17918	6.55445	5.178
60	407	164	147.6	0.0151491	0.49640725	297.3365	337.93653	5.81594	4.665
75	476	157	141.3	0.0147889	0.5287399	267.2391	419.65732	5.0102197	4.471
90	530	142	127.8	0.014634	0.5536199	230.0844	488.24312	3.69953	3.835
105	560	125	112.5	0.0142821	0.57057434	197.16975	530.64332	2.89958	3.507
120	591	103	92.7	0.01455906	0.58862474	157.4867	575.23051	2.4711181	3.742
135	612	87	78.3	0.01445055	0.60043094	130.40634	604.77875	1.945836	3.559
150	635	75	67.5	0.0142409	0.6094122	110.76247	633.6056	1.819706	3.918
165	654	59	53.1	0.01457921	0.6202315	85.61319	659.36993	1.42698	3.975
180	668	51	45.9	0.01429146	0.62589343	73.33517	676.41507	Avg=3.959x10 <sup>-7</sup>	

Table No. 4.34

**Calculation of Thermal Diffusivity**  
 $\infty = ((dTav/dt) \times R) / (3x(dT/dr))$   
 Sample: Iron ore pressed pellet      Radius:=0.6501 Cm.      Density=3507 Kg/m<sup>3</sup>  
 Porosity:=19.93%      To:=30 °C

Time (Sec)	Ts-To ( °C)	Ts-Tc ( °C)	0.9(Ts-Tc) ( °C)	k ( - )	Distance from surface for 0.9(Ts-Tc) temp.drop (Gm)	dT/dr ( °C/Cm)	Tav ( °C)	dT/dr ( °C/sec)	Thermal Diffusivity $\times 10^7$ ( m <sup>2</sup> /Sec)
15	69	52	46.8	0.01885752	0.22627034	206.8322	55.6749	-	-
30	154	112	100.8	0.01061512	0.25073533	402.0175	92.9553	3.1899267	1.719
45	251	168	151.2	0.00892119	0.29896227	505.7494	151.3727	4.0055833	1.716
60	326	197	177.3	0.0083949	0.34515674	513.6797	213.1228	4.2595763	1.796
75	386	204	183.6	0.0085029	0.3905052	470.1602	279.1599	4.276283	1.971
90	433	197	177.3	0.0087504	0.42777398	414.4712	341.4113	4.1275903	2.158
105	471	176	158.4	0.009375	0.46321178	341.9602	402.9877	3.6187367	2.293
120	501	158	142.2	0.0096168	0.4858495	292.6799	449.9734	2.8903267	2.139
135	523	135	121.5	0.0100319	0.50643519	239.9122	489.6975	2.508583	2.266
150	544	113	101.7	0.0104771	0.52365489	194.21188	525.2309	2.14496	2.393
165	560	91	81.9	0.0110126	0.53874743	152.0193	554.0463	1.858423	2.649
180	577	71	63.9	0.0116398	0.5520189	115.7569	580.9836	1.4795767	2.769
195	588	56	50.4	0.01205833	0.56172608	89.72345	598.4336	Avg=2.153x10 <sup>-7</sup>	

Table No. 4.35

**Calculation of Thermal Diffusivity**  
 $\alpha = ((dTav/dt) \times R) / (3x(dT/dr))$

Sample: Iron ore pressed pellet      Radius(R):= 0.7219Cm      Density=3479Kg/m<sup>3</sup>      Porosity:= 20.02%      To=25°C

Time (Sec)	Ts-To (°C)	Ts-Tc (°C)	0.9(Ts-Tc) (°C)	K ( - )	Distance from surface for 0.9(Ts-Tc) temp. drop (Cm)	dT/dr ( °C/Cm)	Tav ( °C)	dTav/dt ( °C/sec)	Thermal Diffusivity $\times 10^7$ (m <sup>2</sup> /Sec)
15	71	46	41.4	0.0289358	0.3498	118.3533	—	—	—
30	167	93	83.7	0.01951314	0.4158	201.299	128.315	4.3716	—
45	261	134	120.6	0.014815	0.44265	272.45	198.219	4.5816	4.047
60	333	151	135.9	0.013181	0.4758	285.6242	265.763	4.3237	3.643
75	391	155	139.5	0.012337	0.5039	276.841	327.932	3.859	3.354
90	438	153	137.7	0.0116864	0.5251	262.235	381.519	3.463	3.178
105	480	147	132.3	0.01127003	0.54325	243.5343	431.818	2.893	2.859
120	499	123	110.7	0.01167018	0.56685	195.2898	468.307	2.224	2.74
135	518	106	95.4	0.01175211	0.5826	163.7487	498.531	2.0342	2.989
150	541	93	83.7	0.01173879	0.5946	140.7669	529.332	1.89197	3.323
165	560	80	72	0.01179339	0.60554	118.9021	555.29	Avg=3.155x10 <sup>-7</sup>	—

Table No. 4.36

**Calculation of Thermal Diffusivity**  
 $\infty = ((dTav/dt) \times R) / (3x(dT/dr))$   
 Sample: Iron ore pressed pellet      Radius(R)= 0.7122Cm      Density=3623 Kg/m<sup>3</sup>  
 Porosity:= 21.24%      To=25°C

Time (Sec)	Ts-To (°C)	Ts-Tc (°C)	0.9(Ts-Tc) (°C)	K (-)	Distance from surface for 0.9(Ts-Tc) temp.drop (Cm)	dT/dr (°C/Cm)	Tav (°C)	dTav/dt (°C/sec)	Thermal Diffusivity $\times 10^7$ (m <sup>2</sup> /Sec)
15	69	54	48.6	0.01634149	0.2162665	224.7227	48.10486	-	-
30	187	125	112.5	0.013426495	0.3282665	342.7094	116.02958	4.749662	3.29~
45	285	168	151.2	0.011745004	0.3885537	389.1354	190.5947	5.574885	3.401~
60	374	182	163.8	0.012004151	0.4518162	362.5368	283.2761	5.392186	3.531~
75	438	187	168.3	0.011348137	0.4826686	348.6865	352.3603	4.7855563	3.258~
90	492	170	153	0.011807558	0.51969745	294.4021	426.8431	4.224705	3.407~
105	532	158	142.2	0.011562366	0.53966456	263.4971	479.1015	3.243938	2.923~
120	558	132	118.8	0.01292475	0.56296856	211.0242	524.1612	2.872981	3.232~
135	584	108	97.2	0.012501998	0.58202254	167.0038	565.2909	2.45132	3.485~
150	607	91	81.9	0.012651128	0.594810961*	137.6908	597.7009	1.871483	3.227~
165	623	75	67.5	0.01283066	0.605748	111.43248	621.4354	1.53213	3.264~
180	640	63	56.7	0.01287963	0.61413286	92.325299	643.6648	1.301397	3.346~
195	654	56	50.4	0.01260388	0.619208963	81.394171	660.4773	Avg=3.306x10 <sup>-7</sup>	

Table No. 4.37

**Calculation of Thermal Diffusivity**  
 $\infty = ((dTav/dt) \times R) / (3x(dT/dr))$

Radius(R):= 0.7543 Cm   Density=3574 Kg/m<sup>3</sup>   Porosity :=22.30%   To=25 °C

Time (Sec)	Ts-To (°C)	Ts-Tc (°C)	0.9(Ts-Tc) (°C)	k (-)	Distance from surface for 0.9(Ts-Tc) temp drop (Cm)	dT/dr (°C/Cm)	Tav (°C)	dTav/dt (°C/sec)	Thermal Diffusivity x10 <sup>-7</sup> (m <sup>2</sup> /Sec)
15	81	63	56.7	0.0167543	0.2347975	241.4846	52.7819	—	—
30	202	143	128.7	0.0115141	0.3105665	414.404	113.4672	4.6782	2.8384
45	305	188	169.2	0.01075266	0.3911607	432.55879	193.1255	5.3909	3.1335
60	384	202	181.8	0.01070625	0.4546527	399.86565	275.1928	5.3971	3.3937
75	448	197	177.3	0.01095453	0.5045138	351.42745	355.0407	4.9839	3.5658
90	497	180	162	0.01128481	0.5428203	298.44131	424.7118	4.2917	3.6157
105	534	155	139.5	0.01178067	0.57439337	242.86492	483.792	3.4592	3.5812
120	560	129	116.1	0.01223437	0.59870337	193.91907	528.4865	2.8647	3.7142
135	588	108	97.2	0.01255256	0.61691387	157.55846	569.7302	2.5876	4.1292
150	614	89	80.1	0.01287572	0.63190188	126.76019	606.1131	2.0129	3.9927
165	630	72	64.8	0.01314578	0.64399118	100.62249	630.1184	1.3887	3.4701
180	645	66	59.4	0.01266442	0.64883686	91.548436	647.7744	1.2385	3.4015
195	659	52	46.8	0.01302297	0.65871075	71.047876	667.2735	Avg=3.599x10 <sup>-7</sup>	

Table No. 4.38

**Calculation of Thermal Diffusivity**  
 $\infty = ((dTav/dt) \times R) / (3x(dT/dr))$   
 Sample: Iron ore pressed pellet      Radius(R)= 0.6758 Cm      Density=3418Kg/m<sup>3</sup>      Porosity:= 22.67 %      To=30 °C

Time (Sec)	Ts-To (°C)	Ts-Tc (°C)	0.9(Ts-Tc) (°C)	K (-)	Distance from surface for 0.9(Ts-Tc) temp. drop (Cm)	dT/dr (°C/Cm)	Tav (°C)	dTav/dt (°C/sec)	Thermal Diffusivity $\times 10^7$ (m <sup>2</sup> /Sec)
15	81	56	50.4	0.024606497	0.292614	172.24	66.882	—	—
30	187	103	92.7	0.01989932	0.392922	235.925	146.3362	5.6613	5.405
45	285	128	115.2	0.017787975	0.447517	257.42	236.7211	5.7971	5.073
60	374	147	132.3	0.01556372	0.4732158	279.576	320.25	4.6625	3.757—
75	431	155	139.5	0.013635772	0.4873811	286.224	376.5901	3.6302	2.857—
90	480	156	140.4	0.012488112	0.5013033	280.07	429.1552	3.2581	2.62—
105	516	147	132.3	0.0119588	0.5166273	256.084	474.339	2.9606	2.604—
120	546	129	116.1	0.0120234	0.5343007	217.293	517.973	2.2573	2.34—
135	565	122	109.8	0.0113541	0.5414793	202.278	542.058	1.6323	1.818—
150	584	113	101.7	0.01095	0.5493062	185.142	566.942	1.6632	2.024—
165	602	101	90.9	0.010819	0.55821679	162.84	591.953	1.6769	2.319—
180	619	85	76.5	0.0110303	0.5688083	134.492	617.251	1.4234	2.384—
								Avg=2.525x10 <sup>-7</sup>	

Table No. 4.39

**Calculation of Thermal Diffusivity**  
 $\alpha_C = ((dTav/dt) \times R) / (3x(dT/dr))$   
 Sample: Iron Ore pressed pellet      Radius(R)=0.7719 Cm      Density=3420Kg/m<sup>3</sup>      Porosity = 23.15%      To=25 °C

Time (Sec)	Ts-To (°C)	Ts-Tc (°C)	0.9(Ts-Tc) (°C)	k ( - )	Distance from surface for 0.9(Ts-Tc) temp.drop (Cm)	dT/dr (°C/Cm)	Tav (°C)	dTav/dt (°C/sec)	Thermal Diffusivity $\times 10^7$ ( m <sup>2</sup> /Sec)
15	74	54	48.6	0.0210054	0.29509	164.6955	55.2439	-	-
30	187	108	47.2	0.0182993	0.42993	226.0833	136.4277	5.728	6.5189
45	297	148	133.2	0.015478	0.48285	275.9764	227.0846	6.6159	6.1682
60	400	159	143.1	0.015376	0.53828	265.8468	334.9039	6.1723	5.9739
75	476	167	150.3	0.0139656	0.56079	268.0148	412.2538	4.4667	4.2881
90	520	155	139.5	0.0134489	0.58443	238.6941	468.905	3.8326	4.1313
105	560	131	117.9	0.0138356	0.61122	192.8929	527.2332	3.2685	4.3599
120	593	122	109.8	0.0131764	0.62255	176.3714	566.9596	2.4548	3.5812
135	621	113	101.7	0.0126218	0.63198	160.9228	600.8783	1.9919	3.2032
150	640	89	80.1	0.0131522	0.64899	123.4225	626.7163	1.8977	3.9562
165	659	80	72	0.0127799	0.6561	109.7394	657.8101	1.8239	4.2764
180	678	55	49.5	0.01395452	0.67309	73.5414	681.4337		
								Avg=3.97x10 <sup>-7</sup>	

Table No. 4.40

**Calculation of Thermal Diffusivity**  
 $\alpha = ((dTav/dt) \times R) / (3 \times (dT/dr))$

Sample: Iron ore pressed pellet      Radius(R):= 0.7790Cm      Density=3327.1kg/m<sup>3</sup>      Porosity:= 23.51%      To=25°C

Time (Sec)	T <sub>s</sub> -T <sub>o</sub> ( °C)	T <sub>s</sub> -T <sub>c</sub> ( °C)	0.9(T <sub>s</sub> -T <sub>c</sub> ) ( °C)	k ( - )	Distance from surface for 0.9(T <sub>s</sub> -T <sub>c</sub> ) temp.drop (Cm)	dT/dr ( °C/cm)	Tav ( °C)	dTav/dt ( °C/sec)	Thermal Diffusivity $\times 10^7$ (m <sup>2</sup> /Sec)
15	50	25	22.5	0.0462098	0.4860619	46.2963	52		
30	137	68	61.2	0.02334911	0.4883074	125.3309	118.4039	4.51188	6.606
45	227	105	94.5	0.0171331	0.50828434	185.9196	187.3565	4.72974	5.468
60	305	123	110.7	0.0151354	0.540296	204.8877	260.2962	4.31462	
75	362	130	117	0.0136548	0.56205238	208.1657	316.7952	3.7271	4.649
90	419	139	125.1	0.01225997	0.57479534	217.6482	372.1079	3.3026	3.94
105	452	128	115.2	0.01201573	0.5962487	193.2079	415.8549	2.8314	3.805
120	485	118	106.2	0.01177887	0.6130014	173.2459	457.0506	2.4284	3.639
135	511	111	99.9	0.01130992	0.623645	160.1873	488.7114	2.0684	3.353
150	537	104	93.6	0.01094405	0.6331194	147.839	519.102	1.8731	3.29
165	555	91	81.9	0.01095823	0.6449819	126.9803	544.9048	1.9063	3.898
180	574	70	63	0.011689634	0.66192024	95.1776	576.2902		
								Avg=3.796x10 <sup>-7</sup>	

Table No. 4.41

**Calculation of Thermal Diffusivity**  
 $\alpha_c = ((dTav/dt) \times R) / (3x(dT/dr))$

Sample: Iron ore pressed pellet      Radius=0.7157 Cm      Density=3170Kg/m<sup>3</sup>      Porosity=28.28%      To=30 °C

Time (Sec)	Ts-To ( °C)	Ts-Tc ( °C)	0.9(Ts-Tc) ( °C)	k ( - )	Distance from surface for 0.9(Ts-Tc) temp drop ( Cm)	dT/dr ( °C/Cm)	Tav ( °C)	dTav/dt ( °C/sec)	Thermal Diffusivity $\times 10^7$ ( m <sup>2</sup> /sec)
15	52	42	37.8	0.01423827	0.18804	201.02106	45.503		
30	137	90	81	0.01400571	0.3395099	238.5792	98.5859	3.8124	3.812
45	232	141	126.9	0.01106617	0.3775068	336.1529	159.872	4.3243	3.069~
60	309	165	148.5	0.01045659	0.4266357	348.0721	228.314	4.7132	3.232~
75	381	177	159.3	0.01022199	0.4659571	341.8769	301.269	4.6634	3.254~
90	429	163	146.7	0.01075229	0.5071666	289.2541	368.215	4.0049	3.303~
105	471	154	138.6	0.01064672	0.5301211	261.1449	421.418	3.2219	2.945~
120	506	146	131.4	0.01035775	0.5457226	240.7819	464.869	2.8152	2.789~
135	534	129	116.1	0.01052284	0.5638824	205.8939	505.871	2.5139	2.913~
150	560	117	105.3	0.01043842	0.5760844	182.7857	540.288	20637	2.694~
165	579	103	92.7	0.01046408	0.5875056	157.7857	567.762	1.7315	2.623~
180	595	87	78.3	0.01068141	0.5991399	130.6873	592.323	1.5775	2.879~
									Avg=2.97x10 <sup>-7</sup>

Table No. 4.42

**Calculation of Thermal Diffusivity**  
 $\rho C_p = ((dTav/dt) \times R) / (3x(dT/dr))$   
 Sample: Iron ore pressed pellet. Radius(R)=: 0.7185 cm Density=  $3106 \text{ Kg/m}^3$  Porosity=:29.73%  $T_0=30^\circ\text{C}$

Time (Sec)	$T_s-T_0$ ( $^\circ\text{C}$ )	$T_s-T_c$ ( $^\circ\text{C}$ )	$0.9(T_s-T_c)$ ( $^\circ\text{C}$ )	K (-)	Distance from surface for $0.9(T_s-T_c)$ temp.drop (Cm)	$dT/dr$ ( $^\circ\text{C}/\text{cm}$ )	$T_{av}$ ( $^\circ\text{C}$ )	$qTav/dt$ ( $^\circ\text{C}/\text{sec}$ )	Thermal Diffusivity $\times 10$ ( $\text{m}^2/\text{Sec}$ )
15	69	51	45.9	0.0201521	0.2651784	173.09117	57.2081	-	-
30	177	108	97.2	0.01646728	0.3771947	257.6918	126.7952	5.9554	5.535
45	288	133	119.7	0.0147246	0.439411	255.1129	235.8686	5.5798	5.238
60	379	182	163.8	0.0122255	0.4593421	356.5969	294.1898	4.4749	3.006-
75	450	188	169.2	0.01163741	0.490003	345.3039	370.1176	4.7321	3.282-
90	501	177	159.3	0.01156063	0.5209442	305.7909	436.1522	4.1312	3.2356-
105	546	165	148.5	0.01139689	0.5423394	273.8138	494.0542	3.5347	3.092-
120	579	146	131.4	0.0114808	0.5670124	233.8027	542.1935	2.8934	2.964-
135	607	131	117.9	0.011358	0.575733	204.7824	580.8546	2.4395	2.853-
150	630	112	100.8	0.01151481	0.5898061	170.9036	615.3789	2.1249	2.978-
165	652	99	81.1	0.01142379	0.5993625	148.6579	644.6043	1.8089	2.914-
180	671	87	78.3	0.01134923	0.6076118	128.8657	669.6467	1.43008	2.658
195	683	74	66.6	0.0113971	0.6157114	108.1676	687.5066	Avg=3.04x10 <sup>-7</sup>	

Table No. 4.43

**Calculation of Thermal Diffusivity**  
 $\infty = ((dTav/dt) \times R) / (3 \times (dT/dr))$   
 Sample:= Iron ore pressed pellet  
 Radius(R):= 0.6762 Cm  
 Density=2922kg/m<sup>3</sup>  
 Porosity=:33.89%  
 To=30 °C

Time (Sec)	Ts-To (°C)	Ts-Tc (°C)	0.9(Ts-Tc) (°C)	K (-)	Distance from surface for 0.9(Ts-Tc) temp.drop (Cm)	dT/dr (°C/Cm)	dTav (°C)	dTav/dt (°C/sec)	Thermal Diffusivity x10 <sup>7</sup> (m <sup>2</sup> /Sec)
15	67	57	51.3	0.01077609	0.1269217	404.1862	45.725	—	—
30	154	107	96.3	0.01213746	0.2898468	332.2445	99.598	3.840283	2.605
45	246	155	139.5	0.0102646	0.34090398	409.2061	160.9335	4.356467	2.3997~
60	326	182	163.8	0.0097148	0.3886294	421.4812	230.292	4.713677	2.5208~
75	400	198	178.2	0.00937591	0.4245726	419.7162	302.3938	4.5643433	2.4512~
90	452	193	173.7	0.00945557	0.4582529	379.0483	367.2223	3.98954	2.3724~
105	497	188	169.2	0.0092586	0.4798676	352.5973	422.03	3.7547033	2.4002~
120	532	163	146.7	0.0098574	0.5088024	288.3241	479.8634	3.384593	2.6459~
135	560	143	128.7	0.0101179	0.5277696	243.8564	523.5678	2.7417267	2.5342~
150	589	130	117	0.0100726	0.5401166	216.6199	562.1152	2.325743	2.42 ~
165	607	108	97.2	0.010463	0.5550286	175.1261	593.3401	1.7265467	2.2222~
180	621	96	86.4	0.0103721	0.5631154	153.4321	613.9116	1.39934	2.041
195	635	80	72	0.0106236	0.5731419	125.6233	635.0203	Avg=2.441x10 <sup>7</sup>	

**Table No.4.44**  
**Variation of thermal diffusivity/conductivity with porosity (Iron ore pressed pellet)**

Serial No.	Weight of Pellet (gram)	Size (cm)	Volume (cm <sup>3</sup> )	Density (Kg/m <sup>3</sup> )	Firing treatment (°C)	True density (Kg/m <sup>3</sup> )	Porosity (%)	Thermal diffusivity (m <sup>2</sup> /sec)	Thermal conductivity (W/mK)
1	3.004	0.5759	0.800073	3754	1050	(4380)	14.29	2.214x10 <sup>-7</sup>	0.8703
2	2.3606	0.5319	0.630345	3745	1050	(4380)	14.5	2.160x10 <sup>-7</sup>	0.8469
3	3.0605	0.588	0.85157	3594	1050	(4380)	17.95	2.035x10 <sup>-7</sup>	0.7958
4	3.9644	0.6424	1.110465	3570	1050	(4380)	18.49	2.129x10 <sup>-7</sup>	0.7957
5	6.3049	0.7413	1.706359	3695	1200	(4600)	19.67	3.844x10 <sup>-7</sup>	1.4872
6	5.4821	0.7155	1.534326	3573	1120	(4450)	19.7	3.959x10 <sup>-7</sup>	1.481
7	4.0361	0.6501	1.150877	3507	1050	(4380)	19.93	2.153x10 <sup>-7</sup>	0.7909
8	5.4821	0.7219	1.575867	3479	950	(4350)	20.02	3.155x10 <sup>-7</sup>	1.1492
9	5.4824	0.7122	1.513194	3623	1200	(4600)	21.24	3.306x10 <sup>-7</sup>	1.2541
10	6.4251	0.7543	1.797715	3574	1200	(4600)	22.3	3.599x10 <sup>-7</sup>	1.3469
11	4.4189	0.6758	1.292835	3418	1100	(4420)	22.67	2.525x10 <sup>-7</sup>	0.9036
12	6.5887	0.779	1.98016	3327	0950	(4350)	23.51	3.769x10 <sup>-7</sup>	1.3223
13	6.5887	0.7719	1.926512	3420	1120	(4450)	23.15	3.970x10 <sup>-7</sup>	1.4215
14	4.8679	0.7157	1.53608	3170	1100	(4420)	28.28	2.970x10 <sup>-7</sup>	0.9857
15	4.8258	0.7185	1.553706	3106	1100	(4420)	29.73	3.040x10 <sup>-7</sup>	0.9885
16	3.7844	0.6762	1.294902	2922	1100	(4420)	33.89	2.441x10 <sup>-7</sup>	0.747

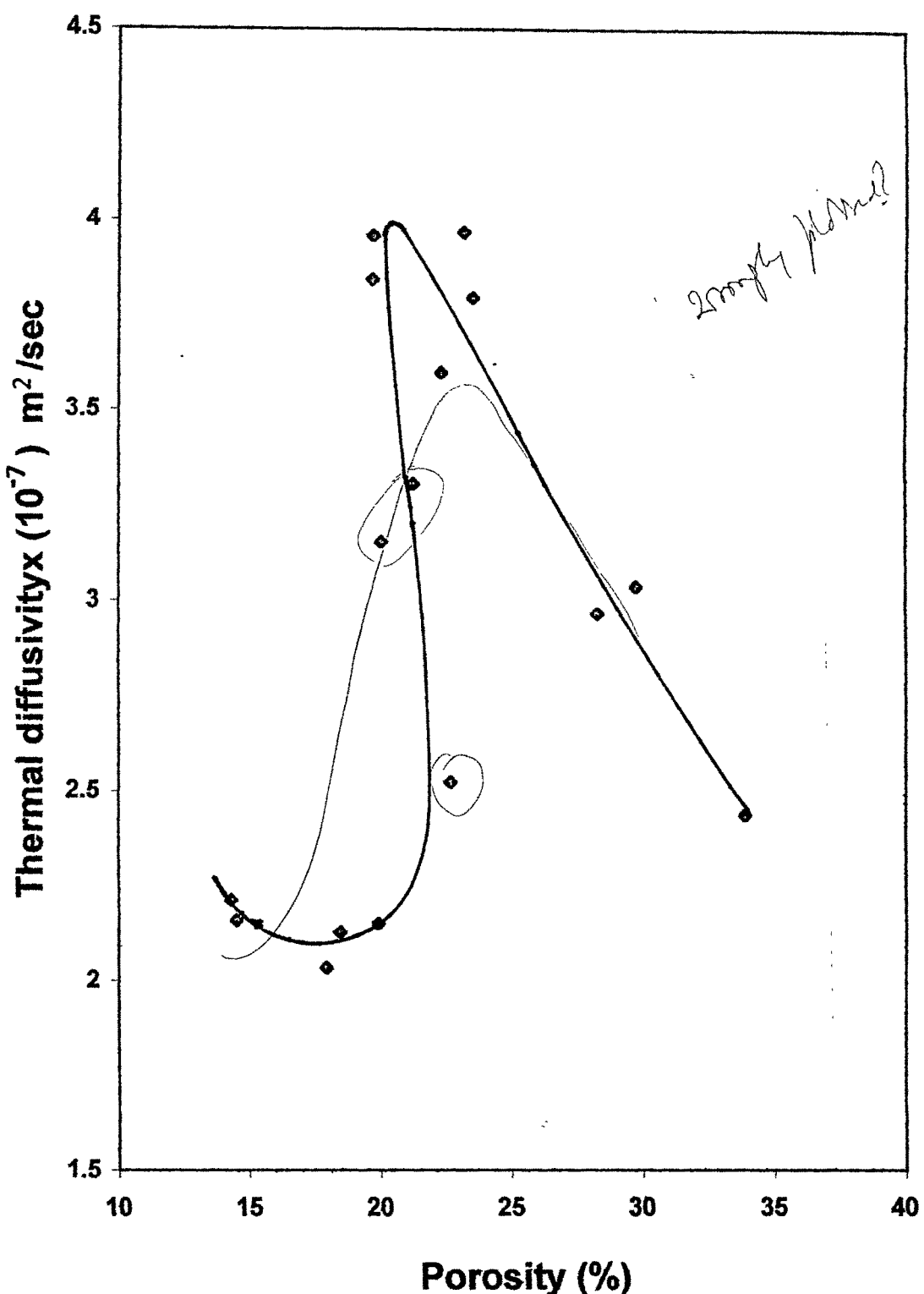


**Fig. 4.102 Effect of porosity on thermal diffusivity of pressed iron ore pellets.**

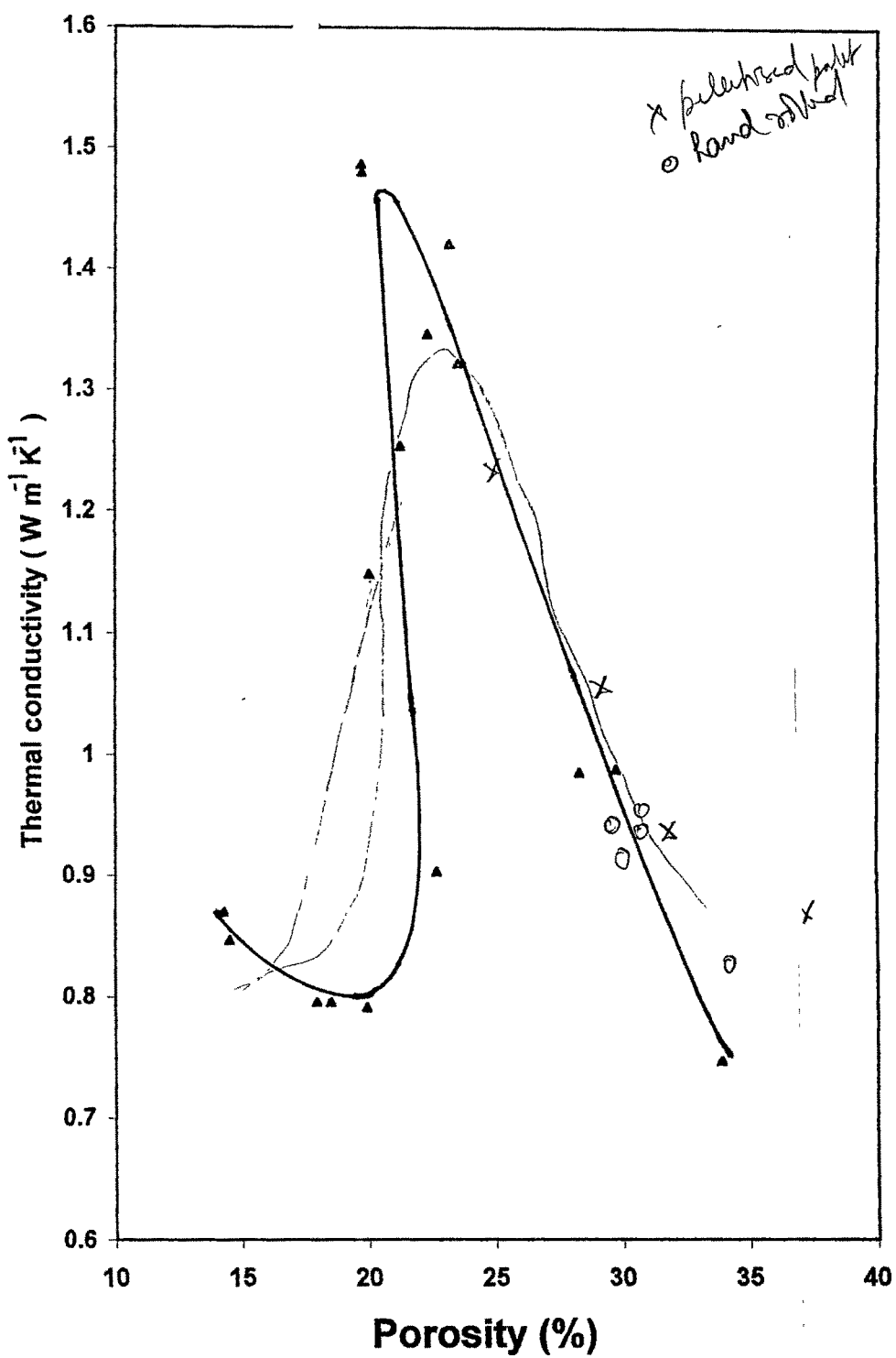


Fig. 4.103 Effect of porosity on thermal conductivity of pressed iron ore pellets.

- 2 At same porosity level, decrease in average pore size increases the pore/solid inter-facial area, increasing resistance to heat transfer and decreasing conduction.

The net change in thermal conductivity with porosity will depend on contribution by above two factor. At high porosity level and with larger pores, decrease in porosity or pore volume will increase particle to particle contact area and decreases the pore/solid interfacial area. However, after certain pore volume/size the increase in contact area is likely to be less pre-dominant than change in particle pore surface area. The decrease in pore size due to closing of pores at constant porosity, will increase pore particle interfacial area with almost no change in particle to particle contact area. This adds resistance to heat flow, decreasing thermal conductivity. The upward rise in thermal conductivity at very low porosity is expected, it will approach to zero porosity conductivity value. More experiments could not be conducted in this low porosity range, as it was difficult to make such pellets.

The effective thermal conductivity of pellets depends on relative proportion of heat transferred by various modes viz solid state conduction, conduction in pore, convection and radiation within pore, which in turn depends on temperature and pore size. The other aspect that could decrease the effective thermal conductivity is lesser pore radiation due to decrease in its average size. The pore radiation is shown to be proportional to its size as indicated in equation 2.47 of chapter 2.

Kasai <sup>32</sup> calculated the contribution of pore radiation towards effective thermal conductivity for coke samples and found it to be negligible. In view of this,

the contribution towards effective thermal conductivity by factors other than conduction is calculated using following equation and taking following parameters:

Kunii's equation,

$$Ke/Ks = \frac{1-e^{2/3}+e^{2/3}}{\left[ (1-e^{1/3}) + e^{1/3} / \{ Kg/Ks + (2/3)(hr.dp/Ks) \} \right]^{-1}}$$

1. Zero porosity conductivity	1.8 Wm <sup>-1</sup> K <sup>-1</sup>
2. Conductivity of air <sup>64</sup>	0.068 Wm <sup>-1</sup> K <sup>-1</sup>
3. Emmisivity of pellet <sup>65</sup>	0.76
4. Temperature	700 °C

It was observed that in porosity range of 5 to 30% and pore size range of 10μm to 50μm the values calculated are very small to justify the change observed in present work and thus eliminating any such possibility. The effect of radiation in the pores of material was estimated and reported by Luikov<sup>49</sup>. The relation suggested:

$$\text{Radiative thermal conductivity in pore} = (2 \varepsilon^2 \delta T^3 dp).$$

The calculation using this formula showed that the coefficient of radiative heat conduction in the pores over the whole temperature range is no more than 1.5% of the molecular heat conduction. This leads to the conclusion that the large drop in thermal conductivity values observed in present case is attributed to decrease in solid-state conduction due to more interfacial resistance.

Figure 4.104 compares the thermal conductivity values of pressed pellet with those of pelletised pellet. The results indicate the value are satisfactorily comparable.

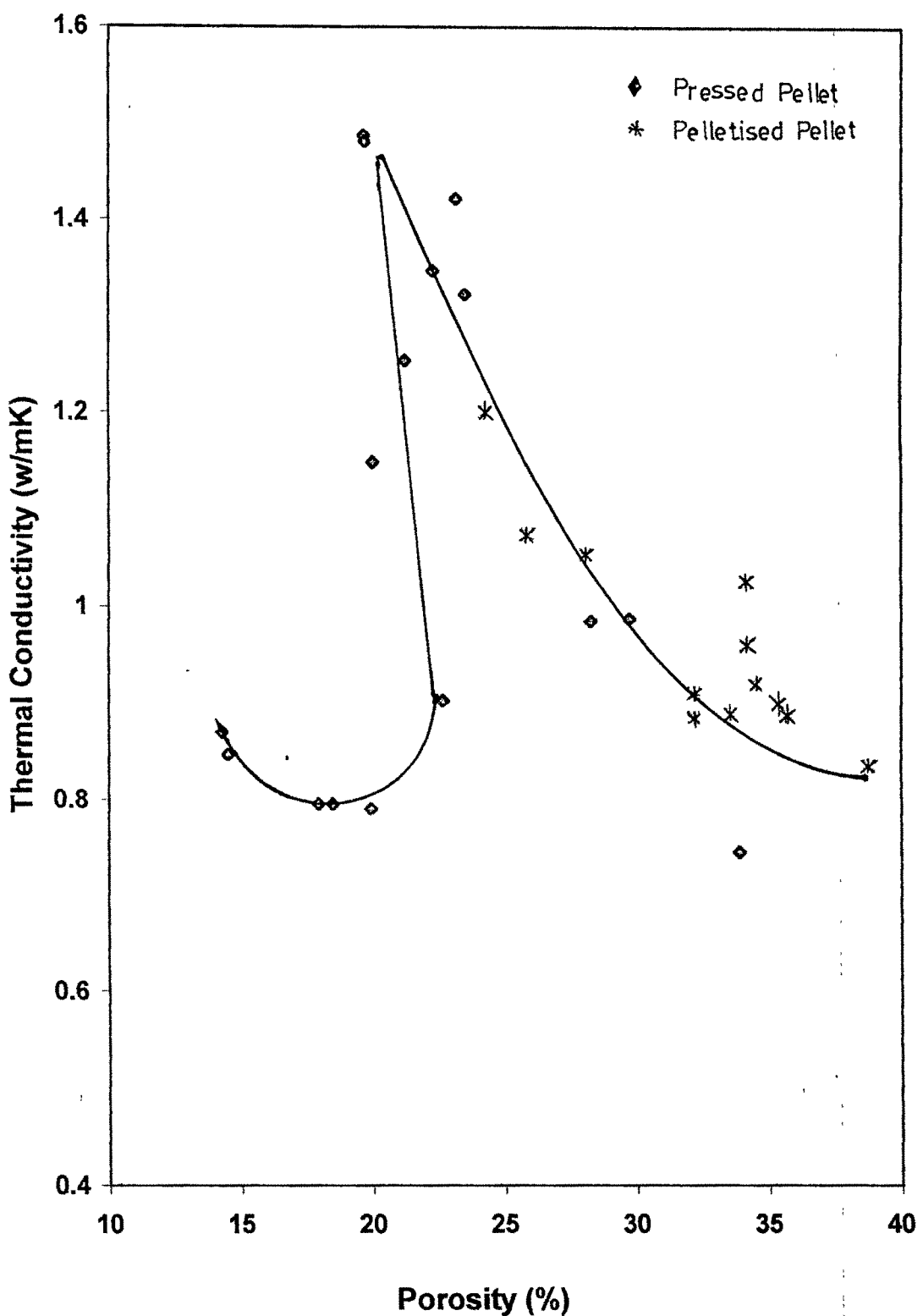


Fig.104 Effect of porosity on thermal conductivity of pressed and pelletized pellets.